THE EVOLUTION OF DIORITIC ROCKS - WITH SPECIAL REFERENCE TO THE HIGH POTASSIUM DIORITES OF THE YEOVAL IGNEOUS COMPLEX, N.S.W.

by
B.L. Gulson

Thesis submitted as a requirement for admission to the Degree of Doctor of Philosophy, Australian National University

February, 1968.

The assistance and instruction given to the author by various people are detailed in the acknowledgements. Except where otherwise indicated, all results presented in this thesis are the author's own, as are all conclusions drawn from the data.

B.L. Gulson

ACKNOWLEDGEMENTS

The author wishes to express his gratitude for the assistance rendered by his supervisors, Dr J.F. Lovering of this department and Dr A.J.R. White of the Department of Geology.

Mrs J. Widdowson instructed the author on the use of the electron microprobe and rechecked a number of analyses.

The major portion of the X-ray fluorescence work was carried out in the Department of Geology and the author gratefully acknowledges the assistance with techniques from Dr B.W. Chappell and Professor D.A. Brown for use of the facilities in his department.

Thanks are due to Dr W. Compston and Mr M. Bofinger for instruction in all aspects of the Rb-Sr geochemistry.

Dr K.S. Heier made the thorium, uranium and potassium determinations by γ-ray spectrometry.

The author is grateful to Dr D.H. Green and Mr W. Hibberson for their assistance with the experimental petrology.

Dr S.R. Taylor, Miss A. Capp and Mrs M. Kaye kindly ran samples on the MS7 and optical spectrograph to cover a wide range of trace elements.

Mr E. Kiss kindly analysed most rock and mineral specimens for ferrous and ferric iron and a number of rocks for Al and Na. His instruction for the determination of a number of elements is gratefully acknowledged.

Mr J. Kleeman assisted in the location and qualitative determination of uranium in two samples of diorite.

The author received guidance in mineral separations from Messrs H. Berry and R. Rudowski.

Messrs E. Pedersen and A. Powell prepared a large proportion of the thin sections, polished thin sections and grain mounts.

This project was begun at the University of New South Wales, Sydney and the guidance of Professor J.J. Frankell and other members of staff is appreciated.

This research has been conducted during the tenure of a G.M.H. Fellowship at the University of New South Wales and an Australian National University Research Scholarship and this financial assistance is gratefully acknowledged.

TABLE OF CONTENTS

CONTENTS (cont)

CONTENTS (cont)

CONTENTS (cont)

1. INTRODUCTION

There is a growing body of opinion amongst petrologists and geochemists in support of the hypothesis that andesitic rocks are "primary" silicate magmas derived from partial melting processes in the earth's upper mantle and/or lower crust (Hamilton 1964; O'Hara 1965; Taylor and White 1966; Taylor 1967; Dickinson and Hatherton 1967). The alternative theories are fractional crystallisation or mixing processes involving a "primary" basalt magma (Bowen 1928; Osborn 1959, 1962; Tilley 1950; Wilcox 1954; Chayes 1956; Joplin 1959; Wilkinson 1966; etc.). However, the current trend is strongly against these "secondary" origins and the possibility that the andesites at least of the volcanic association are the products of partial melting processes within the upper mantle (or lower crust) has stimulated a considerable increase in research activity on andesitic rocks.

Dioritic rocks are members of the coarse-grained or plutonic calc-alkaline association* gabbro-diorite-granodiorite-granite and as such are the equivalents of the andesites in the volcanic calc-alkaline association (basalt-andesite-dacite-rhyolite). By analogy with the arguments

---

*The term "association" is used in preference to "series" which has a genetic implication.

advanced for the "primary" origin of the andesites, it may well be that the diorites are also "primary" and as such represent magmas of andesitic composition which have crystallised at some depth within the earth's upper crust. It is important that the diorite-andesite relationship be well established and further, that the diorites themselves be studied in detail to provide further information on the nature of the "primary" andesitic magma.

The importance of andesites and diorites stems from the fact that the intermediate members of the calc-alkaline association, together with the acid varieties (granodiorites and granites; dacites and rhyolites) are apparently the most voluminous rock types in orogenic areas (e.g. Schmidt 1957; Coats 1962; Hamilton 1964; Taylor and Kolbe 1966; Ewart and Stipp 1967). In addition, the estimated average composition of the continental crust closely resembles that of an andesite (Taylor and White 1966; Taylor 1967). This has led a number of workers to suggest a relationship between the genesis of calc-alkaline rocks and the evolution of continents (Wilson 1954; Engel 1963; Taylor and White 1966; Taylor 1967).

It has been proposed that there is a relationship between orogenesis and the production of the calc-alkaline rocks (e.g. Green and Ringwood 1966).

In this thesis a detailed field, petrographic and geochemical study of the Yeoval diorite complex in central New South Wales is presented in an attempt to elucidate both the particular problem of the Yeoval diorites and the general problem of the calc-alkaline rock association.

1.1 GENERAL FEATURES AND PROBLEMS OF THE CALC-ALKALINE ASSOCIATION

1.1.1. Nomenclature

Basalt-gabbro, andesite-diorite, dacite-tonalite-granodiorite, rhyolite-granite.

It is not usual to speak of a calc-alkaline basalt or gabbro as a distinct type. They are generally of the high alumina basalt type of Kuno (1960) and include occurrences such as New Zealand (Clark 1960) and the Cascades (Powers 1932). Commonly quoted examples of the basic members of the calc-alkaline association are the hornblende gabbro of the Hebridean Islands (the "Central Type" gabbro) and the "Central" basalt (Nockolds 1954).

The diorites can be subdivided in a similar manner to the andesites in that the normal types extend over the silica range from 55-62% SiO_2. With silica contents less than 55%, the diorites tend towards the gabbros, and at the other extreme, to the tonalites or granodiorites. In this SiO_2 range, however, we may have pyroxene-mica diorites, quartz

(mica) diorites, and orthoclase diorites. The calc-alkaline andesites have a much simpler classification, and lacking the minerals such as biotite, quartz and orthoclase (see following section), they are generally grouped together as "andesites", although some distinction such as "basaltic" or "basic" andesite is often made.

Tonalites are as much a problem as the other members of the calc-alkaline association. From a survey of the literature, tonalites appear to be more abundant than diorites in some provinces and invariably display evidence of mixing of two rock types. Although tonalites exhibit a range in composition, they are more closely related to granodiorites or granites (e.g. see Nockolds 1954; p.1015, Table 2) except for their lower potassium contents. There are no tonalites at Yeoval.

Granites (and rhyolites) are generally considered to be the most acid members of the calc-alkaline association. Recent work on the New Zealand calc-alkali province (Rotorua-Taupo region) by Ewart and Stipp (1967) suggests that the rhyolites and ash flow tuffs are not genetically related to the basalts and andesites. A limited examination of the Yeoval granites indicates that they are not genetically related to the diorites. Although the origin of granites is not considered in detail in this thesis,

the formation of the Yeoval granites by partial melting of basic or intermediate material is preferred.

1.1.2 Volume Relationships

Tilley (1950) and others have used volume relationships of the volcanic associations as evidence against fractional crystallisation and mixing of certain rock types for the formation of the calc-alkaline rocks. As is the case for the volcanic rocks, the coarse-grained calc-alkaline types do not follow any pattern with respect to the apparent volume and presence or absence of the respective members. For example, in the Southern California Batholith (Larsen 1948), gabbros constitute approximately 14%, tonalites 50%, granodiorites 34% and granites 2½% of the Batholith; while in the Garabal Hill Glen-Fyne Complex (Nockolds 1941) the gabbros and dioritic types make up less than 10%, and the granodiorites, the remainder. In other areas, such as the Snowy Mountains N.S.W. (Joplin 1958), Bigga (Hasan 1959) and Yeoval districts of Eastern Australia, granites are the dominant rock type.

It should be made clear, however, that these volumes are only approximate and may not give any indication as to the actual volume relationships at depth.

1.1.3. Field Relationships

Diorites and related types are very common as stock-like bodies occurring as minor intrusions about large

granitic batholiths, and are usually considered to be earlier than the granite intrusions. Normally, they invade the country rocks very close to the margin of the batholith, or they may occur just within them. A common associate of the dioritic rocks, usually considered to be an accumulate, is a hornblende- or pyroxene-rich phase. Examples of this include: Arrochar (Anderson 1935), Ben Bullen (Joplin 1937), Glen Falloch (Anderson 1937), Rhodesia (Deans 1938), Garabal Hill (Nockolds 1941), Glen Tilt (Deer 1950), Jersey (Wells and Bishop 1955), Snowy Mountains (Joplin 1958), Bigga (Hasan 1959) and Yeoval (this work).

1.1.4. Mineralogy

Mineralogical and petrographic descriptions of the volcanic and plutonic calc-alkaline rocks are well documented (e.g. Larsen 1948; Nockolds 1941; Williams 1932, 1935; Larsen 1936, 1937, 1938; Ewart 1963, 1965), and so only characteristic features of the diorites will be given in this introductory summary.

(i) In most dioritic rocks, the dominant ferromagnesian mineral is hornblende and it occurs along with pyroxene and biotite (the latter being common in the potassium-rich types and even in very small amounts in the low potassium types.) In the andesites the most commonly reported mineral is pyroxene.

(ii) Quartz is invariably present in varying amounts in diorites but is rarely found in andesites where it is often suggested to be of xenocrystal origin. However, to account for the normative composition of about 10-16% quartz which was the average range for 1,526 Cenozoic volcanics called andesites (Chayes 1964-65), the silica must be present in the groundmass as tridymite, cristobalite or glass.

(iii) Potassium feldspar is present in the high potassium diorites as a late-formed, interstitial phase. In the high potassium andesites, the potassium occurs in the glass. Crystallization of this forms potassium feldspar-silica mineral intergrowths.

1.1.5. Chemistry

The most marked feature of the chemistry of the calc-alkaline association may be seen on a triangular plot of total iron (as FeO), MgO and alkalis (Na_2O, K_2O) of the rocks (the FMA diagram of Poldervaart 1949). Here the calc-alkaline rocks fall in an almost straight band extending from the FeO-MgO side to the alkali apex (Fig.3). There is little or no iron enrichment relative to magnesium. This contrasts with the typical tholeiitic fractionation trend which shows marked iron enrichment in the early and middle stages (e.g. Skaergaard trend in Fig.3). The band is most pronounced for compositions ranging from pyroxene-mica diorite (or

basaltic andesite) to granite (or rhyolite).

There is a broadening of the band at basic compositions and a slight convexity towards the iron apex indicating some iron enrichment relative to magnesium for the basic members of the association. The increased scatter of points at the basic end, particularly for the coarse-grained rocks, may be due to analyses of accumulates.

The basaltic to andesitic members of the volcanic calc-alkaline association often show high alumina contents. They average about 17% Al_2O_3 but range up to approximately 22% as in the Medicine Lake Highlands (Powers 1932). The more basic members of the coarse-grained association (gabbros) have Al_2O_3 contents ranging from 17 to 21%, whereas the reported analyses of dioritic rocks have a lower range (15-17%) although some do extend to about 21%.

1.1.6. High potassium diorites and andesites

In recent years, there has been an awareness of the existence of high potassium andesites, in addition to low, or normal varieties (Dickinson and Hatherton 1967; Green 1967; Taylor, pers. comm.; Joplin, pers. comm.) although the same variations may be observed in diorites. These high potassium rocks have not been adequately defined.

The absence of a definition or an awareness of high potassium varieties is apparent from the average analyses of a number of authors. In his compilation of an average

andesite and quartz diorite, Daly (1933) listed a common value of 2.1% K_2O which included a number of high potassium rocks. In contrast, Nockolds (1954) quoted average contents of 1.33% K_2O for diorites and 1.11% K_2O for andesites, and more recently, Taylor (1967) listed 1.60% K_2O as the average value for andesites.

To clarify the nomenclature of these rock types, it is proposed that a diorite or andesite with a K_2O/SiO_2 ratio greater than 0.034 be classified as a high potassium variety, and those with a ratio less than 0.034 be considered as low potassium or normal andesites and diorites. This ratio is based on a K_2O content of 2.0% and SiO_2 value of 59.5%, the silica being that quoted for the average andesite by Taylor (1967).

The high potassium figures for diorites (such as the Yeoval rocks described in this thesis) do not affect their other properties greatly when compared with the normal types. Important mineralogical changes are the crystallisation of potassium feldspar and slightly greater quantities of biotite. The major element chemistry is essentially the same, except for the higher potassium content. Intimately related to the high potassium are the abundances of trace elements such as Rb, Ba, U and Th. Other high potassium diorites reported

include those from the Snowy Mountains (Joplin 1958) and Bigga (Hasan 1959).

High potassium andesites have also been grossly neglected. Recent data, particularly of trace elements, is meagre. What little data are available for a number of localities, including New Zealand (Ewart and Stipp 1967), Solomon Islands and Fiji (Taylor and Blake, in preparation) indicate a close correlation with high potassium diorites (see Table 48).

Thus, from the little data available so far, there is apparently a transition from very low (e.g. 0.7% K_2O) to high potassium (3.0% K_2O) diorites and andesites, with the possible inclusion of the orthoclase diorites which have K_2O contents of about 4%. This possibility is also suggested by recent observations of Dickinson and Hatherton (1967) who obtained a positive correlation of K_2O content with vertical depth to the Benioff zone for Circum-Pacific andesites.

1.1.7. Origin of dioritic magma

The problem of the origin of dioritic (and andesitic) magmas is treated fully in a later section but it will be sufficient at this stage to point out that there are three main theories of origin:

(1) Fractional crystallisation of basaltic magma

(2) Mixing of basic and acidic rock types

(3) "Primary" dioritic magma derived from the mantle or deep crust.

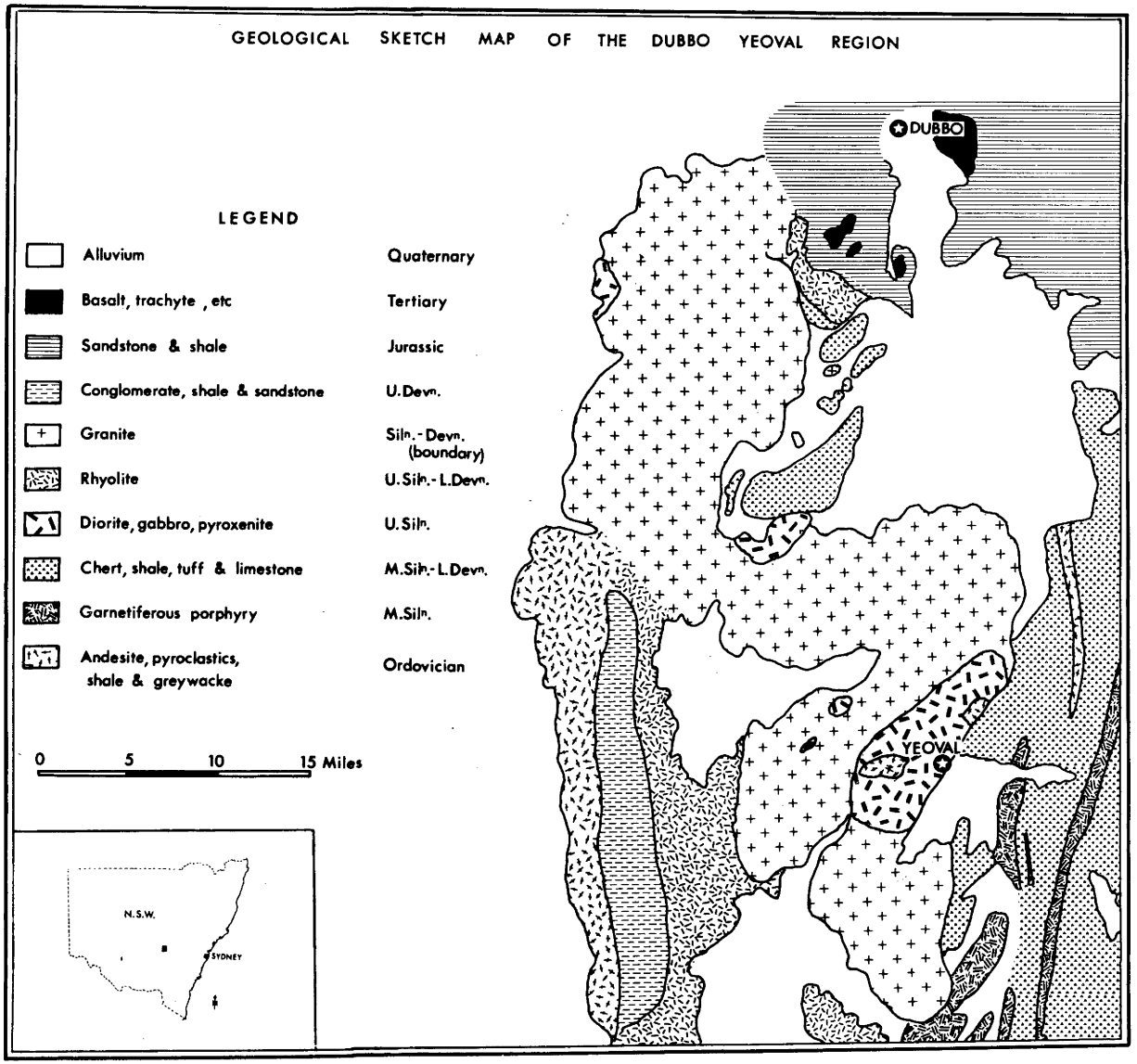
GEOLOGICAL SKETCH MAP OF THE DUBBO YEOVAL REGION
LEGEND
Alluvium
Quaternary
Basalt, trachyte , etc
Tertiary
Sandstone & shale
Jurassic
Conglomerate, shale & sandstone
U.Devn.
Granite
Siln.- Devn. (boundary)
Rhyolite
U.Siln.- L.Devn.
Diorite, gabbro, pyroxenite
U.Siln.
Chert, shale, tuff & limestone
M.Siln.- L.Devn.
Garnetiferous porphyry
M.Siln.
Andesite, pyroclastics, shale & greywacke
Ordovician
0 5 10 15 Miles
DUBBO
YEOVAL
N.S.W.
SYDNEY

Map 1

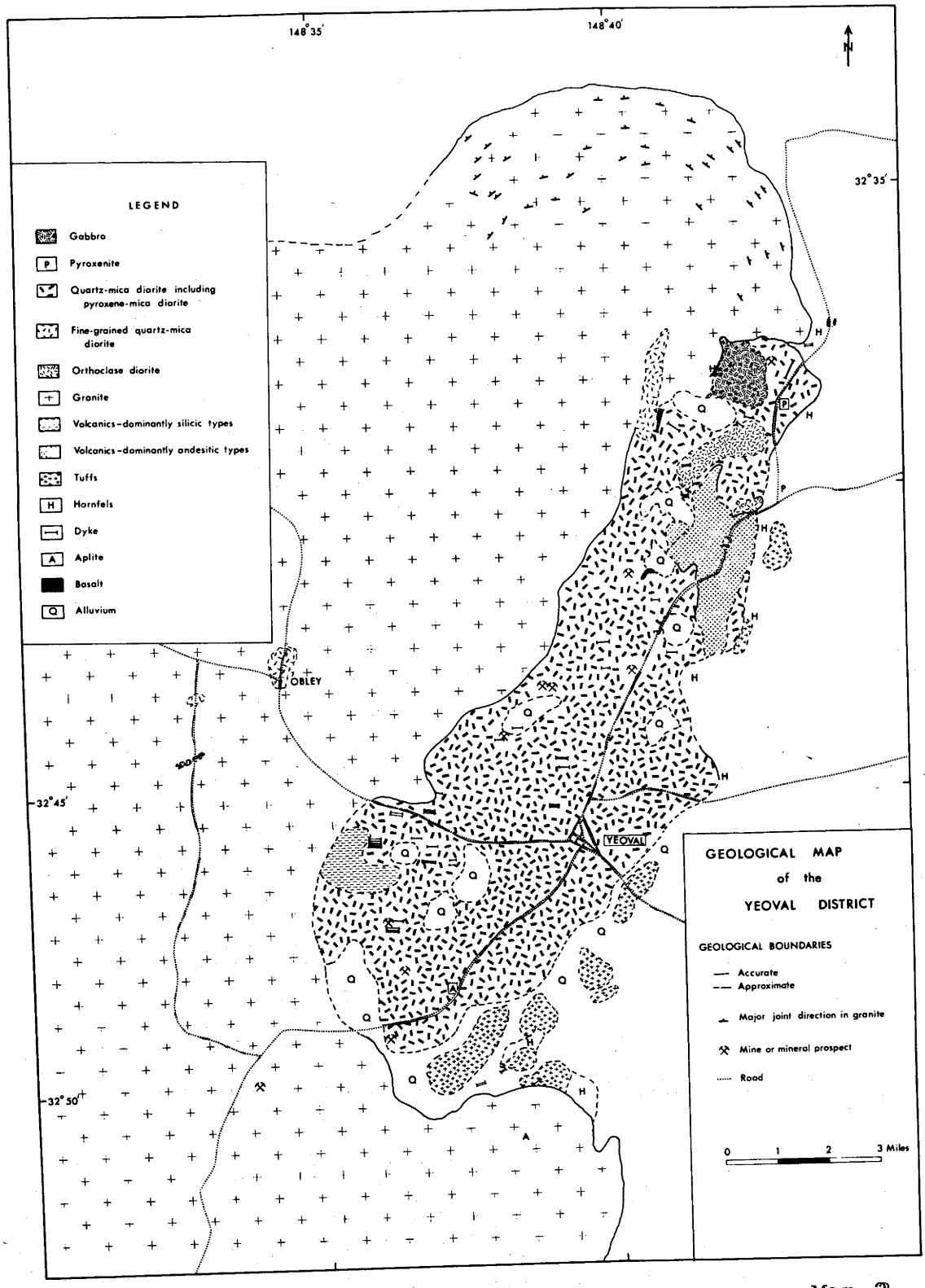
148°35'
148°40'
32°35'
32°45'
32°50'
N
LEGEND
Gabbro
Pyroxenite
Quartz-mica diorite including pyroxene-mica diorite
Fine-grained quartz-mica diorite
Orthoclase diorite
Granite
Volcanics-dominantly silicic types
Volcanics-dominantly andesitic types
Tuffs
Hornfels
Dyke
Aplite
Basalt
Alluvium
OBLEY
YEOVAL
GEOLOGICAL MAP
of the
YEOVAL DISTRICT
GEOLOGICAL BOUNDARIES
Accurate
Approximate
Major joint direction in granite
Mine or mineral prospect
Road
0 1 2 3 Miles

Map 2

THE DIORITES OF THE YEOVAL IGNEOUS COMPLEX

2. GEOLOGICAL SETTING AND FIELD RELATIONSHIPS

2.1. DISTRIBUTION OF ROCK TYPES

The Yeoval Batholith is a complex of igneous rocks, dominantly acid in composition-granites, adamellites and minor granodiorite - with smaller areas of intermediate, basic and ultrabasic types - diorites, gabbros and pyroxenites. Associated with these are a variety of fine-grained rocks, ranging in composition from basic to acid.

The batholith covers approximately 1,200 square miles, although Maggs (1963) has suggested that other granitic bodies to the south are related to the main mass. This would extend the area to some 6,000 square miles.

Map 1 outlines the distribution of the major rock types comprising the complex and it may be seen that, except for the area around the township of Yeoval, the intermediate to ultrabasic rocks occupy a minor area (less than 10% of the complex).

Most of the rock types listed above occur in the Yeoval district (Map 2). Here the dioritic types outcrop over an area of approximately 90 square miles with the granitic rocks enveloping the diorite on three sides. The estimated area of the diorites is very conservative because information obtained from wells sunk for water indicates that diorite exterds for some three miles to the east under the sedimentary cover.

The volcanics occur in three belts, one about 7 miles north, another to the west and the other about 4 miles south of the township of Yeoval. The northern and southern belts consist mainly of intermediate to basic types whereas the western one is dominantly acidic. Field relationships of the acid belt are not clear and in places they seem to be related to the later acid (and basic dykes) which cut the diorite. However they are pre-granite since the granite has contact metamorphosed certain of these volcanic rocks.

2.2. INTRUSIVE RELATIONSHIPS

Relationships of the different rock types in the Yeoval district are not clear. No actual contact between the granite and diorite, granite and gabbro, or gabbro and diorite was observed in the field. However, the following sequence was obtained from field and petrographic evidence:-

1. Andesites (2 square miles) and possibly acid volcanics (1 square mile)
2. (Pyroxenite (30 square yards)
   (Gabbro (1 square mile)
3. Diorite (90 square miles)
4. Granite
5. Dyke Rocks

Evidence for these relationships:

(i) At one locality the diorite was observed to intrude andesites, which were traversed by aplite veins and which were subsequently cut by a basalt dyke.

(ii) Gabbro and diorite - A complete gradation to the north and east exists between these rocks, evidenced in a trend from basic to less basic chemistry, and of increasing amounts of quartz, biotite and finally potassium feldspar. A plot of quartz, feldspars and mafic minerals (Fig.1) clearly brings out this transition.

(iii) Gabbro and granite - Indications from the contact metamorphism of the gabbro (pyroxenes → uralite) and the presence of fine aplitic veins in the gabbro, suggest that the gabbro predated the granite.

(iv) Diorite and pyroxenite - The pyroxenite is entirely surrounded by diorite and a complete gradation exists between the two end members.

(v) Diorite and granite - A number of features support the premise of the intrusion of the diorite by granite.

(a) presence of granite pegmatite consisting of potassium feldspar and quartz intergrowths in the basic diorite

(b) a seven-feet wide quartz-feldspar porphyry dyke extending almost continuously from the granite into the basic diorite.

(c) fine-grained phase of granite (chilled margin) extending down the western contact in a band up to 300 feet wide.

Plate 1 Illustrating the incorporation of blocks of fine-grained diorite and andesite by the granite.

(d) aplite veins cutting diorite and much epidotisation of diorite near the margins at some localities.

(e) fine-grained quartz-mica diorite intruded by granite with incorporation of angular to sub-rounded blocks up to 3 feet wide of diorite in the granite (Plate 1).

(vi) Dioritic types - No contacts were observed between the variations within the main diorite mass, and except for the orthoclase-rich types, it is impossible to subdivide them further. Although no contact was visible between the orthoclase-rich and other types it is of interest to note that the orthoclase diorites tend to occur only in the northern area.

(vii) Tuffs and other rock types - the tuffs are separated by alluvium from all rock types except the andesitic lavas, with which they are intimately associated.

(viii) 'Dyke' rocks - are apparently much later than any of the other rock types and were probably intruded along joints in the granites and diorites.

Occurring in isolated patches are small showings of various ore minerals, usually as sulphides. The late 1890s and early 1900s witnessed some production from the Goodrich Mine (gold and later, copper) and gold at Obley.

2.3. XENOLITHS

Xenoliths are not common in any of the rock types except for the example cited above of the fine-grained diorite and granite. No increase in abundance of xenoliths was observed near the contacts of any members of the complex. The few present in the diorite and granite appear mainly to be of sedimentary or volcanic material which has now been reconstituted, either partly or completely, to a mineralogy comparable with that of the host rock. A number of rounded xenoliths of andesitic rocks were observed in the diorite near the contact.

2.4. COUNTRY ROCKS AND CONTACT EFFECTS

Packham (1960) suggested that the Lachlan Geosyncline of New South Wales be divided into four tectonic components, the western subdivision being the Cowra Trough. It is into this trough that the rocks of the Yeoval Complex have been intruded. Rocks in the trough include greywackes, shales, siltstones, tuffs, sandstones, limestones and a variety of volcanics. The effect of the intrusion of the complex into these is varied. For example, in the Yeoval district, metamorphism of the siltstones by the diorite is of hornblende hornfels facies. Near the contact of the gabbro and granite, a lens of calcium-silicate skarn rock has been produced.

2.5. STRUCTURE

The almost north-south trend of the batholith, as a whole, roughly parallels the regional structure. However, owing to their paucity of outcrop, little can be said of the concordance (or discordance) of the sediments surrounding the batholith. From the meagre data available, the north-south trending boundaries (as distinct from the east-west) of the batholith are concordant with the sediments.

Foliation has not been observed over most of the batholith although, to the west near the Harvey Syncline, mylonites are well developed (Hobbs, pers. comm.).

A major structure to the north of Yeoval is present in the granite and extends into the diorite. In the granite, this is of a circular nature, and is due to a complex joint pattern. Field observations show no evidence of flow banding or multiple injection. This is apparently a post consolidation effect caused by orogenic movement around 370 million years ago, which may be related to the Tabberaberran orogeny of Middle Devonian age (see section on Sr Isotope Chemistry).

Jointing is not well developed in the dioritic types but is fairly consistent in the granites throughout the batholith (except for the circular structure described above). Thus Ringis (1962), Emerson (1962), Frenda (1961), and Steggles

(1962) measured two well developed joint directions over a substantial area of the batholith. Both are vertical (or near vertical); one trending from 0-5° west of north and the other 0-5° north of east. A minor horizontal joint system is also developed in some areas.

The major joint system is considered to be tensional in origin. Snelling (1960) maintained that the E-W joints of the Murrumbidgee Batholith are due to tensional stresses induced in the rock by a major E-W compressive stress, while the N-S joints are tensional joints resulting from the elastic expansion of the rock after the E-W compression had ceased. This hypothesis is supported by the frequent occurrence of acid and basic dykes parallel to these joints (see also Map 2).

3. PETROGRAPHY AND CHEMISTRY OF MAJOR ROCK TYPES

3.1. GABBROS AND PYROXENITES

3.1.1. Gabbros

The gabbros are almost black in colour and show an apparent variation from coarse- (up to 1 cm. long plagioclases) to medium- to fine-grained types. They consist dominantly of plagioclase and pyroxene with or without minor amounts of olivine, amphibole, biotite, opaques, quartz, apatite, spinel and tourmaline. The coarse grain size observed in hand-specimen is not apparent in thin section as the large clear areas are an intergrowth of plagioclase prisms.

Brief notes on the various minerals follow; optical and chemical data on selected minerals are given in a subsequent section.

Plagioclase: occupies from 50-70% of the rock, usually as unzoned simply twinned prisms (An_{80-85}) averaging 3-4 mms in length. A sub-parallel arrangement of crystals is present in restricted areas.

Pyroxene: both clinopyroxene and hypersthene occur, with hypersthene varying from 30 to 70% of the total pyroxene. Pyroxenes may either occur as single anhedral grains or as aggregates of grains (often accompanied by olivine and opaques) up to 4-5 mms across while individual grains average 2-3 mms and do not exceed 4 mms across.

Clinopyroxene is invariably twinned and both pyroxenes exhibit schiller structure. Occasionally, clinopyroxene in contact with plagioclase shows a reaction rim of fibrous amphibole and hypersthene.

Amphibole: is present in two main forms in the gabbro. The minor occurrence is as rims or grains (up to 0.4 mms across) around pyroxene. This amphibole is pleochroic from green to pale yellow brown and is probably "primary" hornblende. Most of the amphibole is a fibrous variety, commonly termed "uralite", and apparently the alteration product of pyroxene. It is pleochroic pale blue-green to colourless and is usually accompanied by fine-grained opaque minerals. The uralite veins, rims, and partially or completely replaces the pyroxene. Occasionally, veinlets of amphibole (up to 0.2 mms wide) extend out from the uralitised pyroxene into the plagioclase crystals.

Olivine: although not present in most specimens, may amount to 8% in others. It occurs in aggregates - often vein-like - consisting of 2 to 5 grains. These aggregates are in turn veined by fine-grained magnetite, a green serpentine mineral and lizardite. Irregular reaction rims with plagioclase are common, the following sequence often being developed along the rim:

$$\text{olivine} \longrightarrow \text{orthopyroxene} \overset{+}{-} \text{clinopyroxene} \longrightarrow$$

$$\text{amphibole} + \text{spinel} \longrightarrow \text{biotite}$$

The biotite formed in the rim is a very pale fawn colour and differs markedly from the deep red-brown biotite associated with the opaque minerals.

Opaque minerals: occur in three distinct habits. The first is as discrete grains or aggregates of grains which consist dominantly of magnetite and a little ilmenite and chalcopyrite. The magnetite usually contains oriented lamellae of ilmenite and/or octahedral intergrowths of ulvospinel(?). The degree of alteration of magnetite to hematite is limited. The other opaque minerals appear to be secondary products associated with the breakdown of pyroxene to uralite. Here the magnetite may assume unusual skeletal intergrowths with pyroxene and plagioclase; both these minerals often being included and veined by the magnetite. The magnetite may also occur as orientated or random blebs in the altered pyroxene.

3.1.2. Pyroxenite

The pyroxenite is a very dark green colour with pyroxene crystals ranging up to 2 cms. Small interstitial patches (up to 2 mm across) of feldspar are scattered throughout the rock.

In thin section, the intimate association of clinopyroxene and amphibole is most evident; they constitute up to 80% of the rock. Coarse crystals of clinopyroxene

have undergone varying degrees of alteration to uralite and fine-grained opaque minerals. The rim alteration is most marked although this usually spreads sporadically throughout the crystals giving them a "mottled" appearance. This pale blue-green amphibole is fibrous, in contrast to the mosaics of well crystallised olive-green amphibole which are interstitial to the clinopyroxene crystals. Well developed twinning and incipient zoning are present in the clinopyroxene crystals.

Prismatic to anhedral crystals of plagioclase are commonly veined by blue-green amphibole. Alteration to clay minerals and white mica is fairly extensive. The plagioclase is not zoned and has a composition of approximately An_{50}.

Moderately pleochroic orthopyroxene occurs as aggregates of anhedral grains in association with altered olivine. Biotite is associated with either amphibole, opaque minerals or orthopyroxene. When apparently replacing orthopyroxene, the biotite is a pale olive-green variety.

Modal analyses of the gabbro and pyroxenite are given in Table 2.

3.1.3. Chemistry

The rocks were analysed by the following techniques:

Si, Al, total iron as Fe^{3+}, Ti, Mn, Mg, Ca and K - x-ray fluorescence spectrography (Norrish and Chappell, 1966; Chappell 1966)

TABLE 1

Chemical Analyses and CIPW Norms of Gabbros and Pyroxenites from the Yeoval District

	Gabbros			Pyroxenites		
	W71	W3	W53	W61	G153	W60
SiO_2	43.66	45.83	47.09	47.68	47.91	50.17
TiO_2	0.54	0.22	0.45	0.31	0.42	0.55
Al_2O_3	17.18	17.62	17.40	8.54	9.36	13.43
Fe_2O_3	0.05	1.69	0.26	1.02	n.d.	n.d.
FeO	10.34	6.69	8.67	9.60	9.16	9.47
MnO	0.22	0.14	0.24	0.30	0.23	0.26
MgO	8.75	10.86	7.90	14.27	13.91	7.92
CaO	16.06	15.36	13.10	14.23	14.83	11.22
Na_2O	0.82	0.76	1.30	0.68	0.57	2.08
K_2O	0.07	0.06	0.16	0.46	0.48	0.60
P_2O_5	0.002	0.007	0.003	0.006	0.054	0.095
H_2O^+	0.70	0.91	0.95	1.75	2.16	1.88
H_2O^-	0.12	0.09	0.11	0.15	0.18	0.14
CO_2	0.09	Nil	0.04	0.11	0.08	0.04
	98.60	100.23	97.67	99.11	99.34	97.85
Q	-	-	-	-	-	-
Or	0.41	0.35	0.95	2.72	2.84	3.55
Ab	1.76	6.43	11.00	5.75	4.82	17.60
An	42.99	44.49	41.17	18.89	21.56	25.54
Ne	2.81	-	-	-	-	-
Di	29.72	25.47	19.34	41.19	41.41	24.16
Hy	-	4.14	15.30	10.24	9.83	20.55
Ol	18.79	15.46	7.53	16.08	15.45	3.11
Mt	0.07	2.45	0.38	1.48	-	-
Il	1.03	0.42	0.85	0.59	0.80	1.04
Ap	-	0.02	-	0.02	0.11	0.20
Cc	0.20	-	0.09	0.25	0.18	0.09
Z	-	-	-	-	-	-
Plag. An	96.08	87.37	78.91	76.65	81.72	59.20

(n.d.=not determined)

Fe^{2+} and total iron as Fe^{3+}	- potentiometry and chelometry (Kiss 1967)
Na and K	- flame photometry (Cooper 1963)
P	- spectrophotometry (Riley 1958)
H_2O^+ and CO_2	- heating the sample in a platinum tube furnace at 1150°C for thirty minutes in a stream of dry argon
H_2O	- weight loss after heating the sample for two hours at 110°C.

Some samples were analysed for a number of elements using, in addition to the above techniques, electron probe analyses on fused rock samples (see Appendix III). Some Al determinations were checked by E. Kiss using wet chemical techniques (Kiss 1967).

Table 1 gives the major element analyses of three gabbros, two pyroxenites and a transition rock. The latter will be discussed in the next section. The main features to be noted in the chemistry of the gabbros are their relatively low SiO_2, very high CaO compared with "Central Type Gabbros" (Nockolds 1954) and low alkalis, particularly

potassium. The pyroxenite is characterised by low Al_2O_3 and alkalis, along with high MgO and CaO.

3.2. DIORITES

Apart from a fine-grained quartz diorite body which is thought to be unrelated to the main diorite mass and is briefly discussed at the end of this section, the diorites may be subdivided into three main groups:

(i) Pyroxene-mica diorites

(ii) Quartz-mica diorites

(iii) Orthoclase diorites

This subdivision is not rigid as transitions exist between the various types and also the pyroxene-mica diorite and the gabbro.

The name "pyroxene-mica diorite" is used here to conveniently distinguish this rock type from the quartz-mica and orthoclase diorites and also the gabbro. In comparison with the pyroxene-mica diorites of Nockolds (1941), the Yeoval variety has substantially lower amounts of pyroxene (3-5% modal pyroxene compared with 25% in Garabal Hill) and no olivine and more quartz (up to 10-12% modal compared with 3%). The chemistry of the Yeoval pyroxene-mica diorite only vaguely resembles Nockolds' (1954) average pyroxene-mica diorite but is very similar to his hornblende biotite diorite (see Table 12, this thesis).

TABLE 2

Micrometric Analyses of Yeoval Rocks

GABBROS

	Qtz.	Plag.	Hbl.	Biot.	Cpx°	Opx	Ol.	Acc.+	K-F	Colour Index
W71	-	58.6	-	-	28.3	1.4	8.4	3.3	-	41.4
W6	-	44.0	-	-	28.2	25.0	-	2.8	-	56.0
W3	-	60.6	-	-	26.7	9.8	trace	2.9	-	39.4
W53	-	63.2	-	-	14.3	21.4	-	1.1	-	36.8
W9	-	65.0	-	-	11.8	20.0	-	3.2	-	35.0
W42	2.1	59.1	-	1.1	36.0	-	-	1.7	-	38.8
Y190	5.5	61.0	3.3	1.8	26.5	-	-	1.9	-	33.5
W65	5.0	60.5	5.0	5.4	22.3	-	-	1.8	-	34.5
W50	7.5	59.6	12.2	5.6	13.8	-	-	1.3	-	32.9
W18	9.0	70.2	0.9	5.4	12.4	-	-	2.1	-	20.8
G66	12.6	56.2	5.4	5.4	14.4	-	-	1.8	4.2	27.0

PYROXENE-MICA DIORITES

	Qtz.	Plag.	Hbl.	Biot.	Cpx°	Opx	Ol.	Acc.+	K-F	Colour Index
Y8	9.6	60.2	19.6	6.6	2.7	-	-	1.3	trace	30.2
G71	12.0	59.9	20.6	4.0	2.4	-	-	1.1	trace	28.1

TABLE 2 (continued)

Micrometric Analyses of Yeoval Rocks

QUARTZ-MICA DIORITES

	Qtz.	Plag.	K-F	Hbl.	Biot.	Acc.*	Colour Index
Y12	23.5	54.0	7.2	8.5	6.0	0.8	15.3
Y14	25.5	43.6	15.0	15.7	0.1	0.1	15.9
Y67	23.5	52.5	8.2	10.4	4.4	1.0	15.8
Y69	23.3	50.0	8.5	13.6	4.1	0.5	18.2
Y71	23.3	48.8	11.2	13.4	2.8	0.5	16.7
Y149	22.4	49.5	10.2	12.4	4.9	0.5	17.8
Y151	25.8	52.9	13.5	5.1	1.8	0.9	7.8
Y195	23.4	56.2	6.3	13.1	0.3	0.7	14.1
G84	23.3	50.5	9.4	9.5	6.6	0.7	16.8
G88	24.3	45.5	12.3	10.6	6.6	0.7	17.9
G91	21.6	52.2	9.7	12.6	3.2	0.7	16.5
G99	24.5	51.9	13.6	6.0	3.4	0.6	10.0
G110	21.9	53.5	10.2	9.2	3.9	1.3	14.4
G72	20.7	46.4	15.6	13.0	3.7	0.6	17.3
G98	20.7	53.8	8.7	11.6	4.1	1.1	16.8
G92	20.0	54.5	8.2	11.1	5.3	0.9	17.3
G90	19.4	54.3	5.6	17.5	2.4	0.8	20.7
Y235	18.5	51.2	14.6	9.5	5.6	0.6	15.7
G96	18.1	53.2	7.6	10.6	9.3	1.2	21.1

TABLE 2 (continued)

Micrometric Analyses of Yeoval Rocks

QUARTZ-MICA DIORITES

	Qtz.	Plag.	K-F	Hbl.	Biot.	Acc.*	Colour Index
Y148	19.2	57.6	2.8	12.0	7.0	1.4	20.4
Y158	16.3	47.0	20.0	14.0	1.8	0.9	16.7
Y227	17.0	52.4	6.1	14.3	9.6	0.7	24.6
G107	16.5	49.5	11.7	14.4	6.5	1.4	22.3
Y245	15.3	51.7	9.4	17.8	5.4	0.4	23.6
G41	15.9	46.8	12.2	19.5	3.3	2.4	25.2
Y161	15.1	52.4	8.1	17.8	5.4	1.2	24.2
Y16	14.9	54.1	11.4	13.3	5.7	0.6	19.6
Y150	14.2	49.4	9.2	16.9	8.3	2.0	17.2
G73	14.6	59.4	6.7	17.6	0.8	0.9	19.3
G101	14.1	49.2	9.2	20.3	5.1	2.1	27.5
Y208	14.3	49.3	14.3	18.7	3.0	0.4	22.1
Y225	14.0	49.0	15.6	14.3	6.2	0.9	21.4
Y147	12.4	58.4	9.1	15.3	1.9	1.9	19.1
G86	12.9	50.5	15.8	15.2	4.4	1.2	20.8
G102	12.0	53.6	12.0	16.2	5.4	0.8	22.4
G105	13.4	52.9	7.4	18.9	5.9	1.5	26.3
Y40	12.0	55.4	9.0	15.9	5.6	2.1	23.6
Y75	12.4	53.6	7.8	20.5	3.9	1.8	26.2

TABLE 2 (continued)

Micrometric Analyses of Yeoval Rocks

QUARTZ-MICA DIORITES

	Qtz.	Plag.	K-F	Hbl.	Biot.	Acc.*	Colour Index
G55	9.8	57.5	13.9	15.2	1.3	2.3	18.8
G106	9.0	52.6	15.0	20.0	2.4	1.0	23.4
G35	8.6	58.2	8.3	23.0	0.7	1.2	24.9
G80	6.4	59.6	14.7	13.8	4.1	1.4	19.3

ORTHOCLASE DIORITE

	Qtz.	Plag..	K-F	Hbl.	Biot.	Acc.*	Colour Index
G57	20.1	32.2	42.3	2.6	1.6	1.2	4.4

GRANITES

	Qtz.	Plag.	K-F	Hbl.	Biot.	Acc.‡	Colour Index
Y64	41.0	-	55.9	2.1	0.8	0.2	3.1
Y53	34.1	25.9	35.7	0.9	2.7	0.7	4.3
Y147B	34.1	27.9	34.5	0.2	2.3	1.0	3.5
R69	7.8	14.4	77.8	trace	trace	trace	

TABLE 2

Micrometric Analyses of Yeoval Rocks

o Includes uralite

\+ Includes opaque minerals, apatite, zircon, spinel, lizardite

* Includes opaque minerals, apatite, zircon, epidote, tourmaline, sphene

‡ Includes opaque minerals, apatite, zircon, epidote, fluorite, rutile

All analyses were performed on a swift point counter, for 2,000 points

All thin sections were stained for differentiation of the feldspars

The analyses were duplicated using stained slabs of rock (mafic minerals are grouped together)

Samples underlined have been chemically analysed

The quartz-mica diorites are most common. These are medium-grained, light and dark speckled rocks which exhibit a marked variation in the colour index (Table 2). The grain size is fairly consistent (average 2-4 mms) although, occasionally, biotite flakes may range up to 8 mms across. Plagioclase is white or pale green and twinning and zoning can be observed. Potassium feldspar is usually difficult to distinguish from plagioclase and quartz except in samples where alteration produces a pink colouration. The pyroxene-mica diorites may be distinguished from the quartz-mica diorites by their much darker colour and lower quartz content and the orthoclase diorites from the quartz-mica diorites by their dominance of pink potassium feldspar.

3.2.1. Petrography

The quartz-mica diorite consists mainly of a granular intergrowth of plagioclase, hornblende, biotite, potassium feldspar, quartz and accessories.

Plagioclase: occupies up to 65% of the rock but averages 55%. Crystals are usually subhedral, commonly twinned and of a fairly even grain size. Zoning is ubiquitous and may be of the "patchy", normal, oscillatory or reverse types. The degree of alteration is extremely varied both between specimens and within the one specimen. Common alteration products are clay minerals and white mica, although epidote and carbonate are sometimes present.

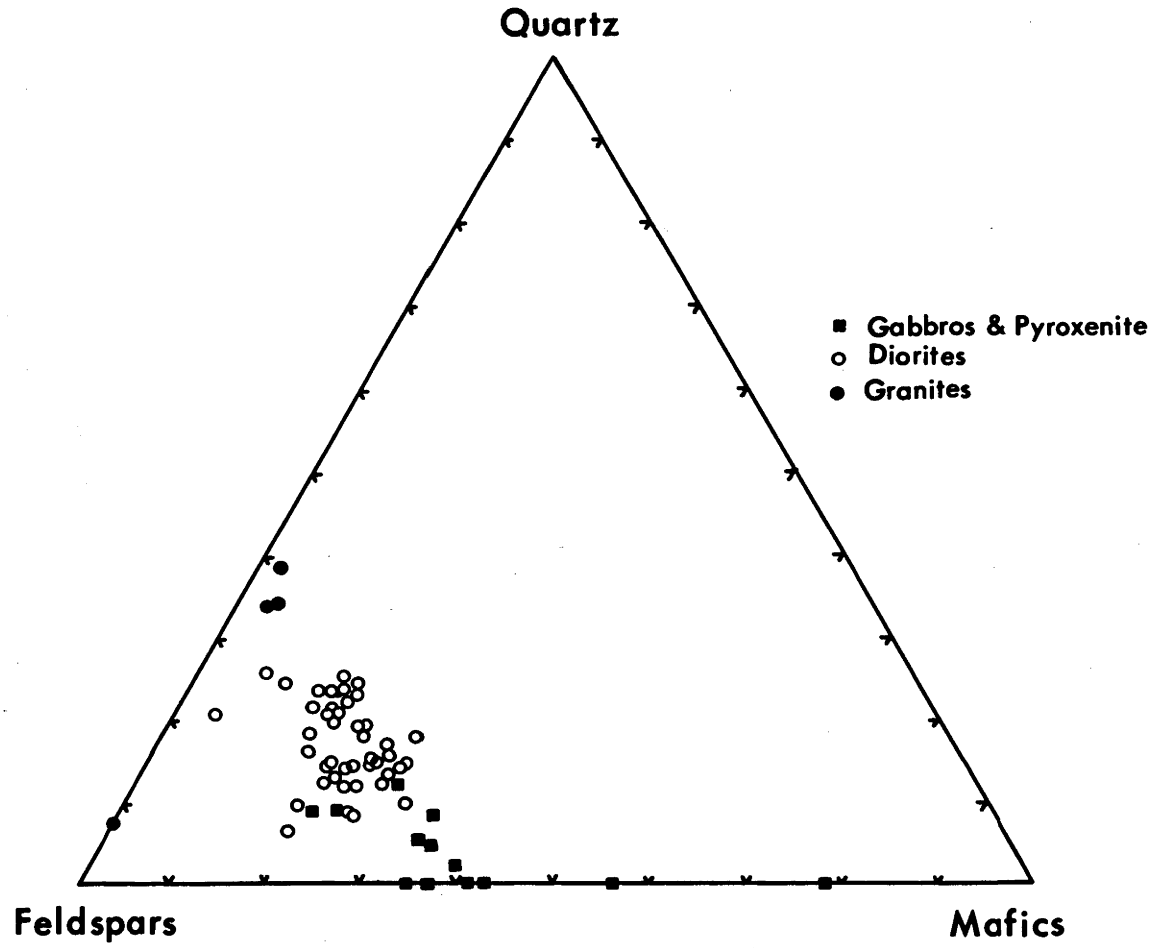

Fig.1 Quartz-Feldspar-Mafics relationships in the Yeoval Rocks.

Hornblende: forms either as euhedral single crystals or crystal aggregates. Simple and/or multiple twinning is common. Apatite, zircon and opaques are often included in the hornblende. Clinopyroxene, when present, occurs as cores or relict patches in the hornblende, but it is usually pseudomorphed by fibrous uralite.

Biotite: may form separate or aggregates of grains but is more commonly intergrown with hornblende. Pleochroism is strong.

$\beta = \gamma$ = red brown >> α = straw yellow.

Wedges of prehnite (?), apatite, zircon and opaques may be present in the biotites. Alteration to chlorite, epidote and iron oxides varies from one specimen to another.

Potassium feldspar: may amount to 20% of the rock. When abundant, it usually forms plates including plagioclase crystals; when in smaller quantities it tends to be interstitial. Incipient development of "string" perthite and microcline twinning is present in some grains, but no significant departure from "zero" triclinicity was observed (see Section 4.6).

Quartz: may amount to 25% but more commonly ranges from 12-15%. It apparently follows potassium feldspar to a certain extent in that it occurs as interstitial "wedges" when present in smaller amounts (<15%) and as irregular grains if in larger quantities.

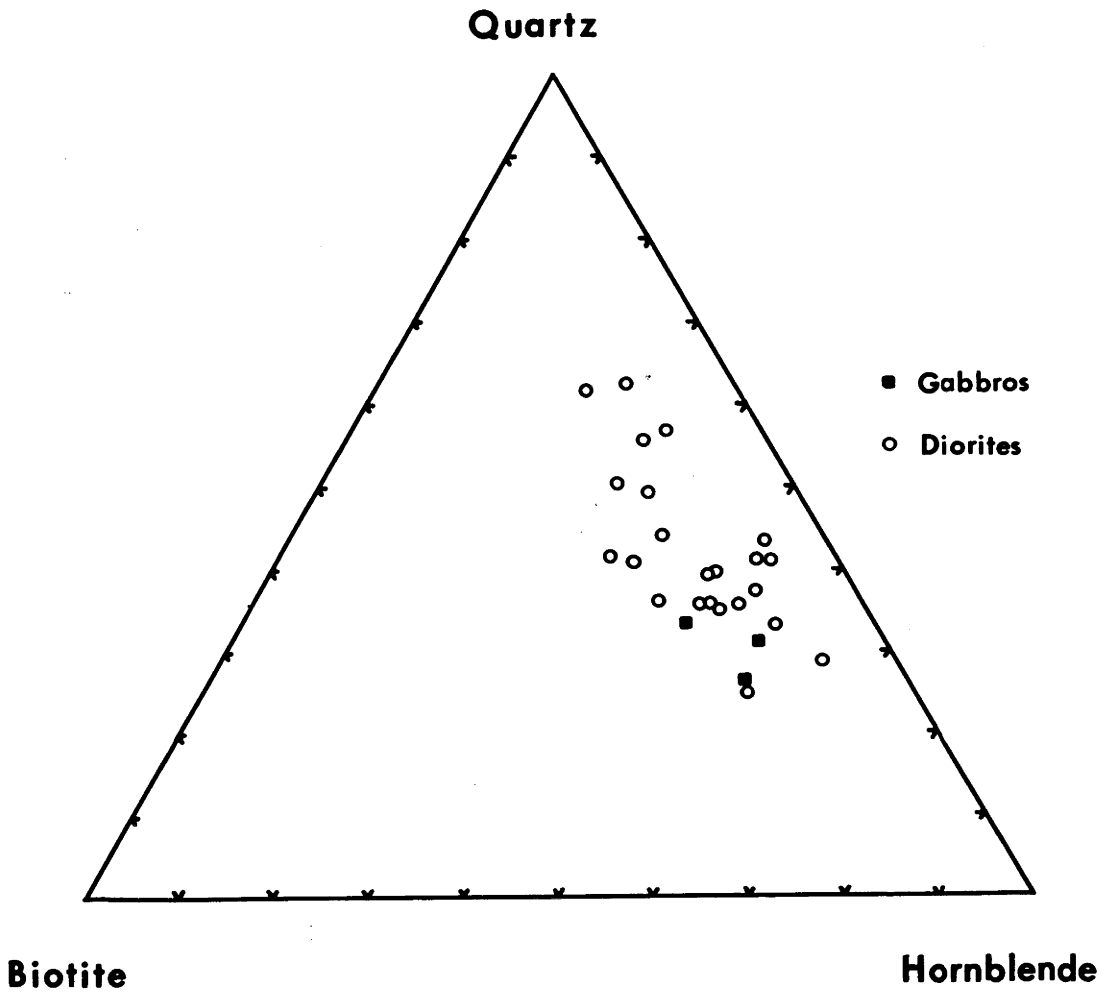

Fig.2 Quartz-Biotite-Hornblende relationships in the Yeoval Rocks.

Opaque minerals: occur as single grains, clusters of grains, inclusions in biotite and hornblende or as alteration products. The dominant opaque mineral is magnetite which shows varying degrees of alteration to hematite. Ilmenite, as single grains and/or lamellae in magnetite, varies in amount. Octahedral intergrowths of ulvospinel (?) may or may not be present in the magnetite. Other opaque minerals include pyrite and chalcopyrite.

There is a transition from the gabbro to the pyroxene-mica diorite and thence to the quartz-mica diorite. In the course of the transition, the following observations have been made:

(i) presence of interstitial quartz, potassium feldspar and biotite in increasing amounts

(ii) pyroxene becoming rimmed by olive-green hornblende and uralite alteration

(iii) crystallisation of olive-green hornblende

(iv) plagioclases become zoned and more albite-rich

(v) increasing amounts of apatite and zircon.

A similar transition exists between the pyroxenite and quartz-mica diorite. In the orthoclase diorites there are increasing amounts of potassium feldspar and quartz, and the plagioclases are often strongly zoned with rims of alkali feldspar.

TABLE 3a

Chemical Analyses and CIPW Norms of Basic Diorites from the Yeoval District

			Pyroxene-Mica Diorites			Basic diorite near margins
	W42	W66	Y8	G154	G71	G131
SiO_2	50.74	54.11	53.68	54.82	55.23	52.86
TiO_2	0.62	0.61	0.66	0.71	0.63	0.74
Al_2O_3	17.79	17.45	17.03	17.20	17.18	17.03
Fe_2O_3	n.d.	n.d.	<0.01	0.01	0.01	n.d.
FeO	8.88	8.24	8.46	7.65	7.23	8.87
MnO	n.d.	0.19	0.23	0.22	0.23	0.27
MgO	6.71	5.21	4.55	4.51	4.66	4.15
CaO	10.12	9.56	8.84	7.50	7.17	8.28
Na_2O	n.d.	n.d.	2.76	3.08	2.87	3.03
K_2O	0.78	0.81	1.08	1.40	1.60	1.74
P_2O_5	n.d.	n.d.	0.037	0.039	0.143	0.501
H_2O^+	n.d.	n.d.	1.10	0.81	1.74	1.51
H_2O^-	n.d.	n.d.	0.09	0.05	0.12	0.20
CO_2	n.d.	n.d.	0.10	0.02	0.18	0.23
			98.53	98.01	98.98	99.41
Q			4.13	4.55	6.11	1.38
Or			6.38	8.27	9.46	10.28
Ab			23.36	26.06	24.29	25.64
An			30.89	28.97	29.27	27.73
Ne			-	-	-	-
Di			10.11	6.55	3.60	7.51
Hy			20.90	21.25	22.48	22.13
Ol			-	-	-	-
Mt			-	-	-	-
Il			1.25	1.35	1.20	1.41
Ap			0.09	0.09	0.31	0.09
Cc			0.23	0.05	0.41	0.52
Z			-	0.02	0.02	0.02
Plag. An			56.95	52.64	54.65	51.96

TABLE 3b

Chemical Analyses and CIPW Norms of Quartz-Mica Diorites from the Yeoval District

	Y158	G107	G41	Y75	Y161	G92	Y225	G120	Y227	Y235	Y150	Y41	Y148	G90	G110	Y71	G46	G118	G99	Y151
SiO_2	54.32	56.40	57.34	57.50	57.70	58.40	58.42	58.61	58.72	59.51	59.51	59.71	59.80	61.23	62.09	62.48	62.70	63.04	63.06	64.40
TiO_2	0.67	0.68	0.54	0.59	0.47	0.56	0.60	0.73	0.54	0.56	0.49	0.62	0.52	0.67	0.51	0.50	0.50	0.40	0.38	0.39
Al_2O_3	15.52	16.72	16.49	16.95	16.27	17.32	16.08	16.28	16.88	16.32	16.67	16.37	16.34	16.30	16.23	16.02	16.42	17.10	17.10	16.10
Fe_2O_3	<0.01	0.58	<0.01	0.02	<0.01	n.d.	<0.01	<0.01	<0.01	<0.01	2.12	<0.01	n.d.	n.d.	<0.01	0.17	<0.01	<0.01	n.d.	<0.01
FeO	7.99	7.20	6.12	7.12	7.39	6.84	5.20	6.93	6.83	6.50	4.55	6.18	5.48	5.68	5.36	4.98	5.25	4.64	4.17	4.10
MnO	0.21	0.18	0.20	0.22	0.20	0.21	0.19	0.18	0.20	0.20	0.22	0.19	0.18	0.28	0.28	0.17	0.19	0.16	0.15	0.17
MgO	5.25	3.20	2.59	3.20	3.20	2.78	3.10	3.38	3.27	3.04	2.86	2.55	2.55	2.30	2.50	2.58	2.51	2.07	2.26	1.99
CaO	8.24	6.77	5.78	7.06	6.52	6.58	5.74	6.22	6.69	5.70	6.73	5.37	5.95	5.79	5.30	5.30	5.26	5.25	4.47	4.83
Na_2O	2.77	3.01	5.63	2.82	2.90	3.28	5.51	2.75	2.93	3.00	2.91	3.24	3.17	2.93	3.11	3.10	2.82	3.30	3.10	3.50
K_2O	2.27	2.40	2.64	2.28	2.48	2.14	2.95	2.62	2.47	2.82	2.26	3.15	2.11	2.16	2.18	2.30	3.02	2.28	2.20	1.99
P_2O_5	0.041	0.240	0.214	0.108	0.128	0.086	0.109	0.042	0.114	0.215	0.102	0.144	0.151	0.143	0.014	0.080	0.151	0.027	0.149	0.082
H_2O^+	1.73	1.51	2.56	1.65	1.76	1.41	1.53	1.03	1.27	1.26	1.04	1.36	1.61	1.45	1.36	1.12	1.34	1.15	1.40	0.79
H_2O^-	0.23	0.16	0.22	0.11	0.19	0.18	0.13	0.18	0.19	0.14	0.13	0.13	0.22	0.21	0.26	0.17	0.17	0.07	0.18	0.12
CO_2	0.21	0.12	0.14	0.18	0.29	0.17	0.18	nil	0.26	0.03	0.25	0.26	0.05	nil	0.09	0.18	0.13	0.17	0.15	0.31
	99.45	99.17	100.46	99.81	99.50	99.96	99.74	98.95	100.36	99.30	99.84	99.27	98.13	99.14	99.28	99.15	100.46	99.66	98.77	98.77
Q	1.83	7.29	-	8.92	8.95	9.14	-	10.27	9.66	10.85	14.53	10.42	13.81	16.59	16.88	17.62	16.53	17.61	21.11	20.87
Or	13.42	14.18	15.60	13.47	14.66	12.65	17.43	15.48	14.60	16.67	13.36	18.62	12.47	12.77	12.88	13.59	17.85	13.47	13.00	11.76
Ab	23.44	25.47	47.64	23.86	24.54	27.76	46.63	23.27	24.79	25.39	24.62	27.42	26.82	24.79	26.32	26.23	23.86	27.92	26.23	29.62
An	23.21	25.02	11.93	26.86	24.05	26.22	10.43	24.34	25.61	22.74	25.75	20.82	24.13	24.95	23.89	23.01	23.23	24.79	20.35	21.53
Ne	-	-	-	-	-	-	-	-	-	-	-	-	-	-	-	-	-	-	-	-
Di	13.36	5.36	12.31	5.36	4.79	4.07	13.52	5.26	4.43	3.40	4.50	2.82	3.52	2.49	1.49	1.40	0.98	-	-	-
Hy	20.39	17.23	0.88	17.77	18.72	16.90	3.67	17.64	17.94	17.25	11.11	15.61	14.12	14.32	15.00	14.22	14.93	13.31	12.94	12.16
Ol	-	-	7.52	-	-	-	4.61	-	-	-	-	-	-	-	-	-	-	-	-	-
Mt	0.01	0.84	-	0.03	-	-	-	-	-	-	3.07	-	-	-	-	0.25	-	-	-	-
Il	1.27	1.29	1.03	1.12	0.89	1.06	1.14	1.39	1.03	1.06	0.93	1.18	0.99	1.27	0.97	0.95	0.95	0.76	0.72	0.74
Ap	0.09	0.52	0.46	0.24	0.28	0.20	0.24	0.09	0.24	0.48	0.22	0.31	0.33	0.31	0.02	0.17	0.33	0.07	0.33	0.17
Cc	0.48	0.27	0.32	0.41	0.66	0.39	0.41	-	0.59	0.07	0.57	0.59	0.11	-	0.20	0.41	0.30	0.39	0.34	0.71
Z	0.02	0.02	-	0.02	0.02	-	0.02	0.02	0.02	0.02	0.02	0.02	0.02	0.02	0.02	0.02	0.02	-	0.02	0.02
C	-	-	-	-	-	-	-	-	-	-	-	-	-	-	-	-		0.12	2.16	0.30
Plag. An	49.75	49.56	20.02	52.95	49.50	48.57	18.28	51.12	50.81	47.25	51.12	43.16	47.35	50.15	47.58	46.72	49.32	47.03	43.68	42.10

TABLE 3c

Chemical Analyses and CIPW Norms of Orthoclase Diorite from the Yeoval District

	Y205	Y206	G57
SiO_2	64.23	63.91	63.52
TiO_2	0.50	0.49	0.52
Al_2O_3	15.79	15.78	15,37
Fe_2O_3	<0.01	<0.01	<0.01
FeO	4.47	4.19	4.30
MnO	0.16	0.13	0.11
MgO	1.46	1.30	1.63
CaO	3.57	3.37	3.88
Na_2O	3.98	4.10	3.79
K_2O	3.83	4.19	4.10
P_2O_5	0.042	0.171	0,187
H_2O^+	0.81	0.82	1.03
H_2O^-	0.14	0.17	0.16
CO_2	0,09	0.06	0.07
	99.07	98.68	98.67
Q	14.08	12.86	13.45
Or	22.63	24.76	24.23
Ab	33.68	34.69	32,07
An	13.91	12.28	12,82
Ne	-	-	-
Di	2.54	2.60	4.11
Hy	10.03	9.04	9.23
Ol	-	-	-
Mt	-	-	-
Il	0.95	0.93	0.99
Ap	0.09	0.37	0.42
Cc	0.20	0.14	0.16
Z	0.03	0.03	0.03
C	-	-	-
Plag. An	29.23	26.14	28.56

3.2.2. Modal Analyses

The variation within, and transitions between, the different phases of diorites is evident in their modes. These are presented in Table 2 and Figs. 1 and 2. The transition between the gabbros and diorites is clearly seen in a plot of quartz-feldspar-mafics, in which a broad band extends from the feldspar-mafics boundary toward the quartz-feldspar boundary. On the quartz-biotite-hornblende plot, the variation in the diorites is found to be a function of the quartz-hornblende ratio with the biotite content fixed between fairly well defined limits.

3.2.3. Chemistry

The major element chemistry of the rocks (Table 3) supports the postulate of a transition between the rock types described above. If W61, W60 and G71 are taken as one transition from pyroxenite through to pyroxene-mica diorite, then the changes are most marked, viz: SiO_2, Al_2O_3 and alkalis increase whereas MgO and CaO decrease. The transition from gabbro to pyroxene-mica diorite is similar except for an increase in TiO_2 and a slight decrease in Al_2O_3. In passing from the pyroxene-mica diorite to the quartz-mica diorite there is an increase in SiO_2 and K_2O, and a decrease in MgO and CaO. From the quartz-mica diorite to the orthoclase diorite, an overall increase in SiO_2 and alkalis, and a decrease in Al_2O_3, MgO and CaO may be noted.

TABLE 4

Chemical Analyses and CIPW Norms of the Fine Grained Quartz-Mica Diorite and Associated Rocks

	G151	Y187	Y189
SiO_2	67.79	46.55	62.62
TiO_2	0.55	3.36	0.86
Al_2O_3	15.87	13.60	16.15
Fe_2O_3	<0.01	<0.01	<0.01
FeO	3.99	15.81	5.79
MnO	0.25	0.29	0.19
MgO	1.97	5.54	1.53
CaO	4.16	10.29	3.57
Na_2O	3.91	3.33	5.65
K_2O	1.66	0.50	2.05
P_2O_5	0.014	0.034	0.154
H_2O^+	0.34	0.77	0.56
H_2O^-	0.16	0.13	0.15
CO_2	0.21	0.37	0.18
	100.87	100.62	99.45
Q	24.29	-	9.09
Or	9.81	2.95	12.12
Ab	33.09	23.37	47.81
An	19.25	20.69	12.65
Ne	-	2.60	-
Di	-	23.23	2.59
Hy	11.79	-	12.05
Ol	-	19.47	-
Mt	-	-	-
Il	1.04	6.38	1.63
Ap	0.02	0.17	0.33
Cc	0.48	0.84	0.41
Z	0.03	0.02	0.16
C	0.59	-	-
Plag. An	36.78	46.95	20.93

3.2.4. Fine-grained quartz-mica diorite

The grain size, mineralogy and chemistry of this rock type is completely different from other diorite.. It occurs as a sausage-shaped body trending in a north-south direction at the northern most part of the main diorite body. It is intruded by the granite (Plate 1) and truncated by the main diorite. In handspecimen it is a dark grey, fine even grained rock. In thin section it consists of plagioclase (60-70%) along with potassium feldspar (up to 15%), pyroxene (up to 15%) and quartz, biotite and opaques. Plagioclase is strongly zoned and the outer margins are fairly sodic. The clinopyroxene is almost completely uralitised.

The major element analysis is shown in Table 4, Anal. 1. This fine quartz-mica diorite is the most common variety present over most of the area of the intrusion but near its contacts with the granite, the rock changes markedly in both grain size and composition and is apparently unrelated to the main fine-grained rock type.

Some varieties are gabbroic but with a coarse grain size and higher specific gravity than the normal gabbro. Compared with the complex mineralogy of the normal gabbro, this rock contains only plagioclase and clinopyroxene and its chemistry is entirely different from the normal gabbro (Table 4, Anal. 2) in that Al_2O_3 MgO and CaO are low, and TiO_2, FeO and Na_2O are high.

At other contacts, the rocks resemble the normal quartz-mica diorite except that they are a much darker grey, contain up to 70% plagioclase, and have more potassium feldspar. The analysis (Table 4, Anal. 3) of this rock resembles the normal quartz-mica diorite except for lower MgO and CaO, and higher Na_2O.

As relationships to the main diorite body are not clear and because the fine-grained quartz-mica diorite has more normal dioritic affinities, it will not be treated in the petrogenesis of the high potassium diorites.

3.3. GRANITES

These vary in composition from adamellites (with approximately equal amounts of plagioclase and potassium feldspar) to granites sensu stricto according to Nockolds (1954) with little or no plagioclase. Throughout this discussion the general term "granite" (Turner and Verhoogen, 1960) will be adhered to.

The granites vary markedly in handspecimen with respect to their grain size and mineralogy. They range from aplitic and granophyric types (with all constituents <1 mm) to granites with plagioclases up to 7 mm long and 4 mms wide.

The most striking features of the granites are their overall fine grain size and paucity of ferromagnesian minerals. Plagioclase, when present, is either white or a greenish colour and is twinned and zoned. The granites can be divided into three groups based on both mineralogy and grain size:

(i) granophyric type

(ii) two feldspar type

(iii) one feldspar type.

The granophyric type is a marginal phase of the granite mass and consists mainly of feldspar in the approximate proportion of 2 potassium feldspar : 1 plagioclase. Both feldspars are fairly altered and are coated with a fine hematite stain. Plagioclase is euhedral to subhedral and is not zoned. Quartz often occurs as euhedral crystals surrounded by spherulites of potassium feldspar as well as in micrographic intergrowths with both feldspars. No ferromagnesian minerals are present. Opaque minerals are sparsely scattered throughout the rocks. They are mainly magnetite, now almost completely altered to hematite, and some pyrite, chalcopyrite and pyrrhotite.

The two-feldspar granites consist mainly of potassium feldspar, plagioclase and quartz in approximately equal amounts along with varying percentages of ferromagnesian minerals. Although the grain size is medium and fairly even (average

2-4 mms), these granites are sometimes porphyritic. Plagioclase is quite strongly zoned (but not as intense as in the diorite) with both normal and "patchy" types developed. The central zone is commonly altered. "String" perthite traverses the potassium feldspar grains. The ferromagnesian minerals, biotite and hornblende, account for less than 1-10% of the rock. The ratio of biotite to hornblende also varies over a wide range e.g. in some rocks biotite is in greater abundance than hornblende, whereas in others, hornblende may be in greater amount. Both tend to occur as single crystals rather than as "clots". Opaques are magnetite (which is extensively altered to hematite) containing a few ilmenite lamellae and minor ulvospinel(?). Zircon, sphene, opaque minerals, fluorite and rutile (rarely) are associated with the ferromagnesian minerals.

The one feldspar granites consist mainly of quartz with minor ferromagnesian minerals. Selectively stained slabs or thin sections of these rocks show that the feldspar is a perthite in which there are equal proportions of potassium feldspar and plagioclase.

Biotite is the usual ferromagnesian mineral, although, in one example, "clots" of hornblende were observed. The hornblende in this instance may be of xenolithic origin. Sphene, zircon, apatite and opaques are common.

TABLE 5

Chemical Analyses and CIPW Norms of Granites from the Yeoval District

	One Feldspar	Two Feldspar			Granophyric	
	Y64	Y53	Y43	Y147B	R69	R77
SiO_2	74.48	74.85	74.23	74.61	73.62	74.87
TiO_2	0.14	0.35	0.28	0.22	0.12	0.18
Al_2O_3	13.08	13.03	13.71	13.38	13.59	13.08
Fe_2O_3	n.d.	<0.01	0.44	n.d.	n.d.	n.d.
FeO	2.07	0.97	1.24	2.97	2.64	1.44
MnO	0.10	0.07	0.05	0.10	0.06	0.06
MgO	0.29	0.48	0.45	0.50	0.29	0.29
CaO	0.51	0.50	1.28	0.95	0.22	0.11
Na_2O	4.44	4.10	3.91	4.05	4.46	4.69
K_2O	4.12	4.56	3.63	3.65	4.00	3.82
P_2O_5	0.019	0.003	0.062	0.022	0.011	0.020
H_2O^+	0.35	0.20	0.40	0.32	0.80	0.52
H_2O^-	0.05	0.04	0.07	0.04	0.10	0.04
CO_2	0.10	0.09	0.03	0.05	0.43	0.05
	99.75	99.25	99.78	100.86	100.34	99.17
Q	29.95	31.39	33.70	32.08	29.77	31.35
Or	24.35	26.95	21.45	21.57	23.64	22.58
Ab	37.57	34.69	33.09	34.27	37.74	39.69
An	1.78	1.91	5.81	4.28	-	0.11
Ne	-	-	-	-	-	-
Di	-	-	-	-	-	-
Hy	4.48	2.53	2.66	6.52	5.48	3.18
Ol	-	-	-	-	-	-
Mt	-	-	0.64	-	-	-
Il	0.27	0.66	0.53	0.42	0.23	0.34
Ap	0.04	-	0.13	0.04	0.02	0.04
Cc	0.23	0.20	0.07	0.11	0.37	0.11
Z	0.05	0.03	0.03	-	-	0.05
C	0.66	0.65	1.22	1.20	1.92	1.19
Plag. An	4.52	5.22	14.93	11.10	-	0.28

Chemistry: Little can be said of the major element chemistry of the granites (Table 5) because of the few analyses available. However, even though there is a marked difference in the type of feldspar in the rocks, no significant difference in the Na_2O/K_2O ratio is apparent. Also the lower values for MgO and CaO are consistent with the lack of ferromagnesian minerals in the granophyric type.

3.4. VOLCANIC ROCKS

The silicic rocks are a pale colour, porphyritic in quartz and feldspar and usually fairly altered. Flow lines are occasionally visible. In thin section the rocks consist mainly of phenocrysts of quartz and potassium feldspar set in a very fine, apparently devitrified groundmass of quartz, potassium feldspar, amphibole (?), opaques and sometimes sphene. Spherulites of potassium feldspar micrographically intergrown with quartz are present in some rocks.

In addition to the rhyolitic types, minor andesites also occur. Table 6, Anal. G128 gives the analysis of an andesite which is slightly metamorphosed by the granite. The slightly high K_2O value (compared with 1.6% for an average andesite; Taylor 1967) may be due to the introduction of potassium feldspar from the granite, which occurs as veins cutting the andesite.

The northern and southern belts consist of an association of various andesitic lavas and pyroclastics.

TABLE 6

Chemical Analyses and CIPW Norms of Volcanic Rocks from the Yeoval District

	G117	G133	G134A	G134B	G140	G128	IV	V	VI	VII	VIII	Average Andesite
SiO_2	55.12	50.91	50.89	53.59	52.45	55.75	50.46	56.65	62.55	50.85	50.71	60.1
TiO_2	0.71	0.74	0.76	0.61	0.72	0.66	0.88	0.67	0.52	1.30	1.04	0.7
Al_2O_3	16.97	17.35	13.89	17.22	17.28	15.72	17.99	20.37	17.46	16.07	17.92	17.2
Fe_2O_3	<0.01	<0.01	<0.01	<0.01	<0.01	n.d.	1.06	1.24	2.37	4.58	5.14	-
FeO	7.94	8.52	10.58	9.10	9.06	7.87	5.76	3.28	2.03	6.45	4.73	-
MnO	0.21	0.30	0.26	0.23	0.19	0.31	0.12	0.08	0.44	0.09	0.09	-
MgO	3.33	8.64	7.62	3.90	4.41	4.11	6.78	3.20	1.43	4.23	4.67	3.5
CaO	8.30	9.49	11.07	9.54	9.42	9.48	10.91	4.31	2.55	7.83	7.28	7.1
Na_2O	2.37	1.26	1.64	2.55	2.33	2.12	0.97	5.65	4.99	2.57	2.49	3.3
K_2O	2.06	0.37	1.06	0.80	1.81	1.80	1.63	2.75	4.78	2.03	2.16	1.3
P_2O_5	0.15	0.15	0.03	0.05	0.02	0.15	0.29	0.29	trace	0.33	0.35	-
H_2O^+	1.08	1.62	1.39	1.01	1.15	0.87	2.38	1.43	0.85	2.41	1.96	-
H_2O^-	0.11	0.16	0.17	0.09	0.12	0.27	0.04	0.11	0.08	0.16	0.62	-
CO_2	0.09	0.09	0.21	0.16	0.11	Nil	1.12	Nil	Nil	0.79	0.48	-
	98.44	99.61	99.57	98.85	99.07	99.11	100.39	100.03	100.05	99.69	99.64	
Q	7.23	3.85	-	5.42	1.50	8.02	6.20	-	7.17	6.48	6.28	
Or	12.17	2.19	6.26	4.73	10.70	10.64	9.63	16.25	28.25	12.00	12.77	
Ab	20.06	10.66	13.88	21.58	19.72	17.94	8.21	47.81	42.23	21.75	21.07	
An	29.58	40.59	27.41	33.18	31.35	28.06	39.92	19.68	11.13	26.32	31.02	
Ne	-	-	-	-	-	-	-	-	-	-	-	
Di	8.54	4.07	21.51	10.81	12.21	15.12	4.39	-	1.23	4.55	-	
Hy	17.79	34.51	26.89	20.40	20.66	16.61	23.23	5.28	4.69	14.41	14.52	
Ol	-	-	0.07	-	-	-	-	4.88	-	-	-	
Mt	-	-	-	-	-	-	1.54	1.80	3.44	6.64	7.45	
Il	1.35	1.41	1.44	1.16	1.37	1.25	1.67	1.27	0.99	2.47	1.98	
Ap	0.33	0.35	0.07	0.11	0.04	0.33	0.63	0.63	-	0.72	0.76	
Cc	0.20	0.20	0.48	0.36	0.25	-	2.55	-	-	1.80	1.09	
Z	0.02	-	0.02	0.02	0.02	0.02	-	-		-	-	
C	-	-	-	-	-	-	-	0.89	-	-	0.12	
Plag. An	59.60	79.20	66.39	60.59	61.39	61.00	82.95	29.16	20.85	54.75	59.55	

G117 Meta-andesite Yeoval N.S.W.
G133 Volcanic Breccia "
G134A Pyroxene Andesite "
G134B Meta-andesite "
G140 Pyroxene Andesite " (Metamorphosed)
G128 Meta-andesite "
IV Porphyritic Basalt Wellington District N.S.W. Anal. M.J. Colditz (1948)
V Augite Hornblende Andesite " "
VI Hornblende Trachyandesite " "
VII Augite Porphyrite " "
VIII Augite Andesite " "
Average Andesite (Taylor & White 1966)

Individual lava flows are impossible to map separately as no flow is continuous over any distance and they often merge into breccias or xenolith-bearing flows. The rock types are porphyritic basalt, pyroxene andesite, orthoclase-bearing andesites and associated pyroclastic rocks including fine-grained tuffs, breccias and agglomerates.

Such a volcanic association is typical of this region and fairly complete petrographic descriptions have been given by a number of authors (Colditz 1948, Maggs 1963, etc.). A number of the andesites have undergone varying stages of contact metamorphism by the diorite, resulting in uralite replacement of pyroxenes.

Chemistry: Table 6 gives analyses of selected andesitic rocks in the Yeoval district as well as Colditz's analyses. For comparison, the average andesite suggested by Taylor (1967) is also given.

Little can be said of the chemical analyses owing to the wide variation in composition and degree of metamorphism. The pyroxene andesites from Yeoval and Wellington (G140 and VIII) are somewhat similar except for the lower CaO content in the Wellington rocks. A comparison of the andesites from Yeoval and Wellington with the average andesite shows SiO_2 and Na_2O to be higher, and FeO, MgO and CaO to be lower, in the average andesite.

3.5. MISCELLANEOUS ROCKS

Included under this section are the tuffs, aplites, dyke rocks, xenoliths and contact rocks. A brief description of each will be given followed by chemical and/or mineralogical data.

3.5.1. Tuffs

The tuffs form a boudinage-like band along the eastern margin of the main diorite mass. The individual areas are separated from each other and from the diorite by alluvium.

The tuffs are a massive crystal variety and in hand-specimen could easily be mistaken for a phase of the diorite. Three types may be distinguished. The first is a grey colour with a fairly even, medium grain size. The second is porphyritic in plagioclase and quartz, the phenocrysts being set in a very dark grey (almost black) matrix. The third has a very uneven grain size and is a light cream colour.

In thin section, the different varieties are somewhat similar and do not even vaguely resemble the diorite. All have large crystals of quartz and feldspar (both plagioclase and potassium feldspar) set in a varying sized groundmass of quartz, feldspar, chlorite, biotite, zircon, apatite, epidote and sphene. The second variety, whose darker colour may be attributed to the presence of abundant chlorite, has definite "flow lines" and could be an ash flow tuff (Ewart,

pers. comm.). In this variety, a number of rounded, fine, even-grained xenoliths were observed. A thin section study revealed the xenolith to consist of a vermicular-like intergrowth of quartz, plagioclase and biotite accompanied by abundant fine apatite needles. Occasionally, a large crystal of altered plagioclase may be present. The third tuff variety contains little or no potassium feldspar and a few "clots" of fairly fresh biotite.

Garnets (amounting to <1%) were observed in the first variety. These are pale pink to colourless, quite fresh, usually anhedral, and traversed by numerous cracks which are often filled by quartz and feldspar. This tuff may well be related to the garnetiferous porphyry occurring to the east of Yeoval and extending for some 60 miles in a N-S direction (see Map 1). The porphyry is intimately associated with a tuffaceous phase and Maggs (1963) suggested that there was no sharp demarkation between the tuff and porphyry.

The garnet is an almandine-pyrope variety, according to the partial probe analysis, given below.

Partial Microprobe Analyses of Garnets from the Yeoval Rocks

	*		
SiO_2	41.9	Garnet Components	(Mol. per cent)
Al_2O_3	20.6	Ti - And.	0.9
FeO	30.0	Gross.	5.2
MnO	1.1	Pyrope	20.1
MgO	4.7	Alm.	72.0
CaO	1.7	Spess.	1.8
	100.0		

*Calculated

TABLE 7

Chemical Analyses and CIPW Norms of Tuffs from the Yeoval District

	G121	G122	G123
SiO_2	67.60	66.32	67.32
TiO_2	0.64	0.66	0.55
Al_2O_3	14.74	15.25	14.72
Fe_2O_3	n.d.	n.d.	n.d.
FeO	3.84	4.42	4.92
MnO	0.11	0.12	0.18
MgO	1.77	2.24	2.92
CaO	3.12	1.76	3.10
Na_2O	2.06	2.09	1.99
K_2O	3.82	4.38	0.82
P_2O_5	0.157	0.148	0.071
H_2O^+	1.40	0.56	2.44
H_2O^-	0.22	0.28	0.20
CO_2	0.11	0.19	0.18
	99.59	98.42	99.41
Q	29.54	27.85	38.41
Or	22.58	25.88	4.85
Ab	17.43	17.69	16.84
An	13.84	6.71	13.83
Ne	-	-	-
Di	-	-	-
Hy	10.61	12.83	15.73
Ol	-	-	-
Mt	-	-	-
Il	1.22	1.25	1.04
Ap	0.35	0.31	0.15
Cc	0.25	0.43	0.41
Z	0.03	0.03	0.03
C	2.14	4.61	5.49
Plag. An	44.26	27.50	45.09

The composition is very similar to the 24 analyses of garnets reported by Green (1967) from a variety of calc-alkaline rocks (rhyodacites, granodiorites) from different localities in Victoria. The compositions of the host rocks are also similar. From his experimental data, Green (1967) has suggested that the garnets from the calc-alkaline rocks formed at pressures somewhere between 9 and 18 Kb (i.e. at the base of the crust or in the upper mantle), under conditions of $P_{H_2O} < P_{LOAD}$.

Chemical analyses of the three types of tuff (Table 7) are fairly similar, the major differences being MgO, CaO and K_2O.

3.5.2. Aplites

Aplite veins are fairly common in the granite showing a tendency to follow the main joint directions. They are usually 2-18 cms. wide although some do attain a width of approximately 80 cms. Contact with the host rock is sharp. Near the diorite-granite contacts veins of aplite frequently cut the diorite. Only one aplite vein, of width approximately 40 cms, was observed in the diorite at any distance from the granite contact.

The aplites in the granite have sparsely distributed phenocrysts of quartz and potassium feldspar set in a dominantly quartz and feldspar groundmass. Minor amounts of

TABLE 8

Chemical Analyses and CIPW Norms of Aplite Veins and Host Rocks from the Yeoval District

	Aplite in Granite		Aplite in Diorite	
	Aplite Y53A	Granite Y53	Aplite Y41A	Diorite Y41
SiO_2	76.04	74.85	74.74	59.71
TiO_2	0.09	0.35	0.14	0.62
Al_2O_3	12.85	13.03	13.13	16.37
Fe_2O_3	<0.01	<0.01	<0.01	<0.01
FeO	0.95	0.97	1.43	6.18
MnO	0.07	0.07	0.09	0.19
MgO	0.33	0.48	0.56	2.55
CaO	0.47	0.50	1.32	5.37
Na_2O	3.82	4.10	2.56	3.24
K_2O	4.57	4.56	5.50	3.15
P_2O_5	0.012	0.003	0.006	0.144
H_2O^+	0.27	0.20	0.55	1.36
H_2O^-	0.03	0.04	0.11	0.13
CO_2	0.05	0.09	0.05	0.26
	99.55	99.25	100.19	99.27
Q	34.20	31.39	34.10	10.42
Or	27.01	26.95	32.50	18.62
Ab	32.33	34.69	21.66	27.42
An	1.96	1.91	6.23	20.32
Ne	-	-	-	-
Di	-	-	-	2.82
Hy	2.55	2.53	3.96	15.61
Ol	-	-	-	-
Mt	-	-	-	-
Il	0.17	0.66	0.27	1.18
Ap	0.02	-	-	0.31
Cc	0.11	0.20	0.11	0.59
Z	0.02	0.03	0.02	0.02
C	0.90	0.65	0.68	-
Plag. An	5.71	5.22	22.34	43.16

very fine biotite may be present. The aplite in the diorite consists mainly of potassium feldspar, plagioclase (in a ratio of about 7:3) and quartz with minor altered biotite. A few slightly coarser zoned crystals of plagioclase are present.

Major element analyses of an aplite in the granite and another in the diorite are presented in Table 8. For comparison, the analyses of the host rocks are also tabulated. The aplite in the diorite has lower SiO_2 and Na_2O, and higher FeO, CaO and K_2O than the granite aplite.

3.5.3. Dyke Rocks

These are intrusive into the diorite along the main E-W joint direction and vary in composition from rhyolitic to basaltic types. The most common types have intermediate to basic compositions.

One of these is a keratophyre. It is a red-brown colour showing sparse phenocrysts of feldspar set in a fine even groundmass. The feldspar is an albitic plagioclase, coated with an iron stain and containing carbonate. Approximately 15% of quartz and minor chlorite (after hornblende or clinopyroxene) is intergrown with the plagioclase. Small needles of apatite and grains of rutile and sphene are present. Chemical analysis of the keratophyre (Table 9) indicates high Na_2O and CO_2 values which are the result of the albitisation and alteration (to carbonate) of the plagioclase.

TABLE 9

Chemical Analyses and CIPW Norms of Dyke Rocks in Diorites from the Yeoval District

	Basalt Y229	Keratophyre G156
SiO_2	46.67	65.36
TiO_2	2.52	0.60
Al_2O_3	13.49	14.72
Fe_2O_3	0.08	n.d.
FeO	11.60	3.60
MnO	0.23	0.16
MgO	9.05	1.22
CaO	9.00	2.97
Na_2O	3.74	4.58
K_2O	0.84	3.10
P_2O_5	0.136	0.155
H_2O^+	1.43	1.60
H_2O^-	0.48	0.29
CO_2	0.22	2.08
	99.49	100.44
Q	-	22.06
Or	4.96	18.32
Ab	21.41	38.76
An	17.54	0.64
Ne	5.54	-
Di	20.43	-
Hy	-	8.96
Ol	21.97	-
Mt	0.12	-
Il	4.79	1.14
Ap	0.31	0.35
Cc	0.50	4.73
Z	0.05	1.01
C	-	3.59
Plag. An	45.03	1.64

Another is a basalt, almost black in colour and occasionally with large crystals of olivine (2 mms.) and amphibole (up to 3 cms. across). In thin section, phenocrysts of clinopyroxene and olivine are set in a very fine, even groundmass of plagioclase, clinopyroxene and opaque minerals. Mosaics of 7 or 8 grains of quartz also form xenocrysts. The basalt is an alkali olivine variety as indicated by nepheline in the norm (Table 9).

The relationship of the keratophyric dyke rocks to the diorite complex is not clear. Since alkali basalts of Late Mesozoic Tertiary age are common in Eastern Australia (Joplin, 1965) at least the basalt dykes are likely to be much later and unrelated to the diorite complex.

3.5.4. Xenoliths

As these are very sparsely distributed throughout most of the rock types in the Yeoval district, a discussion of the xenoliths will be restricted to those in the diorite.

Two main types can be distinguished. One is a medium-grained basic variety which, in thin section, resembles the gabbro in that it consists of a granular aggregate of plagioclase, uralite and minor quartz with very fine-grained

TABLE 10

Chemical Analyses and CIPW Norms of Xenoliths in the Diorite

	Xen. Y151X	Host Y151	Xen. G90X	Host G90
SiO_2	53.00	64.40	54.62	61.23
TiO_2	0.44	0.39	0.70	0.67
Al_2O_3	17.11	16.10	17.25	16.30
Fe_2O_3	n.d.	<0.01	n.d.	<0.01
FeO	7.68	4.10	8.00	5.68
MnO	0.34	0.17	0.25	0.28
MgO	4.82	1.99	3.53	2.30
CaO	8.08	4.83	7.42	5.79
Na_2O	4.16	3.50	3.48	2.93
K_2O	1.51	1.99	1.64	2.16
P_2O_5	0.072	0.082	0.118	0.143
H_2O^+	1.14	0.79	1.79	1.45
H_2O^-	0.20	0.12	0.18	0.21
CO_2	0.07	0.31	Nil	Nil
	98.62	98.77	99.03	99.14
Q	-	20.87	2.84	16.59
Or	8.92	11.76	9.69	12.77
Ab	35.20	29.62	29.45	24.79
An	23.55	21.53	26.61	24.95
Ne	-	-	-	-
Di	13.04	-	7.98	2.49
Hy	3.78	12.16	18.90	14.32
Ol	11.64	-	-	-
Mt	-	-	-	-
Il	0.84	0.74	1.33	1.27
Ap	0.15	0.17	0.26	0.31
Cc	0.16	0.71	-	-
Z	-	0.02	-	0.02
C	-	0.30	-	-
Plag. An	40.09	42.10	47.46	50.15

mosaics of plagioclase and pyroxene occupying smaller areas between the coarser crystals. Flakes of deep red-brown biotite are dotted with inclusions of plagioclase.

The second type of xenolith is very fine and even grained, except for occasional phenocrysts and coarser patches of feldspar and hornblende. This type is the most common and may be up to 20 cms. across, although they usually average 3-4 cms. In thin section the xenolith consists of approximately 50-60% plagioclase and 30-40% hornblende. The plagioclase may be fresh, partially or almost wholly saussuritised. The rest of the xenolith is made up of quartz and an occasional grain of potassium feldspar and opaque mineral.

Table 10 lists two analyses of the second type of xenolith and for comparison, the analyses of the host rocks are repeated. The two xenoliths are somewhat similar, the discrepancies being accounted for in the slightly differing mineralogies, e.g. Y151X has higher MgO, CaO and Na_2O which may be due to the presence of more hornblende and plagioclase. The higher SiO_2 and K_2O contents in G90X are reflected by the presence of small amounts of quartz and potassium feldspar respectively.

When the analyses of the xenoliths and host rocks are compared, no similarities exist. The SiO_2 and K_2O contents

TABLE 11 (continued)

Electron Probe Analyses and Structural Formulae of Minerals in the Skarn

Hedenbergite		Garnet Fe calculated as FeO		Fe calculated as Fe_2O_3		Clinozoisite
			Structural Formulae			
Si)	2.000	Si)	6.093	Si)	5.849	
Al)	-	Al)	-	Al)	-	
Al)	0.042	Al_{2+})	2.335	Al_{3+})	2.242	
Ti)	0.007	Fe^{2+})	2.031	Fe^{3+})	1.940	
Mg_{2+})	0.200	Ti)	0.039	Ti)	0.038	
Fe^{2+})	0.712	Mg_{3+})	-	Mg)	-	
Mn)	0.048	Fe^{3+})	-	Mn)	0.160	
Ca)	0.969	Mn)	0.167	Ca)	5.792	
Na)	-	Ca)	6.034			
K)	-					
Z	2.000	Z	6.093		5.849	
X+Y	1.978	Y	4.405		4.220	
		X	6.201		5.962	
$100\left[\frac{Mg}{Mg+Fe^{2+}}\right]$	21.9	Mole Prop.				
		Grossular	73.2	Andradite	48.8	
		Spess.	2.1	Almandine	-	
		Almandine	24.6	Grossular	48.3	
				Spess.	2.8	

TABLE 11

Electron Probe Analyses and Structural Formulae of Minerals in the Skarn

	Hedenbergite	Garnet Fe Calculated as FeO	Fe Calculated as Fe_2O_3	Clinozoisite
SiO_2	50.9	37.3	37.3	41.3
TiO_2	0.2	0.3	0.3	<0.03
Al_2O_3	0.4	12.1	12.1	27.8
FeO	21.5	14.9	16.5	1.4
MnO	1.4	1.2	1.2	<0.1
MgO	3.4	<0.04	<0.04	0.5
CaO	22.8	34.5	34.5	26.3
Na_2O	<0.04	<0.04	<0.04	<0.04
K_2O	<0.02	<0.02	<0.02	<0.02
	100.6	100.3		97.3

of the xenoliths are very much lower and FeO, MgO, CaO and Na_2O are higher.

3.5.5. Contact Rocks

As the contact effects of the diorite and country rocks are not particularly striking, no detailed study of these were made. Observations on a small number of thin sections indicated the grade of metamorphism to be hornblende hornfels facies. The pelitic hornfelses consist mainly of quartz and altered feldspar with disseminated "clots" of biotite and minor andalusite and possibly cordierite.

A more detailed study was made of a banded calcium-silicate hornfels found as a lens at the contact of the gabbro and granite. It is possible that this hornfels is an undigested block of metamorphosed limestone rather than part of the pre-existing country rock which has been metamorphised "in situ". In hand specimen the most noticeable feature is the discontinuous lenses or "pods" of different minerals. In thin section the hornfels consists mainly of hedenbergite along with plagioclase, quartz, sphene, clinozoisite and garnet. Hedenbergite and sphene commonly occur as monomineraloc "pods" as well as being intimately intergrown with the other minerals.

The hedenbergite is a very deep green and shows faint pleochroism. The garnet is a pale yellowish-orange, and slightly anisotropic. It is a grossular-andradite type

Fig.3 FMA plot for the Yeoval rocks.

Inset shows other natural rock associations

—— Skaergaard trend (Wager 1960)

Shaded area denotes typical calc-alkaline band (Tilley 1950)

Solid circles denote Daly's (1933) average basalt, andesite, dacite and rhyolite (in that order, from FM side towards alkali apex)

Triangles denote Nockold's (1954) average central basalt, andesite, dacite, rhyodacite, dellemite and rhyolite (in that order, from FM side towards alkali apex)

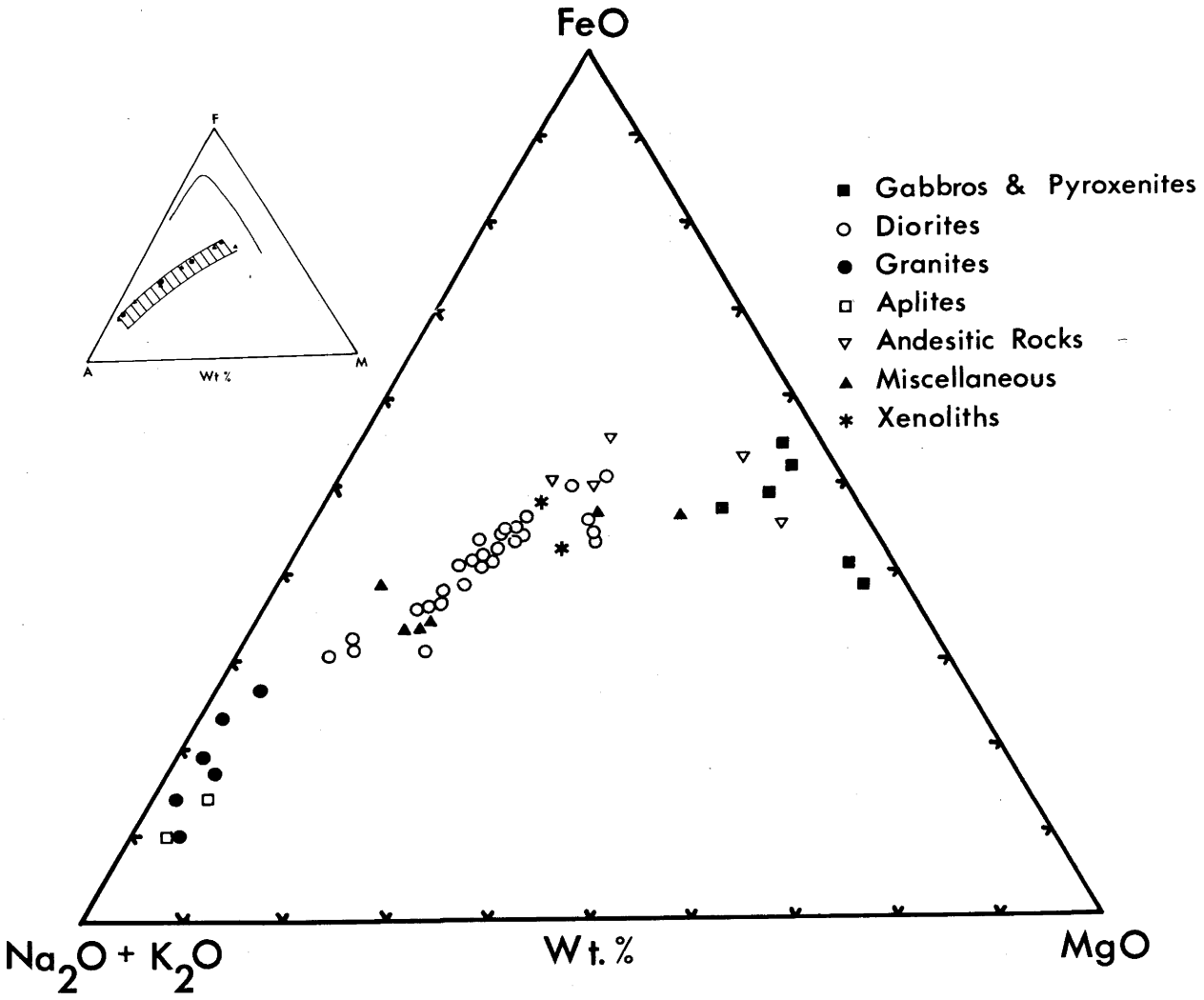
FeO
F
A
M
Wt %
Gabbros & Pyroxenites
Diorites
Granites
Aplites
Andesitic Rocks
Miscellaneous
Xenoliths
Na2O + K2O
Wt. %
MgO

fairly common in contact skarn rocks. The clinozoisite is a pale lemon yellow and under crossed Nicols shows anomalous yellow and blue interference colours.

Electron probe analyses of the hedenbergite, garnet and clinozoisite are shown in Table 11. The clinozoisite analysis is only approximate as the grains are difficult to resolve even with the probe since they are intimately intergrown with the garnet and hedenbergite.

3.6. VARIATION DIAGRAMS

The major element chemistry given in Tables 1, 3-10 has been plotted onto a number of triangular and Harker variation diagrams.

3.6.1. FMA diagram

A triangular plot (Fig.3) of total iron (expressed as FeO), MgO and total alkalis for the rock types described above give a typical calc-alkaline trend i.e. the analyses fall in an almost continuous belt from the FeO-MgO tie line towards the alkali apex. This follows closely the classical trend of Tilley (1950), which, for comparitive purposes, is inset in Fig.3. The scatter of the basic members is quite marked in these and subsequent diagrams. There is an indication of a slight iron enrichment in the basic to intermediate members, fairly typical of most calc-alkaline associations.

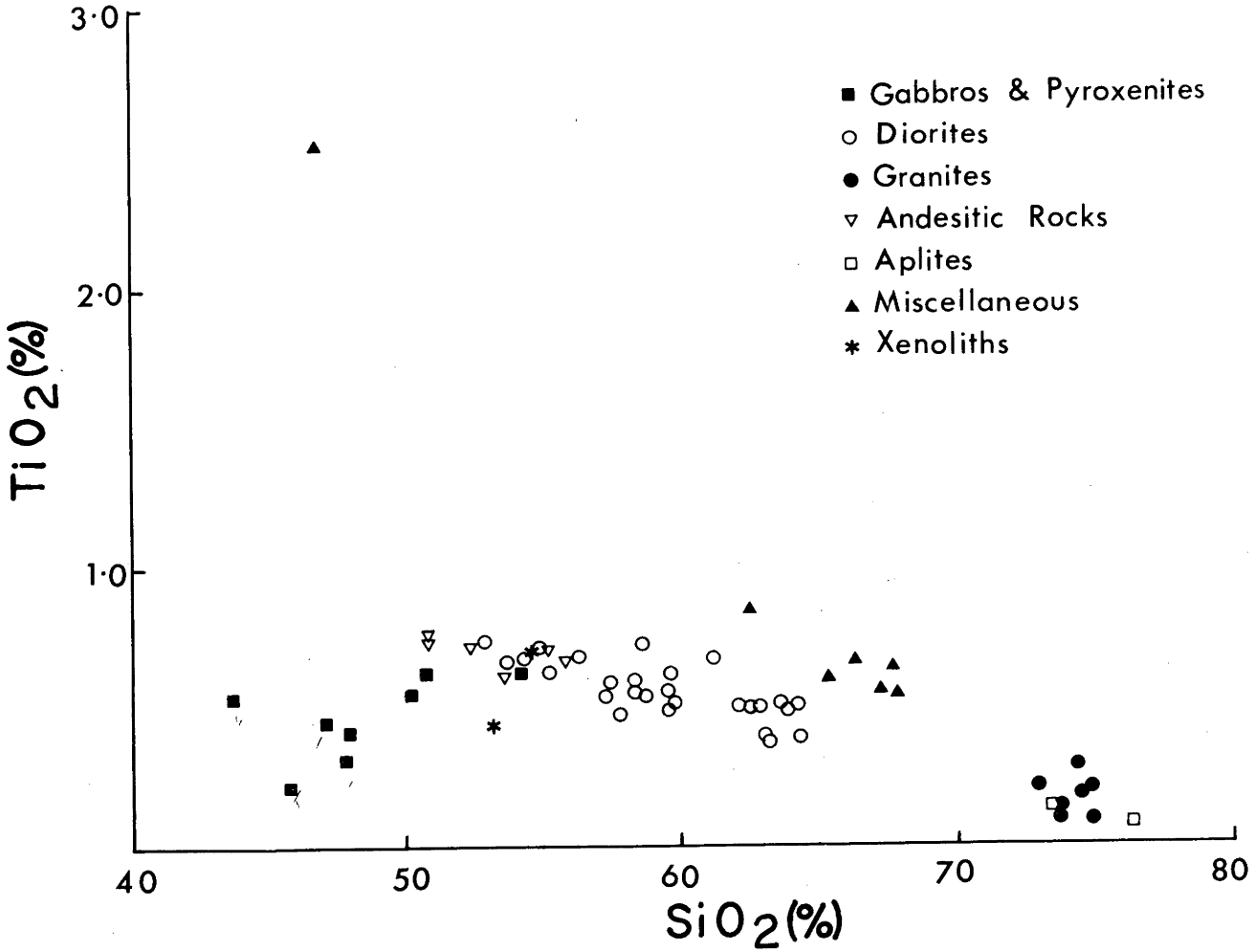

Fig.4 TiO_2 variation diagram for the Yeoval rocks.

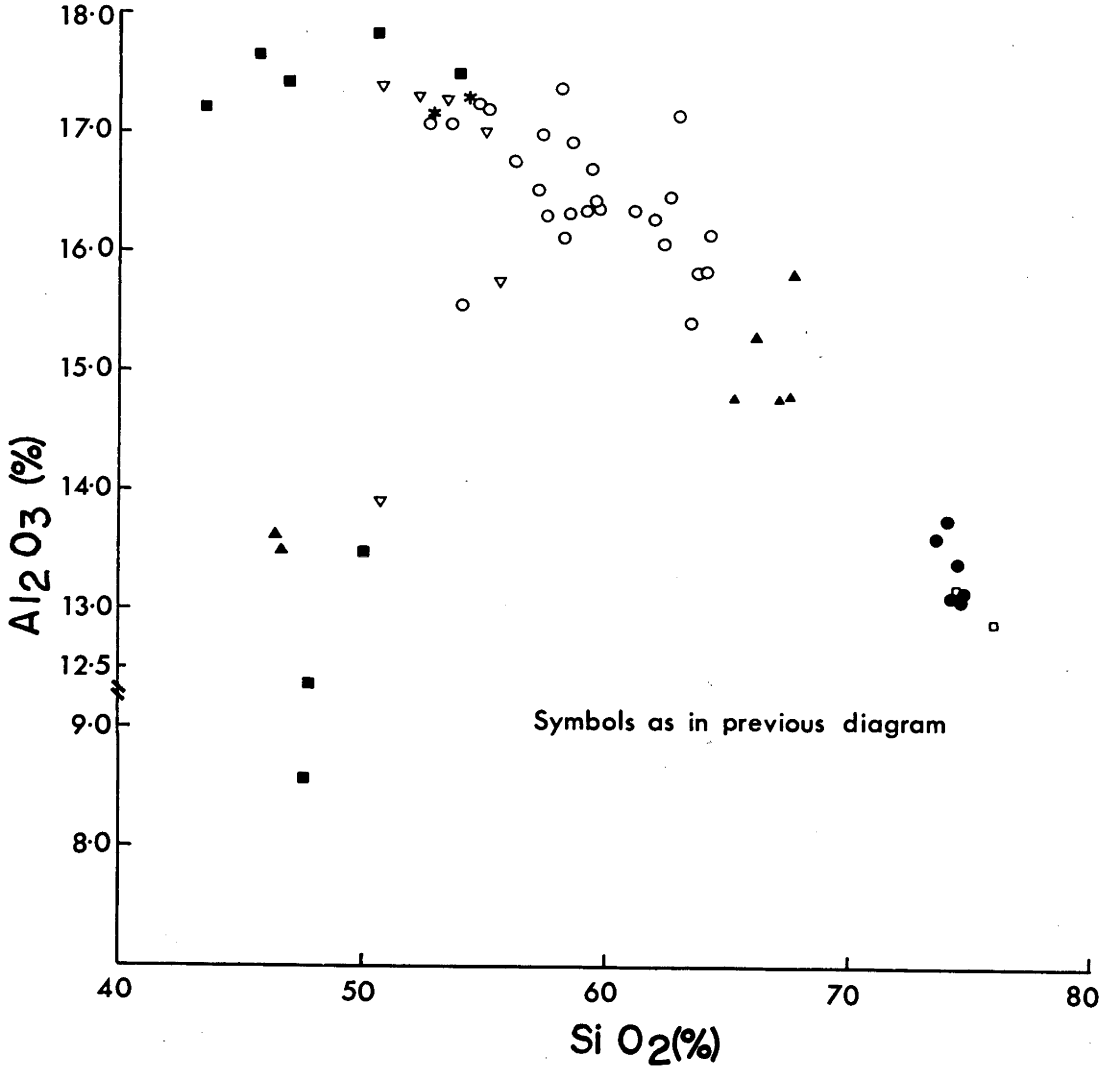

Fig.5 Al_2O_3 Variation Diagram for the Yeoval Rocks.

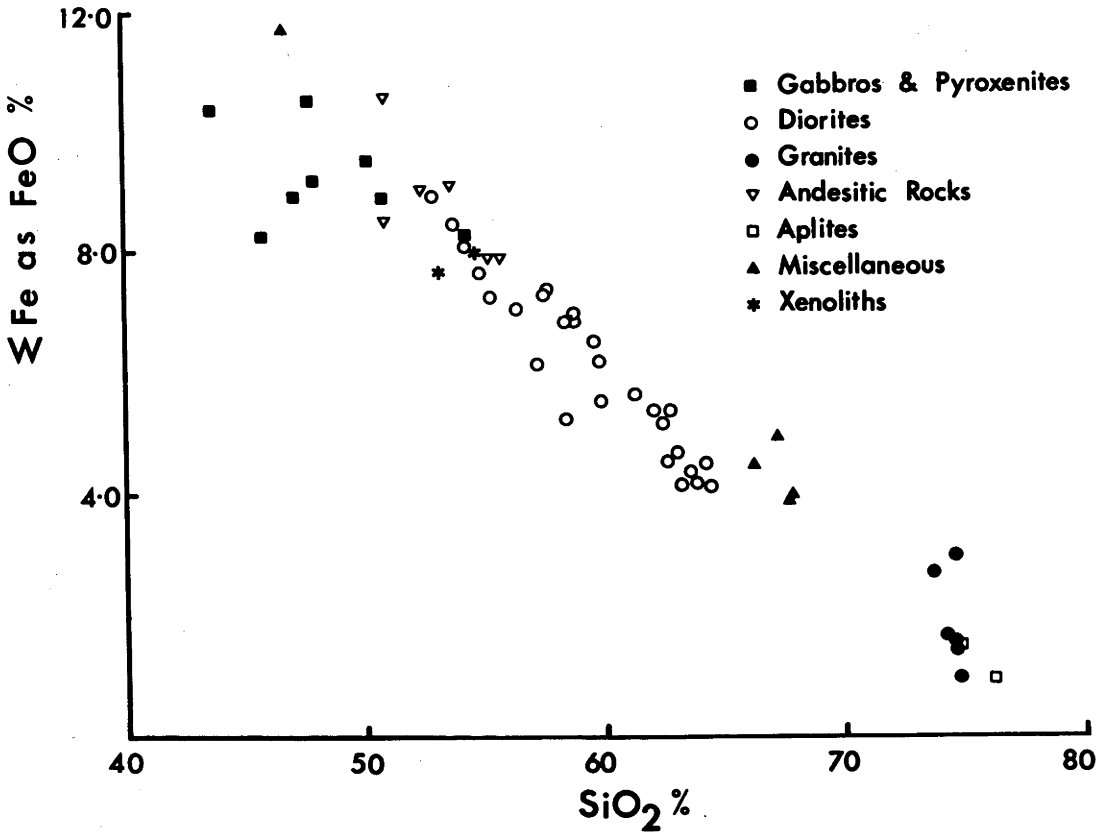

Fig.6a Total iron as FeO variation diagram for the Yeoval Rocks.

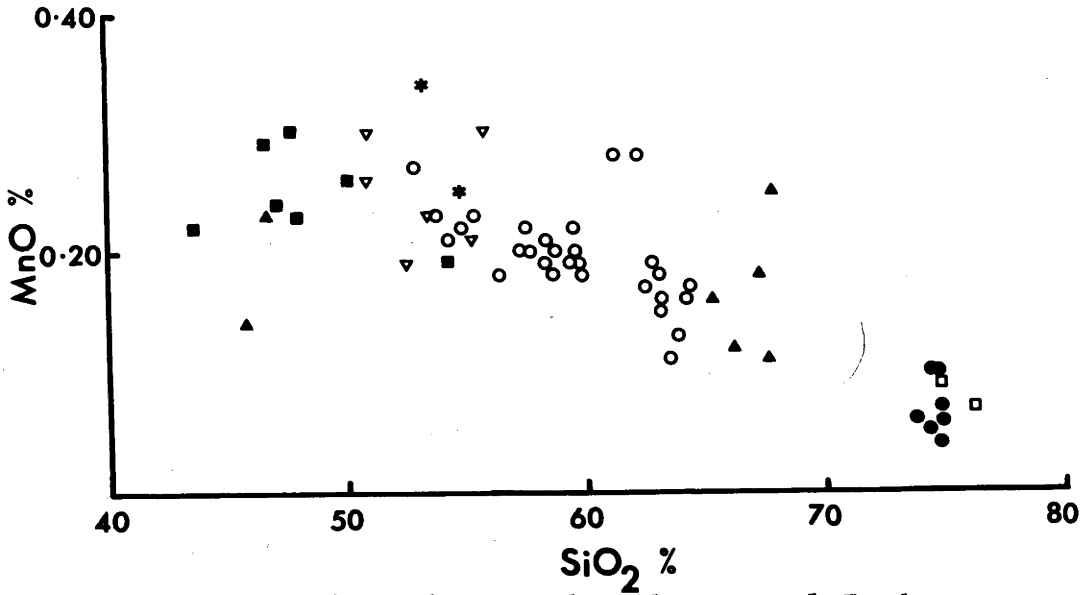

Fig.6b MnO variation diagram for the Yeoval Rocks.

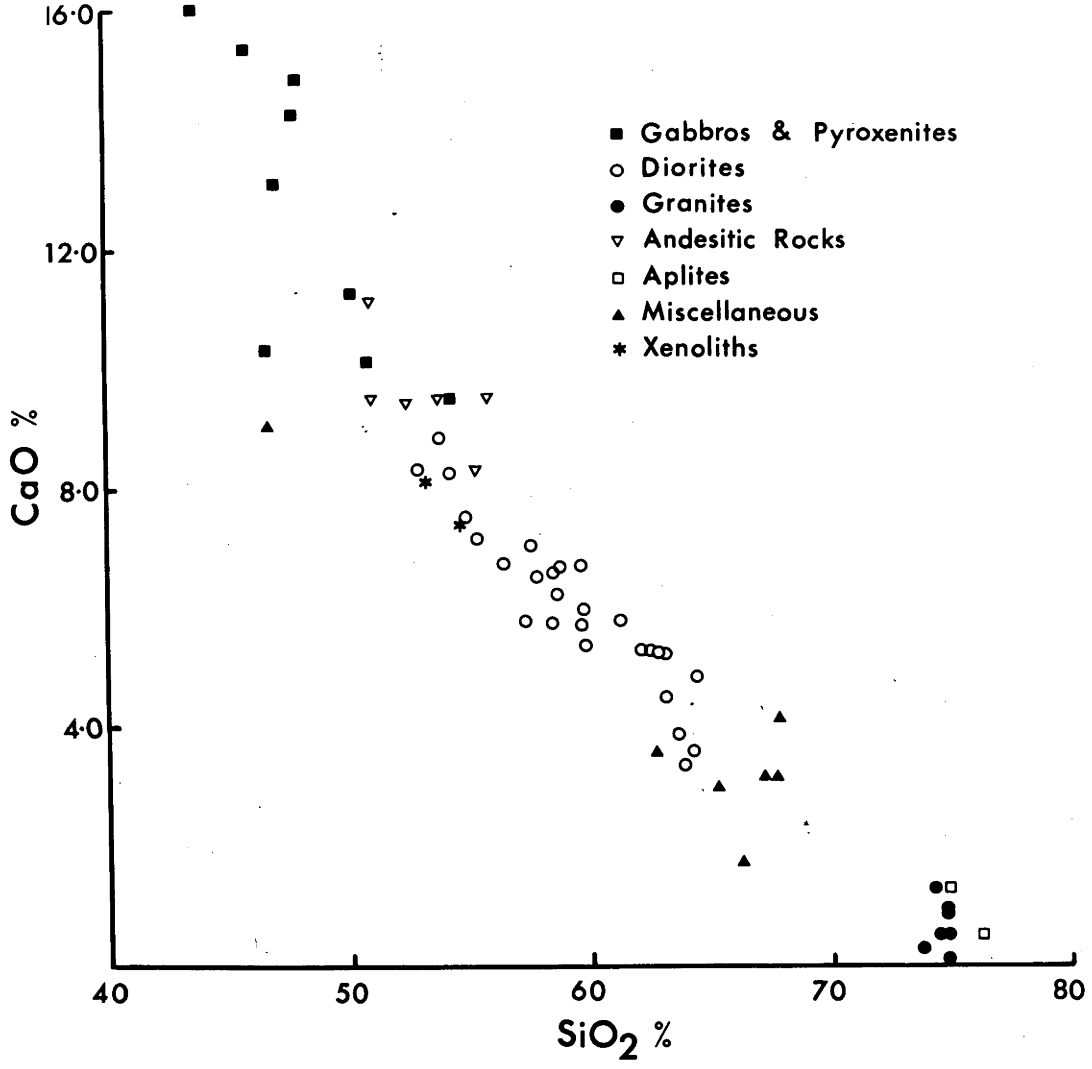

Fig.7 CaO Variation Diagram for the Yeoval Rocks.

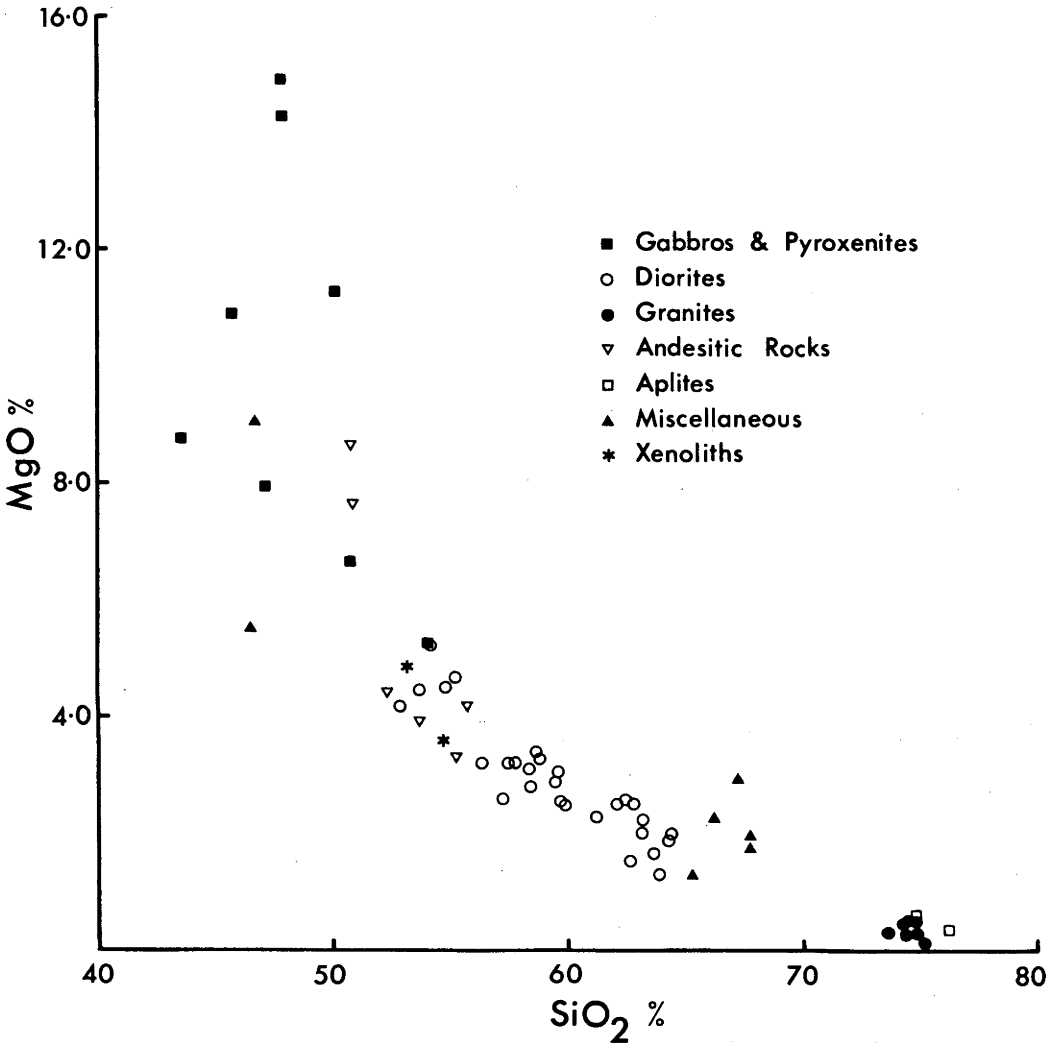

Fig. 8. MgO variation diagram for the Yeoval rocks.

3.6.2. Harker variation diagrams

TiO_2 (Fig.4) Titanium is lower in the gabbros and pyroxenites and has its maximum concentration in the pyroxene-mica diorites. From these rocks it decreases in an irregular fashion to the orthoclase diorites and drops sharply in the granites.

Al_2O_3 (Fig.5) The most striking feature of the silica-variation diagram for Al_2O_3 is the extremely low contents in the pyroxenites. The Al_2O_3 present in these rocks occurs dominantly in the hornblende and minor plagioclase. There is a more or less regular decrease from the gabbros to the orthoclase diorites and a sharp drop of about 2% Al_2O_3 to the granites.

FeO (Fig.6a) Because the ferric iron content of most samples is very low, total iron expressed as FeO is plotted against silica. Although the usual scatter of the "accumulative" rocks is still present, there is a linear trend for the association (disregarding the hiatus between the orthoclase diorites and granites).

MnO (Fig.6b) Superimposed on the scatter of points is an overall decrease in MnO from the gabbros to the granites.

CaO and MgO (Figs.7 and 8) Calcium and magnesium display a wide scatter near the basic end of the association, changing to a fairly smooth trend from the pyroxene-mica to the orthoclase diorites, with the usual break between

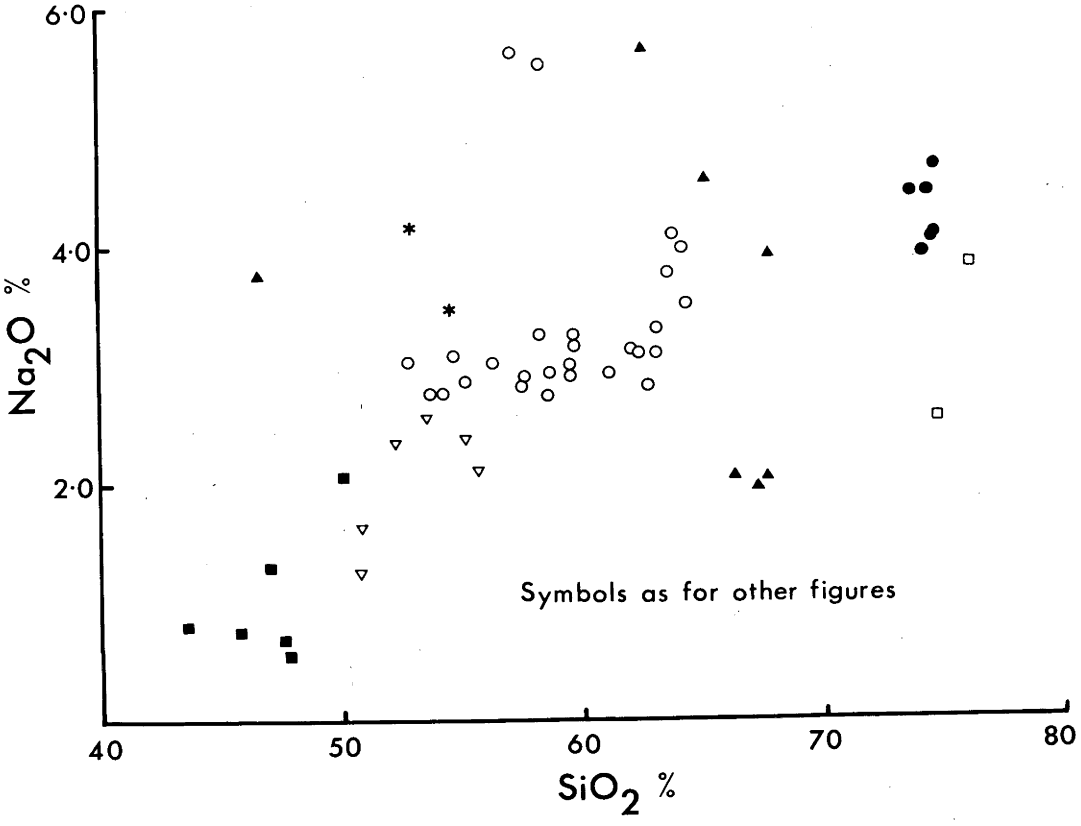

Fig.9 Na_2O Variation Diagram for the Yeoval Rocks.

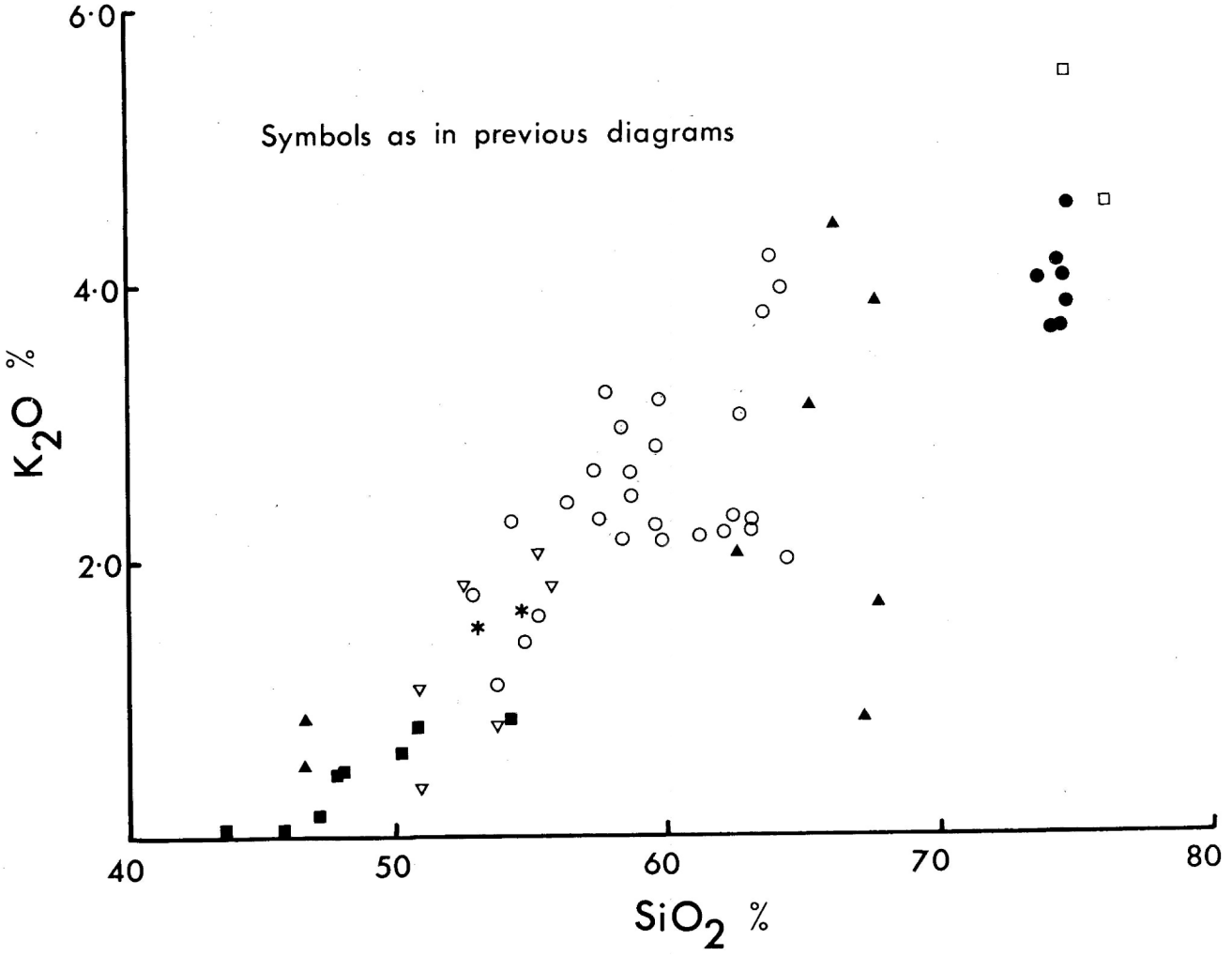

Fig.10 K_2O variation diagram for the Yeoval rocks.

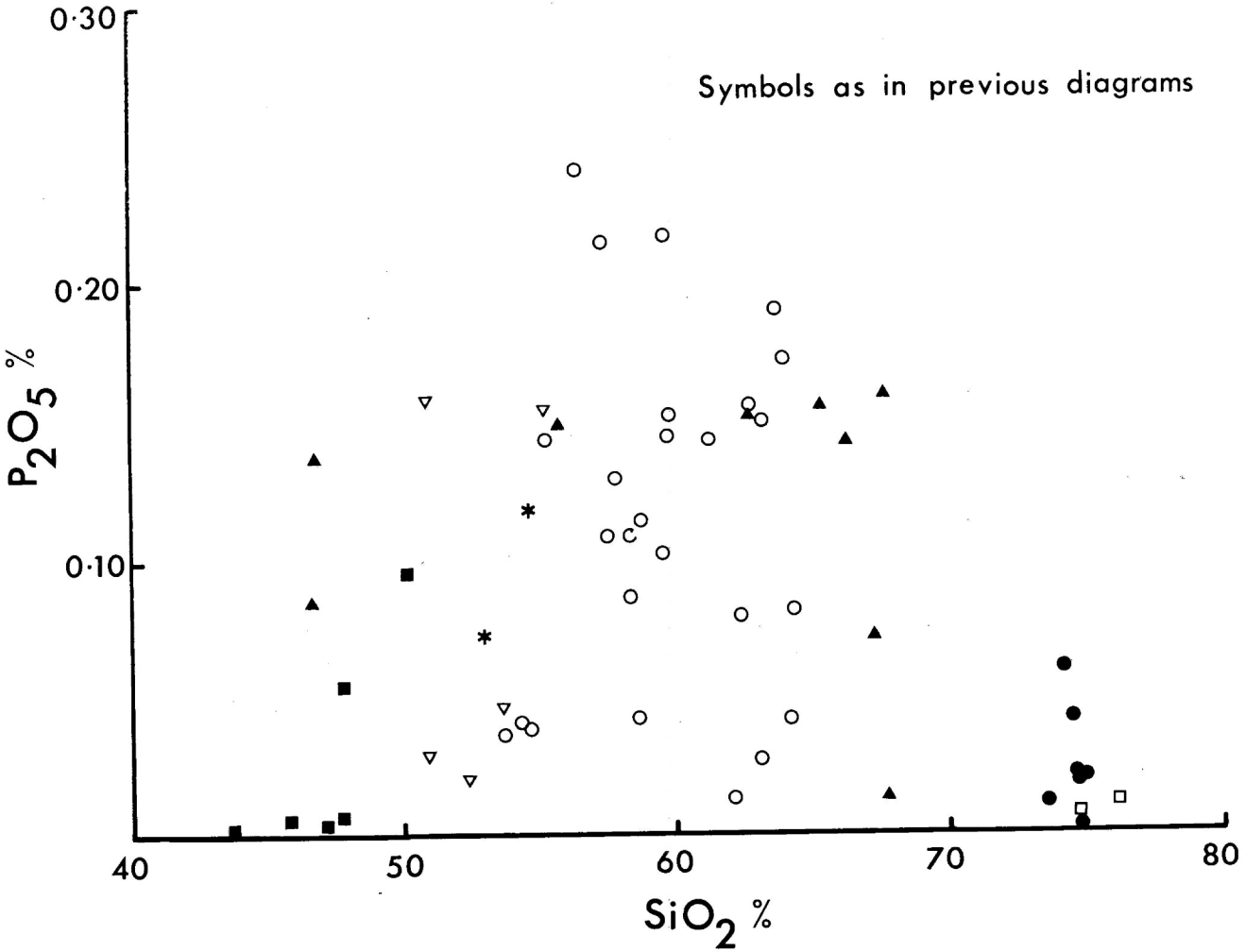

Fig.11 P_2O_5 variation diagram for the Yeoval rocks.

the orthoclase diorites and the granites.

Na_2O (Fig.9) There is an overall increase in Na_2O from the gabbros to the granites, with large variations in the sodium content of the diorites; some containing up to 5.6% Na_2O. The Yeoval gabbros have very much lower Na_2O contents (0.76 to 1.30%) than the average gabbro (2.26% Na_2O) of Nockolds (1954).

K_2O (Fig.10) Potassium follows sodium to a certain extent with low concentrations in the gabbros and pyroxenites and higher concentration in the orthoclase diorites. Two unusual features are

(1) similar K_2O contents of the orthoclase diorites and granites;

(2) apparent divergence from the main trend of a number of samples having K_2O concentrations of about 2.2%.

P_2O_5 (Fig.11) Although no trends are obvious in the phosphorous contents, the low amounts in the gabbros and granites are important features.

3.7. COMPARISON WITH AVERAGE ANALYSES OF NOCKOLDS (1954)

In Table 12 a comparison of the Yeoval rocks is made with Nockolds' (1954) average gabbro, pyroxene-mica diorite, hornblende-biotite diorite and hornblende-biotite mangerite (orthoclase diorite).

TABLE 12

Comparison of Compositions of the Yeoval Diorites with Various Average Compositions Listed by Nockolds (1954)

	Gabbro		Pyroxene-Mica Diorite		Hornblende-Biotite Diorite		Orthoclase Diorite	
	Avge	Yeoval	Avge	Yeoval	Avge	Yeoval Quartz-Mica Diorite	Avge	Yeoval
SiO_2	48.36	43.5	52.63	54.6	52.97	59.7	55.86	63.9
TiO_2	1.32	0.4	1.29	0.7	1.60	0.5	1.09	0.5
Al_2O_3	16.84	17.4	15.58	17.1	18.19	16.5	17.22	15.6
Total FeO	10.22	9.2	8.99	7.8	8.07	6.0	7.64	4.3
MgO	8.06	9.2	6.88	4.5	4.75	2.9	3.42	1.5
CaO	11.07	14.8	8.65	7.8	7.61	6.0	6.75	3.6
Na_2O	2.26	0.9	3.16	2.9	3.50	3.80	3.57	4.0
K_2O	0.56	0.10	1.42	1.36	1.65	2.43	2.82	4.0

The Yeoval gabbros have much lower SiO_2, TiO_2 and alkali contents than Nockolds' average gabbro. They are also exceptionally high in CaO content.

The pyroxene-mica diorites from Yeoval have higher aluminium, and lower iron, magnesium and calcium than Nockolds' average. The average orthoclase diorite of Nockolds is fairly similar to the Yeoval quartz-mica diorite.

SUMMARY

The most important chemical properties of the Yeoval rocks may be summarised as follows:

(i) A break in the silica-variation diagram for all elements in the range 65-75% SiO_2

(ii) Fairly smooth curves of the variation diagrams for compositions ranging from the pyroxene-mica diorites to the orthoclase diorites

(iii) Very high calcium content of the gabbros and pyroxenites

(iv) Low alkali content of the gabbros

(v) Similar compositions of the andesitic rocks and the pyroxene-mica diorites

(vi) High potassium content of the diorites in comparison with other well known calc-alkaline diorites.

TABLE 13

Electron Probe Analyses and Structural Formulae of Olivine and Spinel from the Gabbro

	Olivine (W71)	Olivine (W3)	Spinel (approx. analysis)
SiO_2	35.4	36.7	<0.04
TiO_2	<0.03	<0.03	<0.03
Al_2O_3	<0.04	<0.04	60.1
FeO	27.4	27.9	22.7
MnO	0.6	0.7	0.2
MgO	35.3	35.1	12.5
CaO	<0.04	<0.04	<0.04
Na_2O	<0.04	<0.04	<0.04
K_2O	<0.02	<0.02	<0.04
	98.7	100.4	95.5

Structural Formulae on the Basis of

	4 Oxygen Atoms		32 Oxygen Atoms		
Si	0.964	0.982	Si	-	
Al	-	-	Al^{3+}	15.74	16.00
Ti^{2+}	-	-	Fe^{3+}	0.26	
Fe^{2+}	0.624	0.624	Ti	-	
Mg	1.434	1.400	Mg^{2+}	4.14	
Mn	0.013	0.013	Fe^{2+}	3.96	8.14
Ca	-	-	Mn	0.04	
			Ca	-	
$100\left[\frac{Mg}{Mg+Fe^{2+}+Mn}\right]$	69.2	68.7		49.3	

4. MINERALOGY

In this section the various mineral groups from the three major rock types (gabbro, diorite, granite) will be treated separately in the following order:

olivines, pyroxenes, amphiboles, biotites, plagioclase feldspars, potassium feldspars, zircons, apatites.

Only the major element chemistry will be presented, the trace element data for the total rocks and constituent minerals are given in a later section (section 5.2). Discussion of the distribution of the various elements between the different mineral phases will be deferred until the individual mineral groups have been described. Only limited optical data are available. Except where indicated, all determinations of major elements have been carried out on the electron probe (Appendix I).

4.1 OLIVINES

Olivine is restricted to the gabbros and pyroxenites where it occurs as anhedral, colourless, homogeneous grains. Analyses of olivines from two gabbros are given in Table 13 along with their respective structural formulae. From this table it can be seen that no CaO, Al_2O_3, TiO_2, Na_2O or K_2O were detected, which supports Smith's (1966) claim that any significant amounts (say, above 0.5%) of these elements reported in olivine are due to impurities. The forsterite

TABLE 14

Electron Probe Analyses and Structural Formulae of Pyroxenes from the Yeoval Rocks

	Gabbro (W71)		Diorite (G120)	Pyroxenite (W61)	
	OPX	CPX	CPX	OPX	CPX
SiO_2	53.2	52.1	51.4	53.0	53.7
TiO_2	<0.03	0.5	0.5	<0.03	0.2
Al_2O_3	1.3	2.8	3.1	0.7	1.3
FeO	17.3	8.0	8.8	18.4	6.2
MnO	0.6	0.7	0.4	0.4	0.7
MgO	26.3	14.9	14.7	25.4	16.3
CaO	1.0	21.5	20.9	0.7	23.0
Na_2O	<0.04	0.2	0.4	<0.04	0.1
K_2O	<0.02	<0.02	<0.02	<0.02	<0.02
	99.7	100.7	100.2	98.6	101.5
Structural Formulae on the Basis of 6 Oxygen Atoms					
Si	1.946	1.925	1.983	1.968	1.953
Al	0.057	0.075	0.017	0.031	0.047
Al	-	0.045	0.124	-	0.010
Ti_{3+}	-	0.013	0.015	-	0.007
Fe^{3+}	-	-	-	-	-
Cr	-	-	-	-	-
Mg_{2+}	1.434	0.821	0.845	1.406	0.884
Fe^{2+}	0.530	0.246	0.286	0.571	0.188
Mn	0.018	0.018	0.013	0.013	0.022
Ca	0.040	0.850	0.864	0.027	0.897
Na	-	0.007	0.030	-	0.009
K	-	-		-	-
Z	2.003	2.000	2.000	1.999	2.000
X+Y	2.022	2.000	2.177	2.017	2.017
$100\left[\frac{Mg}{Mg+Fe^2}\right]$	73.0	76.9	74.7	71.1	82.5
Atomic Proportions					
Mg	71.3	42.4	42.1	69.7	44.4
Fe	26.5	13.6	14.9	29.0	10.5
Ca	2.2	43.9	43.0	1.3	45.1

component is approximately 70 molecular %, which compares favourably with 69 to 75% for olivines (composition determined optically) in gabbros from the Southern California Batholith (Miller 1937) and Garabal Hill (Nockolds 1941), and is slightly higher than those reported by Deer et al. (1961) for gabbros in general.

A common product in thereaction rim around olivine against plagioclase is a green spinel. An approximate analysis (Table 13) indicates that it is a magnesian hercynite. A more accurate analysis could not be obtained owing to the very fine grain-size.

4.2. PYROXENES

Both clino- and orthopyroxene occur in the gabbros and pyroxenites whereas clinopyroxene, rimmed by hornblende, is dominant in the diorites; remnant grains of orthopyroxene are sometimes found, particularly in the more basic diorites.

The orthopyroxene in the gabbro and pyroxenite is bronzite but close to hypersthene (Table 14, Fig.12) according to the classification of Deer et al. (1962a). It is pleochroic from pale pink to very pale green to colourless, and is biaxial negative. Analyses (Table 14) of bronzites from the gabbro and the pyroxenite are very similar. The orthopyroxene in basic rocks from Garabal Hill (Nockolds 1941) and the Southern California Batholith (Larsen and Draisin 1948) is hypersthene.

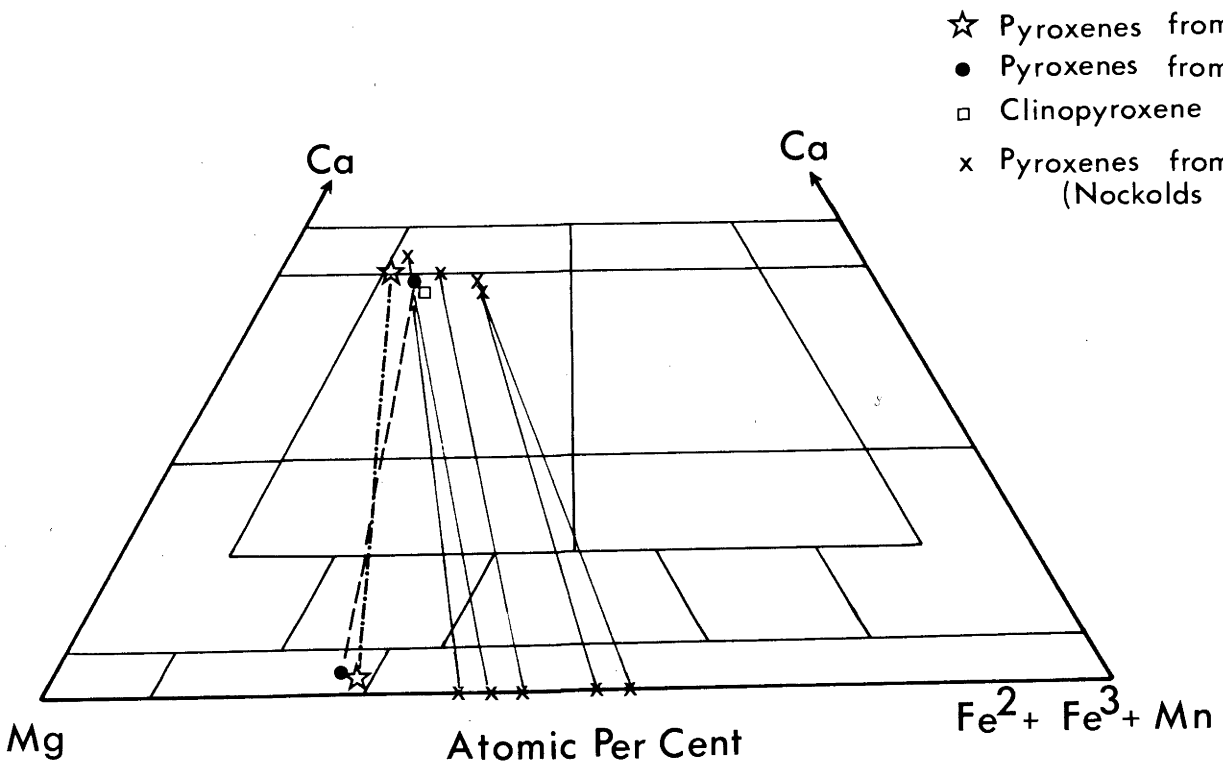

Fig.12 Distribution of pyroxene analyses with respect to Ca, Mg and (Fe^{2+} + Fe^{3+} + Mn) atoms for the Yeoval rocks.

The Yeoval and Garabal Hill orthopyroxenes are plotted on the pyroxene quadrilateral in Fig.12.

Miller (1937), in a study of co-existing plagioclase and hypersthene from the San Marcos gabbro of the Southern California Batholith, observed the anorthite content of the plagioclase to decrease as the iron increased in the hypersthene. Such a correlation is also present in both the Yeoval gabbros and the Garabal Hill rocks.

The clinopyroxene in the gabbros, pyroxenites and diorites is colourless with $Z \wedge C$ ranging from 38° to 44°. The clinopyroxenes from the diorites and gabbros are similar in composition (Table 14) and plot in the augite field of the pyroxene quadrilateral (Fig.12). The clinopyroxene in the pyroxenite has higher SiO_2, MgO and CaO, and lower Al_2O_3 and FeO and plots at the junction of the diopside-salite-augite field (Fig.12).

No compositional variations (within experimental limits) were found in the clinopyroxenes in the gabbro. The alteration to uralite of the clinopyroxenes in the pyroxenites prevent detailed examination of possible zoning. In the diorites, crystals were traversed to check both zoning and other inhomogenieties for the elements Si, Al, Fe, Mg, Ca and Mn. No zoning was observed and the only elements to show any significant variation, were Fe (probably due to fine opaque inclusions) and Ca.

4.3. AMPHIBOLES

Amphibole, as the mineral hornblende, is the dominant ferromagnesian mineral in the diorites and is sparsely distributed in the granites. In the gabbros and pyroxenites it occurs as a fibrous variety, uralite, and replaces pyroxene. The very basic phases of diorite (or more acid phases of gabbro) have primary hornblende rimming the pyroxene which has the same properties as that in the pyroxene-mica and quartz-mica diorites. The optical properties of the hornblendes in the orthoclase diorites are the same as those of the hornblendes in the other diorites. The absorption scheme in the hornblende is always $X \sim Y < Z$ and the pleochroic scheme in the diorites and granites is as follows:

Diorites	Granites
X - pale yellow green	X - pale yellow green
Y - pale green	Y - pale green
Z - deep olive green	Z - brownish green

Twenty-four amphiboles have been analysed (Table 15) - two from the pyroxene-mica diorite, sixteen from the quartz-mica diorite, one from the orthoclase diorite (and two partial analyses), three from the granite and two from the pyroxenite. Totals have not been computed for most samples as water determinations were not carried out due to insufficient sample. Water was determined (along with other major elements)

TABLE 15

Electron Probe, Chemical Analyses and Structural Formulae of Hornblendes from Yeoval Rocks

	Pyroxene-mica Diorite		Quartz-mica Diorite					Quartz-mica Diorite			Quartz-mica Diorite				Quartz-mica Diorite			Orthoclase Diorites		Granites		
	Y8	G154	Y161+	G120	Y75	Y41	Y150	G107+	Y235	Y71	Y148	G110	G99	G92	G118	Y151+	G90	Y227+	Y205	Y206	Y43	Y53	Y64
SiO_2	47.7	47.8	47.71	47.8	47.9	48.0	48.0	48.59	48.8	49.0	49.0	49.1	49.3	49.4	49.7	49.98	50.0	50.05	46.2	n.d.	48.6	45.0	45.4
TiO_2	0.9	0.9	0.86	1.0	0.8	0.9	0.9	0.85	0.9	0.9	0.8	0.8	0.8	0.8	0.8	0.85	0.7	0.77	1.1	n.d.	1.0	1.0	1.13
Al_2O_3	5.4	5.1	5.76	5.1	4.6	5.1	5.2	4.82	5.5	4.4	4.5	4.3	4.5	4.5	4.6	4.14	4.4	4.56	5.2	n.d.	4.4	5.1	4.2
Fe_2O_3	3.71	3.82	4.17	4.22	4.16	4.18	4.92	3.96	4.46	4.67	4.26	3.96	4.53	4.12	3.72	3.54	(6.8)	3.51	4.40	(23.4	6.96	7.3	8.1
FeO	14.07	14.90	12.45	15.52	13.20	14.68	13.39	12.63	14.52	13.37	12.72	14.09	13.55	13.07	13.15	(9.93)	12.2	13.03	15.29	n.d.	15.22	20.3	22.5
MnO	0.5	0.6	0.55	0.5	0.5	0.6	0.6	0.56	0.7	0.6	0.6	0.6	0.5	0.6	0.6	0.78	0.6	0.54	0.6	n.d.	0.7	0.7	0.7
MgO	12.4	12.6	13.26	12.4	13.3	11.9	12.3	13.22	12.6	12.7	13.3	13.2	13.2	13.2	12.8	(15.46)	13.7	12.51	10.7	10.9	11.7	7.3	6.1
CaO	12.4	12.5	11.46	11.5	11.8	11.6	12.7	11.77	12.6	11.1	11.4	11.3	11.7	12.5	11.3	11.44	11.2	11.66	10.0	11.1	11.2	10.8	10.7
Na_2O	0.80'	0.88'	0.50	0.9	0.82'	1.00'	0.85'	0.86	0.86	0.8	0.9	1.04'	0.96'	0.75'	1.10'	0.79	0.50'	0.80	1.13'	n.d.	1.2	1.5	1.55'
K_2O	0.65	0.60	0.55	0.7	0.65	0.65	0.56	0.54	0.56	0.6	0.5	0.61	0.47	0.60	0.52	0.39	0.50	0.59	0.8	n.d.	0.5	0.7	0.56
P_2O_5	n.d.	0.20	0.05	n.d.	n.d.	n.d.	0.07	0.03	0.06	n.d.	n.d.	0.05	0.05	n.d.	0.01	0.06	n.d.	0.03	n.d.	n.d.	n.d.	n.d.	n.d.
H_2O^+	n.d.	n.d.	2.30	n.d.	n.d.	n.d.	n.d.	2.03	n.d.	n.d.	n.d.	n.d.	n.d.	n.d.	n.d.	2.36	n.d.	1.97	n.d.	n.d.	n.d.	n.d.	n.d.
H_2O^-	n.d.	n.d.	0.04	n.d.	n.d.	n.d.	n.d.	0.06	n.d.	n.d.	n.d.	n.d.	n.d.	n.d.	n.d.	0.07	n.d.	0.06	n.d.	n.d.	n.d.	n.d.	n.d.
CO_2	n.d.	n.d.	0.15	n.d.	n.d.	n.d.	n.d.	0.11	n.d.	n.d.	n.d.	n.d.	n.d.	n.d.	n.d.	0.23	n.d.	0.12	n.d.	n.d.	n.d.	n.d.	n.d.
	98.53	99.70	99.81	99.64	97.73	98.61	99.49	100.05	101.56	98.14	97.98	99.05	99.56	99.54	98.40	100.02	100.60	100.20	94.70				
Σ FeO (Chemical)	17.45	18.38	16.24	19.36	16.98	18.48	17.86	16.23	18.56	17.62	16.60	17.70	17.67	16.84	16.54	13.12	20.51	16.19	19.37	n.d.	20.64	n.d.	30.51
Σ FeO (Probe)	17.3	n.d.	n.d.	19.3	17.3	18.4	n.d.	n.d.	n.d.	17.8	16.6	17.6	17.6	16.8	16.7	n.d.	18.3	n,d.	19.4	21.1	18.9	26.9	29.3
	Structural Formulae on the Basis of 23 Oxygen Atoms. Water Free																						
Si	7.045	7.018	7.064	7.034	7.108	7.100	7.035	7.221	7.017	7.218	7.207	7.193	7.173	7.180	7.278	7.292	7.167	7.338	7.122		7.074	6.867	6.950
Al	0.941	0.882	0.936	0.884	0.804	0.888	0.898	0.779	0.931	0.765	0.781	0.743	0.771	0.772	0.722	0.708	0.744	0.662	0.878		0.756	0.917	0.758
Al	-	-	0.069	-	-	-	-	0.066	-	-	-	-	-	-	0.078	0.004	-	0.126	0.067		-	-	-
Ti	0.105	0.117	0.096	0.107	0.089	0.106	0.100	0.095	0.098	0.118	0.088	0.088	0.087	0.087	0.088	0.093	0.076	0.085	0.128		0.109	0.115	0.130
Fe^{3+}	0.412	0.420	0.465	0.465	0.469	0.466	0.341	0.443	0.487	0.521	0.476	0.440	0.493	0.449	0.408	0.386	0.734	0.388	0.511		0.766	0.838	0.933
Fe^{2+}	1.741	1.830	1.542	1.907	1.638	1.818	1.643	1.569	1.744	1.651	1.562	1.727	1.655	1.592	1.617	1,212	1.463	1.598	1.972		1.851	2.590	2.881
Mn	0.062	0.075	0.069	0.062	0.062	0.075	0.075	0.071	0.086	0.075	0.075	0.075	0.062	0.074	0.075	0.096	0.073	0.067	0.079		0.087	0.091	0.091
Mg	2.691	2.724	2.743	2.532	2.817	2.461	2.682	2.802	2.642	2.540	2.712	2.656	2.687	2.805	2.567	3.149	2.646	2.565	2.110		2.285	1.427	1.059
Ca	0.038	0.033	0.182	0.187	0.124	0.162	0.005	0.126	0.058	0.248	0.203	0.226	0.176	0.054	0.227	0,212	0.280	0.168	0.348		0.253	0.234	0.343
	1.962	1.967	1.818	1.813	1.876	1.838	1.995	1.874	1.942	1.752	1.797	1.774	1.824	1.946	1.773	1.788	1.720	1.832	1.652		1.747	1.766	1.657
Na	0.239	0.251	(0.144)	0.256	0.235	0.286	0.241	0.248	0.240	0.228	0.256	0.296	0.275	0.211	0.315	0.228	(0.140)	0.229	0.337		0.339	0.452	0.460
K	0.122	0.113	0.104	0.131	0.123	0.110	0.104	0.102	0.102	0.113	0.094	0.114	0.087	0.112	0.097	(0.070)	0.092	0.106	0.157		0.093	0.136	0.109
Z	7.99	7.90	8.00	7.92	7.91	7.99	7.93	8.0	7.95	7.98	7.99	7.94	7.94	7.95	8.00	8.00	7.91	8.00	8.00		7.83	7.78	7.71
Y	5.01	5.17	4.98	5.07	5.08	4.93	5.04	5.05	5.06	4.91	4.91	4.99	4.98	5.01	4.83	4.94	4.99	4.83	4.87		4.90	5.06	5.09
X	2.00	2.00	2.00	2.00	2.00	2.00	2.00	2.00	2.00	2.00	2.00	2.00	2.00	2.00	2.00	2.00	2.00	2.00	2.00		2.00	2.00	2.00
A	0.35	0.36	(0.25)	0.39	0.36	0.40	0.35	0.35	0.34	0.34	0.34	0.41	0.36	0.32	0.41	0.30	(0.23)	0.34	0.49		0.43	0.59	0.57
$100\frac{Mg}{Mg+Fe^{2+}+Fe^{3+}+Mn}$	55.2	54.2	58.5	52.8	57.6	52.6	54.3	58.4	53.8	55.4	58.0	56.2	56.4	57.5	57.1	(66.5)	56.3	57.1	49.0		48.4	32.1	26.3

\+ FeO and Fe_2O_3 analyses by E. Kiss

' Alkalis (both Na_2O and K_2O) determined by Flame Photometry

n.d. Not determined

Brackets indicate not included in average

in four samples by E. Kiss. The average of these is 2% and assuming this average applies for all hornblendes from the quartz-mica diorite then the totals range from 99.7 to 103.6%.

In the analysis of natural minerals by the electron probe, a variation in composition between grains is apparent, particularly for hornblendes and biotites. The degree of heterogeneity varies significantly from one sample to another, and may well be a function of crystallisation or some other factor such as late stage deuteric alteration. If the heterogeneity between crystals was a function of crystallisation then one could expect some compositional variation within crystals. Zoning of hornblende was checked in a number of polished thin sections, and no variation was detected. Erratic results may be obtained if remnant cores or areas of pyroxene (now uralite) in hornblende are analysed. That the heterogeneities between grains in some samples is due to late stage alteration is supported by the degree of alteration of the co-existing minerals, viz: biotites almost completely altered to chlorite and epidote; plagioclase heavily saussuritised. This suggestion is clearer if reference is made to Table 16 where the analyses of hornblende from a fresh (Y41) and an altered (G92) quartz-mica diorite are compared. Here, the single grain analyses of the fresh diorite show little or no variation for all elements; whereas the Si, Fe and Mg vary

TABLE 16

Comparison of Probe Analyses of 10 Different Hornblende Grains from (a) Fresh and (b) Altered Rock

											Average
(a) Fresh											
SiO_2	47.8	47.7	47.7	48.0	47.9	48.2	47.9	48.2	48.1	48.0	48.0
TiO_2	0.95	0.93	0.94	0.96	0.96	1.00	0.95	0.95	0.96	0.94	0.95
Al_2O_3	5.4	5.5	4.8	5.2	5.3	4.9	4.8	4.9	5.0	4.9	5.1
ΣFe_2O_3	20.5	20.6	20.3	20.2	20.1	20.1	21.0	20.4	20.2	20.3	20.4
MnO	0.60	0.65	0.62	0.62	0.60	0.60	0.61	0.65	0.62	0.60	0.62
MgO	11.6	11.9	12.2	12.0	11.9	11.9	12.3	11.9	11.9	11.7	11.9
CaO	11.7	11.6	11.6	11.5	11.9	11.8	11.9	11.2	11.3	11.6	11.6
Na_2O	1.00	0.99	0.99	1.01	0.99	1.00	0.96	1.00	0.99	0.99	1.0
K_2O	0.67	0.60	0.59	0.64	0.71	0.70	0.66	0.66	0.60	0.64	0.65
(b) Altered Rock											
SiO_2	50.0	49.3	48.4	49.4	50.0	49.0	50.2	49.3	49.0	49.7	49.4
TiO_2	0.81	0.87	0.90	0.84	0.81	0.84	0.79	0.84	0.86	0.83	0.84
Al_2O_3	4.7	4.5	4.4	4.9	4.7	4.7	4.0	4.7	4.5	4.4	4.5
1st run ΣFe_2O_3	18.4	19.3	19.4	17.9	17.8	19.3	17.7	18.5	17.7	18.2	18.4
MnO	0.63	0.59	0.56	0.60	0.57	0.60	0.65	0.56	0.61	0.63	0.60
MgO	13.3	12.9	12.6	13.5	13.7	12.9	13.8	13.2	12.9	13.0	13.2
CaO	12.3	12.4	12.9	12.9	12.3	12.9	12.0	12.5	12.3	12.5	12.5
Na_2O	0.82	-	0.78	0.73	0.72	0.80	0.73	0.75	0.80	0.70	0.75
K_2O	0.60	0.59	0.62	0.58	0.58	0.61	0.59	0.61	0.59	0.59	0.60
2nd run ΣFe_2O_3	20.1	19.2	18.3	19.5	18.9	16.7	17.9	19.4	19.2	17.2	18.6
3rd run ΣFe_2O_3	19.2	18.9	19.6	19.2	17.2	18.1	18.7	19.4	18.8	17.6	18.7

significantly in the hornblende grains from the altered rock. Owing to machine conditions at the particular time, iron was repeated for each run of analyses (i.e. Fe Si Al; Fe Ca Mg; Fe K Na) and the results for two other iron runs are reproduced at the bottom of Table 16. When using grain mounts, it is impossible to analyse exactly the same grains on each run except when there are very few grains. The data in Table 16 indicate that although analyses from grain to grain may vary significantly, the average of a number of grains gives a fairly reliable result. This is born out in Table 15, where the chemical and probe total iron analyses are shown to compare favourably.

Twenty-two analyses of hornblendes from the diorite and granite are presented in Table 15. The structural formulae have been calculated water-free, on the basis of 23 oxygen atoms according to the general amphibole formula:

$$A\ X_2\ Y_5\ Z_8\ O_{22}\ \ (OH, F, Cl)_2$$

where A represents a normally vacant site in amphibole which may be occupied by the alkalis; X = Ca; Y = Mg, Fe^{2+}, Fe^{3+}, Al, Ti, Mn, Cr, Li, Zn; Z = Si, Al.

With the exception of the hornblendes from granites all the analyses contain close to the prescribed number of 5 atoms in the Y site and 8 in the Z site. Except for five analyses, the Z site is slightly less than eight which is due to an

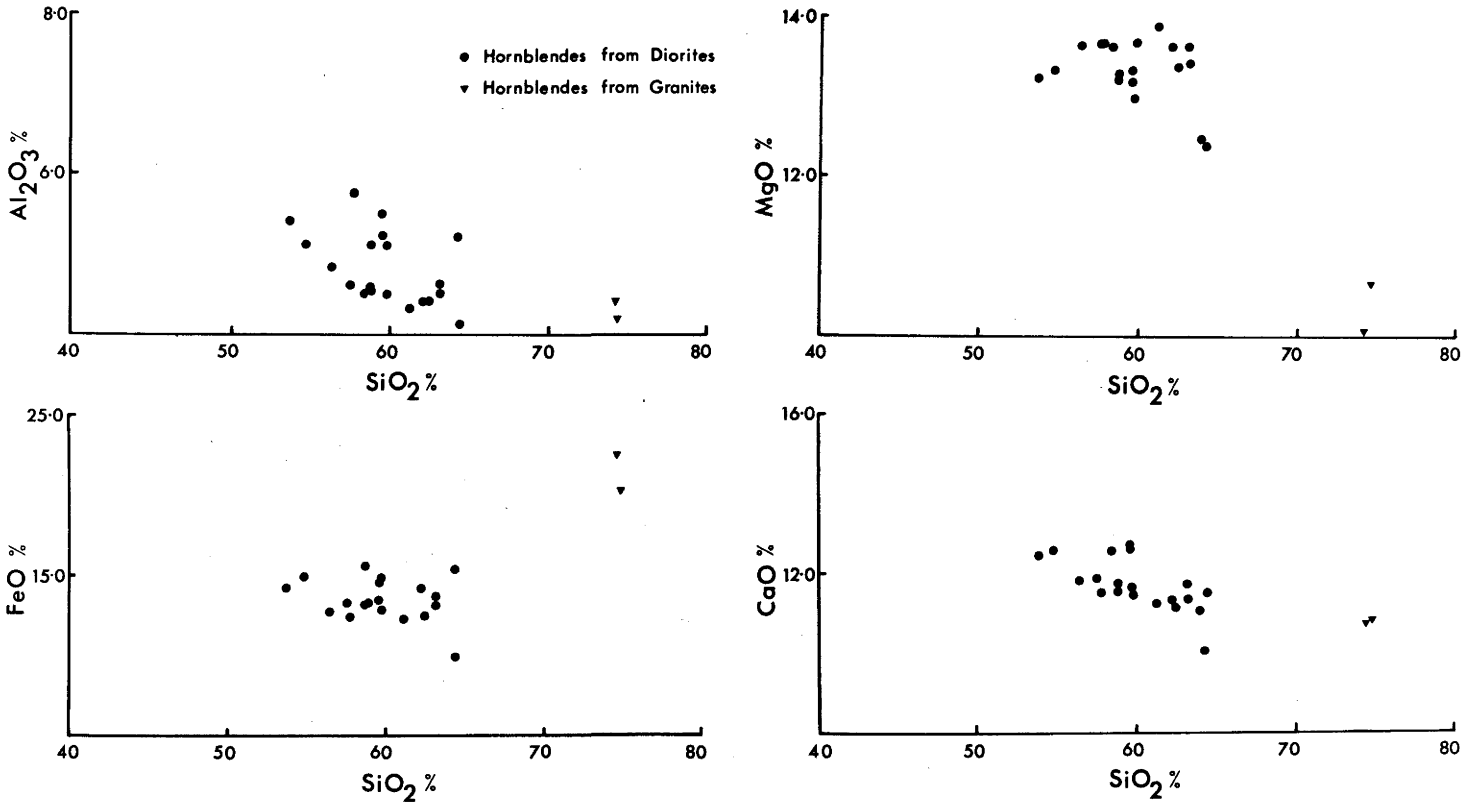

Fig.13 Composition of the hornblendes plotted against position on the variation diagram of the enclosing rock.

apparent aluminium deficiency. All aluminium is taken up in tetrahedral co-ordination, but only in one analysis does the tetrahedrally co-ordinated aluminium exceed 1 atom/formulae unit. The general absence of aluminium in octahedral co-ordination in the Yeoval hornblendes contrasts with published analyses where values range from zero to 0.83 atoms/formula unit. Chappell (1966) also reported low values (0.09 - 0.20 atoms) for aluminium in octahedral co-ordination from hornblendes in the Moonbi granites. He suggested that the high values for aluminium in both tetrahedral (>1) and octahedral co-ordination (>0) in granites and diorites may be due to analytical error inherent in the classical method of aluminium analysis and non-determination of P_2O_5.

The Al_2O_3 content for the amphiboles decreases slightly with increasing SiO_2 in the dioritic host rock (Fig.13) and in the Al_2O_3 versus SiO_2 for the whole rock (Fig.5).

Ti and Fe^{3+} + Fe^{2+} do not show a great deal of variation in the one rock type (i.e. diorite) but in passing from the diorite to granite the hornblendes show a slight increase in Ti (from 0.08 - 0.13 atoms/formula unit) and a marked increase in Fe^{2+} (1.54 - 1.88). This is illustrated (along with other elements) in Fig.13, where the composition of the hornblendes is plotted against the position on the variation diagram of the enclosing rock.

The Ti contents of the hornblendes in the Yeoval diorites and granites are low (average <0.1 atoms formula unit) compared with published analyses. This may be the result of

varying physical conditions of crystallisation of the hornblende, allowing more Ti to enter the structure or it may be analytical error in published analyses. The presence of very fine ilmenite inclusions quite often associated with hornblende would affect the Ti contents considerably whereas analyses with the microprobe eliminate such errors.

Excluding some values which are probably the result of deuteric alteration, the Fe^{3+} contents are fairly constant around 0.4 atoms/formula unit. This is in good agreement with average published values of 0.4 - 0.6.

The replacement of Mg by Fe^{2+}, expressed as the ratio 100 Mg : (Mg + Fe^{2+} + Fe^{3+} + Mn) is fairly constant in the diorite hornblendes ranging from 58.5 to 52.6: it drops to 26.3 in the granite hornblendes.

The distribution of CaO between the hornblendes from the different rocks is shown in Fig.13; a slight decrease from the more basic to silicic rocks is obvious. The Ca contents of a number of hornblendes from the diorite approach the maximum number of 2 atoms per formula unit and range in value from 1.720 - 1.995. In the granite, the CaO contents vary from 1.657 - 1.747 per formula unit. These values are in good agreement with the value of 1.8 $\pm$ 0.1 Ca atoms per formula unit for the majority of hornblendes given by Deer et al. (1963a). Chappell (1966) suggests that "Ca values in hornblendes must

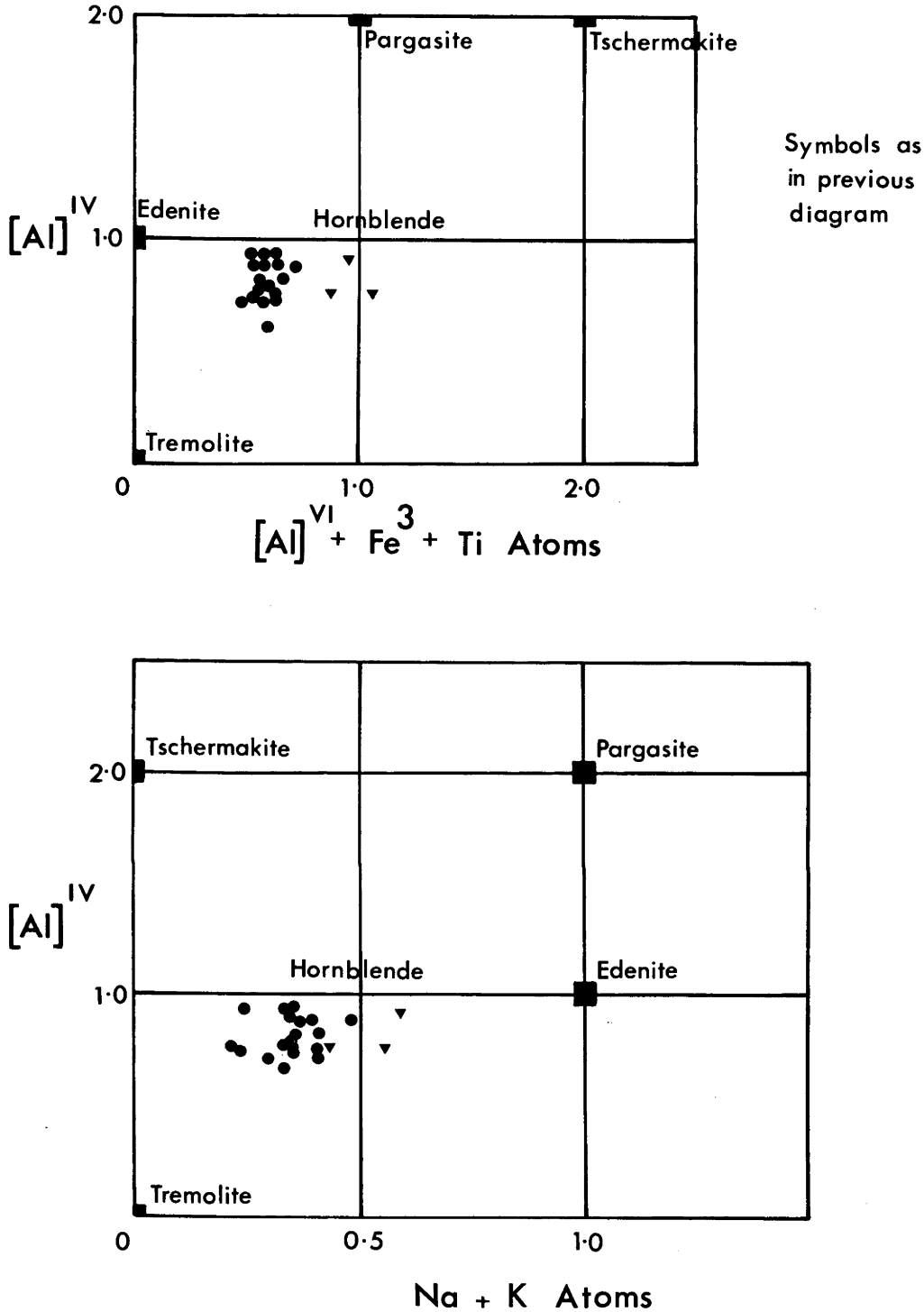

Fig.14 Chemical variation of the calcium-rich-amphiboles expressed as the numbers of ($Al^{VI} + Fe^{3} + Ti$), (Na + K) + Al^{IV} atoms per formula unit. (After Deer et al. 1963a)

generally be in error because of failure to correct for apatite inclusions."

The Na contents of hornblendes in the diorites (disregarding Y161, G90) are generally more than twice that of the K contents and range from 0.21 to 0.31 atoms/formula unit. In the granites the Na extends to 0.46 atoms/formula unit. On the other hand, K contents show no positive trend. The "A" group of atoms for the hornblendes in the diorite are thus much lower (0.36 average) than most published analyses where the average is 0.5 (Deer et al. 1963a; Chappell 1966).

The classification of amphiboles is a matter for some conjecture, but here that of Deer et al. (1963a) is followed. A plot (Fig.14) of Al^{IV} versus (Na + K) and (Al^{VI} + Fe^{3+} + Ti) atoms show that the amphiboles from the Yeoval diorites and granites scatter around common hornblende. However, two points to note are the low (Al^{VI} + Fe^{3+} + Ti) and (Na + K) atom contents in the diorite hornblendes. Perhaps the most interesting features to be noted from the above data on the hornblendes are:

(i) the similarity of the hornblendes in the pyroxene- and quartz-mica diorites

(ii) the gradual increase in Fe and decrease in Mg content from the pyroxene- and quartz-mica diorites through to the orthoclase diorite, with a marked change in the granites.

This is obvious from the ratio 100 Mg : Mg + Fe^{2+} + Fe^{3} + Mn which decreases from 56.0 (average for quartz-mica diorites) to 49.0 (orthoclase diorites) and then drops to 28 in the granites.

(iii) Very slight decrease in Ca from the hornblendes in the diorites to those in the granites.

(iv) Increase in content of A site atoms from 0.36 (average for diorites) to 0.58 in the granite hornblendes.

The misfit in these trends is the hornblende from an adamellite, Y 43. From the optical and chemical data available this hornblende is almost identical to those in the diorite and it is suggested that this particular hornblende could be of xenolithic origin. The trace element data also supports such an origin.

Uralite and Uralitisation

In a previous section the pyroxenite was described as consisting of large crystals of clinopyroxene surrounded by a fibrous amphibole (uralite) with the interstitial areas filled with mosaics of a deep olive-brown hornblende. Analyses of the clinopyroxene, uralite and the olive-brown hornblende are presented in Table 17. For comparison, an analysis of a "hydrothermal fibrous" amphibole from a calcic-hornblende gabbro in the Southern California Batholith (Larsen and Draisin 1948) is given. Structural formulae for the uralite,

TABLE 17

Electron Probe Analyses and Structural Formulae of Minerals from the Pyroxenite

	Clino-pyroxene	Uralite (Alteration of Cpx)	Uralite from S. California Batholith (Larsen & Draisin, 1948)	Olive-Green Hornblende
SiO_2	53.7	49.6	48.55	44.4
TiO_2	0.2	0.6	0.97	1.1
Al_2O_3	1.3	4.2	8.57	7.3
FeO+	6.2	13.3	11.49	15.6
MnO	0.7	0.3	0.09	0.3
MgO	16.3	16.3	14.81	14.1
CaO	23.0	12.4	12.59	12.3
Na_2O	0.1	0.8	0.99	1.4
K_2O	<0.03	0.3	0.16	0.9
Total (Minus H_2O)	101.5	97.8	98.22	97.4

Structural Formulae on the Basis of:

	6 Oxygens	6 Oxygens	23 Oxygens	6 Oxygens	23 Oxygens	23 Oxygens
Si	1.953	1.890	7.246	1.820	6.978	6.688
Al	0.047	0.110	0.722	0.180	1.022	1.296
Al	0.010	0.078	-	0.199	0.431	-
Ti_{2+}	0.007	0.017	0.066	0.027	0.104	0.125
Fe^{2+}	0.188	0.424	1.625	0.360	1.381	1.965
Mn	0.022	0.010	0.037	0.003	0.011	0.038
Mg	0.884	0.926	3.490	0.828	3.111	3.150
Ca	0.897	0.506	0.059) 1.941)	0.506	0.067) 1.939)	0.015) 1.985)
Na	0.009	0.059	0.226	0.072	0.622	0.409
K	-	0.015	0.056	0.008	0.069	0.174
Z	2.00	Z 2.00	7.97	2.00	8.00	7.98
X+Y	2.02	Y) 2.04	5.22)	2.00	5.04	5.28
		X)	2.00)		2.00	2.00
		A	0.28		0.69	0.58
$100\left[\frac{Mg}{Mg+Fe^{2+}}\right]$	82.5	68.6		69.7		61.6
Ti/Fe^{2+}	0.037	0.040				0.064

+Total iron as FeO

calculated on the basis of both 6 and 23 oxygen atoms, is seen to fit both the pyroxene and amphibole structures remarkably well, although there is a slight over-abundance of cations in the Y site of the amphibole.

In the transformation from clinopyroxene to uralite the following major chemical changes may be noted:

(i) Small decrease in SiO_2, and large decrease in CaO content.

(ii) Threefold increase in Al_2O_3; total iron content is doubled; total alkalis increase from 0.1 to 1.1%.

(iii) MgO remains unchanged.

The fibrous amphibole from the Southern California Batholith is remarkably similar to the uralite except for its very high Al_2O_3 content, which seems to be a general feature of the amphiboles from this area (see Larsen and Draisin 1948, Table 3, p.71).

The olive-brown hornblende is completely different from any hornblende present in the diorites or granites, the most marked differences being the low SiO_2, high Al_2O_3, and higher alkalis. The crystallisation of this hornblende will be discussed in a later section dealing with the origin of the pyroxenite.

Compared to the uralite, the olive-brown hornblende has lower SiO_2 and MgO, and higher TiO_2, Al_2O_3, FeO and alkalis, whereas CaO is essentially the same.

4.4. BIOTITES

Biotite occurs in all phases of the diorites, most of the granites and in those phases of the gabbros containing quartz and primary hornblende.

The colour of the biotite varies in the Y (and Z) optical direction from a reddish chocolate-brown to a straw yellow in the X direction. The absorption scheme is always X<Y = Z.

Structural formulae have been calculated on the basis of 22 oxygen atoms, water free, and are given in Table 18a.

Only half the biotites in Table 18a contain sufficient Si and Al to fill the tetrahedral sites indicating a deficiency of Al, a feature which is also common to the hornblendes. The octahedral sites, capable of accommodating 6 atoms per formula unit (for a tri-octahedral mica), only contain from 5.72 to 5.97 atoms. Chappell (1966), in a compilation of 52 analyses of biotites from granitic rocks, found this deficiency in the Y site to be a general feature. Deer et al. (1962b) states that "the octahedral sites are rarely completely filled and it appears that more vacancies occur as the trivalent iron content and the Fe^{2+}:Mg ratio increase". The structural formulae of the biotites from the Yeoval granites have higher Fe^{3+} contents and higher Fe^{2+}:Mg ratios than the biotites from the diorites, yet they have a more complete occupancy of the octahedral sites. The biotites in the diorites show the relationship suggested by Deer et al. (1962b) with respect to Fe^{3+} variation but not for the variation of Fe^{2+}:Mg.

TABLE 18a

Electron Probe Analyses and Structural Formulae of Biotite Co-existing with Hornblende in the Yeoval Diorites and Granites

	Pyroxene-mica Diorite		Quartz-mica Diorite						Granite	
	Y8	G154	G120	Y41	Y235	G107	Y150	Y227	Y43	Y53
SiO_2	35.8	36.6	37.0	36.9	35.6	36.6	36.3	35.8	35.6	34.0
TiO_2	3.5	3.4	3.5	3.8	3.3	3.9	3.1	3.4	3.7	3.5
Al_2O_3	13.3	13.7	13.6	13.3	13.2	13.5	13.2	13.5	12.6	12.4
Fe_2O_3	2.8	6.0	4.8	2.5	4.4	9.3	8.0	9.4	8.2	8.3
FeO	19.7	16.8	20.0	19.6	18.7	13.8	15.2	13.6	17.2	21.7
MnO	0.5	0.6	0.5	0.5	0.6	0.5	0.7	0.6	0.7	0.6
MgO	10.5	10.8	9.6	10.8	10.4	10.9	10.8	10.7	8.8	6.6
CaO	0.1	0.1	0.1	0.1	0.2	0.1	0.1	0.1	0.1	0.1
Na_2O	0.13	0.16	0.14	0.14	0.13	0.13	0.17	0.16	0.12	0.15
K_2O	7.97	7.70	7.91	7.15	7.45	7.24	8.47	7.89	7.58	6.80
P_2O_5	0.009	0.024	0.037	0.101	n.d.	n.d.	n.d.	0.013	0.094	0.137
H_2O^+					5.22		3.66		4.97	
Σ Fe as FeO	22.2	22.2	21.9	21.9	22.7	22.2	22.4	22.1	24.6	29.2
					99.2		99.7		99.6	
	Structural Formulae on the Basis of 22 Oxygen Atoms. Water Free									
Si	5.570	5.570	5.596	5.653	5.544	5.497	5.518	5.455	5.537	5.435
Al	2.430	2.430	2.404	2.347	2.423	2.390	2.366	2.424	2.310	2.336
Al	0.008	0.028	0.019	0.054	-	-	-	-	-	-
Ti	0.409	0.390	0.398	0.438	0.387	0.440	0.354	0.390	0.433	0.421
Fe^{3+}	0.327	0.688	0.547	0.289	0.517	1.051	0.915	1.080	1.052	0.999
Fe^{2+}	2.563	2.138	2.530	2.511	2.436	1.734	1.993	1.738	2.237	2.901
Mn	0.065	0.071	0.064	0.064	0.080	0.063	0.090	0.078	0.093	0.082
Mg	2.434	2.450	2.164	2.466	2.414	2.439	2.447	2.430	2.039	1.571
Ca	0.017	0.016	0.016	0.016	0.033	0.014	0.016	0.016	0.017	0.017
Na	0.038	0.048	0.042	0.042	0.038	0.038	0.049	0.048	0.036	0.046
K	1.587	1.494	1.525	1.407	1.490	1.388	1.648	1.536	1.508	1.387
Z	8.00	8.00	8.00	8.00	7.97	7.89	7.88	7.88	7.85	7.77
Y	5.81	5.77	5.72	5.82	5.83	5.73	5.74	5.72	5.85	5.97
X	1.64	1.56	1.58	1.47	1.56	1.44	1.71	1.60	1.56	1.45
$100\left[\frac{Mg}{Mg+Fe^{2+}+Fe^{3+}+Mn}\right]$	45.2	45.8	40.8	46.3	44.3	46.1	45.4	45.6	37.6	28.3

Nockolds (1949) and Chappell (1966) suggest that biotites co-existing with hornblende contain very low or negligible amounts of Al in the octahedral sites and close to 5.5 atoms of Si and 2.5 atoms of Al in the tetrahedral sites. The biotites from the Yeoval diorites agree remarkably well with these conclusions, in that they have an average of 5.55 atoms of Si and 2.40 atoms of Al in the tetrahedral sites. The biotites from the granites have an average of 5.49 atoms of Si and 2.32 atoms of Al in the tetrahedral sites.

The Ti, Mn, and Mg and total iron contents of the biotites from the diorites show little variation so that the Mg:Fe ratio for these biotites is constant. The Mg:Fe ratio is lower for the biotites in the granites. This relationship is parallelled by the biotites from rocks of the Southern California Batholith (Larsen and Draisin 1948), in the Garabal Hill-Glen Fyne complex (Nockolds 1941) and the Carsphairn igneous complex (Deer 1937).

The variation in Fe^{3+}/Fe^{2+} ratio may explain the differences in Z site occupancy for the Yeoval biotites. That is, where the Fe^{3+}/Fe^{2+} is large, there is an insufficient number of ions/formula unit in the Z site. Some support for this may be gained from a study of published biotite analyses, especially those co-existing with hornblende (see Chappell 1966, Table 33). The structural formulae of the Yeoval

TABLE 18b

Biotite Structural Formulae Iron Recalculated as Total FeO

	Y8	G154	G120	Y41	Y235	G107	Y150	Y227	Y43	Y53
Si)	5.612	5.635	5.748	5.689	5.609	5.630	5.635	5.574	5.659	5.527
Al)	2.388	2.365	2.252	2.311	2.391	2.370	2.365	2.436	2.341	2.376
Al)	0.069	0.121	0.414	0.105	0.061	0.078	0.051	0.041	0.020	-
Ti)	0.413	0.394	0.409	0.441	0.391	0.451	0.362	0.399	0.442	0.428
Fe^{2+})	2.911	2.859	2.845	2.824	2.991	2.856	2.908	2.878	3.271	3.970
Mn)	0.066	0.079	0.065	0.065	0.080	0.065	0.092	0.080	0.095	0.083
Mg)	2.453	2.478	2.222	2.482	2.422	2.498	2.499	2.483	2.084	1.598
Ca)	0.017	0.017	0.017	0.017	0.034	0.017	0.017	0.017	0.017	0.018
Na)	0.039	0.043	0.043	0.043	0.039	0.039	0.050	0.049	0.036	0.047
K)	1.599	1.512	1.566	1.416	1.507	1.422	1.683	1.716	1.542	1.670
Z	8.000	8.000	8.000	8.000	8.000	8.000	8.000	8.000	8.000	7.903
Y	5.912	5.931	5.955	5.917	5.965	5.948	5.912	5.881	5.912	6.079
X	1.655	1.577	1.626	1.476	1.580	1.478	1.750	1.782	1.595	1.735

biotites have been recalculated with total iron expressed as FeO (Table 18b). From this it can be seen that the Z site is now filled and the number of atoms in the octahedral position increases almost to the maximum permissible, i.e. 6.0. The amount of octahedrally co-ordinated Al also increases.

A plot of the octahedrally co-ordinated atoms ($Mg:Fe^{2+}$ + Mn:Al + Fe^{3+} + Ti) in biotite co-existing with potassium feldspar and magnetite shows a trend in the field of biotite in the diorites towards the (Al + Fe^{3+} + Ti) - Mg join brought about by the oxidation of the Fe^{2+} to Fe^{3+} (indicated by the arrow in Fig.15). The biotites in the granite, particularly Y53, do not plot near the diorite field which would indicate that the biotites in these two rock types formed under different conditions of pressure, temperature and oxygen fugacity (Wones 1964), assuming, of course, that Ti does not affect the system.

Chloritisation of Biotite

Five of the biotite analyses (Table 18a; G107, Y150, Y227, Y43, Y53) have approximately one Fe^{3+} atom per formula unit which is exactly twice the amount suggested by Chappell (1966) as being the upper limit for the Fe^{3+} content of biotites (co-existing with magnetite) in igneous rocks. This high Fe^{3+} content is tentatively suggested due to the chloritisation of these biotites. A visual estimate from a number of thin

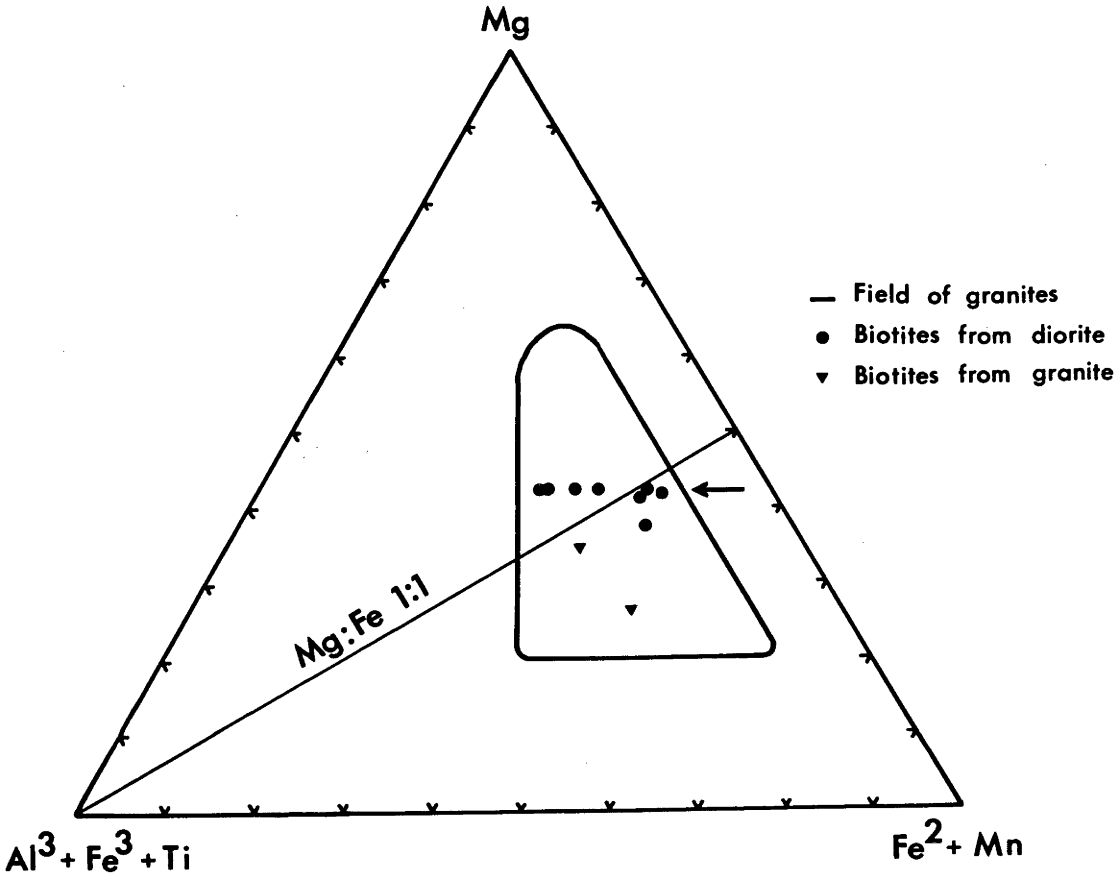

Fig.15 Plot of octahedrally co-ordinated atoms (Mg: Fe^{2+} + Mn: Al + Fe^{3+} + Ti) in biotites. The field of granites are from Foster's (1960) diagram.

sections supports this postulate in that the rocks with the highest Fe_2O_3 contents are those in which the biotite appears to be most chloritised. The presence of chlorite was checked by X-ray diffractometry, but no estimate of the chlorite abundance was possible.

The number of inter-layer alkali atoms per biotite formula unit is very much less (1.44 - 1.71) than the maximum value of 2 atoms and may well be due to leaching of potassium during chloritisation of the biotite. Some of the grain mounts for probe analyses contained many partly chloritised biotites so that a comparison between various degrees of chloritisation were made. The chloritised, or partly chloritised, biotites were obvious because they showed a marked decrease in SiO_2 to almost half the amount in fresh biotites; a loss of potassium was easily recorded. However there appears to be no correlation between the degree of iron oxidation and the potassium content (see Table 18a).

4.5. PLAGIOCLASE FELDSPARS

Plagioclase feldspar is present in all major rock types except for the one-feldspar granites. Plagioclase is unzoned in the gabbros but is strongly zoned in most varieties of the diorite and granite.

Nineteen plagioclases were separated - three from the gabbro, two from the pyroxene-mica diorite, thirteen from the quartz-mica diorite and one from the granite. However, except for the plagioclases from the gabbro, these separates are not representative of the rocks as a whole, because of zoning and the fact that a concentrate free of potassium feldspar and quartz could only be obtained by removing the more albitic fractions of the plagioclase. These concentrates were used for trace element studies.

It was apparent that these concentrates would yield little information, so a study of zoning, using the electron probe was made.

4.5.1. Plagioclases in the Gabbros

Ten to fifteen crystals were analysed from each sample and the results averaged. Potassium contents were below the detection limit (approximately 0.1% K_2O). The compositions in each rock are fairly uniform and the crystals show no zoning. In two samples, the CaO content varies from 17.3 - 17.9 (average 17.7%; An_{85}). Another sample of gabbro has a slightly lower average CaO content (17.3%; An_{80}). Finer plagioclase crystals intergrown with the coarser ones give a slightly lower CaO content (16.1%; An_{77}).

Several optical determinations were made on the plagioclases from the gabbro using the method of Rittman and

Plate 2

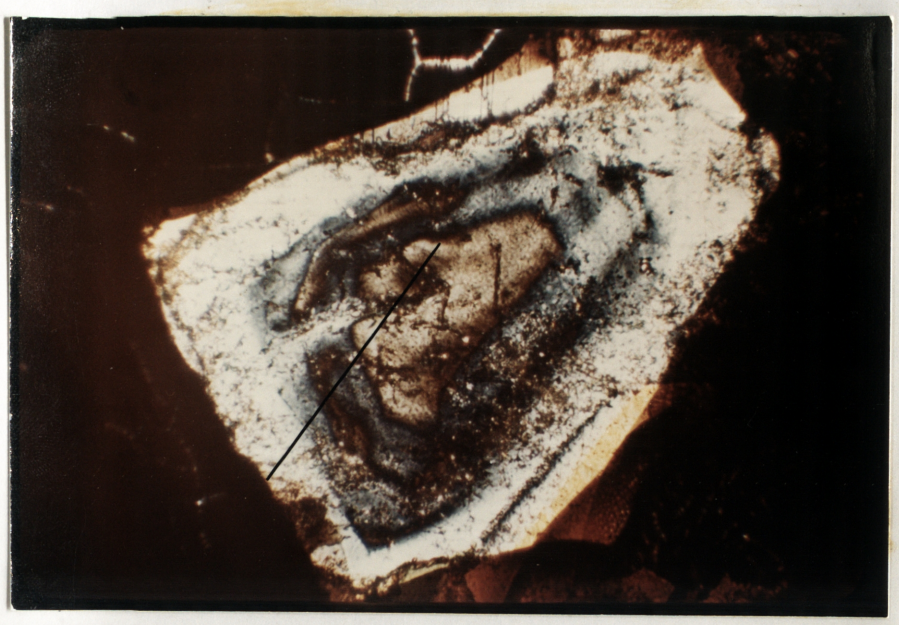

Plate 2, Fig. 16 Compositional variations for a normally zoned corroded plagioclase. (Numbers on the figure indicate the anorthite contents. Line on the plate is the probe traverse.)

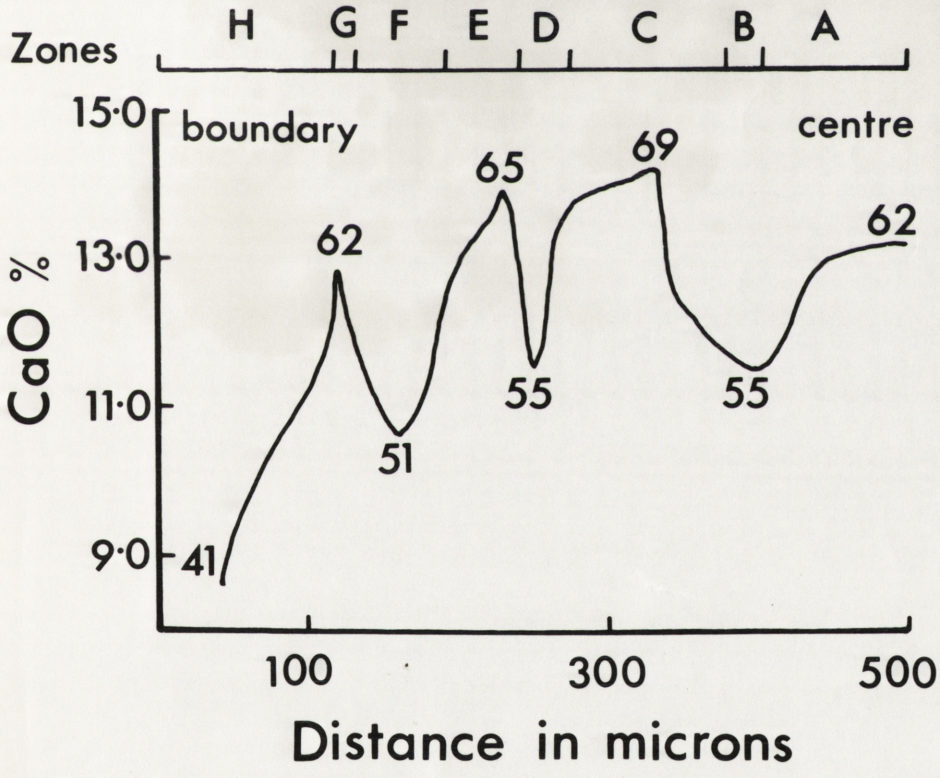

TABLE 19

Electron Probe Analyses of a Normally Zoned Corroded Plagioclase from the Pyroxene-Mica Diorite

Zone	Colour (Plate 2)	CaO (Wt %)	K_2O (Wt %)	Na_2O (Wt %)	Anorthite (mol %)
A (centre)	brown	13.0	0.13	4.6	62
		12.6	0.13	4.7	60
	deep blue to brown	11.9	0.14	4.9	57
		11.5	0.13	5.2	55
B	brown	11.9	0.13	5.0	57
		12.2	0.14	4.8	58
		12.6	0.15	4.4	61
		14.4	-	3.8	69
		13.9	0.12	4.0	65
		13.6	0.12	4.1	65
C	deep blue	12.7	0.16	4.3	61
		11.5	-	5.0	55
D	brown	13.9	0.11	4.0	65
		13.4	-	3.0	64
		12.6	0.12	4.7	61
E	deep blue	11.1	0.14	5.5	53
		10.6	0.15	5.6	51
		11.3	0.13	5.3	54
F	pale brown	12.0	0.14	5.0	57
		12.9	0.12	4.4	62
G (boundary)	deep blue	11.6	0.12	5.1	55
		11.1	0.15	5.4	53
		10.5	0.13	5.7	50
		10.3	0.13	6.0	49
	pale blue	9.9	0.13	6.6	47
	white	8.6	0.14	6.9	41

El Hinnawi (1961). However, the extinction angles (of the order of 50^{o}) fall on the curves in region of very low slope. Previously, some 200 crystals had been measured using the method of Michel-Levy which gave anorthite contents ranging from 64-72%. These are grossly inconsistent with the results obtained by electron probe analysis.

4.5.2 Plagioclase in Diorites

In order to check the coincidence of the spot analyses and the zones in selected diorite plagioclases, photographs of the crystals were taken in transmitted and reflected light. The "contamination spots" from the electron beam could then be correlated with the observed zoning.

Plagioclases in the Pyroxene-mica diorite

Pronounced zoning is common in most plagioclase crystals in the pyroxene-mica diorite. The plagioclase may exhibit oscillatory zoning, reverse zoning or normal zoning as well as corrosion by more sodic feldspar. The range in composition of the zones varies considerably from one crystal to another; the maximum in a single crystal ranging from 13.9% CaO (An_{65}) to 8.6% C_aO (An_{41}).

(1) Normally zoned corroded plagioclase-(Plate 2, Fig. 16, Table 19). The line of traverse for 43 spot analyses is indicated on the photograph. It appears that the brownish core in the centre (zones A and C) and the small brownish

Plate 3

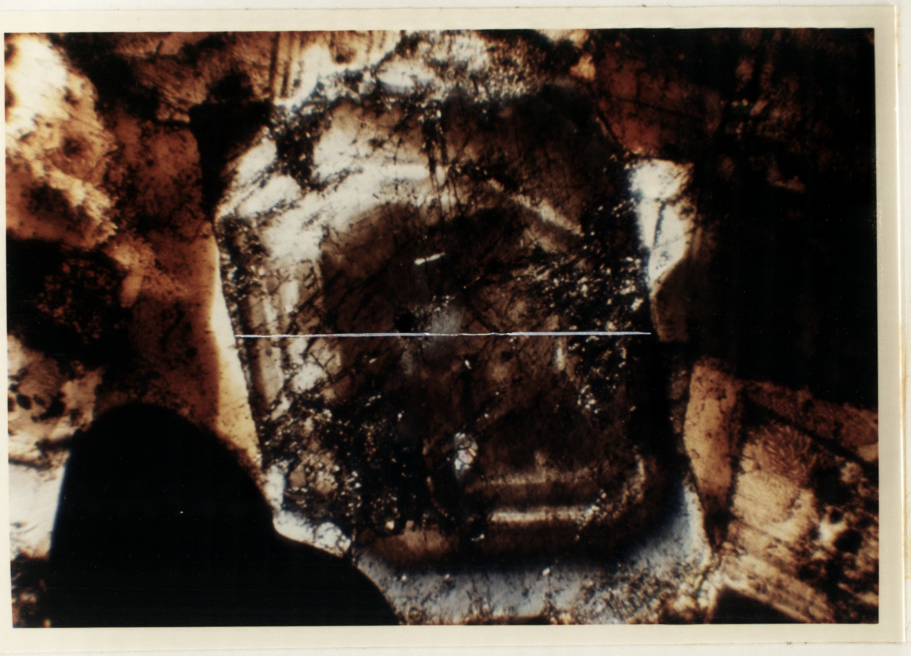

Plate 3, Fig.17 Compositional variations for a plagioclase crystal showing oscillatory zoning and containing a sodic core.

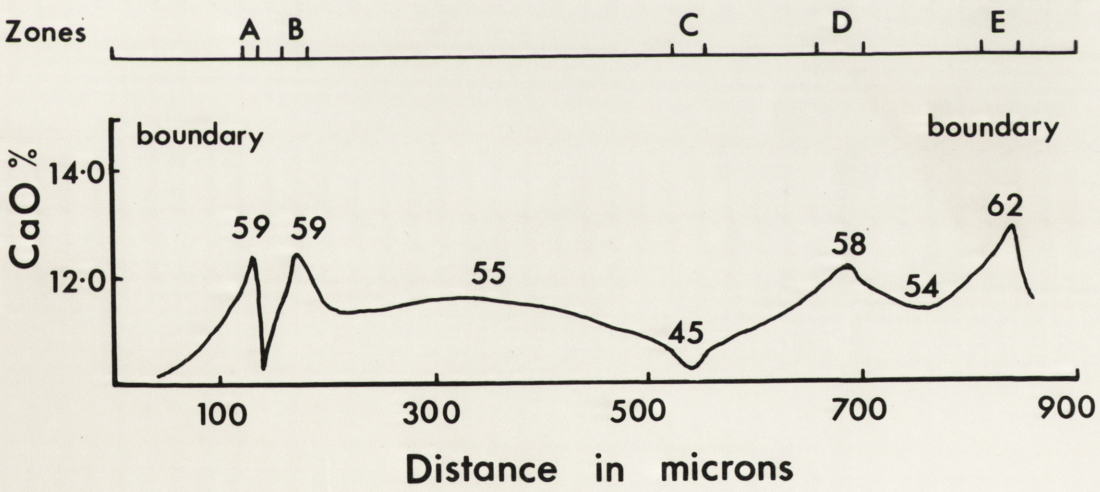

TABLE 20

Electron Probe Analyses of an Oscillatory Zoned Plagioclase Containing a Sodic Core from the Pyroxene-Mica Diorite

Complete Traverse

Zone	Colour (Plate 3)	CaO (Wt %)	K_2O (Wt %)	Na_2O (Wt %)	Anorthite (mol %)
		10.3	0.12	6.0	48
		11.1	0.12	5.6	52
A	white	11.7	0.13	5.3	55
		12.4	0.14	4.7	59
		10.3	-	5.7	48
		11.3	0.13	5.5	53
		11.7	0.13	5.3	55
B	white	12.4	0.13	4.9	59
		12.1	0.12	5.0	57
		11.4	0.11	5.2	53
		11.4	0.11	5.2	53
		11.5	0.12	5.3	54
C	pale blue	9.8	-	6.4	45
		11.6	0.11	5.3	55
		11.1	0.12	5.6	52
		10.6	0.15	5.7	49
		10.1	0.15	6.0	47
		10.6	0.15	5.7	49
		10.8	0.14	5.5	50
		11.5	0.12	5.1	54
D	white	12.1	0.13	5.0	58
		11.8	0.12	4.8	56
		11.5	0.13	5.1	55
		11.3	0.12	5.3	54
		11.7	0.13	5.2	56
E	white	12.4	-	4.9	59
		12.9	-	4.7	62
		11.5	0.13	5.2	55

slivers (zone G) separated from the core by blue areas (zone F) were part of a single crystal which has been corroded. This is supported by the observation that the analyses of the brown areas (zones A, C, E and G) are similar (Table 19). At the crystal boundary (very pale blue-white area of zone H) the plagioclase has a CaO content of 8.6% (An_{41}) which gradually increases to 11.1% CaO (An_{53}) as the deeper blue part of zone H is approached. At the brownish zone (G) the CaO content increases but not as markedly as might be expected: because of the size of zone G where traversed, resolution was limited. In zone F the composition decreases to approximately 11.2% CaO (An_{53}) in accord with the previous value for the deep blue part of zone H. Between zone F and the centre, the composition increases to 13.4% CaO (An_{64}) near the outer margins of the core and then to 13.9% CaO (An_{65}) about 30 microns into the core (zone E). In the traverse across the core a number of incursions (zones D and B) by more sodic-rich material are obvious from the decrease in CaO content. The most calcic part of the core is near its centre where a value of 14.4% CaO (An_{69}) was recorded.

(2) Oscillatory zoning and a sodic core -(Plate 3, Fig. 17, Table 20). In a plagioclase crystal from the pyroxene-mica diorite, two sets of zones may be distinguished towards the outer crystal boundaries and there is a central portion of

Plate 4

Plate 4, Fig. 18 Compositional variations for a twinned plagioclase showing coarse oscillatory zoning.

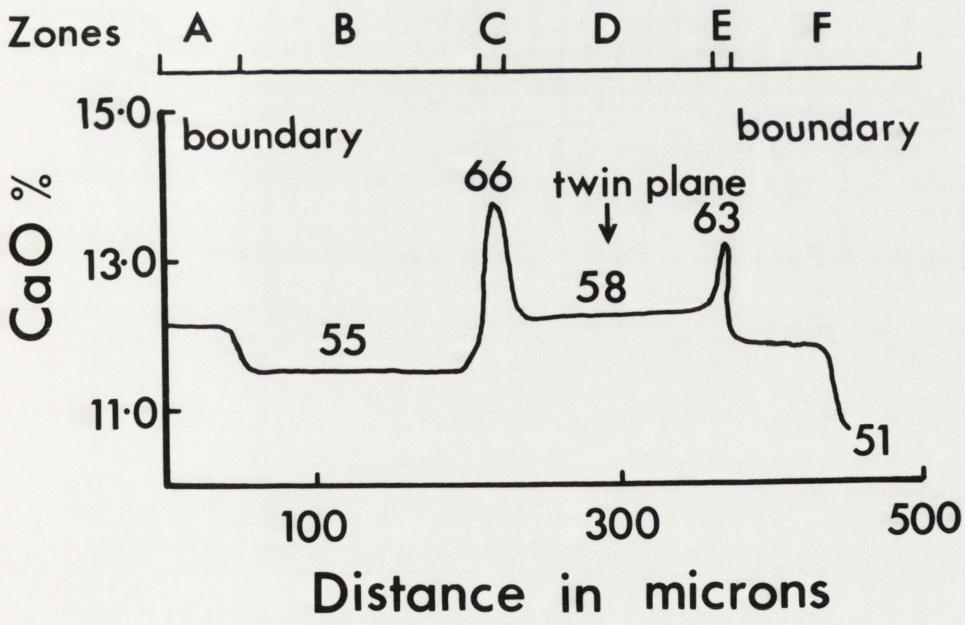

TABLE 21

Electron Probe Analyses of a Twinned Plagioclase with Oscillatory Zoning from the Pyroxene-Mica Diorite

Two Traverses (Plate 4)

Zone	Zone Width (microns)	CaO (Wt %)	K_2O (Wt %)	Na_2O (Wt %)	Anorthite (mol %)
1. Cross over twin plane to outer edge					
B	40	11.8	0.15	5.1	56
C	20	13.7	0.12	3.9	66
D	160	12.2	0.14	5.0	58
E	10	13.2	0.13	4.3	63
F	70	11.8	0.11	4.9	56
		10.7	0.18	5.2	51
2. Centre to outside					
B	110	11.3	0.12	5.2	54
A	40	12.2	0.15	5.0	58

variable composition. The minor fluctuations are indicated by the "blotchy" appearance of the whole central portion of the crystal between zones B and D. Within this central portion is a core (zone C) with exceptionally low CaO content (An_{45}). Oscillatory zones are also normal types (c.f. Vance 1962, Bottinga et al. 1966) and the most calcic parts of these (zones A and B) are seen as two sets of white lines near the crystal margins (see Plate 3). The more albite-rich outer zones were not analyzed although they are undoubtedly of a similar composition to that given for the previously described crystal (i.e. approximately 9% CaO). No corrosion of the crystal edges could be observed.

(3) Twinned plagioclase showing coarse oscillatory zoning - (Plate 4, Fig. 18, Table 21). Traverses were made across this crystal at two places and the data in Table 21 and Fig. 18 are an attempt to combine these two sets of analyses. The most important point to note from these analyses is the fairly constant composition of the central part of the crystal (zone D) with an average of 12.2 CaO (An_{58}) with no change in composition on either side of a central twin plane. At the edge of this central zone, the CaO content increases to more than 13% (zones C and E) and from this point, almost to the crystal boundaries, the composition is fairly constant (11.8 to 11.3% CaO) decreasing to 10.7% CaO as one boundary (zone F) is

Plate 5

Plate 5, Fig.19 Compositional variations for a normally zoned plagioclase.

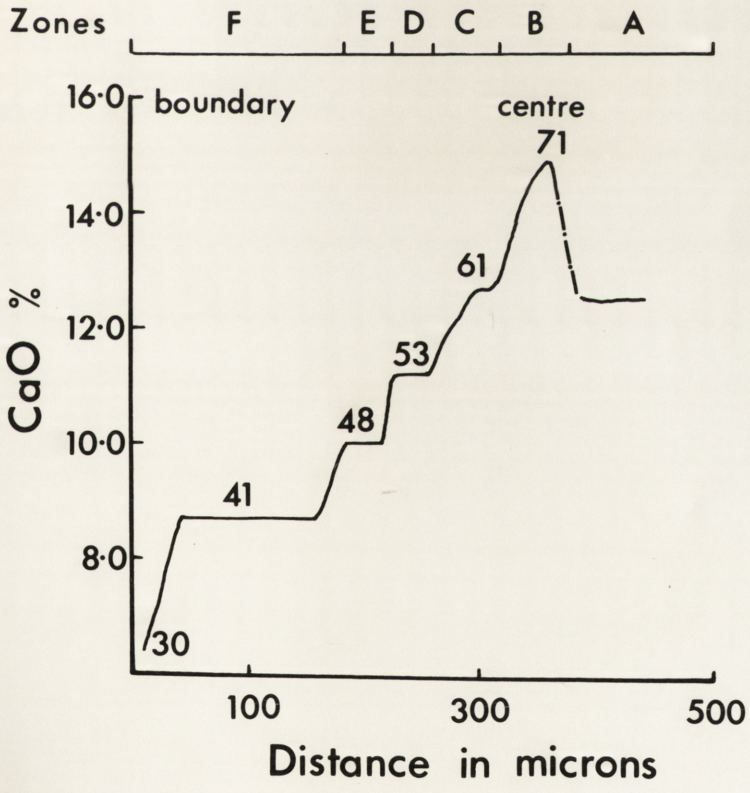

TABLE 22

Electron Probe Analyses of a Normally Zoned Plagioclase in the Quartz-Mica Diorite

Traverse from Inner to Outer Crystal Edge

Zone	Colour (Plate 5)	CaO (Wt %)	K_2O (Wt %)	Na_2O (Wt %)	Anorthite (mol %)
A (centre)	grey-brown	12.5	0.14	4.4	60
		14.1	0.12	3.9	67
B	white	14.9	0.12	3.6	71
		14.1	-	4.0	67
C	grey-brown	13.3	0.13	4.1	64
		12.7	0.14	4.7	61
		12.1	0.14	4.9	58
D	deep grey-brown	11.7	0.15	5.1	56
		11.2	0.16	5.5	53
E	deep blue	10.0	0.18	6.0	48
F (boundary)	pale blue to white	9.5	0.19	6.1	45
		9.2	0.20	6.1	44
		8.7	0.20	6.5	41
		7.8	0.21	6.9	37
		7.0	-	7.1	33
		6.4	-	7.3	30

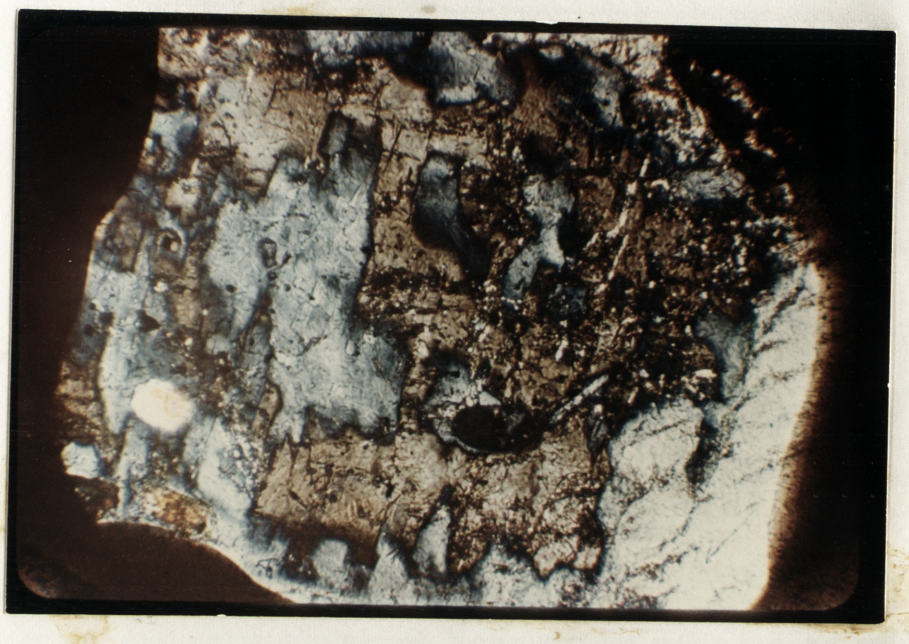

Plate 6 "Patchy" zoning of a plagioclase crystal in the quartz-mica diorite.

approached (Fig. 18).

Plagioclase in the quartz-mica diorite.

In the quartz-mica diorites, zoning in the plagioclase differs in three ways from that of the pyroxene-mica diorite:

(i) normal zoning is common;

(ii) "patchy" zoning is abundant;

(iii) the outer zones are usually more albite-rich than those in the pyroxene-mica diorite and so a greater range of composition exists.

(1) Normally zoned plagioclase - (Plate 5, Fig. 19, Table 22).

Analyses from the centre to the outer crystal boundary indicate that the very white inner zone (B) is the most calcic part of the crystal (14.9% CaO; An_{71}) and from here the composition changes in a step-like manner (Fig. 19) to the crystal edge which has a composition of 6.4% CaO (An_{30}). There is a very good correlation between interference colour and composition of zones in this crystal (Fig. 19). Where the colour is fairly homogeneous (as in the outer pale bluish-white area in Plate 5, Zone F in Fig. 19) the composition is consistently about 8.7% CaO. In contrast, where there is a gradation in colour (as in the grey-brown regions, zones D and C), the composition varies normally from 11.1 to 12.7% CaO towards the centre of the crystal.

(2) "Patchy" zoning - (Plate 6). This zoning is the same as

Plate 7

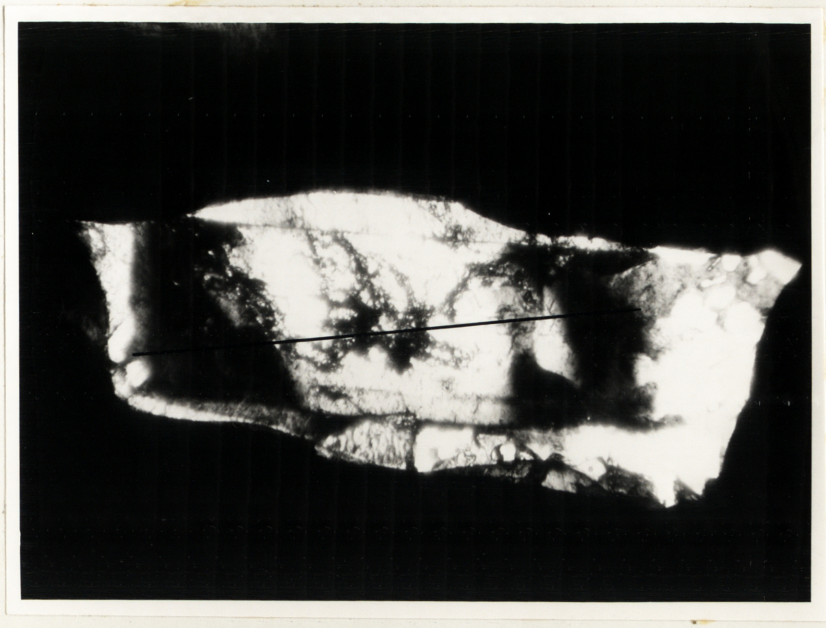

Plate 7, Fig.20 Compositional variations of a plagioclase crystal containing homogeneous calcic core and exhibiting irregular oscillatory zoning.

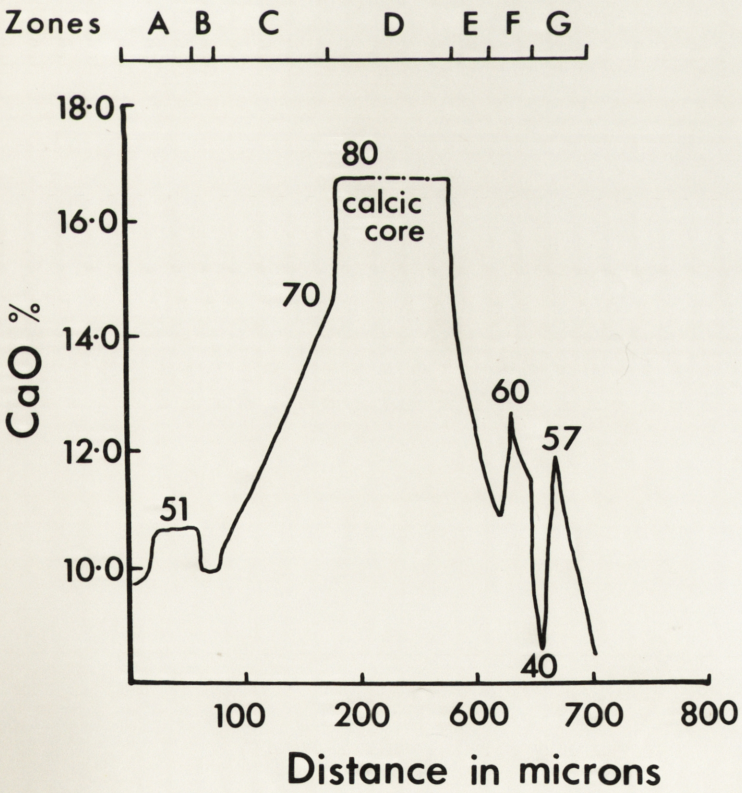

TABLE 23

Electron Probe Analyses of Plagioclase in the Quartz-Mica Diorite Containing a Calcic Core and Oscillatory Zoning

Almost Complete Traverse of Crystal (Plate 7)

Zone	Zone Width (microns)	CaO (Wt %)	K_2O (Wt %)	Na_2O (Wt %)	Anorthite (mol %)
A (boundary)	50	9.8	0.15	6.4	47
		10.7	0.13	5.6	51
B	20	9.9	0.15	6.3	47
C	100	10.6	0.13	5.6	51
		11.6	0.13	5.1	55
		12.4	0.12	4.9	59
		13.8	0.11	3.9	66
		14.4	0.11	3.8	69
D (core)	540	16.7	-	2.2	80
E	50	14.8	0.10	3.6	71
		13.5	0.11	4.1	65
		12.8	0.11	4.7	62
		11.7	0.12	5.3	56
		10.8	0.13	5.5	51
F	40	12.6	0.13	4.4	60
		11.8	0.11	5.0	56
		11.5	0.13	5.1	55
		8.4	0.19	6.8	40
G (boundary)	40	11.9	0.12	5.0	57
		10.4	0.12	5.7	50
		9.7	0.13	6.4	46
		8.6	0.15	6.9	41

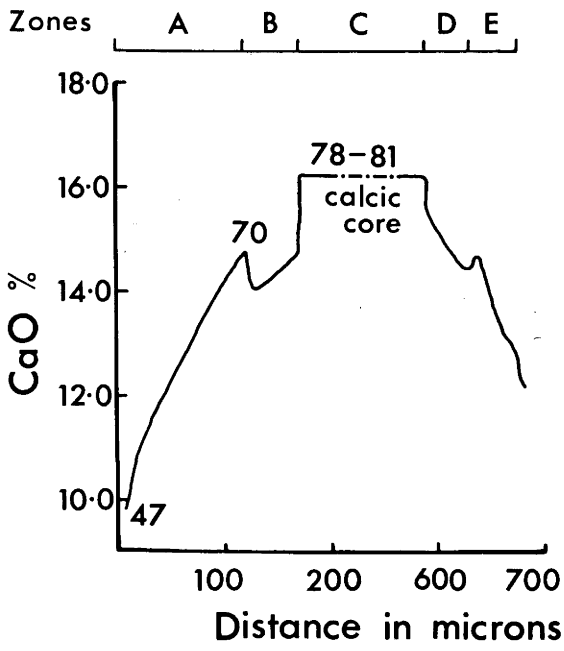

Fig.21 Compositional variations of a plagioclase crystal containing a heterogeneous calcic core and exhibiting regular oscillatory zoning.

TABLE 24

Electron Probe Analyses of Plagioclase in the Quartz-Mica Diorite with a Calcic Core and Minor Oscillatory Zoning

Almost Complete Traverse (Figure 18)

Zone	Zone Width (microns)	CaO (Wt %)	K_2O (Wt %)	Na_2O (Wt %)	Anorthite (mol %)
A (boundary)	140	9.9	0.16	6.5	47
		11.0	0.15	5.6	52
		11.8	0.15	5.0	56
		12.3	0.14	4.9	59
		12.7	0.14	4.7	61
		12.9	0.13	4.4	62
		13.9	0.13	4.0	67
		14.2	0.12	3.9	68
		14.7	0.12	3.6	70
B	50	14.0	0.13	4.1	67
		14.7	0.12	3.6	70
C (core)	360	16.2-17.1	0.10	2.6-2.2	78-81
D	50	15.5	-	2.9	74
		15.2	0.11	3.0	73
		14.8	0.11	3.6	71
		14.4	0.11	3.7	69
E (boundary)	60	14.7	0.11	3.6	70
		13.8	0.12	4.1	66
		12.6	0.12	4.4	60
		12.3	0.13	4.9	59
		12.0	0.14	5.0	57
		11.2	0.15	5.5	54

that described as "patchy" by Vance (1965). The grey-brown areas ("included plagioclase" of Vance) have a composition varying from 14.6 - 15.8% CaO (An_{70-76}). They are corroded and replaced by a more sodic plagioclase (8.0 - 8.9% CaO; An_{38-42}). The replacement appears to have been controlled by the two cleavage directions in the plagioclase.

(3) Calcic cores - (Plate 7, Fig. 20, Table 23). These are easily distinguished under the microscope by their irregular boundaries and cross-cutting cracks. A traverse from one crystal boundary, through the core to the other boundary (Fig. 20) shows that compositional changes are extremely marked. At one extremity (zone A) the plagioclase exhibits a regular type of oscillatory zoning, in that there is little change in composition of the zones as a whole (e.g. zone A to zone B). There is a gradual increase in CaO content towards the core (zone D) where a sharp change from 14.4 to 16.7% CaO (An_{69} to An_{80}) is apparent. The core is fairly homogeneous (less than 1% by weight variation). The extreme changes in composition on the opposite side of the core (zones E to G) cannot be correlated with the minor fluctuations on the previously described side of the crystal.

The analysis of another calcic core is given in Table 24 and illustrated in Fig. 21. Although the composition of the core is similar and more variable than that described above,

Plate 8

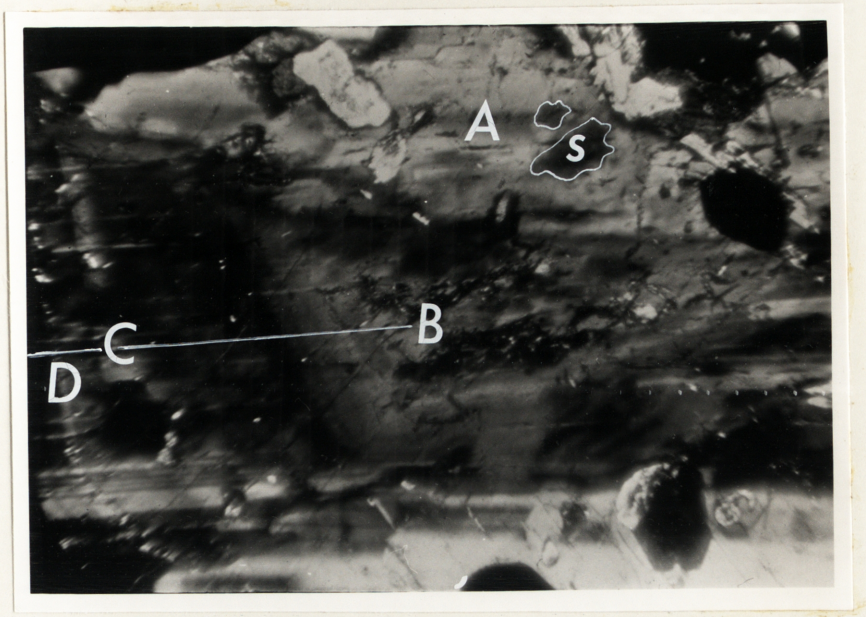

Plate 8, Fig.22 Compositional variations of a plagioclase crystal containing sodic remnants and exhibiting oscillatory and reverse zoning.

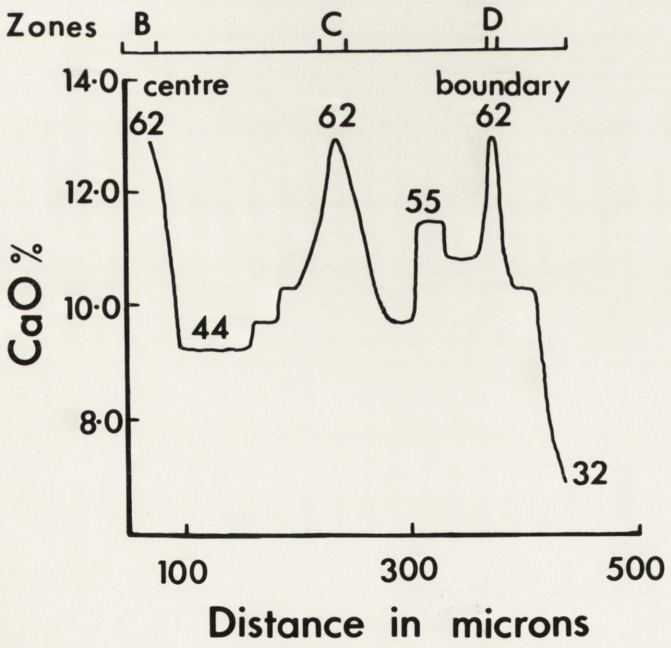

TABLE 25

Electron Probe Analyses of a Plagioclase Crystal from the Quartz-Mica Diorite Containing Sodic Remnants, Corroded Areas and Oscillatory Zoning

---

AREA DESIGNATED A:
For 3 different locations of analysis give:

	CaO (Wt %)	Na_2O (Wt %)	Anorthite (mol %)
(1)	9.8	4.8	47
(2)	10.2	4.7	49
(3)	10.1	4.8	48

Zone	CaO (Wt %)	Na_2O (Wt %)	Anorthite (mol %)
B (centre)	12.9	3.2	62
	11.9	3.7	57
	10.9	4.3	52
	9.2	5.5	44
	9.8	5.2	47
	10.3	5.0	49
	10.7	4.8	51
	11.4	4.7	55
C	12.9	3.6	62
	12.3	4.2	59
	11.8	4.5	57
	10.4	5.3	49
	9.7	5.7	46
	11.4	4.8	55
	10.8	5.0	52
	11.1	4.4	53
D	13.0	3.7	62
	11.8	4.5	56
	10.2	5.2	49
	8.3	6.5	40
	8.0	6.7	38
(boundary)	6.8	7.3	32

the extremes in CaO content of the outer zones (A, B, and D, E) are not apparent. They show a gradual increase in CaO content from the crystal boundaries to the core associated with minor oscillatory zoning.

(4) Sodic Cores - (Plate 8, Fig. 22, Table 25). In contrast with the calcic cores of the last two examples, other crystals in this same sample contain sodic cores. They can be distinguished optically by their slight difference in extinction angle. In Plate 8 the main sodic core is labelled 'S'. The other parts of this crystal show an exceedingly complex compositional variation (Table 25). For example, the area (designated A) containing the sodic cores has outer rims of about 8.2% CaO (An_{39}) whereas the inner parts of this area remain fairly constant at about 9.9% CaO (An_{46}).

The central, slightly altered area (zone B, Fig.22, Plate 8) has a higher overall CaO content, ranging from 10.9 to 12.9% (An_{52}-An_{62}). From this more central calcic area, the calcium content decreases to 9.2% CaO (An_{44}) and then increases again at zone C to 12.9% CaO (An_{62}). The composition then becomes less anorthite-rich until the thin zone (D) is reached whereupon the CaO content rises sharply to 13.0% (An_{62}). From this area, normal zoning prevails to the outer uncorroded edge of the crystal, which has a composition of 6.8% CaO (An_{32}). Thus, from the centre of the crystal, there are three main

Plate 9

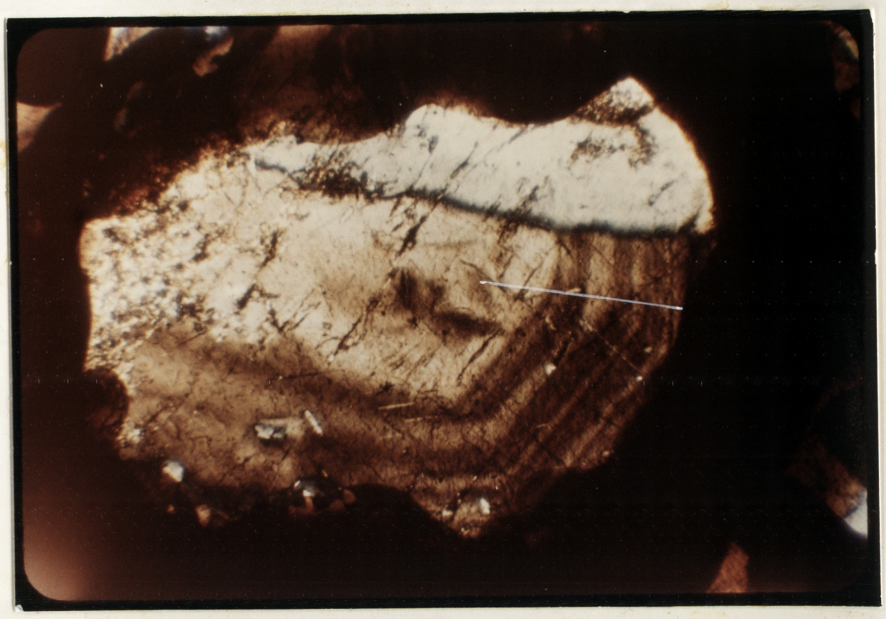

Plate 9, Fig.23 Compositional variations of a plagioclase crystal showing normal, reverse and oscillatory zoning.

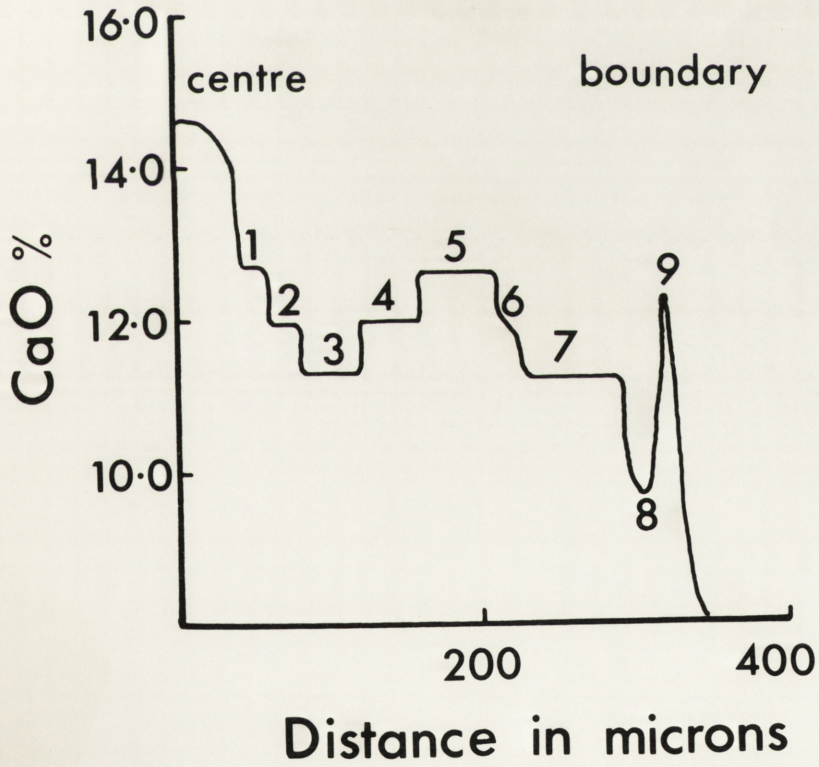

Plate 10

Plate 10, Fig.24 Compositional variations of a corroded plagioclase crystal exhibiting coarse oscillatory zoning.

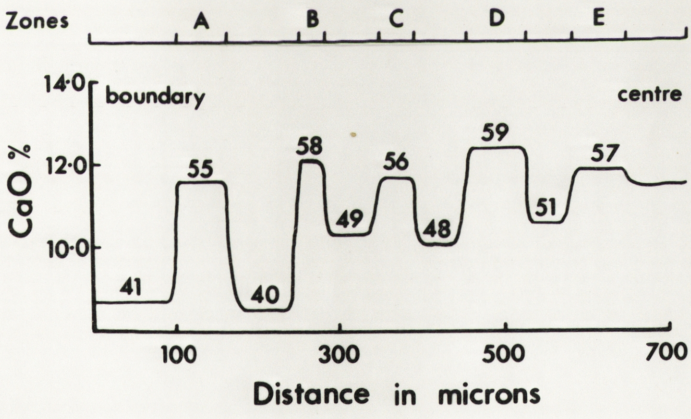

TABLE 26

Electron Probe Analyses of an Oscillatory Zoned Crystal with Corroded Rims from the Quartz-Mica Diorite

Zones	Colour (Plate 10)	CaO (Wt %)	K_2O (Wt %)	Na_2O (Wt %)	Anorthite (mol %)
A	blue	8.7	0.14	6.7	41
	brown	11.6	0.14	5.2	55
B	blue	8.5	0.15	6.8	40
	dark brown	12.1	0.13	4.9	58
		10.9	0.15	5.5	52
	light brown	10.3	0.16	5.7	49
		10.6	0.15	5.6	51
C	dark brown	11.7	0.14	5.2	56
		11.0	0.16	5.5	53
	light brown	10.1	0.17	6.0	48
		11.0	0.16	5.5	53
D	dark brown	12.3	0.14	4.8	59
		11.7	0.15	5.2	56
	light brown	10.6	0.16	5.7	51
		11.2	0.16	5.5	53
E	dark brown	11.9	0.15	4.9	57

TABLE 27a

Electron Probe Analyses of Plagioclase Crystals from Selected Samples of Quartz-Mica Diorite

Sample Y151

		CaO (Wt %)	K_2O (Wt %)	Na_2O (Wt %)	Anorthite (mol %)
Unzoned Crystals	1	9.7	0.24	5.6	46
	2	9.8	0.24	5.5	47
	3	9.7	0.24	5.8	46
	4	9.0	0.25	6.3	43
	5	9.7	0.25	5.5	46
Normal Zoning (70 micron traverse from centre)		10.1	0.23	5.6	48
		9.6	0.25	6.0	46
		8.7	0.25	6.5	41
Oscillatory zoning (traverse from centre)		11.4	0.18	4.8	54
		10.9	0.18	5.2	52
		10.4	0.23	5.4	50
		11.3	0.17	4.8	54
		10.9	0.17	5.2	52
		10.1	0.23	5.5	48
Crystal with oscillatory zoning in centre and two lines of inclusions		9.6	n.d.	5.5	46
		11.0	n.d.	5.0	52
		9.6	n.d.	5.4	46
		10.3	n.d.	5.2	49
	(1)	10.4	0.23	5.4	50
then oscillatory zones, and					
	(2)	9.6	n.d.	6.2	46
		8.5	n.d.	6.4	40
		6.6	n.d.	8.2	31

n.d. = not determined

TABLE 27b and c

Electron Probe Analyses of Plagioclase Crystals from Selected Samples of Quartz-Mica Diorite

Associated Mineral	Wt % CaO	Wt % K_2O	Wt % Na_2O
Sample Y227			
Potassium Feldspar	7.8	0.12	6.6
Potassium Feldspar	8.1	0.12	6.2
Mosaic of plagioclase	10.5	0.10	5.0
Biotite	6.5	0.30	7.2
Mosaic of plagioclase	10.6	0.11	4.9
Mosaic of plagioclase	10.2	0.11	5.1
Quartz	8.8	0.13	5.6
Sample Y150			
	Wt % CaO	Wt % K_2O	Wt % Na_2O
Crystal containing lines of inclusions			
	10.7	0.10	5.3
	11.4	0.11	4.9
	10.1	0.10	5.5
	12.9	0.15	3.7
Line of inclusions			
	9.6	0.11	5.8
	7.4	0.15	7.1

TABLE 28

Electron Probe Analyses of Plagioclases from the Granite

		CaO (Wt %)	K_2O (Wt %)	Na_2O (Wt %)	Anorthite (mol %)
Unzoned Crystals	1	2.4	0.27	9.7	12
	2	3.9	0.16	8.7	20
	3	4.1	0.14	8.5	21
	4	3.5	0.27	8.9	18
	5	3.9	0.16	8.8	20
Oscillatory zoned crystal (centre to boundary) (Zones approximately 10μ wide)		4.6	-	8.4	22
		3.8	-	8.8	19
		3.4	-	9.0	17
		3.2	-	9.1	16
		2.8	-	9.6	14
		3.3	-	9.4	17
		2.8	-	9.6	14
		3.3	-	9.4	17
		2.4	-	9.9	12
Normally zoned crystal (centre to outside)		2.6	0.23	9.4	13
		2.3	0.27	9.7	12
		1.9	0.30	10.0	10
		1.6	0.37	10.1	8
		1.4	0.38	10.3	7

oscillatory zones with a CaO content of approximately 12.9% associated with both reverse and normal zoning.

A similar pattern of normal, reverse, and oscillatory zoning is illustrated in Fig. 23 and Plate 9. This (and observations for other crystals) add support to the suggestion of Bottinga et al. (1966) that the number of oscillations in the long dimension of a crystal is greater than in the short dimension.

(5) Crystal boundary corrosion and coarse oscillatory zoning - (Plate 10, Fig. 24, Table 26). The group of repeated zones (A, B, C, D and E) are fairly similar in composition, and the data clearly illustrates the sharp break between zones, (Fig. 24) which contrasts with other types of oscillatory zones showing a gradation in composition (e.g. Fig. 17). In addition to the zoning, the crystal boundaries are corroded by a more sodic plagioclase (8.6% CaO), which differs markedly from any in the oscillatory zones.

Other analyses of plagioclases from the quartz-mica diorite are listed in Table 27.

4.5.3. Plagioclases in the Granites

As in the diorites, there are unzoned crystals of fairly constant composition, as well as both normal and oscillatory zoned types. The zoning is more delicate than in the diorites and there are not such large variations in composition. Plagioclase analyses in a two-feldspar granite are given in Table 28.

TABLE 29

Flame Photometric Determinations of K_2O and Na_2O and Triclinicity Measures of Potassium Feldspars from Yeoval Rocks

Rock Type	Specimen No.	Na_2O	K_2O	Triclinity	
				Peak 1	Peak 2
Pyroxene-mica Diorite	G154	1.90	12.80	0	0.72
Quartz-mica Diorite	G120	1.68	11.70	0	0.72
	Y41	1.90	12.71	0	-
	Y71	1.93	12.82	0	0.78
	G110	1.54	12.95	0	0.72
	Y151	1.81	12.36	0	-
	G118	2.14	11.75	0	-
	Y235	1.63	12.80	0	0.72
	G107	1.42	13.52	0	0.72
	Y75	1.22	14.04	0	-
	Y150	1.69	13.50	0	-
	Y227	1.70	12.70	0	0.70
	G99	1.58	13.03	0	0.72
Orthoclase Diorite	Y205	2.81	11.23	n.d.	n.d.
Granite	Y43	4.57	10.07	0.78	0.30
	Y53	4.26	9.71	0.72	-
	Y64	4.64	9.03	0.76	0.31
	R77	3.99	9.86	0.82	0.45

4.6 POTASSIUM FELDSPARS.

Potassium feldspar occurs in all granites and all except the most basic phases of the diorites. In the diorites, it is weakly perthitic and faint cross-hatched twinning is sometimes developed. Coarse perthite is abundant in the granites.

Potassium feldspars from 14 diorites and 4 granites have been separated and partial chemical analyses are presented in Table 29.

X-ray diffractometer determinations of the (131) and ($1\bar{3}1$) spacings have been used for the calculation of triclinicity according to the method of Goldsmith and Laves (1954) who defined the triclinicity (Δ) by the relationship:

$$\Delta = 12.5\ (d_{131} - d_{1\bar{3}1})$$

The triclinicity gives a measure of the degree of disorder in the potassium feldspar lattice so that the most triclinic microcline (fully ordered) has a value very close to 1 and in the monoclinic feldspars it is 0. The triclinicity of potassium feldspars from the diorite was zero. In most samples, a small peak giving a triclinicity of approximately 0.72 was observed and this may possibly be a microcline phase.

In the potassium feldspars from the granites, 3 peaks of similar dimensions were recorded. This indicates that there are two main phases, microcline (Δ = 0.82) and orthoclase.

The potassium feldspars from the diorites show variable

contents of Na_2O (1.22 - 2.14%) and K_2O (11.70 - 13.52%). The potassium feldspar from the orthoclase diorite shows an increase in Na_2O and decrease in K_2O compared with those from the quartz-mica diorites.

The calcium contents of four samples of potassium feldspar determined using the electron microprobe, ranged from 0.1 to 0.3% CaO. The higher values were coupled with correspondingly higher Na_2O and lower K_2O contents which would indicate that cryptoperthite was present in the orthoclase.

4.7 ZIRCONS

Introduction

Most published data on zircons in granitic rocks up to a decade ago were concerned with a study of the physical properties such as colour and inclusions, crystal faces, and elongation (including rounding and corrosion). An excellent summary of this work is given by Poldervaart (1956). Although not held in very high regard at the present time, such zircon studies have been used to distinguish connected and disconnected intrusives, to trace differentiates of the same magma, and to separate them from differentiates of other magmas In applying the study of these physical properties to the petrogenesis of calc-alkaline rocks, two basic assumptions are necessary. Firstly, that of the early formation of zircon; and secondly, the short range of crystallisation of zircon

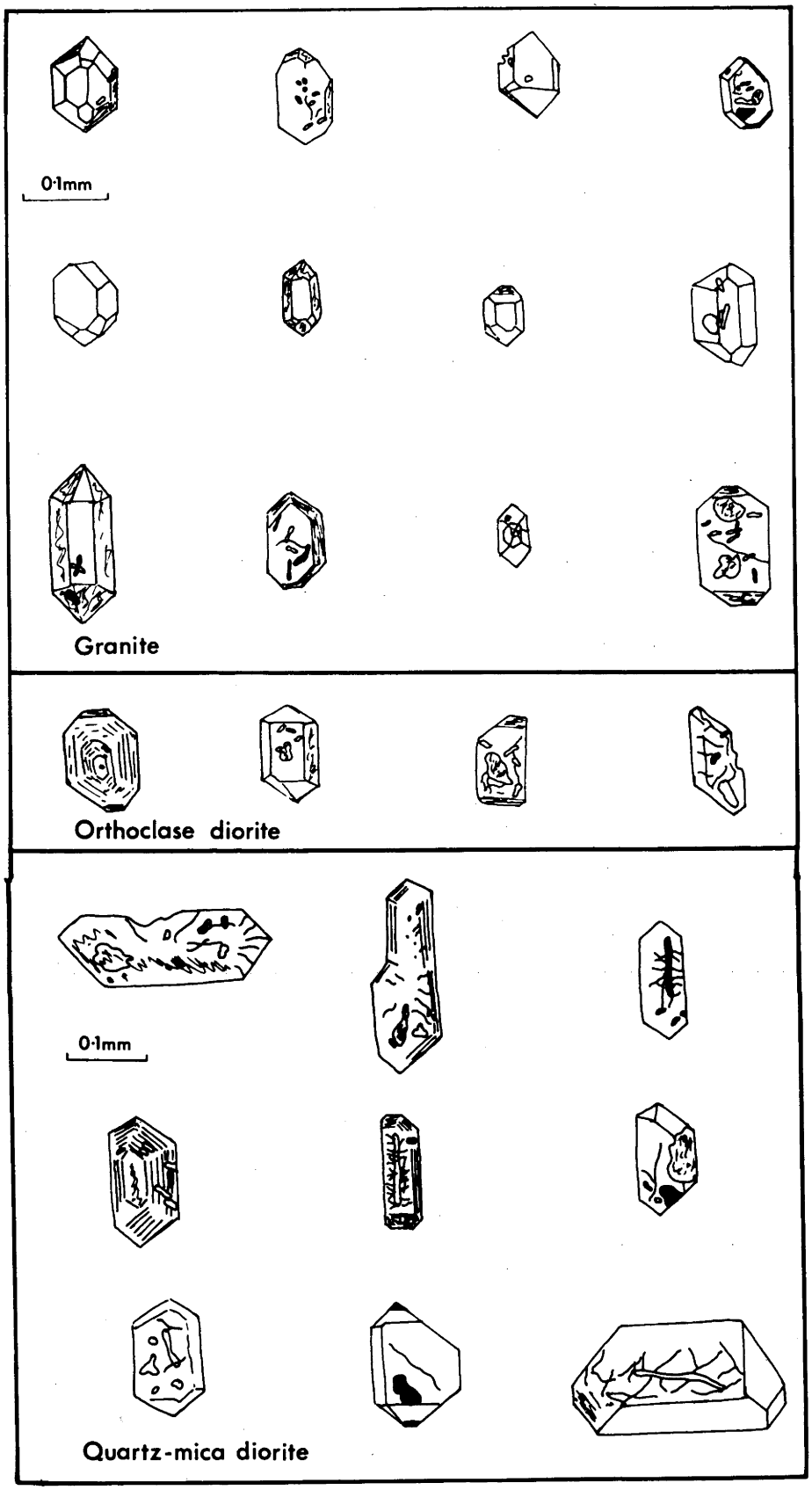

Fig.25 Selected crystal drawings of zircons from the Yeoval diorites and granite.

(Larsen and Poldervaart 1957, Murthy 1958). If the physico-chemical conditions are nearly uniform throughout a magmatic body shortly after its emplacement and before the crystallisation of the major mineral phases, a uniform zircon population should be expected from all parts of the body (except perhaps the chilled margin).

To test this hypothesis, a study was made of the physical properties and chemistry of zircons from the coarse-grained Yeoval rocks. Zircon concentrates, made using the method of Poldervaart (1955), were separated from twenty-one rocks - one pyroxenite, four gabbros, nine quartz-mica diorites, three orthoclase diorites, and four granites. In the gabbros, crystals are irregularly shaped and few in number. They increase in number in the diorites and reach a maximum concentration in the granites.

Length and breadth measurements were not possible for all samples, particularly from some of the diorites and gabbros, because of the small numbers of zircons separated. Polished thin sections were prepared in order to study the variation in composition, if any, of zircons present in different mineral phases. Grain mounts of the two major size fractions (-60 + 100 mesh, -100 mesh) were prepared for a number of samples. Details of standards used and operating conditions of the probe are given in the Appendix.(I).

Physical Properties

The physical properties of the zircons from the various

TABLE 30

Summary of Physical Properties of Zircons in Dominant Rock Types from Yeoval

Feature	Granites		Orthoclase Diorites	Quartz-Mica Diorites	Gabbros
	Coarser Types	Granophyric Types			
Average Length (mms)	0.06-0.08	0.04-0.06	0.04-0.08	0.08-0.22	0.10-0.20
Length/Breadth	2.0 -2.2	1.6 -1.8	1.6 -2.2	2.0 -2.6	
Colour	Colourless	Colourless	Colourless & pale lilac	lilac	lilac
Crystal face Development	Excellent	Excellent	Excellent	fair	poor
Cracks	If present are very fine		Fine Cracks	Usually coarse & very abundant	very coarse

rock types are summarised in Table 30. Selected crystal drawings of zircons from the granite and diorite are given in Fig. 25. From these, the zircons from the granite are distinctly different to those in the diorite. No malacons were observed in the diorites and gabbros although a few rare crystals were observed in the granite, particularly in those varieties which contained fluorite. This supports Poldervaart's (1956) view that hydrothermal activity is associated with the production of malacons (see also Akhmanova and Leonova, 1961, on metamictisation of zircons). Histograms of length and length/breadth ratios have been constructed. For both these parameters, the zircons from the granite show a very limited range of variation while those from the diorite show a much wider distribution. An interesting feature of the parameters for the granites is the slight difference the coarser and granophyric types. In the coarser granites the mean length ranges from 0.06 to 0.08 mms. with an average L/B ratio of 2.0 to 2.2 which contrasts with a mean length of 0.04 to 0.07 mms and L/B ratio of 1.6 to 1.8 for the granophyric types. Thus, it appears that the rapid crystallisation of the granophyric types, which are suggested as being chilled margins of the granite against the gabbro and diorite, is also reflected in the zircon population.

Chemistry

Because of the close relationship of hafnium and zirconium (similar ionisation potentials, ionic radii, and charge) any variation in conditions of crystallisation should be reflected in the Zr:Hf ratio of the zircon. Fleischer (1955) compiled all published determinations of HfO_2 content and hafnium-zirconium ratio of minerals and rocks up to 1955. However, owing to insufficient data given by the authors he was not able to make a grouping determination on zircons according to the composition of the host rock.

Since that time a number of Russian workers have made detailed studies of zircons from granitic rocks. Kosterin et al. (1958), Shevaleevskii et al. (1960), Meliksetyan (1960) and Kosterin et al. (1960) have shown that the Zr/Hf ratios in zircons from calc-alkaline rocks generally decrease from values of about 60 for zircons from basic, early-formed, types (gabbro and diorite) to about 30-40 for zircons from granites.

Lyakhovick and Shevaleevskii (1962) found the Zr:Hf ratio in zircons from quartz diorites and granodiorites to range from a maximum of 40-53, to a fairly constant 35-40 in the biotite granites and a minimum of 21-23 in salic rocks such as alaskites.

However, Kosterin et al. (1963) found, in only one group of rocks from north Kazakhstan, a regular decrease in the Zr/Hf

TABLE 31a

Electron Probe Analyses of Grain Mounts of Zircons from the Yeoval Rocks

Rock Type	Rock No. & Mesh Size	Crystal No.	HfO_2	ZrO_2	SiO_2	Total	Zr/Hf
Gabbro	W54 -36+72	1	1.71	64.8	32.3	98.8	33
		2	1.43	65.5	32.1	99.0	40
		3	1.77	66.9	32.5	101.2	33
		4	2.15	66.9	32.8	101.9	27
		5	1.63	65.5	32.4	99.5	35
Gabbro	W69 -36+72	1	1.90	64.6	33.2	99.7	30
		2	2.23	64.7	32.9	99.8	25
		3	3.18	65.9	33.7	102.8	18
		4	2.55	65.2	34.1	101.9	22
		5	2.24	66.6	33.7	102.5	26
		6	2.09	67.2	34.1	103.4	28
Pyroxene-mica diorite	G71 -72+100	1	2.30	66.4	33.5	102.2	25
		2	2.16	65.4	32.2	99.8	26
		3	2.29	66.0	33.2	101.5	25
		4	2.22	65.9	33.2	101.3	26
		5	2.36	65.7	32.6	100.7	24
		6	2.21	66.2	33.6	102.0	26
		7	2.04	66.1	33.5	101.6	28
Pyroxene-mica diorite	Y8 -72+100	1	1.53	65.6	32.1	99.2	36
		2	1.44	65.0	32.1	98.5	39
		3	1.71	65.3	32.0	99.0	33
		4	1.58	65.3	32.3	99.2	36
Quartz-mica diorite	G107 -72+100	1	1.70	65.5	32.4	99.6	34
		2	1.88	65.5	32.5	99.9	31
		3	1.91	65.4	32.6	99.9	30
		4	1.97	65.5	32.6	100.1	30
		5	1.88	65.4	32.8	100.1	31
Quartz-mica diorite	Y235 -72+100	1	1.72	65.8	31.8	99.3	33
		2	1.56	65.7	31.8	99.1	37
		3	1.65	65.8	32.4	99.9	35
		4	1.54	65.8	31.7	99.0	37
		5	2.04	65.7	32.9	100.6	38

TABLE 31a (continued)

Electron Probe Analyses of Grain Mounts of Zircons from the Yeoval Rocks

Rock Type	Rock No. & Mesh Size	Crystal No.	HfO_2	ZrO_2	SiO_2	Total	Zr/Hf
Quartz-mica diorite	Y235 -100+150	1	2.22	66.2	33.1	101.5	26
		2	1.99	66.3	33.3	101.6	29
		3	2.04	66.3	33.2	101.5	28
		4	2.06	66.1	33.0	101.2	28
		5	2.16	66.1	33.2	101.5	27
Quartz-mica diorite	Y148 -100+150	1	1.54	66.0	32.7	100.2	37
		2	1.18	64.9	30.5	96.6	48
		3	1.41	65.9	31.2	98.5	41
		4	1.69	65.7	31.5	98.9	34
		5	1.50	65.2	31.3	98.00	38
		6	1.37	64.7	30.8	96.9	41
Quartz-mica	Y148 -150	1	1.99	66.0	32.9	100.9	29
		2	2.04	66.0	32.8	100.8	28
		3	2.10	66.3	33.3	101.7	28
		4	2.04	66.0	32.8	100.8	28
		5	2.08	66.2	33.1	101.4	28
Quartz-mica diorite	G46 -72+100	1	1.60	63.0	32.0	96.6	34
		2	2.02	63.6	32.1	97.7	28
		3	1.92	64.4	32.8	99.1	29
		4	1.81	66.0	33.5	101.3	32
		5	2.02	65.0	33.3	100.3	28
Quartz-mica	G92 -72+100	1	1.56	65.1	29.1	95.8	37
		2	1.79	65.4	29.9	97.1	32
		3	1.86	65.4	29.7	97.0	31
		4	1.73	65.1	28.9	95.7	33
		5	1.78	65.2	29.0	96.0	32
		6	1.72	65.3	29.2	96.2	33
		7	1.72	65.2	28.8	95.7	33
Quartz-mica diorite	G92 -100+150	1	1.69	65.3	33.1	100.1	34
		2	1.71	65.4	32.8	99.9	33
		3	1.51	65.2	32.5	99.2	38
		4	1.75	65.5	33.1	100.4	33
		5	1.66	65.5	33.3	100.5	34

TABLE 31a (continued)

Electron Probe Analyses of Grain Mounts of Zircons from the Yeoval Rocks

Rock Type	Rock No. & Mesh Size	Crystal No.	HfO_2	ZrO_2	SiO_2	Total	Zr/Hf
Quartz-mica diorite	G92 -100	1	1.84	65.5	32.5	99.8	31
		2	1.53	65.4	33.3	100.2	37
		3	1.70	65.4	32.9	100.0	34
		4	1.84	65.5	32.9	100.2	31
		5	1.82	65.4	33.1	100.3	31
		6	1.75	65.5	32.7	100.0	31
		7	1.78	65.5	32.6	99.9	32
	Breadth	8a)	1.78	65.5	32.3	99.6	32
	Length	8b)	1.88	65.5	32.3	99.7	31
Quartz-mica diorite	G86 -72+100	1	2.02	62.8	32.7	97.5	27
		2	1.90	64.9	33.2	100.0	30
		3	1.89	64.9	33.4	100.2	30
		4	2.09	65.6	33.3	101.0	27
		5	1.85	65.4	33.6	100.9	31
Quartz-mica diorite	G99 -100+150	1	2.12	66.2	33.3	101.6	27
		2	2.30	66.0	33.1	101.5	25
		3	1.96	66.5	33.4	101.9	30
		4	2.30	66.5	33.0	101.8	25
		5	2.12	66.6	33.5	102.2	27
Quartz-mica diorite	G99 -150	1	2.12	66.9	33.8	101.9	28
		2	1.93	66.5	33.6	102.1	30
		3	2.42	66.3	33.6	102.3	24
		4	2.32	66.1	33.6	102.1	25
		5	2.23	66.3	33.4	101.9	26
Quartz-mica diorite	Y150 -36+72	1	1.83	65.4	33.3	100.5	31
		2	1.89	65.3	33.3	100.6	30
		3	2.15	65.5	32.7	100.4	27
		4	2.39	65.5	32.7	100.6	24
		5	2.09	65.4	32.9	100.4	27
		6	1.98	65.3	33.0	100.3	29
		7	2.30	65.4	33.2	100.9	25
		8	1.94	65.3	33.3	100.5	29

TABLE 31a (continued)

Electron Probe Analyses of Grain Mounts of Zircons from the Yeoval Rocks

Rock Type	Rock No. & Mesh Size	Crystal No.	HfO_2	ZrO_2	SiO_2	Total	Zr/Hf
Quartz-mica diorite	Y150 -100+150	1	2.04	64.8	32.6	99.4	28
		2	1.70	64.7	32.8	99.2	33
		3	1.85	64.6	32.6	99.1	31
		4	2.04	64.6	32.6	99.2	28
		5	2.00	65.2	32.8	100.0	28
Quartz-mica diorite	Y150 -100	1	2.27	65.4	33.2	100.9	25
		2	2.04	65.2	33.7	100.9	28
		3	2.22	65.3	33.2	100.7	26
		4	2.23	65.3	33.0	100.6	26
		5	1.95	65.3	33.4	100.6	29
		6	2.57	65.3	33.5	101.4	22
		7	2.08	65.3	33.3	100.7	28
		8	2.02	65.3	33.3	100.6	28
Quartz-mica diorite	Y147 -72+100	1	1.77	65.3	33.1	100.2	32
		2	2.42	62.4	33.3	98.1	23
		3	1.53	64.2	32.6	98.3	37
		4	1.92	65.5	33.4	100.8	30
		5	1.73	64.6	32.7	99.0	33
		6	1.96	66.3	33.5	101.8	30
Orthoclase diorite	G57 -100	1	1.86	65.5	33.8	101.1	31
		2	1.99	65.7	33.6	101.3	29
		3	2.02	65.4	33.5	100.9	28
		4	1.92	66.0	33.7	101.6	30
		5	2.05	65.7	33.7	101.5	28
Granite	Y147B -100	1	1.53	65.4	32.3	99.2	36
		2	1.71	64.4	32.1	98.2	33
		3	1.70	63.9	32.4	98.0	33
		4	1.58	64.6	32.5	98.7	36
		5	1.66	64.4	32.1	98.2	34

TABLE 31a (continued)

Electron Probe Analyses of Grain Mounts of Zircons from the Yeoval Rocks

Rock Type	Rock No. & Mesh Size	Crystal No.	HfO_2	ZrO_2	SiO_2	Total	Zr/Hf
Chilled Granite Margin	R68 -100	1	1.36	66.9	30.5	98.8	43
		2	1.75	68.5	31.1	101.4	34
		3	1.48	67.8	30.7	100.0	40
		4	1.39	65.7	29.8	96.9	41
		5	1.39	65.7	29.8	96.9	41
		6	1.48	67.8	30.2	99.5	40
Granite	Y43 -72+100	1	2.07	66.1	31.7	99.9	27
		2	1.87	66.4	32.3	100.6	31
		3	1.68	65.8	32.9	100.3	36
		4	1.82	65.2	33.0	99.3	31
		5	1.69	65.6	32.6	99.9	34
		6	1.90	65.9	32.3	100.1	29
Granite	Y43 -100+150	1	2.08	63.1	32.1	97.3	27
		2	1.98	67.8	33.0	102.8	30
		3	2.04	66.0	32.8	100.8	28
		4	2.12	66.7	32.9	101.7	27
		5	2.25	65.4	32.6	100.3	25
		6	1.95	65.3	32.4	99.7	29
Granite	Y43 -150	1	2.15	66.4	32.5	101.0	27
		2	2.03	66.0	32.5	100.5	28
		3	1.98	68.9	32.8	103.7	30
		4	1.98	67.2	32.7	101.9	30
		5	2.05	67.9	32.7	102.6	29
		6	2.24	65.3	32.4	99.9	25
Aplite	Y53A -100	1	2.25	68.3	32.9	103.4	27
		2	2.01	68.7	33.3	104.0	29
		3	1.98	70.1	33.5	105.6	31
		4	(2.38	68.7	33.2	104.3	(26
			(1.89	68.8	33.3	104.0	(32
		(centre)	(1.94	68.6	33.0	103.5	(32
			(2.30	68.7	33.2	104.2	(27
		5	2.24	68.1	32.6	102.9	27

TABLE 31b

Electron Probe Analyses of Polished Thin Sections Containing Zircons from the Yeoval Rocks

Rock Type	Rock No.	Host Mineral(s)	HfO_2	ZrO_2	SiO_2	Total	Zr/Hf
Granite	Y53	Biot-Qtz	2.02	66.7	33.7	102.4	29
		Qtz	2.32	65.5	33.6	101.4	25
		K-F-Hbl	(2.43			101.3	(24
		(centre)	(1.99	65.4	33.5	100.8	(29
			(2.12			101.0	(27
			(2.32			101.2	(25
		K-F-Magnet	1.76	65.7	33.6	101.1	33
		Hbl	2.11	65.5	33.7	101.3	27
		Biot-Feld	2.11	66.1	33.7	101.9	27
Granite	Y43	Qtz	1.53	65.8	33.4	100.7	37
		Biot-Feld	2.04	65.2	33.2	100.4	28
		Qtz-K-F	(2.17			100.1	(26
		(centre)	(2.00	65.5	33.5	101.0	(29
			(1.77			100.8	(32
			(2.17			101.2	(26
		K-F	1.69	65.2	33.5	100.4	34
		K-F-Biot	2.88	65.1	33.6	101.6	20
		K-F-Biot	2.04	65.2	33.1	100.3	28
		Magnet-K-F	4.21	65.7	33.7	103.6	14
Quartz-mica diorite	Y161	Hbl-Plag	2.05	66.7	33.2	101.9	28
		Plag	2.01	66.8	33.0	101.8	29
		Qtz	2.81	65.5	32.5	100.8	20
Quartz-mica diorite	Y150	Hbl	2.47	65.5	33.7	101.7	23
		Hbl-Plag	2.15	65.2	33.1	100.5	27
		Qtz-Plag	2.05	65.3	32.7	100.1	28
		Qtz-Plag	2.26	65.5	32.5	100.3	25
		Plag	2.15	65.9	33.3	101.4	27
Quartz-mica diorite	G110	Qtz	2.28	66.8	32.8	101.9	26
		Plag	2.03	65.5	32.9	100.4	28
		Plag	1.88	67.2	33.1	102.2	31
Quartz-mica diorite	Y71	Plag	1.92	65.5	33.2	100.6	30
		Biot-Magnet	1.99	66.8	32.9	101.7	29
		Hbl	2.01	63.5	33.6	99.1	28
		Uralite	1.97	67.4	33.0	102.4	30
		K-F	1.96	67.0	33.0	102.0	30

ratio in zircons from mafic to felsic rocks. The Zr/Hf ratio in the diorites, quartz diorites and granodiorites varied from 23-83 and this was attributed to assimilation of enclosing rocks.

The Zr and Hf and Zr/Hf ratios in zircons from the Yeoval rocks are given in Table 31. These results show no decrease in the Zr/Hf ratio from the gabbros to diorites and granites as observed by many Russian workers; in fact, there is an overlap in the Zr/Hf ratios for all the rocks. No trend is obvious in the Zr/Hf ratios of zircons from the different crystal sizes i.e. in some samples the Zr/Hf ratio decreases in going from the coarser to finer grainsize (Y235, Y148, Y43) while in others it remains essentially the same (G99, G92, Y150). There is a tendency for the Zr/Hf ratio to be more constant in the zircons from the finer grainsizes, than those in the coarser fractions.

The presence of zircon crystals either as inclusions in all mineral phases or at the grain boundaries of different minerals would suggest that the crystallisation range of zircon was not short. If this is the case then the Zr/Hf ratio might be expected to change with change in composition of the magma. However, as can be seen from Table 31, the Zr/Hf ratio in the diorites in some cases decreases as the crystallisation trend changes from hornblende and plagioclase (early

crystallisation products) to quartz and potassium feldspar (last minerals to crystallise); in others it increases; while in others it remains essentially constant. In the zircons from the granites the variation in Zr/Hf is extremely random. If the markedly different ratios are disregarded the Zr/Hf ratios in zircons in the minerals from the diorites are remarkably consistent in the range 27-30. This also agrees with the average Zr/Hf ratio of about 30 for all zircon in the diorites which would suggest either that the range of crystallisation of zircons was limited or the Zr and Hf contents of the magma did not greatly change with time. An interesting correlation of the Zr and Hf contents and physical properties is notable in the "chilled" margins. With the exception of one crystal the Zr/Hf ratio of R68 is about 40, which is very much higher than that in any zircons from the other granites. The crystals are smaller than those in the other granites, and it has been suggested that these were a result of the rapid crystallisation of the rock. This is supported by the lower Hf contents (i.e. higher Zr/Hf ratios) in the centres of zoned zircons from other samples of granite.

To make comparisons of Zr/Hf ratios between rock types even more difficult, a number of zircons from the granites are zoned. The variation in composition of the zones almost covers the whole range of values of Zr/Hf ratios observed in

the different rock types. The trend of variation in the zones is from Hf-poor core to Hf-rich rim. Although quite a number of zircons in the diorite appear optically zoned, no variation was detectable on the probe; the crystals are remarkably homogeneous. No relationship of zirconium with hafnium was observed in the zircons from the Yeoval rocks. This contrasts with the work of Steiger and Wasserburg (1966), the figures (Fig. 10) from which show a negative correlation of Zr and Hf in zircon from the Sandia Granite, New Mexico.

No Fe, Mg or U could be detected in the zircons.

Thus from an examination of the zircons from the different Yeoval rock types it may be concluded that:

(i) the physical properties suggest different physico-chemical conditions for the crystallisation of the dioritic and granitic rocks resulting in completely different zircon populations for the two rock groups

(ii) no trend in Zr/Hf ratios in zircons from basic to acid rocks or their constituent minerals is present

(iii) the Zr/Hf ratio cannot be used as a basis for distinguishing between the various rock types.

4.8 APATITE.

Apatite is the most common accessory mineral apart from the opaques. It usually occurs as stubby crystal inclusions in all major mineral phases. This is the reason for at least

TABLE 32

Electron Probe Analyses of Apatites Included in Different Mineral Phases from the Pyroxene-Mica Diorite

Host Mineral Phase	CaO	P_2O_5	SiO_2	Cl	Total
Biotite	52.7	42.1	0.21	1.8	96.8
Magnetite and Biotite	52.4	42.2	0.19	1.6	96.4
Plagioclase	53.8	43.1	0.19	1.4	98.5
Hornblende	52.4	41.8	0.21	1.2	95.6
Quartz and Magnetite	54.3	42.8	0.21	1.8	99.1
Quartz	52.5	41.9	0.23	1.6	96.2
Plagioclase	53.1	42.1	0.19	1.4	96.8

a small amount of phosphorus being detected in every analysed phase (e.g. up to 0.1% P_2O_5 in the hornblendes). Apatite is more abundant in the diorites than any other major rock type in the Yeoval district and it is from the diorites that the partial electron probe analyses of apatites were obtained (Table 32).

The main objectives of the analyses were: firstly, to ensure that there were inclusions of apatite in each mineral phase; and secondly, to see if any changes in their chemistry were apparent with changes in the composition of the host mineral.

Mn, Mg, Fe, Al, Zr, Sr and S were below the limits of detection, and at the time of analysis, fluorine determinations were not possible.

The results indicate that the composition of apatite does not significantly change from one mineral phase to another. Some rocks, particularly those in which xenoliths are present, have a second generation of apatite, occurring as very fine needles and cutting across the grain boundaries of all minerals. The needles are up to 3-4 mms. long but are rarely any more than 10 microns wide, making electron probe analyses difficult. An approximate analysis of fifteen needles indicates that the CaO and P_2O_5 contents are slightly lower than the coarse apatites in the diorites, and the chlorine content is much lower

(approximately 0.6%). It is suggested that these late stage apatite needles contain more fluorine and water.

It is interesting to note the consistency of the silicon results in crystals from both generations of apatite i.e. about 0.2% $\pm$ 0.2. This is not due to fluorescence from the enclosing minerals as apatite in the magnetite has similar silicon contents to those in the silicates, even when the host is quartz. This data supports the suggestion of Koritnig (1965) and Cruft (1966) that the Si^{IV} ion is admitted by P^{V} rather than the silicon being present as inclusions of quartz in the apatite.

4.9 DISTRIBUTION OF ELEMENTS BETWEEN CO-EXISTING MINERALS

The distribution of the various major elements between co-existing mineral phases in the gabbros, diorites, and granites is discussed in this section. The distribution of certain trace elements between co-existing mineral phases is given in the following section. In the gabbros(and pyroxenites) the distribution study is restricted to the pairs, olivine-orthopyroxene olivine-clinopyroxene and clino-orthopyroxene. In the diorites and granites, the feldspars are not discussed because of the wide variation in composition of the plagioclases and because the potassium feldspars were only partially analysed.

Theoretical considerations

When two (or more) minerals of variable composition

co-exist in a rock, a certain regularity in the distribution of the elements between the minerals is to be expected. Equilibrium, which may or may not have been attained in the rocks under consideration, is necessary for distribution to be regular.

Ramberg and De Vore (1951) developed a general relationship for the distribution constant (K) for co-existing olivine and orthopyroxene.

$$K = \frac{Xo}{1-Xo} \cdot \frac{1-Xp}{Xp} = \exp. \left[\Delta F/(RT)\right] \qquad \ldots\ldots\ldots(1)$$

where $Xo = Mg/Mg+Fe^{2+}$ in olivine and $Xp = Mg/Mg+Fe^{2+}$ in orthopyroxene, both expressed as atomic ratios. ΔF is the change of free energy in the exchange reaction, R is the gas constant and T the absolute temperature. Equation (1) applies only when the mineral phases are ideal solid solutions.

Kretz (1959, 1960, 1961, 1963) used this relationship to study a number of co-existing mineral phases:

a) orthopyroxene-clinopyroxene;

b) clinopyroxenes-calcic amphiboles-biotites;

c) garnet-biotite-hornblende;

d) orthopyroxene-garnet.

Mueller (1960, 1963) used atomic fractions (e.g. $Mg/Mg+Fe^{2+}$) in order to obtain distribution coefficients for co-existing olivine-pyroxene, clinopyroxene-orthopyroxene,

and amphibole-biotite.

Another distribution coefficient has been suggested by Matsui and Banno (1965) and Matsui et al.(1966). This is the apparent partition (or distribution) coefficient and is defined as follows:

$$K_A^1 \frac{X.Y}{M.Fe} = (M/Fe)_x/(M/Fe)_y \quad \ldots\ldots\ldots(2)$$

where X and Y refer to silicate phases under consideration and M denotes a divalent ion of similar size to Mg and Fe. The apparent partition coefficient is approximately equal to the equilibrium constant in the exchange reaction;

$$(M)_x + (Fe)_y = (Fe)_x + (M)_y \quad \ldots\ldots\ldots(3)$$

A plot of log $(M/Fe)_x$ against log $(M/Fe)_y$ should then, if the solid solutions are ideal, give a straight line with a slope of 45^o. If the solid solutions are non-ideal, then the ratio $(M/Fe)_x/(M/Fe)_y$ will not be constant. This plot differs from that of Kretz (1960) who calculates the atomic ratio of one element, for example Mn, as: the number of Mn atoms/total number of octahedrally co-ordinated atoms (minus Al). Kretz plotted this ratio for co-existing minerals and where the points defined a smooth curve he suggested (p.171) that "equilibrium was attained and that the effect of numerous compositional variables has not been great enough to alter the distribution coefficient noticeably". If a scatter of points

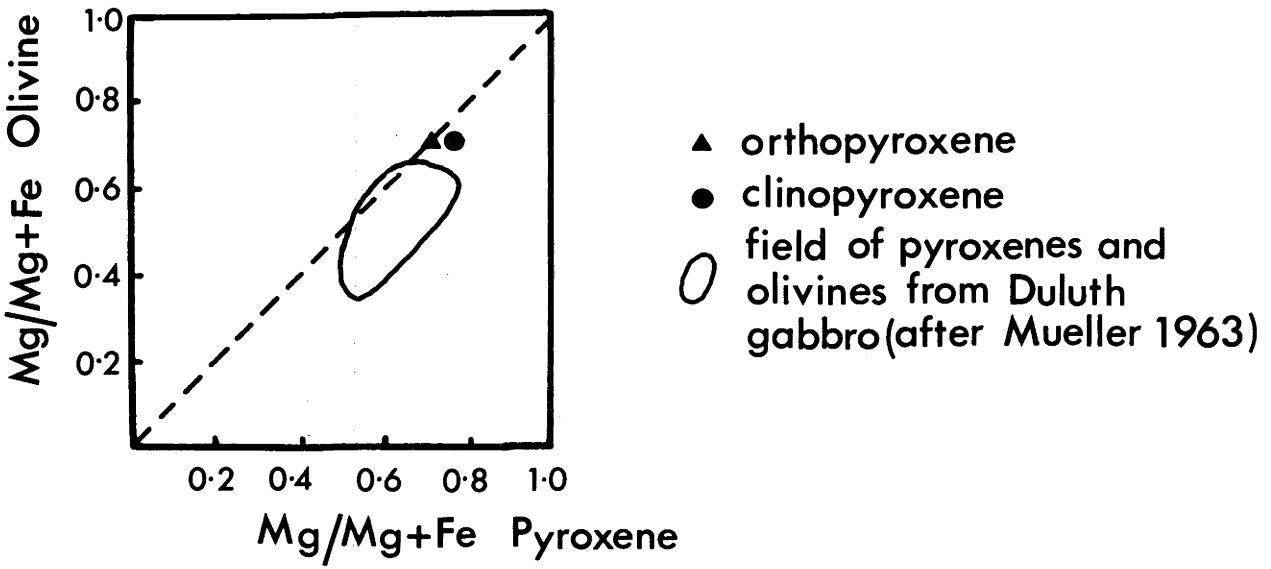

Fig.26 Relation between the atomic fractions of magnesium in co-existing pyroxenes and olivines.

results the distribution coefficient was said to be displaced by the variable concentration of another element in one or both minerals (the scatter may also result from other factors which are discussed on p. 84 of this thesis). In his study of the distribution of Fe and Mg between olivine and pyroxene, Mueller (1963) plots Mg/Mg+Fe in olivine vs. Mg/Mg+Fe in pyroxene and interprets his results in a similar manner to Kretz and Matsui et al. (1966). Kretz (1963), in evaluating the distribution of Mg and Fe between ortho- and clinopyroxene, used the same plot as Mueller (1963).

Distribution of Elements between Olivine and Pyroxene

Published data on the distribution coefficients involving olivine and pyroxene are very limited. Sahama and Torgeson (1949) implied that olivine and orthopyroxene are ideal solutions and so Mg and Fe should give a simple distribution curve. Ramberg and De Vore (1951) observed in natural assemblages that olivines contain less Mg than the co-existing orthopyroxene as long as the average mole fraction (Xo + Xp)/2 is less than about 0.65, where Xo and Xp are the same as in equation (1). Mueller (1963), using Snyder's (1959) analyses of co-existing olivines and pyroxenes from the Duluth gabbro, obtained a scatter of points below the 45° line for the ratio Mg/Mg+Fe which he suggests is what might be expected from a poorly equilibrated assemblage. Another explanation of the

TABLE 33

Distribution and Apparent Partition Coefficients for Co-existing Olivine and Pyroxene from the Yeoval Rocks

	FeO	MgO	CaO	MnO	Mg/Fe	Apparent Partition Coefficients	Mg/Mg+Fe	Distribution Coefficients
Ol	27.4	35.3	-	0.6	2.298		0.697	
Opx	17.3	26.3	1.0	0.6	2.706	KA Ol-Opx=0.85	0.730	KD Ol-Opx=0.85
Cpx	8.0	14.9	21.5	0.7	3.337	KA Ol-Cpx=0.69	0.769	KD Ol-Cpx=0.69

Where Ol = Olivine
Opx = Orthopyroxene
Cpx = Clinopyroxene

scatter is that neither olivine nor orthopyroxene are ideal solid solutions; a premise which is also suggested by Ramberg and De Vore (1951, p.199).

Data on co-existing olivine and pyroxene in the Yeoval rocks are given in Table 33 along with their respective ratios. In this simple system, the computation of both apparent partition and distribution coefficients give the same result. The distribution of Mg between co-existing olivine and orthopyroxene is much closer to unity than that for the olivine-clinopyroxene, this aspect being more clearly seen in Fig. 26. For comparitive purposes, the field of co-existing olivines and pyroxenes from the Duluth complex (after Mueller, 1962) is also given.

Although nothing positive can be stated because of insufficient data, it is suggested that the olivines and pyroxenes of the Yeoval gabbro crystallised under equilibrium conditions. Additional information to support this will be given in later sections.

Distribution of Elements between Orthopyroxene and Clinopyroxene

Published analyses of co-existing orthopyroxene and clinopyroxene show that orthopyroxene has lower Mg/Fe and Mn/Fe ratios, and less Ti and octahedrally co-ordinated Al, than clinopyroxene.

Only two sets of analyses (Table 33) of co-existing pyroxenes are available for the Yeoval rocks; one pair from the gabbro and one from the pyroxenite.

As for olivine, the distribution (or partition) coefficients, calculated according to Kretz (1963) and Matsui et al. (1966), give similar results. In the gabbro, the distribution coefficient is 0.82 while in the pyroxenite it is 0.53. Kretz (1961, 1963) and Bartholomé (1961) suggested that the distribution coefficient for co-existing clinopyroxene and orthopyroxene (or pigeonite) in rocks known, or presumed, to be of magmatic crystallisation was displaced towards unity. Kretz (1963) gives a range of coefficients from 0.51 - 0.65 in high grade metamorphic rocks and 0.65 - 0.86 in rocks derived from crystallisation of a magma. Similar results have been obtained by Mueller (1963).

A graphical representation of the distribution of Mg and Fe^{2+} (expressed as Mg/Mg+Fe) between co-existing pyroxenes from the Yeoval gabbro and pyroxenite shows the points to lie close to the curves obtained by Kretz (1963, p.779, Fig.1) for magmatic and metamorphic rocks respectively.

Distribution of Elements between Hornblende and Biotite.

Much of the literature on element distribution between co-existing hornblende and biotite is restricted to high grade metamorphic rocks (Kretz 1959, 1960; Mueller 1960; Saxone 1966) with little or no attention being given to igneous assemblages since equilibrium is more likely attained in high

TABLE 34

Percentages of Each of Ti, Total Iron (expressed as FeO), Mn and Mg of Total Y Group Cations in Biotite and Hornblendes from the Yeoval Diorite and Granite

		Y8		G154		G120		Y41		Y235		G107		Y150		Y227		Y43		Y53		Average for Diorites
		Bi	Ho	Bi	Ho	Bi	Ho	Bi	Ho	Bi	Ho	Bi	Ho	Bi	Ho	Bi	Ho	Bi	Ho	Bi	Ho	
Ti	(%)	7.07	2.08	6.78	2.25	7.38	2.03	7.59	2.08	6.62	1.91	7.68	1.86	6.18	1.98	6.83	1.73	7.50	2.08	7.04	2.17	3.55
	(Bi/Ho	3.40		3.01		3.64		3.65		3.47		4.13		3.12		3.95		3.61		3.24		
Total Iron as FeO	(%)	49.82	42.66	49.20	43.35	51.34	45.19	48.60	44.91	50.67	43.65	48.65	39.48	49.61	43.35	49.27	40.75	55.51	47.89	65.30	64.78	1.16
	(Bi/Ho	1.17		1.13		1.14		1.08		1.16		1.23		1.14		1.21		1.16		1.01		
Mn	(%)	1.13	1.24	1.36	1.45	1.17	1.18	1.12	1.48	1.36	1.66	1.11	1.38	1.57	1.49	1.37	1.38	1.61	1.65	1.37	1.70	0.91
	(Bi/Ho	0.91		0.94		0.99		(0.76)		0.82		0.80		(1.05)		0.99		0.98		0.81		
Mg (Total)	(%)	41.98	54.02	42.65	52.97	40.10	51.60	42.72	51.52	41.03	52.75	42.56	57.31	42.64	53.19	42.51	56.13	35.37	48.38	26.29	31.33	0.78
	(Bi/Ho	0.78		0.80		0.78		0.83		0.78		0.74		0.80		0.76		0.73		0.84		
Mg/Fe	(Ratio	0.84	1.27	0.87	1.22	0.78	1.14	0.88	1.15	0.81	1.21	0.87	1.45	0.86	1.23	0.86	1.38	0.64	1.01	0.40	0.48	0.67
	(Bi/Ho	0.66		0.71		0.68		0.76		0.67		(0.60)		0.70		0.62		0.63		0.83		
	(Ho/Bi	1.51		1.40		1.46		1.31		1.49		(1.67)		1.43		1.60		1.58		1.20		1.46

TABLE 35a

Selected Molecular Ratios for Coexisting Biotite and Hornblende from Yeoval Rocks

(Total Iron Expressed as FeO)

		Y8	G154	G120	Y41	Y235	G107	Y150	Y227	Y43	Y53	Average (Diorite)
Biotite	Mg/Fe	0.84	0.87	0.78	0.88	0.81	0.87	0.86	0.86	0.64	0.40	0.84
	Mn/Fe	0.023	0.028	0.023	0.023	0.027	0.023	0.032	0.028	0.029	0.021	0.026
	Ti/Fe	0.142	0.138	0.144	0.156	0.131	0.158	0.124	0.139	0.135	0.108	0.141
	Na/K	0.024	0.032	0.027	0.030	0.026	0.027	0.030	0.029	0.023	0.028	0.028
Hornblende	Mg/Fe	1.27	1.22	1.14	1.15	1.21	1.45	1.23	1.38	1.01	0.48	1.26
	Mn/Fe	0.029	0.033	(0.026)	0.033	0.038	0.035	0.034	0.034	0.034	0.026	0.034
	Ti/Fe	0.049	0.052	0.045	0.046	0.044	0.047	0.046	0.042	0.043	0.033	0.046
	Na/K	1.863	2.221	1.962	2.331	2.359	2.437	2.324	2.159	3.670	3.338	

TABLE 35b

Selected Apparent Partition Coefficients for Biotite and Hornblende from Yeoval Rocks

Biotite/ Hornblende	Mg/Fe	0.66	0.71	0.68	0.77	0.67	0.60	0.70	0.62	0.63	0.83	0.68
	Mn/Fe	0.79	0.85	0.88	0.70	0.71	0.66	(0.94)	0.82	0.85	0.81	0.77
	Ti/Fe	2.90	(2.65)	3.20	3.39	2.98	3.36	(2.70)	3.31	3.14	3.27	3.19
	Na/K	0.013	0.014	0.014	0.013	0.011	0.011	0.013	0.013	0.006	0.008	0.013

grade metamorphic rocks.

Comparison of the element distribution between hornblende and biotite is simplified by expressing the amount of each element as a percentage of the total Y group cations (Table 34). The structural formulae for both minerals have been recalculated, with total iron expressed as FeO, because of the variation in Fe^{3+} of the biotites . For the diorites, titanium is more abundant in the biotites than in the hornblendes, the average value for the ratio of the percentage of Ti in the biotite Y sites to the percentage in the hornblende Y sites being 3.55. This is much higher than the average ratio of 2.21 for 18 co-existing biotites and hornblendes from granitic rocks (Chappell 1966, Tables 33 and 37) and 2.94 for 8 biotites and hornblendes from the Moonbi granites (Chappell 1966, p.175). The biotites and hornblendes from the Yeoval granite have a lower ratio (3.24), which is the result of the higher Ti content of the hornblendes. Little can be said on the Fe^{3+} distribution because of the poor results in the biotites. Manganese and magnesium are more abundant in the hornblendes whereas Fe^{2+} is more abundant in the biotites.

The treatment of the distribution of Ti, total iron, Mn and Mg between co-existing biotite and hornblende follows that of Matsui and Banno (1965) using equations (2) and (3) given previously. The calculated ratios (M/Fe) and apparent partition

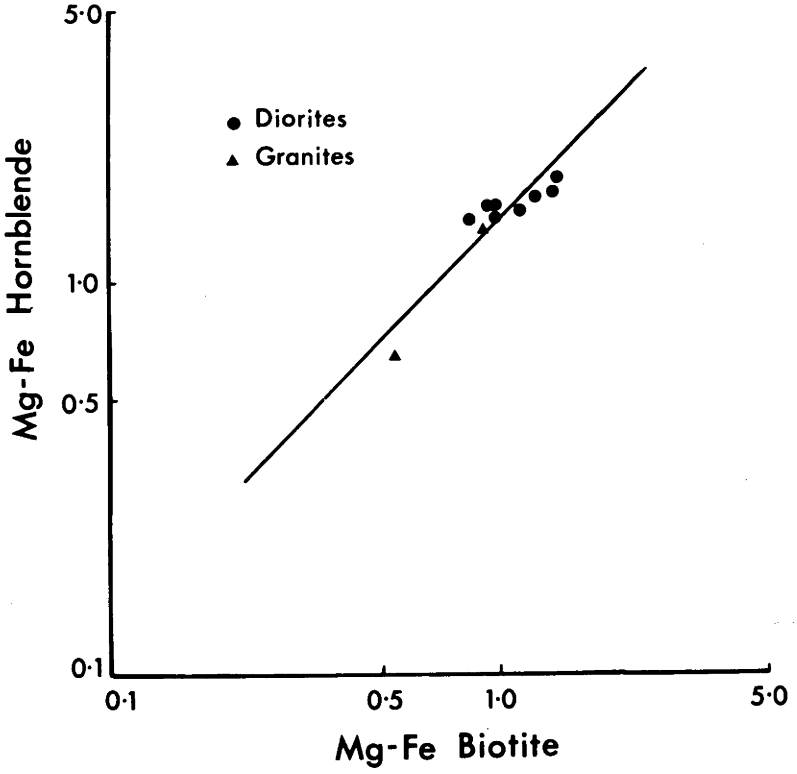

Fig.27a Mg-Fe distribution between co-existing hornblende and biotite in diorites and granites from the Yeoval district. (Straight line is of 45° slope).

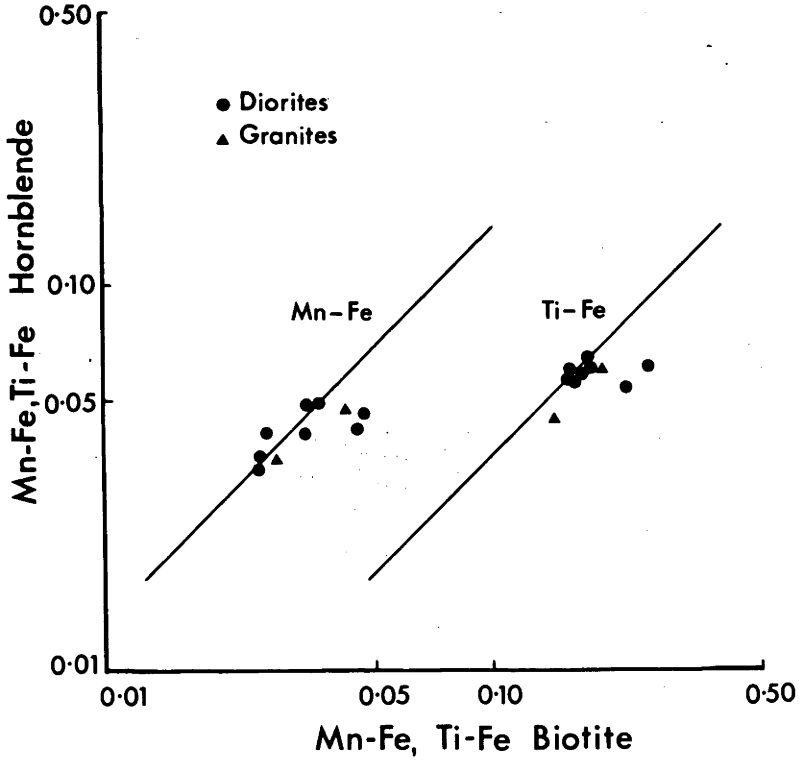

Fig.27b Mn-Fe and Ti-Fe distribution between co-existing hornblende and biotite in diorites and granites from the Yeoval district.

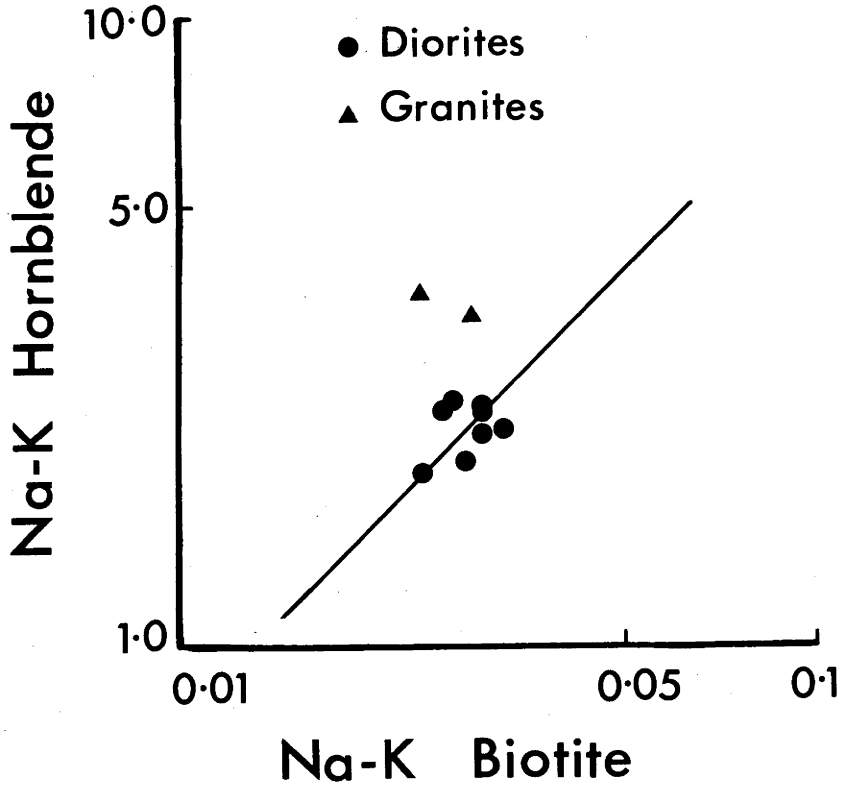

Fig.27c Na-K distribution between co-existing hornblende and biotite in diorites and granites from the Yeoval district.

coefficients are presented in Tables 35a and 35b respectively. The log-log plots of the Mg-Fe^{2+}, Mn-Fe^{2+} and Na-K distributions for the co-existing hornblendes and biotites are shown in Fig. 27a, b, c. The points, although lying fairly close to a straight line of 45^{o} slope, are somewhat randomly scattered. This scatter is slightly reduced if the results are plotted using total iron (as FeO) rather than Fe^{2+}.

The scatter of points may be due to:

(i) Non-ideality of biotite and hornblende - partition coefficients are calculated on the assumption that the co-existing minerals are ideal solid solutions.

(ii) Variable concentration of another element in biotite or hornblende (Kretz 1960).

(iii) Incomplete mineral separation and inaccurate chemical analyses.

(iv) Chemical equilibrium - probably the most important factor causing the scatter is possible disequilibrium between biotite and hornblende. The zoning of plagioclase indicates at least some disequilibrium between mineral phases within the rock.

(v) Size of system -Kretz (1960) suggests that the size of natural chemical systems has a bearing on the interpretation of distribution studies. Unless the volumes of rock chosen for analyses are relatively small, irregularities in element distribution may appear, even though local equilibrium was attained.

5. TRACE ELEMENT CHEMISTRY

The Yeoval rocks and selected minerals have been analysed for the following trace elements:

Rb, Sr, Ba, Y, Zr, Nb - by x-ray fluorescence spectroscopy (XRF) according to the methods of Norrish and Chappell (1966).

U and Th (rocks only) by gamma-ray spectroscopy.

Emphasis is directed toward the trace element chemistry of the most important rock types, viz: gabbros, diorites and granites.

5.1 TRACE ELEMENT CHEMISTRY OF THE MAJOR ROCK TYPES.

5.1.1 Gabbros, Diorites and Granites (Table 36)

Rubidium and K/Rb Ratios - Rubidium increases from the gabbros (<3 ppm) and pyroxenites (20 ppm) to the pyroxene-mica diorites (40 ppm) and quartz-mica diorites (80 ppm). The higher Rb content of the pyroxenites, relative to the gabbros, is a reflection of the hornblende in the pyroxenite (even though the Rb content of hornblende is itself low), and the lack of any Rb in any mineral phase in the gabbro. For the pyroxene-mica diorites, quartz-mica diorites and orthoclase diorites, the presence of potassium feldspar may accomodate the increasing quantity of Rb in these rocks.

The Rb content of the aplite in the granite is similar to the enclosing granites, although much higher than the average granite of the region, whereas the aplite in the diorite is considerably enriched (193 ppm) relative to the host rock.

TABLE 36

Trace Element Chemistry of the Main Rock Types at Yeoval

	Gabbros					Pyroxenites		
	W71	W3	W53	W42	W66	W61	G153	W60
Rb^{+}	2	1	3	n.d.	n.d.	17	25	18
Ba^{2+}	75	35	84	194	263	113	105	168
K^{+} (%)	0.06	0.03	0.13	0.47	0.66	0.38	0.40	0.50
Sr^{2+}	506	390	392	n.d.	n.d.	112	141	268
K/Rb	300	300	433	-	-	224	160	278
Ba/Rb	38	35	28	-	-	6.6	4.2	9.3
Ba/Sr	0.15	0.09	0.21	-	-	1.01	0.74	0.63
Rb/Sr	0.004	0.003	0.008	-	-	0.15	0.18	0.067
Y^{3+}	6	6	10	n.d.	n.d.	11	12	16
Th^{4+}	<1	<1	1.9	2.0	2.6	0.8	1.6	1.2
U^{4+}	<1	<1	0.4	0.5	0.8	0.2	0.4	0.3
Zr^{4+}	11	5	13	n.d.	n.d.	21	25	38
Nb^{5+}	<1	<1	<1	n.d.	n.d.	<1	<1	<1
Th/K	-	-	4.89	4.26	3.97	2.00	3.87	2.47
U/K	-	-	1.06	1.11	1.14	0.59	0.93	0.60
Th/U	-	-	4.60	3.85	3.49	3.39	4.17	4.12

TABLE 36 (continued)

Trace Element Chemistry of the Main Rock Types at Yeoval

	Pyroxene-Mica Diorites				Quartz-Mica Diorites			
	Y8	G154	G71	G131	Y158	G107	G41	Y75
Rb^{+}	32	42	49	55	79	77	107	72
Ba^{2+}	343	407	586	486	458	650	612	580
K^{+}(%)	0.90	1.17	1.33	1.45	1.89	1.99	2.19	1.90
Sr^{2+}	390	385	446	628	489	560	536	525
K/Rb	281	279	271	264	239	258	205	264
Ba/Rb	10.7	9.7	12.0	8.8	5.8	8.4	5.72	8.1
Ba/Sr	0.88	1.06	1.31	0.77	0.94	1.16	1.14	1.10
Rb/Sr	0.082	0.11	0.11	0.088	0.16	0.14	0.20	0.14
Y^{3+}	23	25	21	24	21	26	n.d.	21
Th^{4+}	3.9	5.7	4.3	5.81	8.6	8.3	9.5	8.0
U^{4+}	1.0	1.3	0.9	1.7	2.5	1.6	2.2	2.3
Zr^{4+}	64	82	98	74	83.2	106	n.d.	97
Nb^{5+}	<1	<1	<1	<1	<1	3	n.d.	3
Th/K	4.36	4.85	3.24	4.22	4.55	4.16	3.93	4.21
U/K	1.10	1.07	0.71	1.00	1.34	0.79	0.92	1.50
Th/U	3.97	4.52	4.57	4.19	3.41	5.29	4.28	2.82

TABLE 36 (continued)

Trace Element Chemistry of the Main Rock Types at Yeoval

	Quartz-Mica Diorites								
	Y161	G92	Y225	G120	Y227	Y235	Y150	Y41	Y148
Rb^{+}	87	67	97	95	74	89	67	109	48
Ba^{2+}	623	547	681	565	619	759	557	731	665
K^{+} (%)	2.07	1.78	2.46	2.18	2.06	2.35	1.87	2.61	1.76
Sr^{2+}	535	577	498	316	524	478	585	507	477
K/Rb	238	266	254	230	278	264	279	240	367
Ba/Rb	7.2	8.2	7.0	5.9	8.4	8.5	8.3	6.7	13.9
Ba/Sr	1.16	0.95	1.37	1.79	1.18	1.59	0.95	1.44	1.39
Rb/Sr	0.16	0.12	0.20	0.30	0.14	0.19	0.11	0.21	0.10
Y^{3+}	24	22	27	31	19	26	22	29	20
Th^{4+}	8.8	7.1	9.7	10.7	7.9	9.0	8.4	11.8	5.4
U^{4+}	2.0	1.7	2.1	2.4	2.2	2.1	2.9	2.8	1.5
Zr^{4+}	127	95	112	134	113	136	97	112	96
Nb^{5+}	2	<1	5	6	<1	3	<1	5	<1
Th/K	4.28	3.99	3.96	4.91	3.86	3.84	4.49	4.50	3.10
U/K	0.86	0.95	0.87	1.12	1.07	0.90	1.22	1.08	0.85
Th/U	4.46	4.21	4.55	4.38	3.59	4.25	3.69	4.18	3.63

TABLE 36 (continued)

Trace Element Chemistry of the Main Rock Types at Yeoval

	Quartz-Mica Diorites							Orthoclase Diorites
	G90	G110	Y71B	G46	G118	G99	Y151	Y205
Rb^{+}	63	72	68	105	71	69	68	119
Ba^{2+}	661	746	694	680	733	779	622	858
K^{+}(%)	1.80	1.82	1.92	2.52	1.90	1.87	1.66	3.19
Sr^{2+}	449	400	416	469	431	452	438	397
K/Rb	286	253	282	240	268	271	244	268
Ba/Rb	10.5	10.4	10.2	6.5	10.3	11.3	9.2	7.2
Ba/Sr	1.47	1.87	1.67	1.45	1.70	1.72	1.42	2.16
Rb/Sr	0.14	0.18	0.16	0.22	0.16	0.15	0.16	0.29
Y^{3+}	25	25	21	23	n.d.	20	20	32
Th^{4+}	6.0	6.2	8.9	12.8	7.4	7.2	8.5	15.49
U^{4+}	1.7	1.7	1.7	2.5	1.0	2.0	2.1	2.63
Zr^{4+}	104	131	113	120	n.d.	110	113	163
Nb^{5+}	4	3	3	5	n.d.	n.d.	3	5
Th/K	3.86	3.42	4.66	5.06	3.86	3.82	5.10	4.86
U/K	0.96	0.98	0.89	0.99	0.51	1.05	1.28	1.14
Th/U	4.04	3.49	5.25	5.13	7.65	3.66	3.99	4.26

TABLE 36 (continued)

Trace Element Chemistry of the Main Rock Types at Yeoval

	Orthoclase Diorites		Granites					
	Y206	G57	Y64	Y53	Y43	Y147B	R69	R77
Rb^{+}	113	145	125	160	108	127	113	99
Ba^{2+}	912	709	579	162	671	684	775	887
K^{+}(%)	3.49	3.42	3.43	3.21	3.01	3.04	3.40	3.18
Sr^{2+}	405	294	31	34	117	103	54	32
K/Rb	309	236	274	201	279	239	301	321
Ba/Rb	8.1	4.9	4.6	1.0	6.2	5.4	6.9	9.0
Ba/Sr	2.25	2.41	18.70	4.76	5.74	6.64	14.35	27.72
Rb/Sr	0.28	0.49	4.03	4.71	0.92	1.23	2.09	3.09
Y^{3+}	31	29	63	57	22	n.d.	n.d.	60
Th^{4+}	15.00	19.28	17.8	14.5	14.2	12.5	14.6	11.0
U^{4+}	4.11	5.48	4.1	3.2	3.1	3.0	2.1	2.1
Zr^{4+}	173	184	293	142	165.	n.d.	n.d.	281
Nb^{5+}	5	6	24	17	15	n.d.	n.d.	18
Th/K	4.30	5.64	5.20	4.52	4.89	3.81	4.29	3.46
U/K	1.18	1.60	1.20	1.00	1.06	0.93	0.62	0.65
Th/U	3.65	3.52	4.32	4.51	4.60	4.10	6.88	5.35

TABLE 36 (continued)

Trace Element Chemistry of the Main Rock Types at Yeoval

	Aplites in Granite		Xenoliths in Diorite	
	Y53A	Y41A	Y151X	G90X
Rb^{+}	161	193	27	61
Ba^{2+}	177	332	396	558
K^{+}(%)	3.79	4.58	1.25	1.36
Sr^{2+}	34	154	479	500
K/Rb	235	237	463	223
Ba/Rb	1.1	1.7	14.7	9.1
Ba/Sr	5.21	2.16	0.83	1.12
Rb/Sr	4.74	1.25	0.006	0.12
Y^{3+}	30	12	23	21
Th^{4+}	n.d.	43.0	n.d.	4.9
U^{4+}	n.d.	13.4	n.d.	1.9
Zr^{4+}	138	98	35	39
Nb^{5+}	19	n.d.	n.d.	<1
Th/k	-	9.40	-	3.62
U/K	-	2.94	-	1.38
Th/U	-	3.20	-	2.63

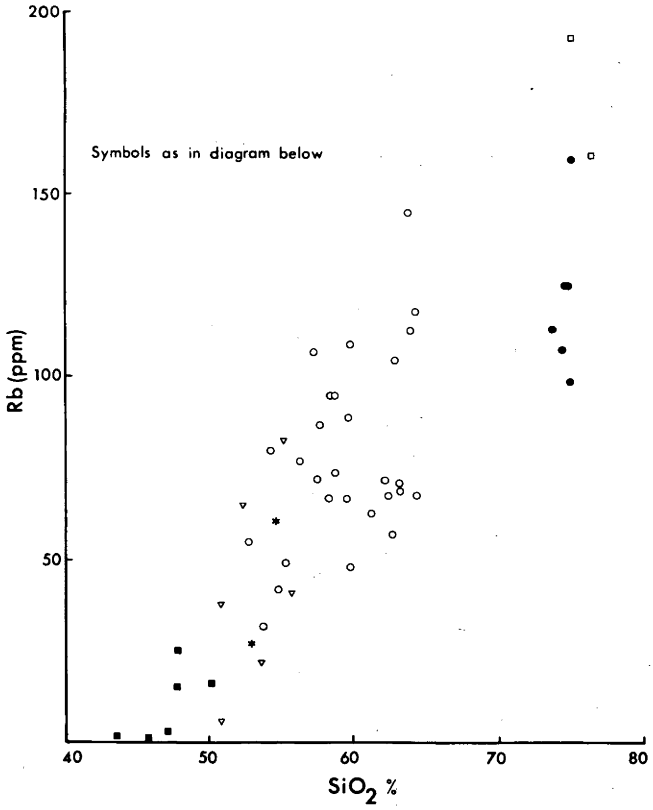

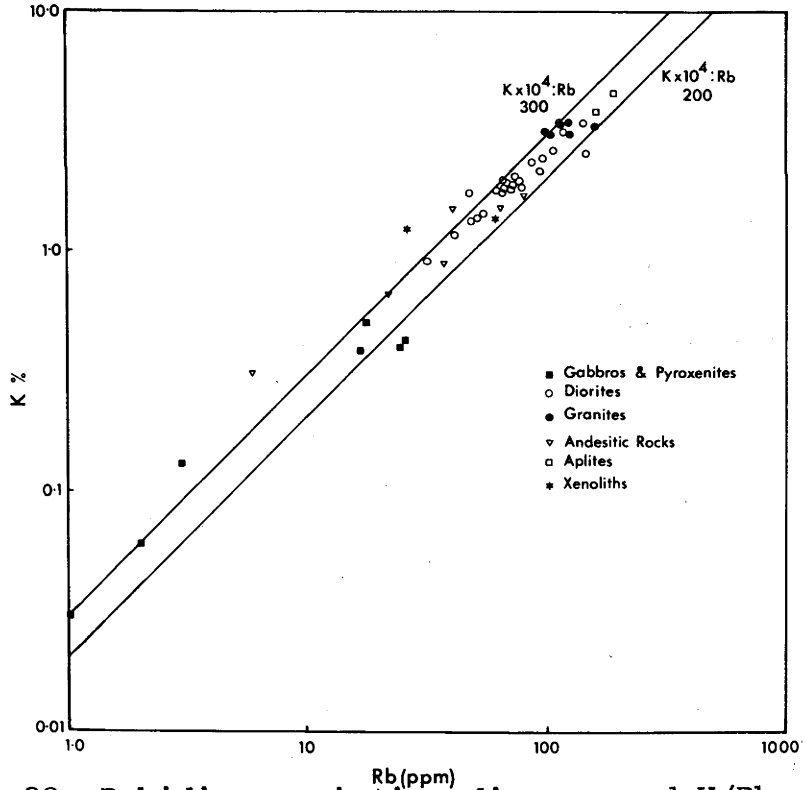

Fig.28 Rubidium variation diagram and K/Rb relationship for the Yeoval rocks.

The xenoliths in the diorite have low Rb contents in keeping with their lower K contents.

The SiO_2 variation diagram for Rb (Fig. 28) shows a wide scatter although there is a general increase in Rb towards the higher SiO_2 contents. The increased scatter in the 60 - 65% SiO_2 range on the SiO_2 variation diagram for Rb is also apparent for the elements Th, Zr and Y. Rubidium and Th closely follow potassium (Taylor 1966). A check of potassium contents of those rocks showing the greatest scatter towards lower values of the above trace elements was made. It revealed that such rocks had low potassium and were the most altered, particularly in the degree of chloritisation of biotite (see section 4.4, p.90 this section).

Because of the marked coherence of K and Rb, the K/Rb ratio has been cited as an important geological parameter in determining fractionation trends (Taylor 1966, Volkov and Savinova 1961). The K/Rb ratio for 80% of the Yeoval rocks lies between 200-300 (Fig. 28). The average K/Rb for the diorites (25 samples) is 263 which is higher than the crustal average of 240 (Taylor 1967). The average Rb content of 82 ppm for the diorites is similar to the crustal abundance of 85 ppm (Taylor 1967). The average Rb content (112 ppm) and K/Rb ratios of the granites

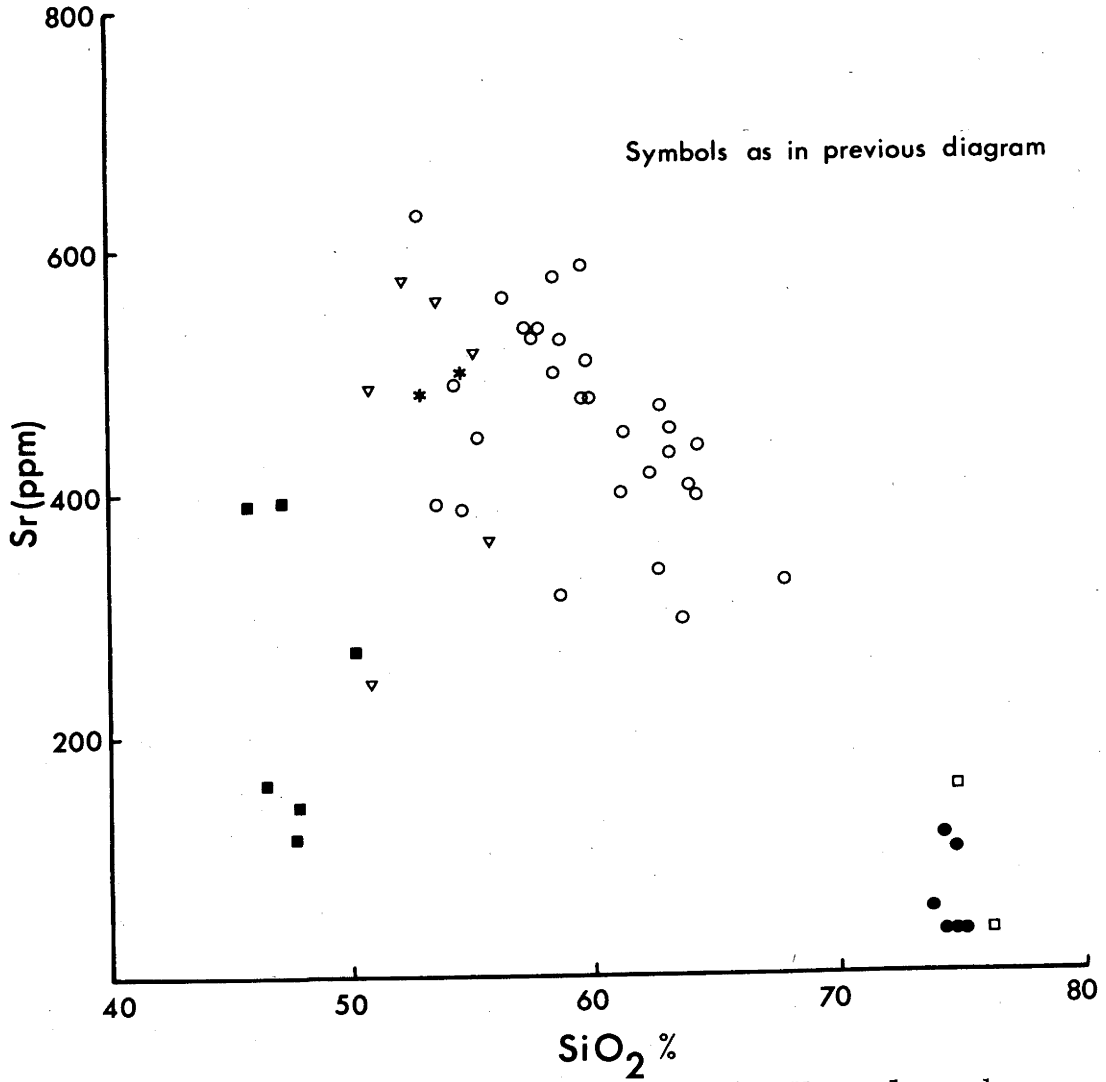

Fig.29 Strontium variation diagram for the Yeoval rocks.

is slightly higher than the average diorite. The average K/Rb ratios are identical (Fig. 28).

There are few previous determinations of Rb in diorites and associated rocks. All Rb values measured by Nockolds and Mitchell (1948), Nockolds and Allen (1953) on the Scottish Caledonian rocks are much higher (quite often by an order of magnitude) than the Yeoval rocks. Similarly, the Rb values for the Southern California Batholith are high compared with the Yeoval rocks, although not to the same extent. The K/Rb ratios are fairly constant for both areas but are considerably lower (~150) than the Yeoval rocks.

Average values of 70, 170 and 250 ppm Rb were obtained by Tauson and Stavrov (1957) for the diorite, granodiorite and granite phases of the Susamyr batholith.

Such low values suggest that there may be an error in the optical spectrographic determinations of Nockolds and Mitchell (1948). This suggestion is supported by the XRF and isotope dilution data of Summerhayes (1966). For diorites of the Garabal Hill-Glen Fyne complex he measured Rb values ranging from 42.3 - 63.5 ppm which are at least half those reported previously.

Strontium - Strontium values for the supposed accumulative rocks (i.e. gabbros and pyroxenites) give a scatter of points at the basic end of the silica-variation diagram (Fig. 29).

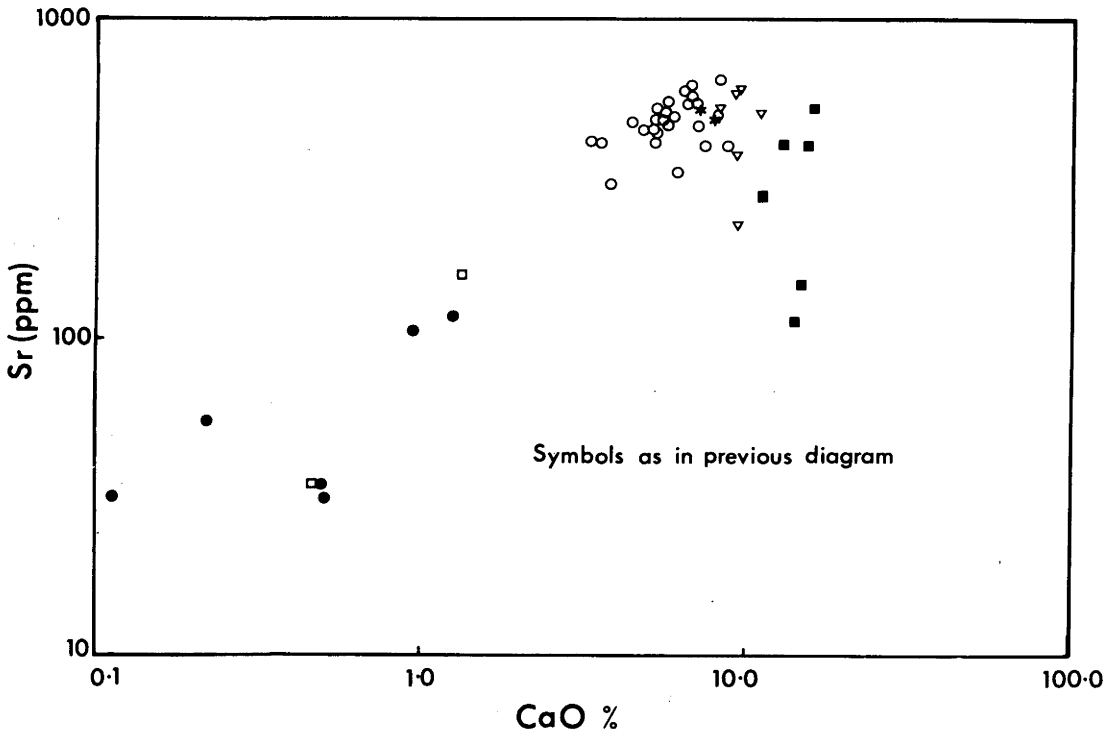

Fig.30 Ca/Sr relationship for the Yeoval rocks.

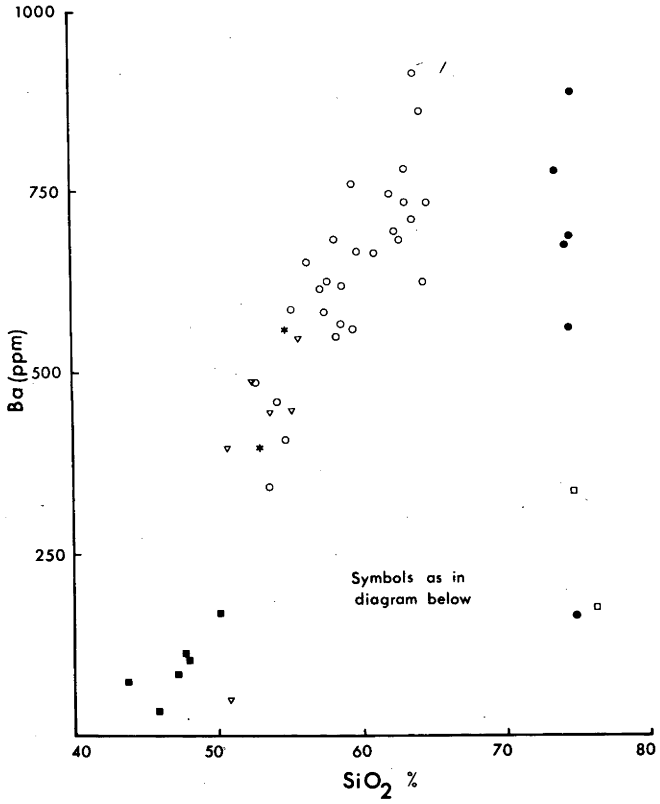

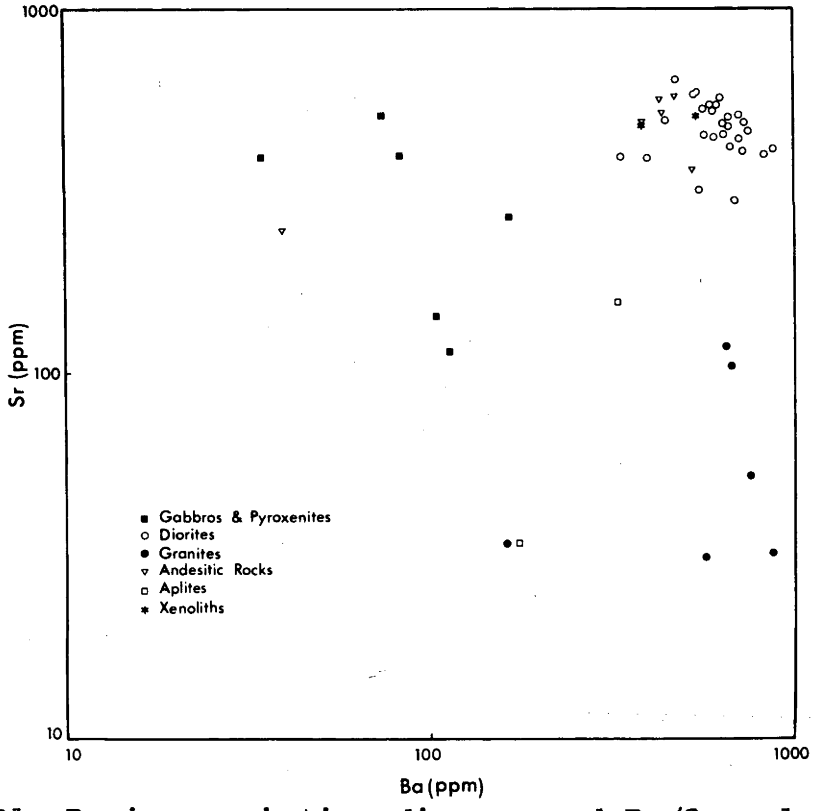

Fig.31 Barium variation diagram and Ba/Sr relationship for the Yeoval rocks.

A more or less linear decrease is evident from the diorites through the orthoclase diorites to the granites. Consequently, the Rb/Sr ratio increases in the same direction. The low Sr contents of the aplites are in keeping with those of the granites, although that of the aplite in the diorite is considerably higher than any value recorded in the granites.

As for Rb, the Sr values reported for rocks of the Garabal Hill - Glen Fyne complex (Nockolds and Mitchell 1948, Nockolds and Allen 1953) are too high in comparison with the XRF and isotope dilution values of Summerhayes (1966). For example, Nockolds and Allen (1953) report values of 1000 ppm for 3 samples of pyroxene-mica diorite which contrasts with 484 ppm obtained by Summerhayes. The lower result is consistent with values of ~400 ppm obtained on Yeoval pyroxene-mica diorites.

A plot of CaO versus Sr displays a scatter for the gabbro and pyroxenites at the high calcium end but the diorite data show little scatter (Fig. 30). However, there is a marked hiatus between the diorites and granites, the latter being distinctly lower in both CaO and S_r.

Barium - The silica-variation diagram for Ba (Fig. 31) shows an approximately linear trend from the gabbros through to the orthoclase diorites. The Ba contents of the granites are extremely variable although the SiO_2 variance is very small.

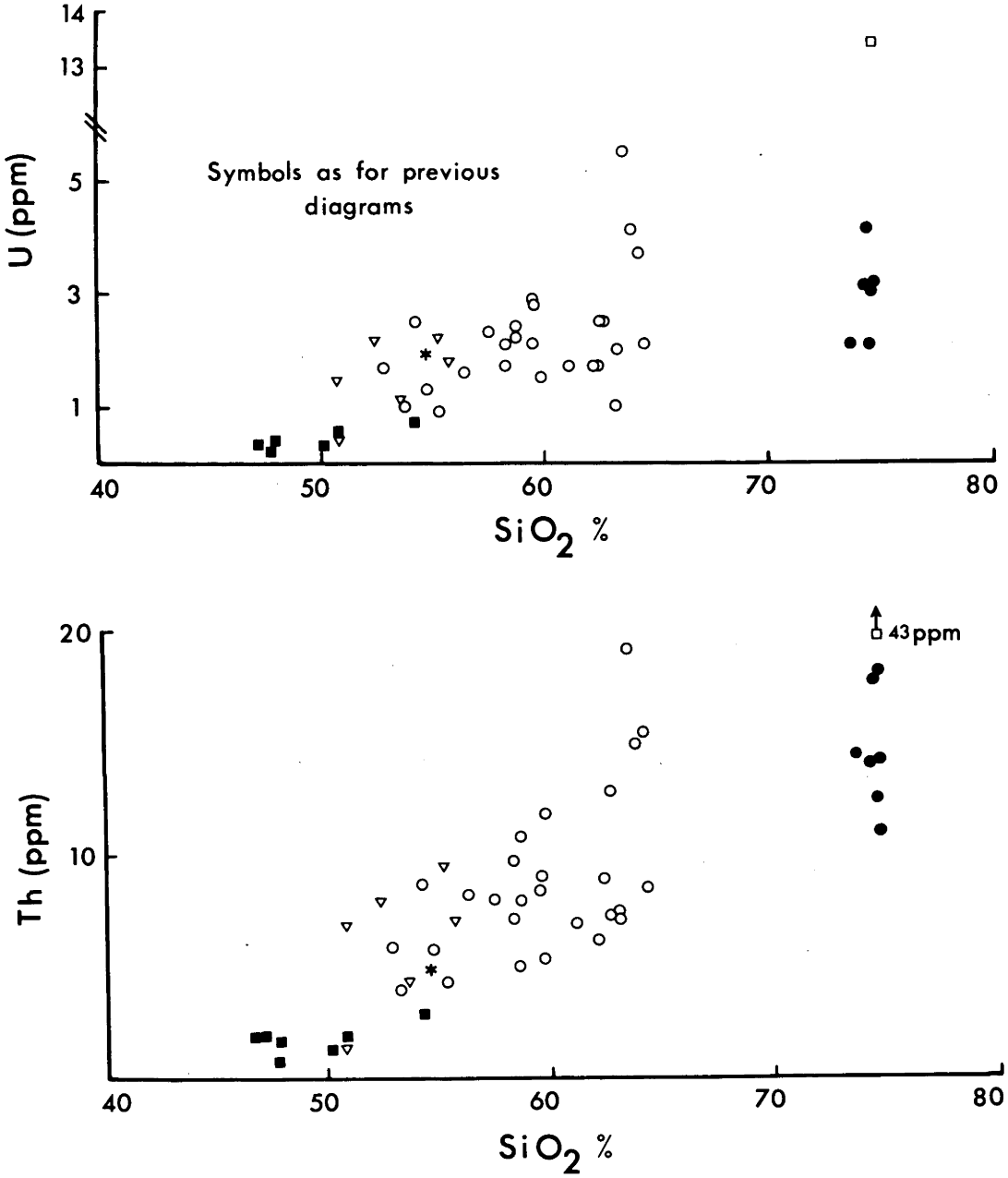

Fig.32 Uranium and Thorium variation diagrams for the Yeoval rocks.

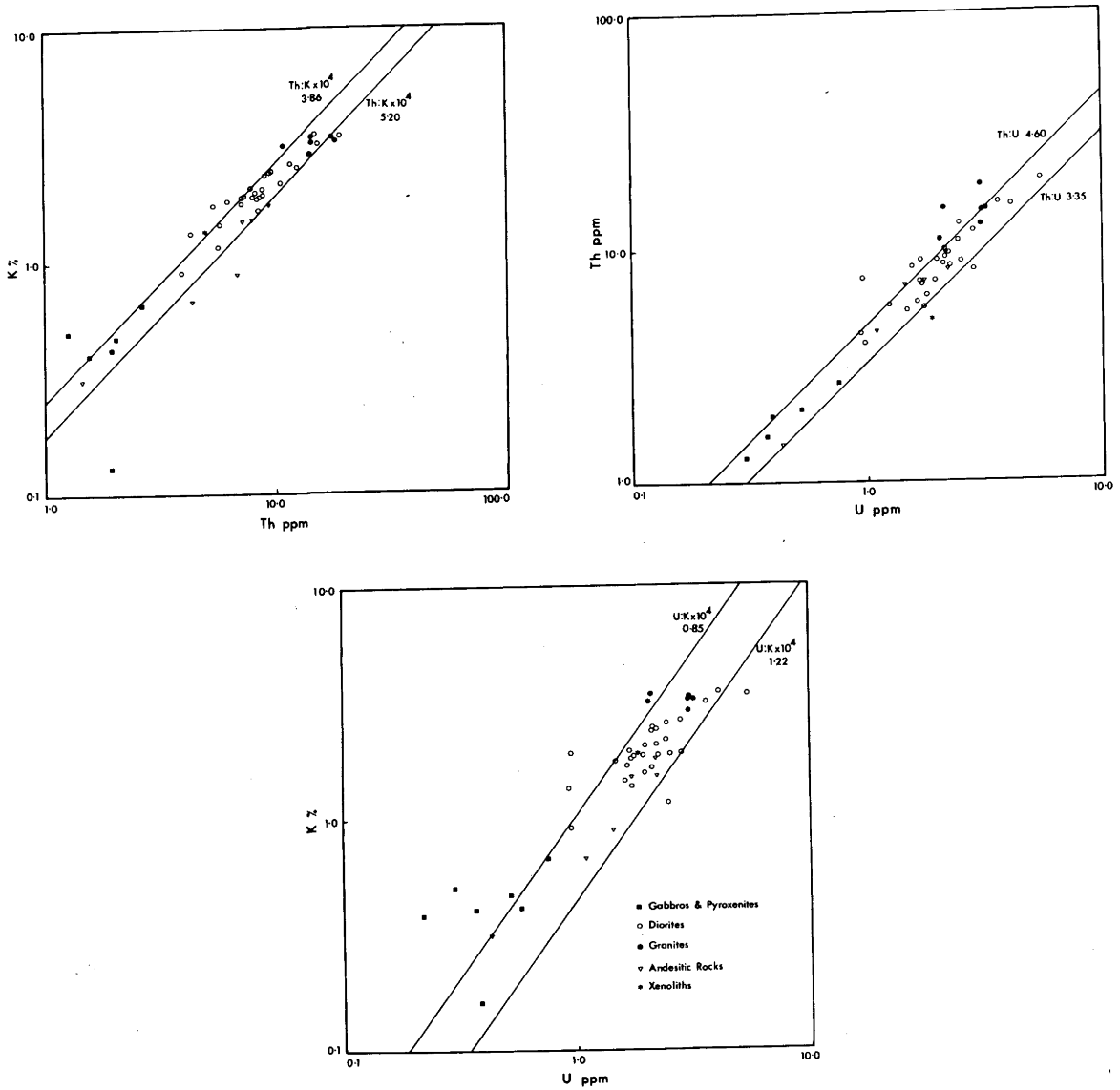

Fig.33 Th/K, Th/U, K/U relationships for the Yeoval rocks.

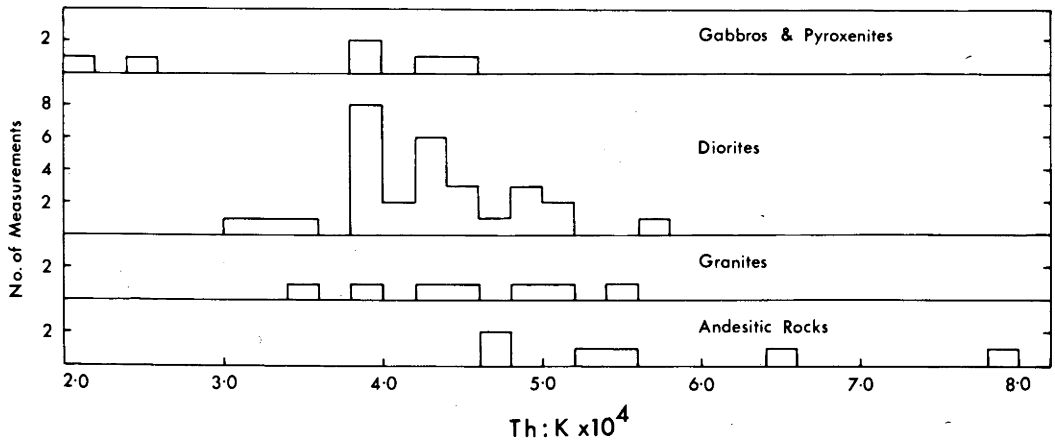

Fig.34a Histograms for the Th/K ratio.

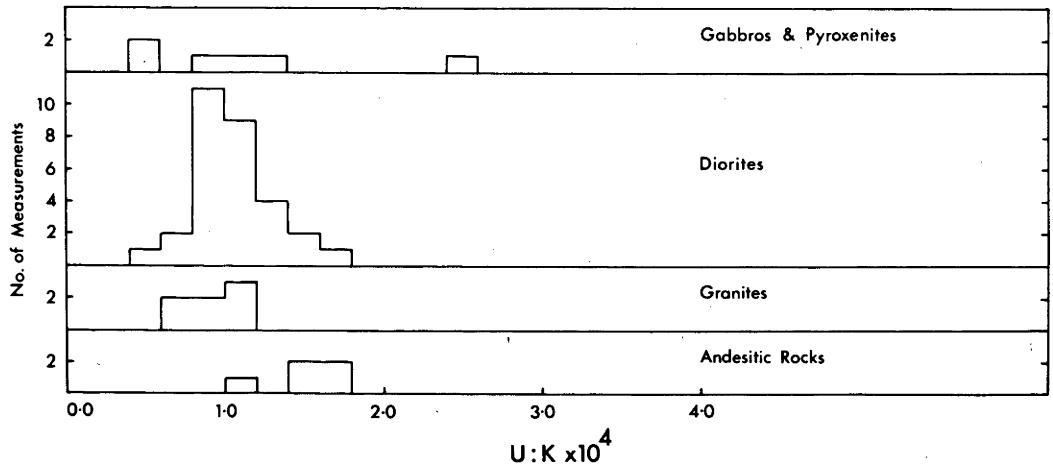

Fig.34b Histograms for the U/K ratio.

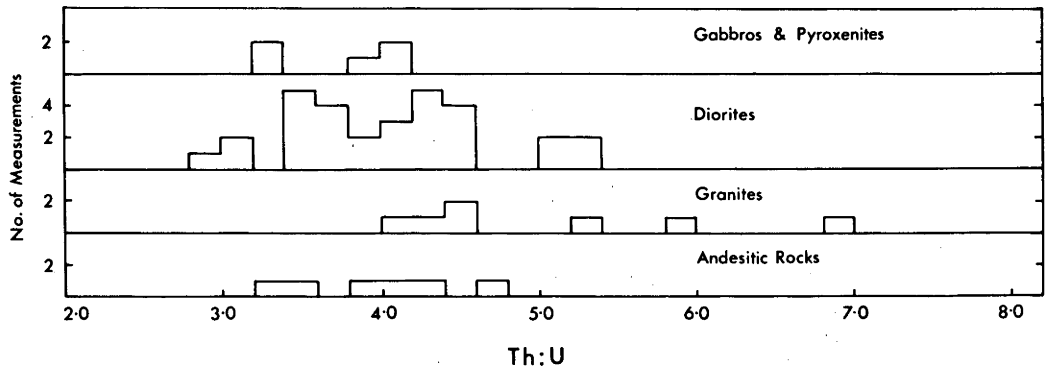

Fig.34c Histograms for the Th/U ratio.

The Ba-Sr relationship, suggested by Taylor (1966) to be an indicator of fractionation, (Fig. 31) shows a similar, distinct separation between the diorites and granites, to that of the CaO-Sr relationship.

Uranium and Thorium - The uranium values for the Yeoval rocks (Fig. 32) show a slight increase from the gabbros (<1 ppm) through to the orthoclase diorites (4.4 ppm). The pyroxene- and quartz-mica diorites have average uranium contents of 1.1 and 2.0 ppm respectively.

Thorium contents increase with increasing SiO_2 (Fig. 32). In the diorites, the pyroxene-mica types average 4.6 ppm Th, which increases to 8.0 ppm for the quartz-mica diorites and then rises to 16.6 ppm for the orthoclase varieties. The granites average 14.7 ppm and there is a sharp increase to 43 ppm in the aplite.

Although there is a trend of increasing U and Th from gabbro to granite there is no marked change in the Th/K, U/K and Th/U ratios (Figs. 33 and 34). The increase of Th and U during "differentiation" of calc-alkaline rocks has been noted by a number of authors: Abramovich (1959), Whitfield et al. (1959), Rogers and Ragland (1961), Smirnov (1962), Heier and Rogers (1963), Leonova and Balashav (1963). Rogers and Ragland (1961) and Heier and Rogers (1963) noted, in contrast to the Russian authors, that the Th/U ratio was apparently

unchanged during "differentiation", which agrees with the data for the Yeoval rocks (Figs. 33 and 34). As mentioned previously, the Yeoval rocks also show very little or no change in the Th/K and U/K ratios. This conflicts with the data of Heier and Rogers (1963) which shows an increase in the Th/K and U/K ratio with "differentiation" in the Southern California Batholith.

The scatter in U and Th contents (particularly U) and the above ratios for the one rock type may be due to a number of factors, including composition of the rock or to secondary processes such as leaching of U and Th associated with deuteric alteration. The importance of the latter process is evident in the diorites; those rocks (Y71, Y148, G90, G92, G118) containing lower amounts of Th and U than the average (8.0 and 2.0 respectively) are the rocks which have undergone the most severe alteration - biotites almost completely chloritised, plagioclases heavily saussuritised.

Uranium distribution.

Uranium distribution in two samples of quartz-mica diorite was made by fission track registration in Lexan plastic prints following the method of Kleeman and Lovering (1967). One of these samples (G92) showed extensive alteration.

In the unaltered rock (Y41), zircon has the greatest concentration of U (about 400 ppm), apatite about 8 ppm, well

crystallised epidote (late stage crystallisation rather than an alteration product) about 100 - 250 ppm, prehnite (?) wedges in the biotite contain approximately 30 ppm U, and chlorite borders of biotite have about 6 - 15 ppm U. The other phases, plagioclase, potassium feldspar and hornblende contain less than 0.1 ppm U. From an estimate of the relative amounts of each mineral in the rock, it would appear that the U is concentrated mainly in the accessories, zircon and sphene.

In the altered rock (G92), uranium is concentrated in zircon (400 ppm) and apatite (18 ppm) as in the fresh rock. However, it is fairly evenly distributed throughout altered plagioclase grains in amounts up to 4.5 ppm although it more commonly averages 1.6 ppm. The U is probably located in the fine-grained alteration products of the plagioclase such as white mica and epidote. White mica (as alteration products of biotite and possibly plagioclase) contains up to 39 ppm U, with an average of about 6 ppm. Chlorite (after biotite) has a U content of approximately 5 ppm but rarely increases to 100 ppm. Sphene, as an alteration product of opaque minerals (e.g. titanomagnetite), contains up to 25 ppm U.

The apparent ease of migration of U in the altered quartz-mica diorite described above, and its low U content compared

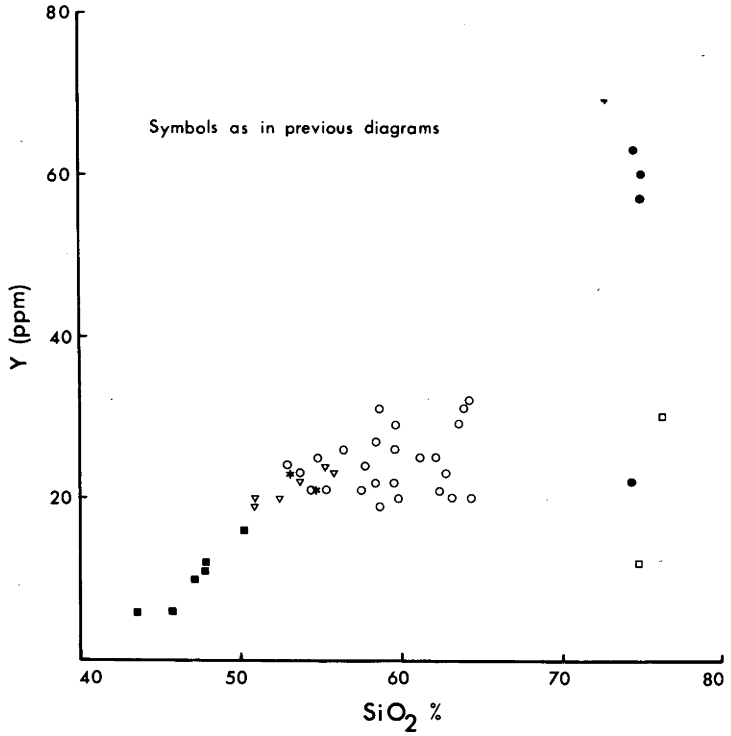

Fig.35 Yttrium variation diagram for the Yeoval rocks.

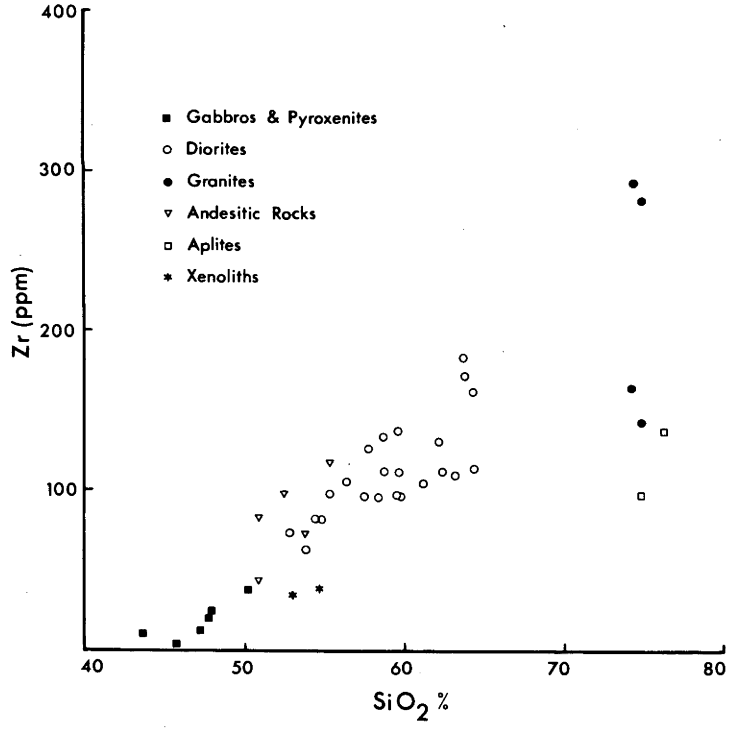

Fig.36 Zirconium variation diagram for the Yeoval rocks.

with the fresh sample, implies that the altered rock was an open chemical system. This is supported by the Sr isotope data (section 6) which indicated that at least some rocks remained open up to 80 million years after their time of intrusion. The isotope data for the fresh sample suggested that even it was an open chemical system.

Zirconium - Zirconium increases with increasing SiO_2 (Fig.36). In the gabbros, the Zr content averages 10 ppm, 81 ppm in the pyroxene-mica diorites, and 111 ppm in the quartz-mica diorites. A marked increase to 173 ppm occurs in the orthoclase diorites. Little can be said of the granites because of the wide scatter of results, although they do have higher Zr contents than the diorites and some samples show a threefold increase. The aplites are depleted in Zr relative to the granites.

Similar trends have been noted for other calc-alkaline rocks (Nockolds and Allen 1953), i.e. in general, the Zr content is low at the basic end, and then tends to rise after which it remains more or less constant until the extreme acid end (aplites) when it tends to fall.

Yttrium - The Y content of the gabbros is low (average 7 ppm) and increases sharply in the pyroxene - and quartz-mica diorites where it remains fairly constant (24ppm). The orthoclase

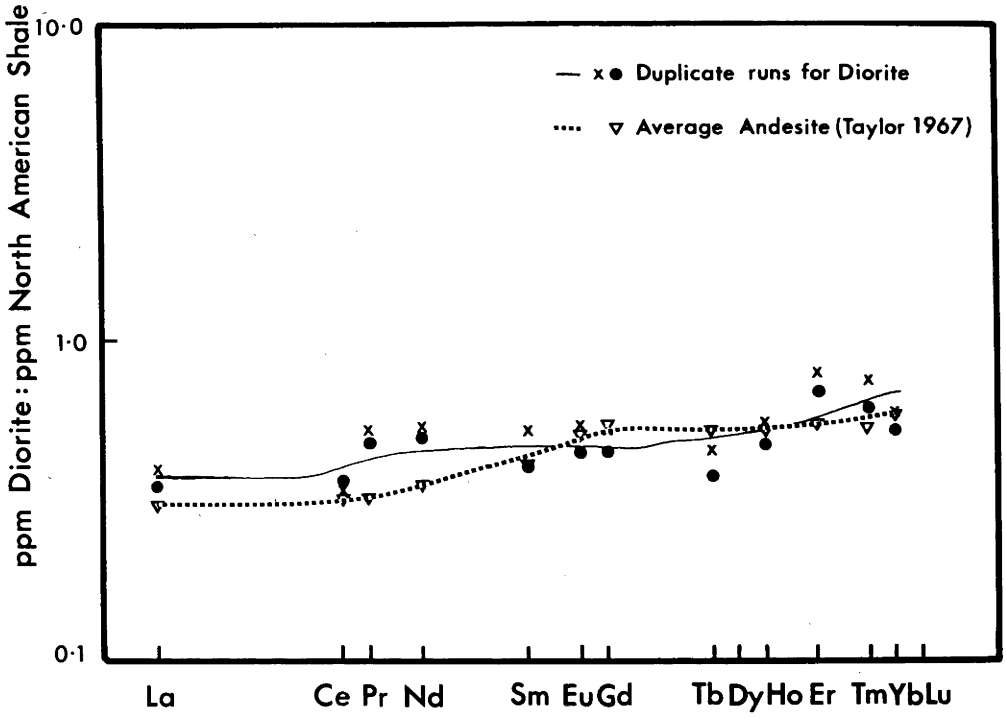

Fig.37a Rare earth data for Yeoval diorite (Y8) and average Andesite ratioed to standard North American Shale.

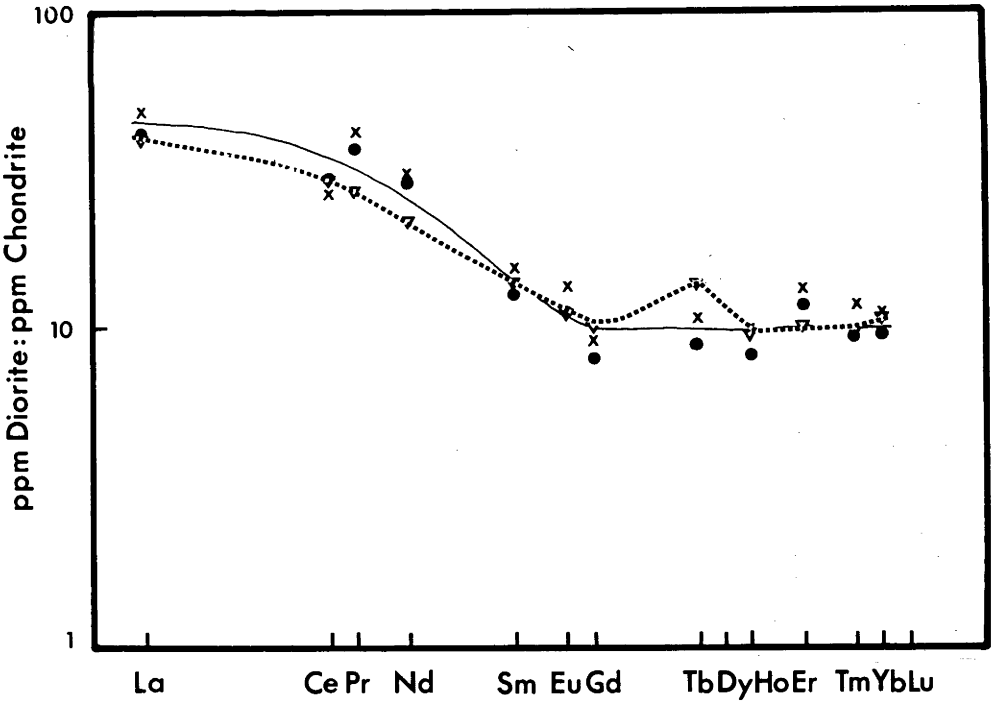

Fig.37b Rare earth data for Yeoval diorite (Y8) and average Andesite ratioed to chondritic pattern.

TABLE 37

Other Trace Element Data for Yeoval Diorite (Y8) Compared with Average Andesite (Taylor 1967)

	Rare Earths					
	ppm		Ratioed to Chondritic Pattern		Ratioed to North American Shale Pattern	
	Y8	Andesite	Y8	Andesite	Y8	Andesite
La	14.5	11.9	49	40	0.37	0.30
Ce	26	24	31	29	0.35	0.32
Pr	5.2	3.2	44	27	0.51	0.31
Nd	19	13	33	22	0.52	0.35
Sm	3.2	2.9	15	14	0.46	0.41
Eu	1.0	(~0.8)	14	(~11)	0.50	(~0.5)
Gd	3.0	3.3	9	10	0.49	0.54
Tb	0.5	0.7	11	14	0.41	0.52
Ho	0.7	0.7	10	10	0.52	0.51
Er	3.0	2.1	14	10	0.74	0.53
Tm	0.4	0.3	12	9	0.68	0.52
Yb	1.9	1.9	11	11	0.56	0.56

	Y8		Andesite
Cs	0.8		1.3
Hf	1.4		2.3
Sn	1.0		0.8
Pb	3.3		6.7
Th	4.0	3.9+	2.2
U	0.9	1.0+	0.7

+determined by γ-ray spectrometry

diorites have slightly higher amounts of Y (31 ppm) and there is a sharp increase in the granites to 60 ppm (Fig. 35). The aplites are depleted in Y relative to the granites; the aplite in the granite containing 30 ppm and that in the diorite only 12 ppm.

Niobium - Niobium was not detected in the gabbros, pyroxenites and pyroxene-mica diorites. It has a maximum concentration of 4 ppm in the quartz-mica and orthoclase diorites and increases to 19 ppm in the granites. The aplite in the granite contains the same amount of Nb as its host, in contrast to the aplite in the diorite which has no Nb.

Other trace elements - A sample (Y8) of pyroxene-mica diorite was analysed in duplicate by Dr S.R. Taylor by spark source mass spectrometry (MS 7) for the elements listed in Table 37.

The rare earths for the diorite, illustrated in Fig. 37, are ratioed to the chondritic and standard North American Shale rare earths patterns (Taylor, pers. comm).

A comparison of the diorite and average andesite data (Taylor 1967) shows a very close correlation between these two rock types (Table 37, Fig. 37).

For the lighter rare earths (i.e. La-Eu), the andesites and diorite have about one-third the abundance of the

TABLE 38

Trace Element Chemistry of the Andesitic Rocks at Yeoval

	G117	G133	G134A	G134B	G140	G128
Rb^{+}	83	6	38	22	65	41
Ba^{2+}	448	50	395	442	484	544
K^{+}(%)	1.71	0.31	0.88	0.67	1.51	1.50
Sr^{2+}	514	244	486	558	572	360
K/Rb	206	517	232	305	232	366
Ba/Rb	5.4	8.3	10.4	20.0	7.4	13.3
Ba/Sr	0.87	0.20	0.81	0.79	0.85	1.51
Rb/Sr	0.16	0.002	0.08	0.04	0.11	0.11
Y^{3+}	24	19	20	22	20	23
Th^{4+}	9.5	1.4	6.9	4.4	8.0	7.1
U^{4+}	2.2	0.4	1.5	1.1	2.2	1.8
Zr^{4+}	117	44	83	74	98	102
Nb^{5+}	3	<1	<1	<1	<1	<1
Th/K	5.41	4.70	7.80	6.55	5.29	4.76
U/K	1.26	1.41	1.65	1.64	1.47	1.17
Th/U	4.30	3.33	4.74	3.99	3.60	4.07

standard North American Shale, while the heavier rare earths (Gd-Lu) are approximately half as abundant (Fig. 37a). The heavier rare earths content of the diorite (and andesites) is about ten times that of chondrites (Fig. 37b).

The trace elements, besides the rare earths, listed in Table 37, are all very similar to the average andesite. The MS 7 values for U and Th correspond perfectly with those obtained by X-ray spectrometry, the results of which are given in Table 37.

5.1.2 Andesitic rocks

The trace element chemistry of the andesitic rocks is given in Table 38 and the trends with varying SiO_2 contents and individual ratios are plotted on the diagram given previously (Figs. 25 - 36). The andesites (excluding the basalt G133), in comparison with the average Yeoval diorite, have lower Rb, Ba, Th, U, Zr, and Nb contents, and similar Sr and Y contents. In a number of these elements the andesitic rocks more closely resemble the pyroxene-mica diorite.

5.2 TRACE ELEMENT CHEMISTRY OF THE MINERALS

Potassium feldspars, biotites and hornblendes have been analysed for Rb, Sr, Ba, Y and Nb; and olivines pyroxenes and plagioclase for Rb, Sr, Y and Nb. Only passing reference is made to the plagioclasesbecause, as indicated in an earlier section, the concentrates are not representative of the whole

TABLE 39

Potassium Feldspar Trace Element Chemistry

Rock Type	Specimen No.	Rb^{+}	Ba^{2+}	K^{+}(%)	Sr^{2+}	$Kx10^{4}/Rb$	Ba/Rb	Ba/Sr	Rb/Sr	Ba/Kx10	$Y3^{+}$	Nb^{5+}
Pyroxene-Mica Diorite	G154	132	3225	10.62	391	805	24.4	8.2	0.34	30.4	6	<1
Quartz-Mica Diorite	G120	237	2800	9.71	470	410	11.8	6.0	0.50	28.8	7	<1
	Y41	317	2362	10.55	525	333	7.5	4.5	0.60	22.4	7	<1
	Y71	218	2752	10.64	411	488	12.6	6.7	0.53	25.9	8	<1
	G110	227	2822	10.75	413	474	12.4	6.8	0.54	26.3	12	<1
	Y151	276	2497	10.26	320	372	9.1	7.8	0.86	24.3	5	<1
	G118	236	2243	9.76	299	414	9.5	7.5	0.79	23.0	9	<1
	Y235	260	2704	10.63	443	409	10.4	6.1	0.59	25.4	10	<1
	G107	320	2211	11.22	494	351	6.9	4.5	0.65	19.7	3	<1
	Y75	272	2745	11.66	631	429	10.1	4.4	0.43	23.5	7	<1
	Y150	183	3354	11.21	839	613	18.3	4.0	0.22	29.9	16	<1
	Y227	245	1764	10.54	418	430	7.2	4.2	0.59	16.7	5	<1
	G99	296	2973	10.82	328	366	10.0	9.1	0.90	27.5	8	<1
Orthoclase Diorite	Y205	283	1645	9.33	265	330	5.8	6.2	1.07	17.6	7	<1
Granite	Y43	255	1262	8.36	46	328	4.9	27.4	5.54	15.1	10	<1
	Y53	310	973	8.05	79	260	3.1	12.3	3.92	12.1	13	<1
	Y64	282	801	7.49	31	266	2.8	25.8	9.10	10.7	14	<1
	R77	196	976	8.19	30	418	5.0	32.5	6.53	11.9	23	<1

rock.

5.2.1. Potassium Feldspars

Although the potassium feldspars from the diorites and granites display a significant variation of trace elements amongst themselves (Table 39), certain overall trends are obvious.

Rb - is lower in the potassium feldspar from the pyroxene-mica diorite but is otherwise not different in the quartz-mica diorite, orthoclase diorite or granite. The K/Rb ratio decreases sharply in the quartz-mica diorite compared with the pyroxene-mica diorite. It is slightly lower in the orthoclase diorite and even more so in the granites.

Ba - is highest in the potassium feldspar from the pyroxene-mica diorite and decreases linearly to the orthoclase diorite. It decreases to almost one-third the amount in the potassium feldspars from the granite. The Ba/Rb and Ba/K ratios decrease in the same direction as the Ba contents.

Sr - displays no particular trend in the pyroxene - and quartz-mica diorites but it decreases sharply in the potassium feldspars from the orthoclase diorites and even more so in the granites. The Ba/Sr is highest (except for G99) in the potassium feldspars from the pyroxene-mica diorite; it shows a large scattering in the quartz-mica diorite and increases sharply in the granites. The Rb/Sr increases in the potassium

TABLE 40

Trace Element Chemistry of Biotites from the Yeoval Rocks

	Pyroxene-Mica Diorites		Quartz-Mica Diorites							Granites	
	Y8	G154	G120	Y41	Y235	G107	Y75	Y150	Y227	Y43	Y53
Rb^{+}	316	338	517	436	344	259	324	464	365	597	344
Ba^{2+}	1792	1699	548	1961	985	3291	n.d.	730	3098	1884	584
K^{+}(%)	6.62	6.39	6.56	5.93	6.18	6.01	5.69	7.03	6.55	6.29	5.64
Sr^{2+}	10	16	8	20	40	20	22	8	20	6	11
K/Rb	209	189	128	136	180	232	176	152	179	105	164
Ba/Rb	5.7	5.0	1.1	4.5	2.9	12.7	-	1.6	8.5	3.2	1.7
Ba/Sr	179.2	106.2	68.5	98.1	24.6	164.6	-	91.3	154.9	314.0	53.1
Rb/Sr	32	21	65	22	9	13	15	58	18	100	31
Ba/Kx10	27.1	26.6	8.4	33.1	15.9	54.8	-	10.4	47.3	30.0	10.4
Y^{3+}	8	11	11	16	11	10	5	10	8	94	175
Nb^{5+}	23	18	38	49	46	34	41	38	36	328	369

n.d. Not Determined

feldspars from the granites compared with those from the diorites.

Y - has no particular trend in the potassium feldspars.

Zr and Nb - are not present in detectable amounts.

5.2.2. Biotites

The trace element contents for biotites in the diorites and granites are given in Table 40. As stated previously, except for the first four listed, the biotites are chloritised, which may account for the lack of any trends for Rb, Ba and Sr (and K) and their corresponding ratios. In contrast, the granite biotites are enriched by an order of magnitude in Y and Nb compared with the biotites in the diorite. The Nb contents of the biotites from the pyroxene-mica diorite are half those of the quartz-mica diorite which may indicate an insensitiveness of Y and Nb to alteration effects in biotite.

Owing to the close association of Rb and Ba with potassium, any variation in the latter should be reflected in the Rb and Ba contents. The large spread of the K/Rb and Ba/K ratios suggests that no correlation of trace element content with alteration can be made. If only the fresh biotites are considered, Rb(and Nb) show an increase in the biotite from the quartz-mica diorite compared with those from the pyroxene-mica diorite.

TABLE 41

Trace Element Chemistry of the Hornblendes from the Yeoval Rocks

Rock Type	Specimen No.	Rb^{+}	Ba^{2+}	K^{+}(%)	Sr^{2+}	$Kx10^{4}/Rb$	Ba/Rb	Ba/Sr	Rb/Sr	Ba/Kx10	$Y3^{+}$	Nb^{5+}
Pyroxenite	W61	3	65	0.65	51	2167	21.7	1.3	0.06	10.0	42	2
Pyroxene-Mica Diorite	Y8	4	59	0.54	40	1350	14.8	1.5	0.10	10.9	382	12
	G154	4	57	0.49	31	1235	14.3	1.8	0.13	11.6	323	12
Quartz-Mica Diorite	G120	5	2.	0.58	24	1160	0.4	0.08	0.21	0.3	443	24
	Y41	4	26	0.54	58	1350	6.5	0.45	0.07	4.8	608	50
	Y158	4	55	0.33	43	835	13.8	1.28	0.09	16.7	170	16
	Y71	2	32	0.50	33	2500	16.0	0.97	0.61	6.4	460	24
	G90	3	72	0.42	47	1400	24.0	1.53	0.06	17.1	379	21
	G110	3	64	0.51	34	1686	21.3	1.88	0.09	12.5	493	36
	Y151	4	25	0.32	21	800	6.2	1.19	0.19	7.8	489	25
	G118	7	115	0.43	83	614	16.4	1.39	0.08	26.7	410	32
	Y235	3	29	0.47	35	1553	9.7	0.83	0.09	6.2	334	25
	Y161	1	21	0.50	25	5000	21.0	0.84	0.04	4.2	269	19
	G107	3	38	0.45	38	1500	12.6	1.00	0.08	8.4	272	24
	Y75	2	35	0.54	50	2700	17.5	0.70	0.04	6.5	374	23
	Y150	5	<1	0.47	39	930	-	-	0.13	-	339	17
	Y227	3	41	0.50	31	1667	13.7	1.32	0.10	8.2	291	23
	G99	3	39	0.39	36	1290	13.0	1.08	0.08	10.1	437	35
	G92	4	17	0.50	42	1250	4.2	0.40	0.10	3.4	331	28
	Y148	3	80	0.42	47	1400	26.7	1.70	0.06	19.1	332	20
Orthoclase Diorite	Y205	5	25	0.75	29	1500	5.0	0.86	0.17	3.3	742	65
Granite	Y43	71	244	0.42	9	592	3.4	27.1	7.89	58.1	1079	233
	Y53	8	15	0.60	10	750	1.9	1.5	0.8	2.5	1787	403
	Y64	10	77	0.50	4	500	7.7	19.3	2.50	15.4	1638	546

5.2.3 Hornblendes

Trace element data for the hornblendes from the diorites and granites are listed in Table 41. The data for a mixed concentrate of the two types of amphibole (uralite and hornblende) in the pyroxenite are also given.

Rb - shows no variation in the diorite hornblendes but increases slightly in the hornblendes in the granite, giving a corresponding decrease in the average K/Rb ratio from 1400 to 614 in the same direction.

Ba and Sr contents of the hornblendes from the diorites are extremely variable, disguising any trends. A similar feature is observed in the granite hornblendes for Ba whereas the Sr content is much lower.

Y - has a very low concentration in the hornblende from the pyroxene-and quartz-mica diorites but increases by a factor of two in the hornblende in the orthoclase diorite. A fivefold enrichment relative to the hornblendes in the quartz-mica diorite occurs in the granite hornblendes.

Nb - displays a similar, although more marked, trend to that of Y.

5.2.4 Plagioclases

The trace element data presented in Table 42 indicates that Rb increases in the plagioclases from the diorites compared with those from the gabbro (where it is present in almost negligible amounts), and then decreases sharply in the

TABLE 42

Trace Element Chemistry of Plagioclases from the Yeoval Rocks

Rock Type	Specimen No.	Rb^{+}	Sr^{2+}	Rb/Sr	Y^{3+}	Nb^{5+}
Gabbro	W71	2	936	0.002	6	<1
	W53	2	637	0.003	7	<1
	W3	2	693	0.003	4	<1
Pyroxene-Mica Diorite	Y8	14	638	0.022	11	<1
	G154	33	641	0.051	15	<1
Quartz-Mica Diorite	G120	49	542	0.090	13	<1
	Y41	45	801	0.056	13	<1
	Y71	46	712	0.065	11	<1
	G110	41	717	0.057	11	<1
	Y151	35	844	0.041	10	<1
	Y235	63	846	0.074	16	<1
	G107	28	896	0.031	10	<1
	Y75	19	706	0.027	9	<1
	Y150	30	909	0.033	14	<1
	Y227	36	920	0.040	14	<1
	G99	55	720	0.076	14	<1
	G118 (Fresh)	41	817	0.050	11	<1
	G118 (Altered)	119	675	0.176	15	<1
Granite	Y43	15	237	0.063	12	<1

TABLE 43

Trace Element Chemistry of Olivines and Pyroxenes from the Yeoval Gabbro and Pyroxenite

	Olivine		Clinopyroxene		Orthopyroxene	
	W71	W3	W71	W3	W3	W53
Rb^{+}	2	1	1	2	1	2
Sr^{2+}	9	6	35	25	7	8
Rb/Sr	0.22	0.17	0.03	0.08	0.14	0.25
$Y3^{+}$	<1	<1	59	71	12	30
Nb^{5+}	<1	<1	<1	<1	<1	<1

granite plagioclase (if it is present). Little can be said of Sr except that it follows Rb with regard to the diorites and granites. The Y content is low in the gabbroic plagioclases and remains fairly constant in the diorites and granites.

5. Minerals in the Gabbro

Trace element data are given in Table 43 for olivine, clinopyroxene and orthopyroxene. These minerals contain little or no Rb or Nb. Sr is concentrated in the clinopyroxene relative to olivine and orthopyroxene. Y was not detected in olivine but is more abundant in the clinopyroxene than the orthopyroxene.

5.3 DISTRIBUTION OF TRACE ELEMENTS BETWEEN COEXISTING MINERALS

From the preceding data, Rb is concentrated in the biotite relative to the late-formed potassium feldspar, often in the ratio of 2:1. The Rb content of the rock is thus largely dependent on the concentrations of Rb in these minerals, with minor contributions from plagioclase and hornblende.

Barium, as near as can be estimated because of alteration of the biotite, is concentrated in the potassium feldspar relative to the biotite. Strontium is apparently concentrated in the early formed plagioclase, although a substantial amount enters the potassium feldspar.

Yttrium is found mainly in the hornblendes. It does not appear to have entered the early apatite occurring as inclusions

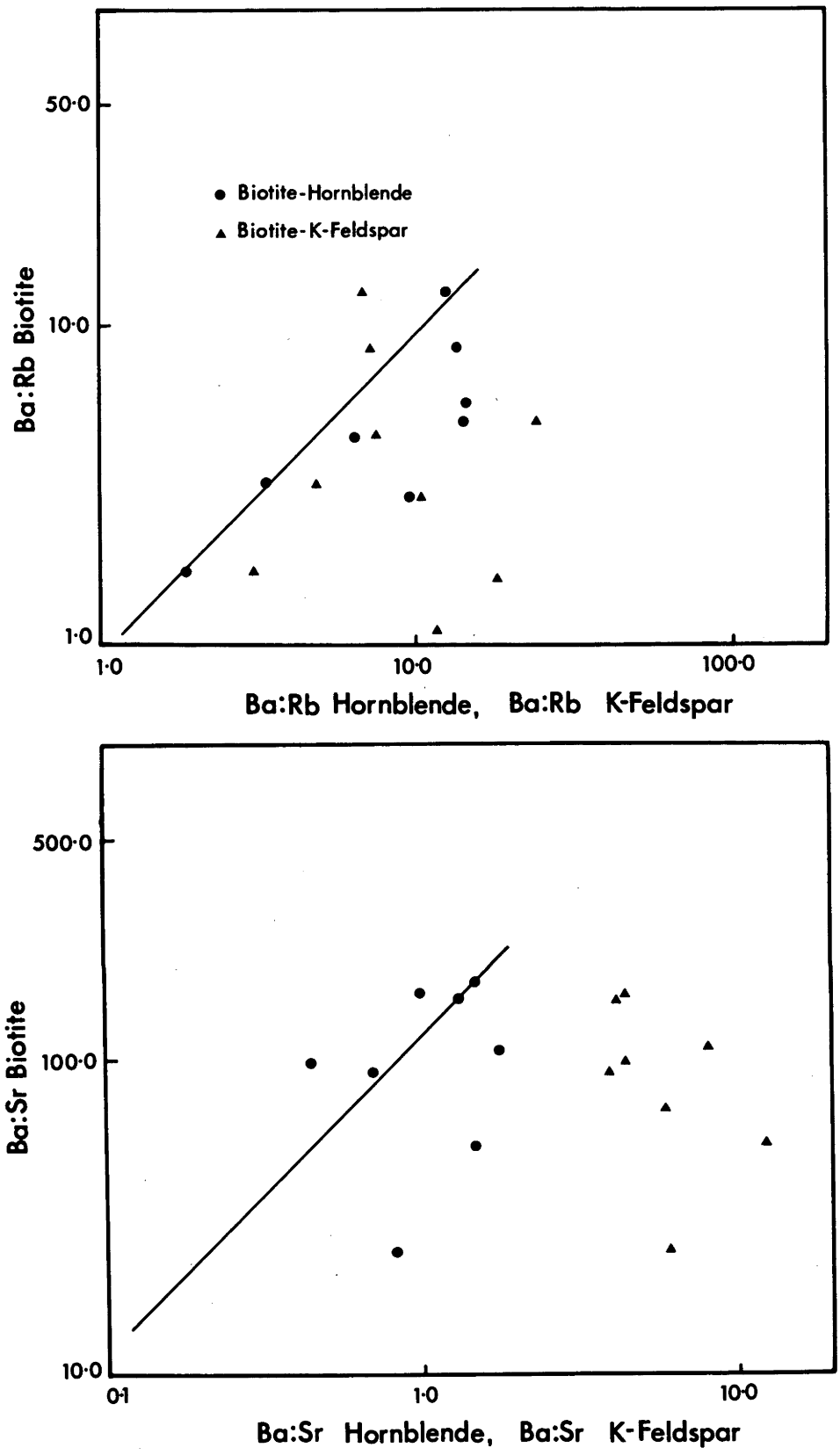

Fig.38 Log-Log distribution of Ba/Rb and Ba/Sr in co-existing biotite, k-feldspar and hornblende from the Yeoval diorites and granites.

in hornblende and biotite. This is suggested by the phosphorus and yttrium contents of the hornblendes. That is, if it is assumed that most phosphorus in the hornblende is accounted for in apatite, and if Y is concentrated in this mineral, then there should be a direct relationship between the phosphorus and Y concentrations. However, no such correlation is observed.

Niobium concentrates in the early formed hornblende and biotite where it is thought to associate with titanium (Taylor 1966).

As stated in a previous section (p. 75), if equilibrium has been established between coexisting mineral phases, then a log to log plot of specific elemental ratios should delineate a straight line of 45^{o} slope. The trace elements Ba, Rb and Sr in coexisting hornblende biotite and potassium feldspar were examined in this way and the results presented graphically in Fig. 38. The random scatter of the Ba/Rb and Ba/Sr for the minerals pairs suggests that conditions of equilibrium did not prevail at the time of crystallisation of the hornblende, biotite or potassium feldspar from the Yeoval diorites.

6. RUBIDIUM-STRONTIUM ISOTOPE GEOCHEMISTRY

The aim of the Rb-Sr isotope study of the Yeoval rocks was to determine the age and isotopic composition of the various members, with a view to elucidating, in association with other data, their complex crystallisation history.

6.1 EXPERIMENTAL METHODS

The method of extraction of Rb and Sr from rock and mineral samples for isotope dilution analyses is described in detail in Compston et al. (1965).

The mass spectrometer used for all measurements was built in the Department of Geophysics and Geochemistry, and designated the MS-X. It is similar to the Metropolitan Vickers MS2-SG but with higher precision; tails of the order of 0.02% under Sr^{87} are normally measured after 20 minutes pumping compared with 0.1% after 2 hours pumping for the MS2 (Compston et al., 1965).

For Rb, two sets of Rb^{85}/Rb^{87} were determined independently on each side filament and the mean weighted Rb^{85}/Rb^{87} value determined. For Sr, using a single Sr^{84} spike, a minimum of 10 comparisons for each set of ratios were measured in the sequence 88/86, 86/84, 88/86, 87/86, 88/86. A check on the Rb^{87} contamination of the Sr^{87} peak was made by measuring the Rb^{85} before and after the 87/86 set of ratios. Approximate values of Rb and Sr were obtained by using X-ray fluorescence

(Norrish and Chappell 1966) for accurate "spiking" and to check the suitability of samples for age determination. A comparison of X-ray fluorescence and isotope dilution values are given in Appendix II.

The Sr ratios are normalised to a Sr^{88}/Sr^{86} of 8.3752 or Sr^{86}/Sr^{88} of 0.1194 as used by Faure and Hurley (1963) and normal Rb^{85}/Rb^{87} considered to be 2,600 (Shields and Garner 1963). The decay constant (λ) of Rb^{87} used throughout this work is 1.39×10^{-11} year $^{-1}$ (Aldrich et al. 1956).

The data are presented graphically following the method of Hales (1960) and Nicolaysen (1961) in which a plot of Rb^{87}/Sr^{86} versus Sr^{87}/Sr^{86} is made. The slope of the isochron is proportional to the age and the Sr^{87}/Sr^{86} ratio estimated at $Rb^{87}/Sr^{86} = 0$ gives the initial Sr^{87}/Sr^{86}. The statistical treatment of the data is by the "two-error" regression method of McIntyre et al. (1966). A test of the goodness of the fit of points to the isochron is given by the magnitude of the mean square of weighted deviates (MSWD) which is a measure of the residual variance. If all error associated with the isochron is experimental, then the statistical expectation of the MSWD of a sufficient number of samples is unity. Any significant increase in this value may be attributed to geological variation. A conservative estimate of the significance of the value of the MSWD is an F-variate with N-2, 34 degrees of freedom (McIntyre et al. 1966). An indication of those samples which fit the isochron with least precision is given

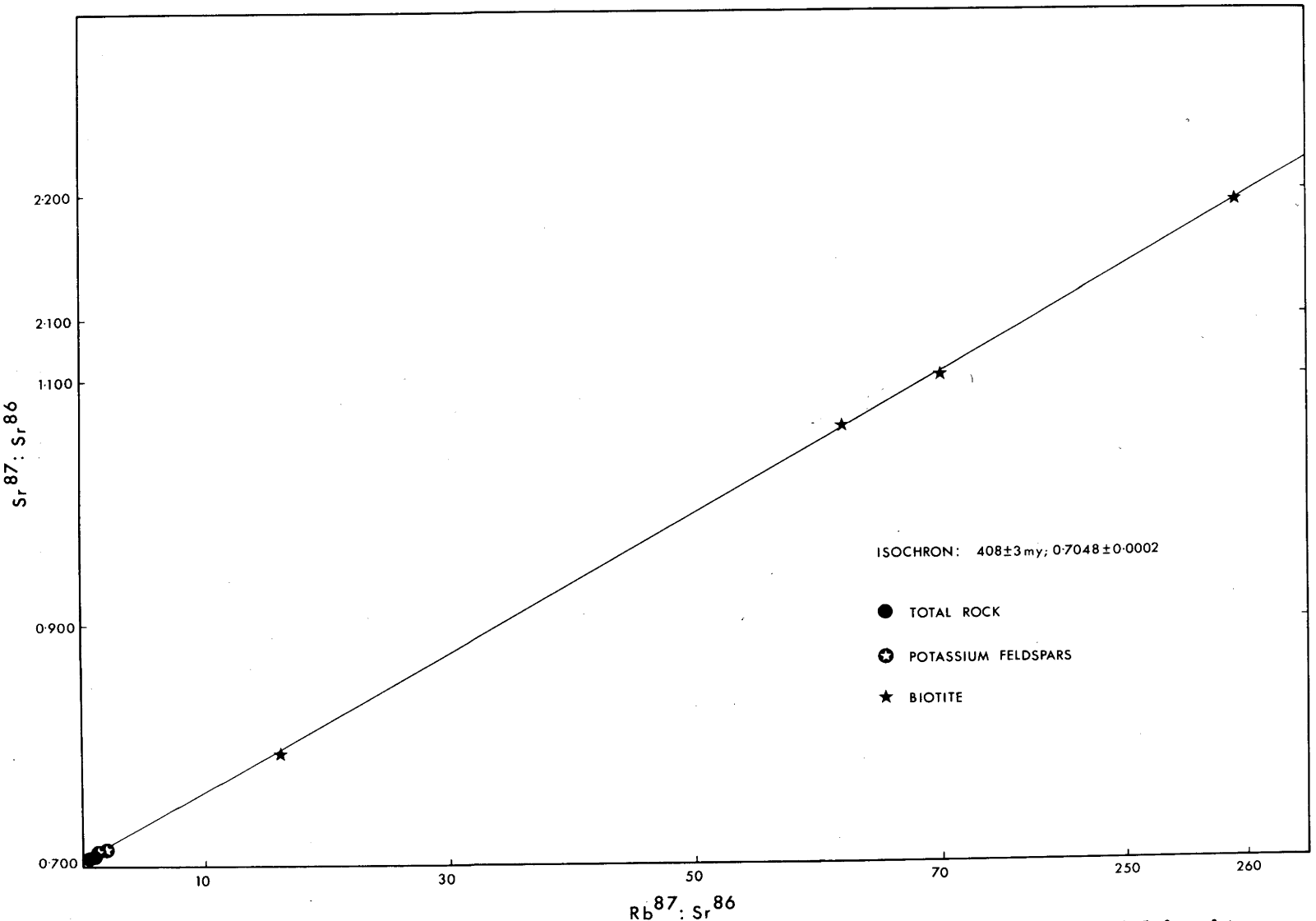

Fig.39 Rb-Sr isochron plot of total rock, potassium feldspars and biotites from the Yeoval diorite.

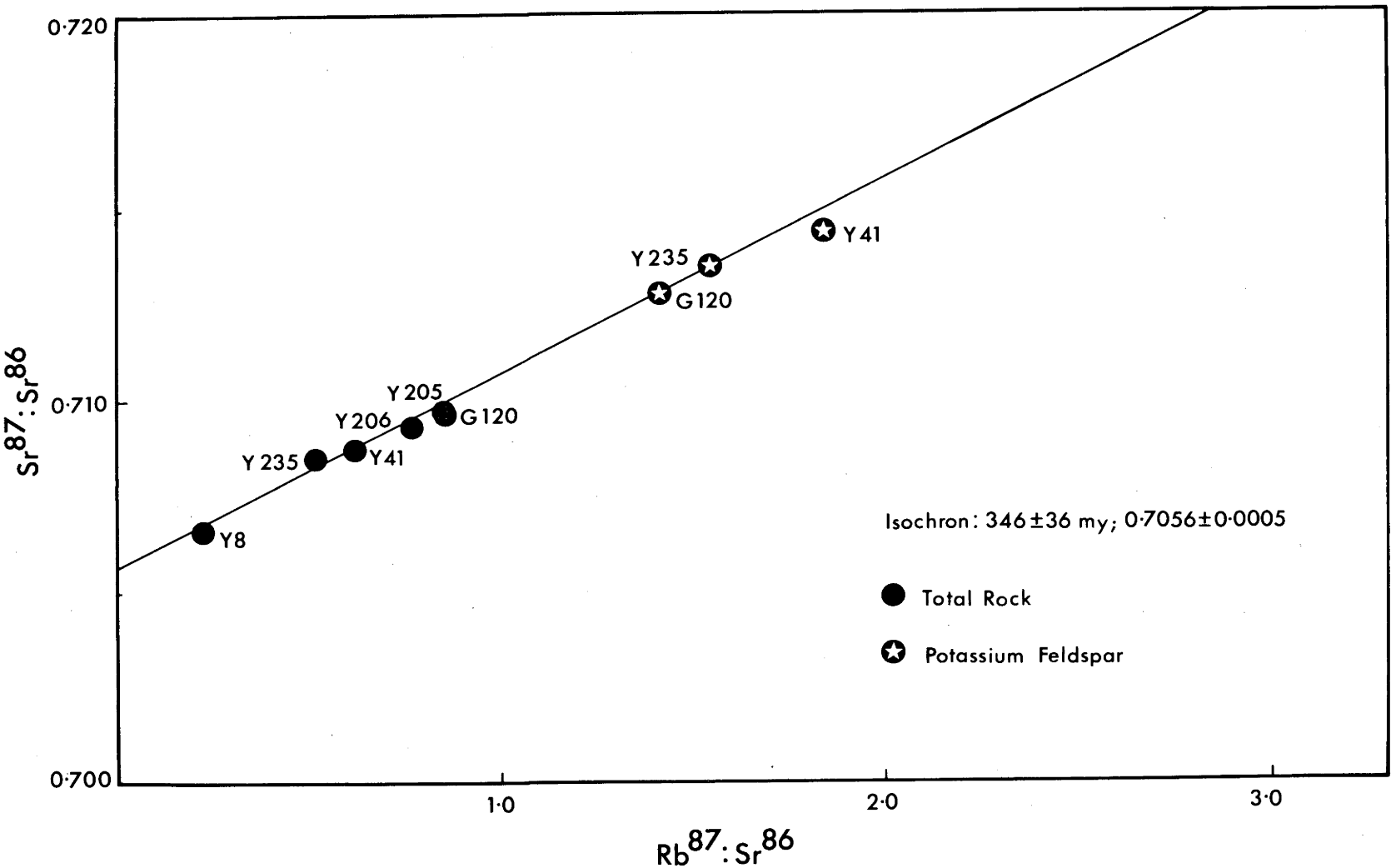

Fig.40 Rb-Sr isochron plot of total rock and potassium feldspars from the Yeoval diorite.

TABLE 44 (continued)

Rb-Sr Data for Yeoval Diorites

Rock Type & No.	Sample	Rb ppm	Sr ppm	Rb^{87}/Sr^{86}	Calculated Sr^{87}/Sr^{86}	Age (my)
Orthoclase diorite (Y205)	Total rock	118.9	402.5	0.8521	0.7095	
Orthoclase diorite (Y206)	Total rock	103.3	395.4	0.7538	0.7093	

TABLE 44

Rb-Sr Data for Yeoval Diorites

Rock Type & No.	Sample	Rb ppm	Sr ppm	Rb^{87}/Sr^{86}	Calculated Sr^{87}/Sr^{86}	Age (my)
Pyroxene-mica diorite (Y8)	Total rock	30.5	394.4	0.223	0.7067	
	Biotite	324.0	15.0	62.240	1.0631	415
Quartz-mica diorite (Y41)	Total rock	106.4	498.4	0.616	0.7086	
	Potassium felspar	324.5	507.9	1.843	0.7143	
	Biotite (Uncrushed)	462.6	19.08	69.956	1.1028	410
	(Crushed)	444.1	22.9	56.015	1.0256	413
	Plagioclase	44.8	866.6	0.149	0.7052	
Quartz-mica diorite (Y235)	Total rock	91.7	511.6	0.517	0.7085	
	Potassium felspar	269.3	502.7	1.546	0.7134	
	Biotite	357.6	63.8	16.174	0.7946	406
		357.9	63.8	16.183	0.7945	405
Quartz-mica diorite (G120)	Total rock	95.3	319.4	0.861	0.7095	
	Potassium felspar					
	(Uncrushed)	244.6	499.9	1.412	0.7127	
	(Crushed)	243.6	497.0	1.414	0.7135	
	Biotite (Uncrushed)	559	6.2	259.138	2.1929	412
	(Crushed)	554	6.7	238.712	2.1647	439

by the value: Difference/standard error; for an ideal situation this value should be close to zero.

Variance values used are as follows:

$$\text{var. } Rb^{87}/Sr^{86} = C. (Rb^{87}/Sr^{86})^2$$

where C is 25.51×10^{-6} which is a pooled variance based on 34 degrees of freedom (Turek 1966). The variance for Sr^{87}/Sr^{86} is a measured value of 0.10×10^{-6} (53 degrees of freedom).

6.2 EXPERIMENTAL RESULTS

Diorites - Rb and Sr isotope data have been measured on four total rocks and biotites, and three potassium feldspars from the quartz-mica diorite. Two total rock samples of orthoclase diorite are incorporated in the results in Table 44 and displayed in Fig. 39. Regression of all data for the diorites results in a model III isochron (MSWD = 4.36) which suggests that geological factors (for example, variation in the initial Sr^{87}/Sr^{86} between samples) have caused the displacement of data points about the isochron. The apparent age is 408 $\pm$ 3 m.y. and initial Sr^{87}/Sr^{86} ratio is 0.7048 $\pm$ 0.0002 at the 95% confidence level (Fig 39). The degree of enrichment in radiogenic Sr^{87} is sufficiently high for the biotite ages to be almost independent of the initial Sr^{87}/Sr^{86} ratio (assuming either 0.70 or 0.71). Their resulting ages average 410 m.y. and range from 405 to 415 m.y. The data for the total rocks (including the orthoclase diorites) and potassium feldspars

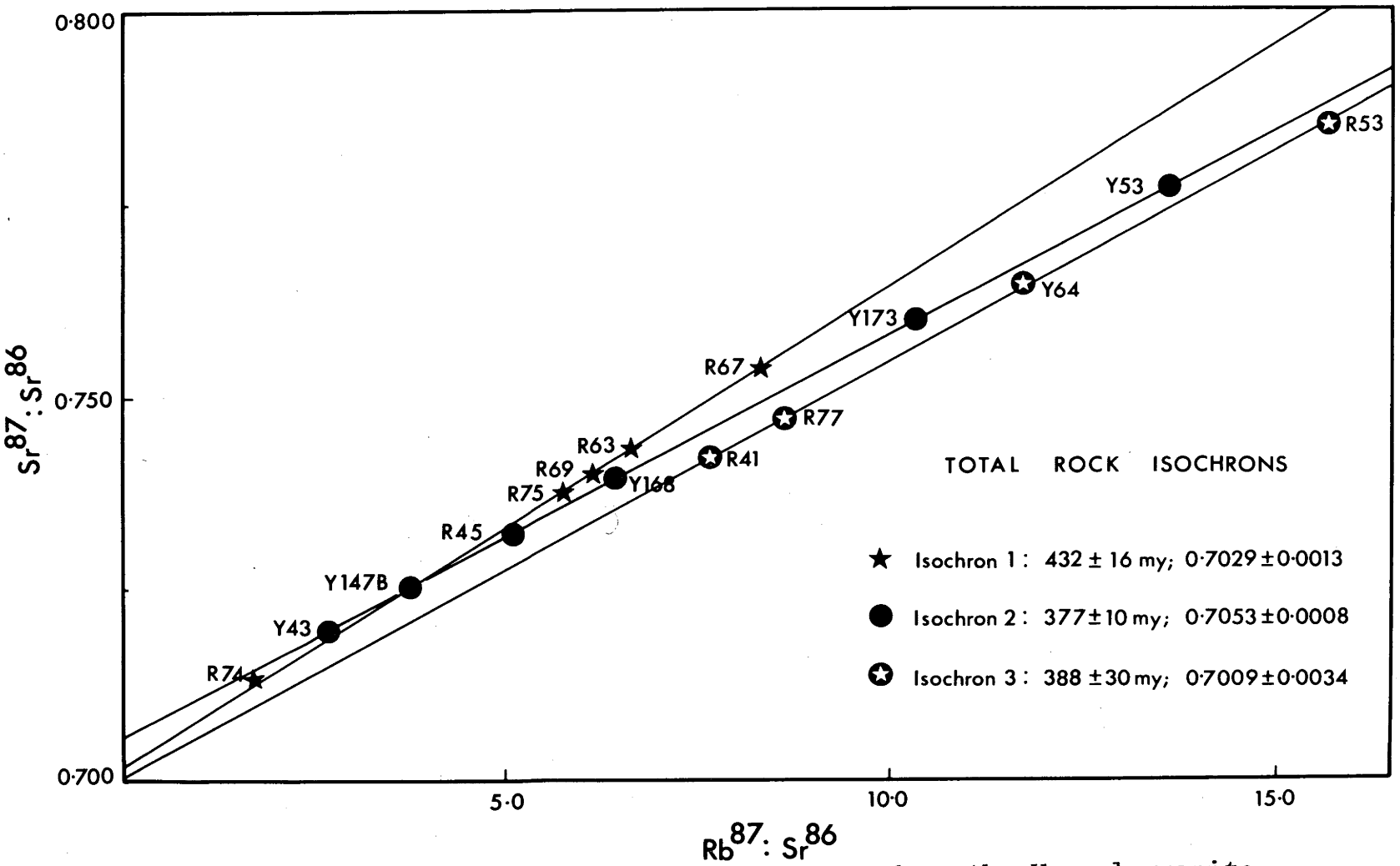

Fig.41 Rb-Sr isochron plot of total rocks from the Yeoval granite.

TABLE 45

Rb-Sr Data for Yeoval Granites

Sample No.	Rb ppm	Common Sr ppm	Rb^{87}/Sr^{86}	Calculated Sr^{87}/Sr^{86}
R74	95.2	158.6	1.731	0.7135
R75	124.2	61.9	5.788	0.7373
R69	117.3	55.2	6.116	0.7397
R63	118.8	51.5	6.661	0.7430
R67	128.6	44.6	8.314	0.7535
Y43	84.3	92.1	2.640	0.7187
Y147B	103.9	85.0	3.693	0.7249
R45	103.8	58.8	5.092	0.7322
Y168	128.5	58.1	6.388	0.7392
Y173	139.7	39.1	10.305	0.7598
Y53	159.2	33.8	13.603	0.7761
R41	116.3	43.6	7.695	0.7428
R77	97.3	32.5	8.648	0.7472
Y64	124.9	30.8	11.706	0.7645
R53	120.9	22.3	15.639	0.7854
Y53 Biotite	491.8	13.8	102.77	1.2687

alone, results in a model I isochron (MSWD = 0.69) shown in Fig. 40. The apparent age is 346 ± 36 m.y. and initial Sr^{87}/Sr^{86} ratio is 0.7056 ± 0.0005. A regression analysis for the total rocks only also gives a Model I isochron (MSWD = 0.49) with a similar age (309 ± 116) and initial ratio (0.7059 ± 0.0011). The large confidence limits in this and the previous analysis are due to the restricted range in Rb^{87}/Sr^{86} of the samples.

Granites - Rb and Sr isotope data have been measured on fifteen total rock samples and one biotite. Results are given in Table 45 and illustrated on the isochron diagram (Fig. 41). Fig. 41 shows that the data cannot define a single isochron. This discrepancy may be resolved by the fitting of three separate model I isochrons, the two lower ones having very similar slopes. Statistical treatment supports this.

The apparent ages and initial ratios of the three isochrons are:

Isochron	Age	Initial Sr^{87}/Sr^{87}	M.S.W.D.
1	432 ± 16	0.7029 ± 0.0013	1.20
2	377 ± 10	0.7053 ± 0.0008	1.55
3	388 ± 23	0.7009 ± 0.0034	1.21

Isochron I is defined by R74, R75, R69, R63, and R67; isochron 2 by Y43, Y147B, R45, Y168, Y173, and Y53; while isochron 3 is defined by the four samples R41, R77, Y64 and R53. Isochrons 1 and 2 have a number of points (particularly

Y43 and Y147B) which may lie on either line. Regression analyses of the data, with or without these points, gives no significant difference in the results (only in the confidence limits). However, for geological reasons they are grouped with isochron 2 data.

The testing of the isochrons 2 and 3 to see if the ages are statistically distinct follows the method of Turek (1966). As the test indicated that the gradients of the separate isochrons are not statistically different (at the 95% confidence level) a weighted mean common age can be computed, based on the assumption that the samples have in fact a common age or that they reflect a common event. This age is 383 $\pm$ 14 m.y. Similar testing and pooling of isochrons 2 and 3, separately and as an average isochron, with isochron 1 indicated that the ages and intercepts are statistically distinct at the 99.9% confidence level.

A similar statistical treatment of the mean weighted granite isochron (2 and 3) and the total rock and potassium feldspar isochron of the diorites led to the conclusion that there is no significant difference (at the 95% level of confidence) in these two isochrons so that a weighted mean average age of 380 $\pm$ 12 m.y. can be calculated.

As a further indication that granite isochrons 1 and 2 are statistically distinct, regression analyses were carried out on isochron 2, incorporating singly and then all together the samples constituting isochron 1 (i.e. R74, R75, R69, R63, R67).

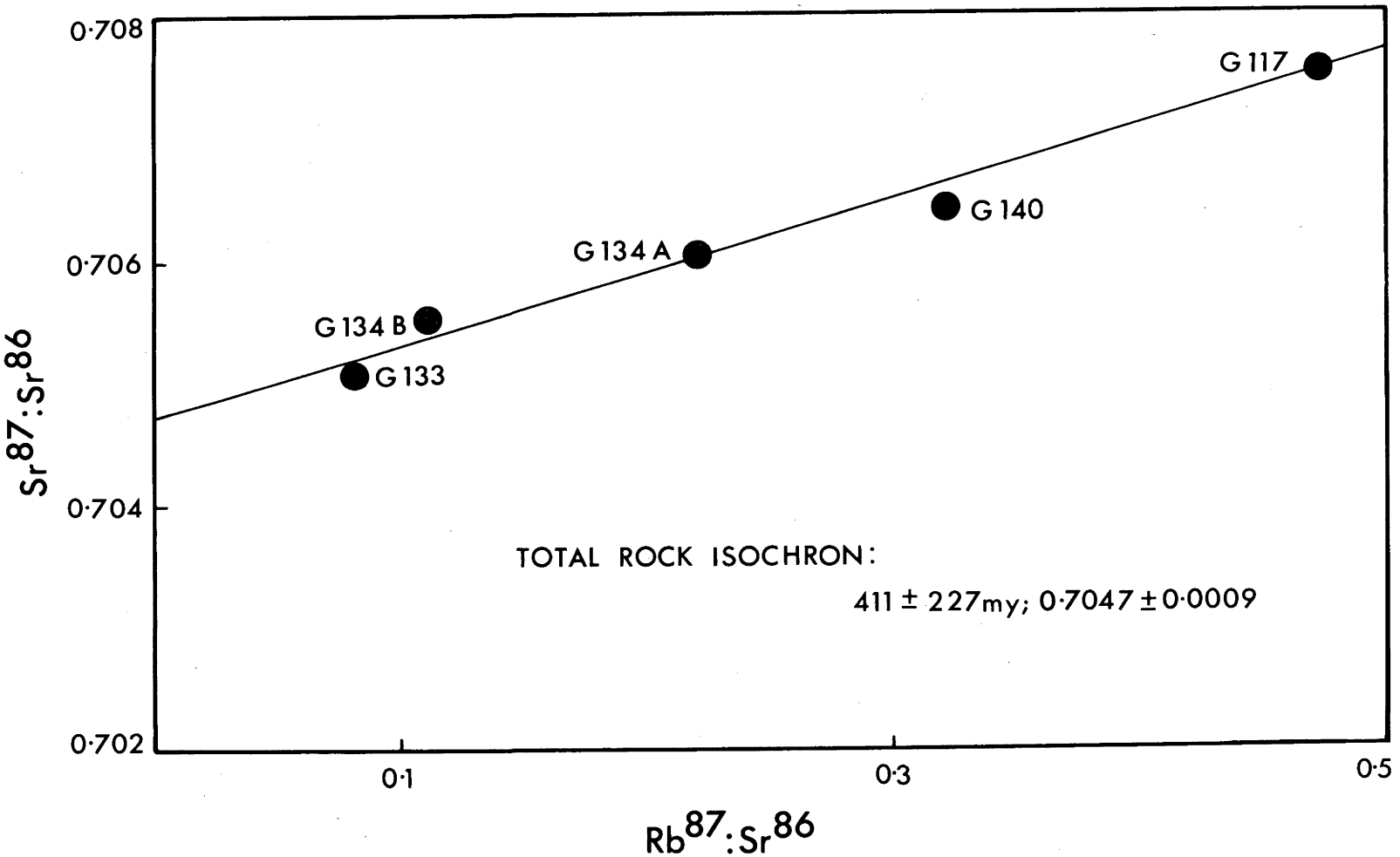

Fig.42 Rb-Sr isochron plot of total rocks from the Yeoval andesites.

TABLE 46

Rb-Sr Data for Yeoval Andesitic Rocks

Sample No.	Rb ppm	Common Sr ppm	Rb^{87}/Sr^{86}	Calculated Sr^{87}/Sr^{86}
G117	33.5	509.3	0.472	0.7075
G133	7.0	245.6	0.083	0.7051
G134A	38.1	489.7	0.225	0.7061
G134B	22.0	566.1	0.112	0.7055
G140	65.2	585.8	0.321	0.7064

These regressions show that the data for isochron 1 cannot possibly fit isochrons 2 and 3. There are geological reasons (discussed later) supporting this division. Thus statistically and geologically there is a separate isochron defined by five samples of granite.

The one sample of biotite analysed is sufficiently enriched in radiogenic Sr to give an age independent of the initial Sr^{87}/Sr^{86} ratio viz. 394 m.y. This is slightly higher than the age of the pooled isochrons and is a minimum age compared with isochron 1.

Gabbros and Associated Rocks - Present day Sr^{87}/Sr^{86} values were measured on one sample each of gabbro and pyroxenite and a complete isotope dilution analyses for the calc-silicate skarn associated with the gabbro. Rb and Sr contents for the unspiked runs were obtained by X-ray fluorescence.

Sample	Rb, ppm	Sr ppm	Rb^{87}/Sr^{86}	Calculated Sr^{87}/Sr^{86}	Measured Sr^{87}/Sr^{86}
Gabbro	2	395	0.015		0.7048
Pyroxenite	17	113	0.433		0.7097
Skarn	30	159	0.551	0.7085	

Andesitic rocks - The results of Rb and Sr isotope measurements on five total rock samples of andesites are given in Table 46 and displayed in Fig. 42. Application of the "two-error" regression method results in a model I isochron of apparent age 411 $\pm$ 227 m.y. and initial Sr^{87}/Sr^{86} of 0.7047 $\pm$ 0.0009. The large confidence limits for these rocks is due to the very

restricted range in Rb^{87}/Sr^{86} i.e. from 0.083 to 0.472. The age obtained for the andesites is a minimum as the field evidence demonstrates that the diorites intrude the andesites.

6.3 DISCUSSION OF RESULTS

The age of 432 m.y. (equivalent to about 408 m.y. using $\lambda = 1.47 \times 10^{-6}$ year^{-1}) for the granites place them on the geological time scale (Kulp 1961) near the Silurian-Devonian boundary. This is compatible with the geological control of the granites intruding Lower to Middle Silurian sediments and overlain unconformably by Upper Devonian sediments.

The most important facts to be gained from the Rb-Sr isotope data are:

(i) the statistically indistinct ages and initial Sr^{87}/Sr^{86} ratios of certain granites, the diorites (total rock and potassium feldspar), gabbros and the andesites.

(ii) the older age of the biotites from the diorite compared with the total rock and potassium feldspar ages.

(iii) the 3 isochrons for the granites; one indicative of the age of intrusion, and the other two of lower age.

These facts point to an event, approximately 380 m.y. ago which led to the readjustment of a large proportion of the rocks in the Yeoval district (and possibly the whole complex), leaving them with a similar imprinted age and initial Sr^{87}/Sr^{86}. That the younger ages are related to a post-crystallisation deformation event is suggested by the circular structure in the

granite (p. 16) which continues into the gabbro and diorite. Samples taken from this area plot exactly on the second granite isochron. This deformation was apparently fairly widespread, affecting the whole of the Yeoval Complex, as suggested by the K-Ar age of 376 m.y. for a sample of quartz syenite near Dubbo, some 30 miles to the north (Evernden and Richards 1962). However, textural evidence in the rocks, particularly the granites, is not indicative of a very severe deformation.

The true age of granite intrusion of about 432 m.y. is reflected in the fine-grained granophyric varieties which are usually marginal to the diorite and are thought to be chilled phases. The retention of their age for these types may be the result of two factors. Firstly, if the finer-grained rocks were less susceptible to deformation than the coarser-grained types, they might be expected to lose less radiogenic Sr and so retain their ages. Secondly, the larger volume of "pore" space and grain boundaries may restrict diffusion of radiogenic Sr out of the rock. This apparently older age of the granite relative to the diorite may be due to incorporation of radiogenic Sr from, say, sedimentary material. Objections to such a hypothesis are based on field and petrographic evidence (absence of xenoliths and any ferromagnesian minerals in the marginal phase, which should be present if sedimentary material was incorporated into the magma) and the low initial Sr^{87}/Sr^{86} ratio of the chilled margin.

It is apparent from the Rb-Sr isotope data that the diorites

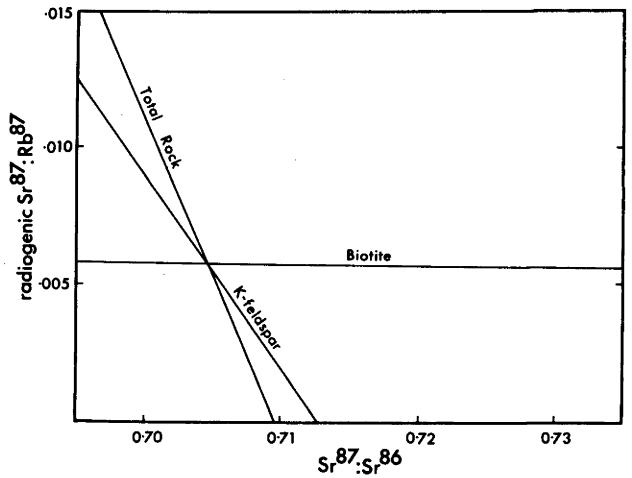

Fig.43a Rb-Sr data for sample G120

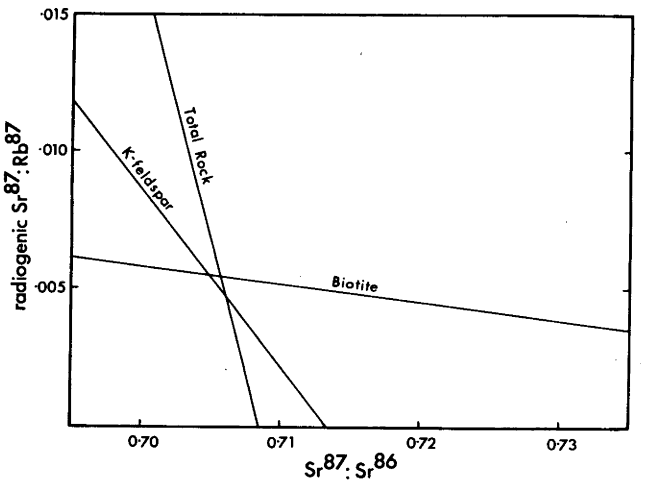

Fig.43b Rb-Sr data for sample Y235

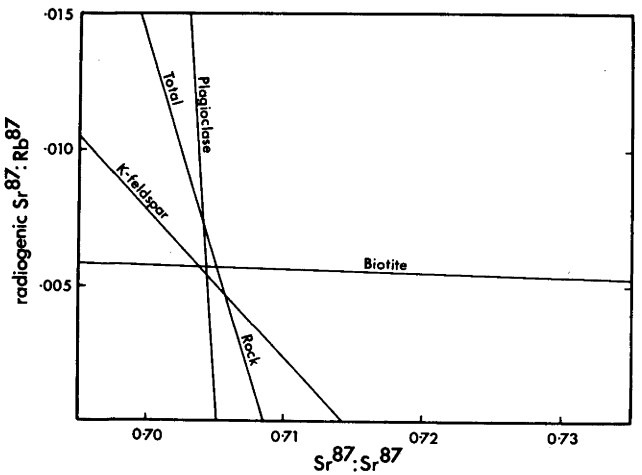

Fig.43c Rb-Sr data for sample Y41

(i.e. their constituent minerals) have lost radiogenic Sr, indicated by their lower ages relative to the granite (of age 432 m.y.) and which intrudes the diorite. The biotites are the least affected as they have retained an age of about 410 m.y. The high biotite age relative to the total rock may be due to:

(i) radiogenic Sr^{87} gain

(ii) Rb loss; or

(iii) it is a relict age.

(i) gain of radiogenic Sr^{87} in biotites has not been established; in fact, the general tendency is for biotites to lose radiogenic Sr^{87}.

(ii) the loss of Rb from the biotite is a possibility, but the concordance of age between random samples (some up to 10 miles apart) indicates that the fractional loss of Rb must be proportional to the concentration (as the biotites have markedly different contents of Rb). This unlikely possibility, combined with the fact that the diorites are older than the granite (and so the biotite age for the diorite is a minimum), precludes the suggestion of Rb loss from the biotites to account for their high age, relative to the total rock.

(iii) since it is not (i) and (ii), the biotite has apparently retained its age to a higher degree relative to the total rock.

The loss of radiogenic Sr^{87} from constituent mineral phases is more clearly seen if reference is made to Figs. 43 a', b' and c'. Here, the ratio of radiogenic Sr^{87}/Rb^{87} is plotted against

Sr^{87}/Sr^{86} for three samples of diorite and their constituent potassium feldspar and biotite after the method of Compston and Jefferey (1959). The convergence of the lines for G120 (Fig. 43a) suggests that there was complete homogenisation between the biotite and potassium feldspar within the total rock. Regression analyses for the biotite, potassium feldspar and total rock delineate a perfect model I isochron (MSWD = 0.0) with an apparent age of 412 $\pm$ 27 m.y. and an initial Sr^{87}/Sr^{86} of 0.7046 $\pm$ 0.0043. As this is a minimum age, then the rock must have initially been an open chemical system which, after homogenisation, closed. This contrasts with Y41 and Y235, the Figs. 43b and c and regression analyses of which indicate that, although the biotite closed around 400 m.y., other phases and the total rock, remained open chemical systems, possibly for another 50 m.y. (A comparison may be drawn between sample G120 in the diorite and the samples defining the main isochron (1) for the granite. Both sets of samples have apparently retained (or nearly so) their age and it is significant to point out that they represent chilled margins of the two rock types).

This suggests that some mineral phase (or phases) is present (besides biotite) which has lost a considerable amount of radiogenic Sr^{87}. Hornblende can be disregarded because of its extremely low Rb content, leaving potassium and plagioclase feldspar as the only phases present in any significant quantity, capable of accommodating Rb and Sr. The loss of radiogenic Sr from potassium feldspar is well documented (e.g. Arriens et al. 1966, Brooks 1966). In a number of such cases, the radiogenic

Sr has been redistributed into the co-existing plagioclase resulting in an apparently older age of this mineral. Only one sample of plagioclase (Y41) was analysed by the method of isotope dilution and as it is not considered to be representative of the mineral as a whole, little can be said of its effect on relative mineral ages. Loss of radiogenic Sr^{87} from plagioclase or its alteration products may account for the observed trends. This possibility is suggested by the Rb and Sr data for a fresh and altered concentrate of plagioclase separated from the one rock (G118). The fresh plagioclase occurs mainly in the outer zones of the crystals while the altered material is in the cores of higher specific gravity. The alteration products are dominantly fine-grained white mica and clay minerals.

	Fresh Plagioclase	Altered Plagioclase
Rb (ppm)	41	119
Sr (ppm)	817	675

The Rb is concentrated, by a factor of 3, in the altered fraction. If the radiogenic Sr^{87} was lost from the alteration products (assuming the Rb to be present in these) this may explain the open system chemistry observed in the rocks. Such a postulate is in contrast to that of Arriens et al. (1966) and Brooks (1966) who found in certain granitic rocks, discordant ages for the feldspars, the potassium feldspar having a low, and the plagioclase, a high age. However, their total rocks and biotites had similar ages, which led them to invoke internal

isotopic redistribution as the mechanism to account for the discrepancies. Arriens et al.(1966) also noted that muscovite (including sericite) retains radiogenic Sr longer or more completely than other Rb-rich minerals which is incompatible with the postulate that the alteration products of the plagioclase in the Yeoval diorites have lost radiogenic Sr^{87}. However, Brooks (1966) implied that muscovite in the white series A of the Heemskirk granite lost radiogenic Sr but not to the same degree as biotite. Thus it is possible that the potassium feldspar, plagioclase feldspar and the total rock of a number of samples of quartz-mica diorite may have been open chemical systems as a result of the metamorphic event discussed previously.

The spread of values in the age of the biotites is most likely a reflection of geological, rather than experimental influences. The lower ages of all the biotites, and particularly Y235 and Y53, may be the result of partial chloritisation, the effects of which are discussed on p. 50. Brooks (1966) suggested that chloritisation of biotite led to an increase in the Sr^{86} content, a decrease in the Rb^{87} content, and a decrease in the radiogenic Sr^{87}/Rb^{87}, resulting in a low age. This is supported by the lower age of Y235 and Y53 biotites, both of which show a greater degree of chloritisation than the other biotites.

6.4 RECALCULATION OF INITIAL Sr^{87}/Sr^{86} RATIOS

Assuming the age of granite intrusion (432 m.y.) to be the minimum age of the diorite and gabbro, it is possible to calculate the initial ratios of the various rock types (relative to the granite age) which have been affected by the metamorphism accord-

TABLE 47

Recalculated Initial Sr^{87}/Sr^{86} Ratios for Yeoval Rocks

Rock Type	Rb^{87}/Sr^{36}	Sr^{87}/Sr^{86}_{P}	Sr^{87}/Sr^{86}_{O}
Gabbro	0.015	0.7048	0.7047
Pyroxenite	0.433	0.7097	0.7071
Diorites (Average of 25)	0.608	0.7048	0.7011

ing to the equation:

$$(Sr^{87}/Sr^{86})_o = (Sr^{87}/Sr^{86})_p - Rb^{87}/Sr^{86} (e^{\lambda t} - 1)$$

where $e^{\lambda t} - 1$ is the slope of the granite isochron (0.006038)

The recalculated initial ratios for the rock types are given in Table 47 along with their "present day" Sr^{87}/Sr^{86} ratios. For the diorites, results are averaged from 25 samples, the Rb and Sr data for 18 of these being obtained by x-ray fluorescence.

The most noteworthy points of interest are the extremely low (0.7011) initial Sr^{87}/Sr^{86} ratio for the diorites and the higher ratios for the gabbro and pyroxenite. This anomaly, from apparently cogenetic rocks, and its relation to the genesis of the Yeoval diorites will be discussed in the following section.

6.5 EFFECT OF CRUSHING ON MINERAL AGES AND INITIAL Sr^{87}/Sr^{86}

For extraction of Rb and Sr from minerals, the coarsest grain-size of pure material is dissolved. For this work, biotite of -72 + 100 mesh and potassium feldspar of -100 + 150 mesh was used. Two samples of biotite and one of potassium feldspar were crushed in a mechanical agate mortar and pestle for 1 hour and then analysed for Rb and Sr by isotope dilution. These results are compared with the coarser samples in Table 44. The crushed biotites give lower Rb and higher Sr contents, and lower present day Sr^{87}/Sr^{86} ratios. The data for the crushed potassium feldspar is not significantly different from the uncrushed material.

7. PETROGENESIS OF DIORITIC ROCKS

In this section the ideas for and against the various theories of the origin of dioritic rocks, are presented with particular reference to the Yeoval diorites. It should be remembered at the outset, that the Yeoval diorite is a high potassium type, which is most likely a reflection of the bulk composition of the original magma. Also, no one theory can satisfactorily explain all occurrences of diorite rocks,

7.1 THEORIES OF ORIGIN OF DIORITIC ROCKS

Three main hypotheses have been proposed to explain the origin of dioritic rocks. These are parallel to current theories for the origin of andesites.

1. fractional crystallisation from a parent basalt magma
2. mixing of rock types
3. primary diorite magma derived from the mantle or deep crust.

7.1.1 Fractional Crystallisation

According to the classical Bowen (1928) hypothesis of fractionation under near surface conditions there should be a sequence found in the field from:

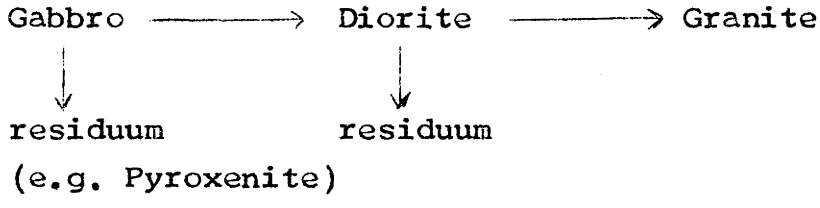

Assuming that the rocks seen in the field at Yeoval are those involved in this fractional crystallisation scheme, then in the derivation of the diorite from the gabbro there would be an increase in the SiO_2 content by more than 10%, and a decrease in the MgO and CaO contents by approximately 6 and 9% respectively. This requires crystallisation and separation of one or more of the phases seen in the gabbro (olivine, pyroxene, plagioclase). The pyroxenite could not be the residuum in this case because the removal of say, pyroxene, with very low aluminium content (less than 1% Al_2O_3) would enrich the magma in Al_2O_3. The analyses show that the Al_2O_3 content is lower in the diorites than the gabbros. Removal of anorthite and olivine may bring about this composition change, but these are only minor minerals in the pyroxenite.

If pyroxenite is the residuum from the formation of diorite from gabbro, then some mixture of the pyroxenite and diorite should give gabbro composition. The SiO_2, Al_2O_3 and alkali contents are incompatible with this hypothesis.

Another objection to the formation of the diorites by fractional crystallisation, and a characteristic of calc-alkaline rocks in general is their lack of iron enrichment. This is illustrated on an FMA diagram (Fig. 3) along with typical tholeiitic trends which show iron enrichment.

Osborn (1959, 1962) modified Bowen's theory to account for the lack of iron enrichment in calc-alkaline rocks by appealing to crystallisation under

conditions of high and constant oxygen fugacity. This gives rise to early crystallisation of magnetite so that fractionation proceeds without iron enrichment.

A number of objections have been raised against this mechanism:

(i) there is no evidence of the large scale accumulation, or early crystallisation of magnetite in the calc-alkaline rocks.

(ii) calc-alkaline rocks are not strongly oxidised. For example the Yeoval diorites contain very little, if any, ferric iron.

(iii) rocks formed by fractional crystallisation should lie on smooth variation diagrams. The Yeoval diorites and associated rocks give a scatter of points on Harker diagrams, as do the replotted Garabal Hill-Glen Fyne and Southern California Batholith rocks.

(iv) Wilkinson (1966) suggested that certain aspects of the mineral chemistry of some calc-alkaline rocks are not consistent with crystallisation under conditions of relatively high oxygen fugacity. In fact, the ulvöspinel content of titanomagnetites from Japanese andesites (Akimoto 1954, 1955) implies crystallisation under conditions of low oxygen fugacity.

(v) Carmichael (1967) suggested, on the basis of data from iron-titanium oxides in some acid calc-alkaline rocks, that the oxygen fugacity has not remained constant during fractionation.

From the data presented above it is concluded that

fractional crystallisation of a basaltic magma, has played no role in the formation of diorites, and probably, calc-alkaline rocks in general.

7.1.2 Mixing of Rock Types

Included in this discussion are mixing of basaltic and granitic magma, mixing of basaltic magma with metasedimentary crustal material ("sialic" material), and mixing of basic rock and acid magma.

A. Mixing of basaltic and granitic magma has been frequently cited for the formation of rocks of intermediate composition. For the Yeoval rocks, mixing of basic and acid magmas of similar composition to the gabbro and granite may explain the following:

(i) high K, Rb, Ba, Th and U contents (cf. normal andesites, see Table 48)

(ii) the calcic and possibly sodic cores in the plagioclases (see Plate 7).

Objections to this hypothesis include:

(i) field relationships show no evidence of mixing - there is no transition between the diorite and granite or gabbro and granite; in fact, for most of its length, the granite exhibits a "chilled" margin against the diorite so that any mixing would have to occur at depth.

(ii) major and trace element variations show no transition between the diorites and granites - in most Harker variation diagrams, there is a sharp break in the 65-75% SiO_2 range.

(iii) there is a marked difference in the zircon population from the granite and diorite (see section 4.7). If the diorite was formed by mixing of the granite and gabbro (or even another magma) it might be expected that two zircon populations would be observed in the diorite.

(iv) Initial Sr^{87}/Sr^{86} isotope ratios of 0.705 for the gabbro, 0.701 for the diorite and 0.703 for the granite indicate that mixing of granite and gabbro could not result in a diorite of lower initial Sr^{87}/Sr^{86}.

B. Mixing of basaltic magma and "sialic" material - This hypothesis offers a plausible explanation, as does the mixing of magmas, for certain major and trace element abundances in the diorites. However, Sr isotope data for the Yeoval diorites give an initial Sr^{87}/Sr^{86} ratio (0.701) far lower than can be obtained by mixing of basaltic magma and crustal material such as the greywackes, shales, etc. of the Tasman Geosyncline. Certain shales of the Tasman Geosyncline have initial Sr^{87}/Sr^{86} ratios of the order of 0.72 (Bofinger, pers. comm.) whereas the Hamilton Shales of Pennsylvania and New York studied by Whitney and Hurley (1964) have an initial ratio of about 0.707. Other Sr isotope data for coarse-grained calc-alkali rocks of intermediate composition is scarce; values of 0.705 initial Sr^{87}/Sr^{86} ratio have been obtained for Garabal Hill-Glen Fyne complex (Summerhayes 1966), 0.704 - 0.705 for certain of the Moonbi rocks in New England (N.S.W.). The high value of 0.7073 ± 0.0010 for the majority of the coarse-grained rocks of the Sierra Nevada Batholith led Hurley et al. (1965)

to suggest that the Sierra magmas either represent a mixture of oceanic basalt and crustal sial, or the partial melting within a geosyncline containing fairly recent volcanic material and some terrigenous detritus. Such low initial Sr isotope ratios preclude the possibility of any sizeable addition of "sialic" material to a basaltic magma.

Taylor (1967) calculated that in order to raise the silica percentage from 50 to about 60% would require the addition of either 50% of material of granitic, 60-70% of granodioritic, or 20% quartzitic composition to the basalt mix. Such large amounts of added material would give anomalous initial Sr^{87}/Sr^{86} ratios and trace element chemistry.

Other information from the fine-grained rocks does not support this mixing hypothesis. For example:

(i) Waters (1955) found no evidence of sialic contamination for large areas of basalt in theCascade-Coast Range province of the western United States.

(ii) Andesites are common both in areas of continental crust (Japan, New Zealand, Cascades) and in island arcs (Aleutians, Marianas, Solomons) where little or no "sialic" material is available.

C. Mixing of basic rock and acid magma - This mechanism, involving the mixing of crystalline (or nearly crystalline) basic material with acid magma, has been the most commonly invoked hypothesis for the formation of dioritic rocks e.g.

Brown (1928), Pabst (1928) Wells and Wooldridge (1931), Thomas and Smith (1932), Nockolds (1932, 1934), Brammal and Harwood (1932), Deer (1935, 1950), Wells and Bishop (1955), Akaad (1956), Chayes (1956), Joplin (1958, 1959), Hutchinson (1964), Read and Haq (1965), Wilkinson (1966) and Chappell (1966). In some cases, it is attributed a minor role as in the Southern California Batholith (Larsen 1948) and Garabal Hill (Nockolds 1941). The basic rocks may or may not be associated with the granitic rocks in the field. The abundance of basic, rather than surrounding country rock, xenoliths in the majority of these areas and the fairly homogeneous distribution of xenoliths throughout the magma, suggests this process takes place at depth. This is a plausible mechanism for a number of dioritic (or more correctly, tonalitic) types although it is not applicable to all occurrences.

Assuming that the gabbro and granite (magma) are the end members involved in the production of the Yeoval diorite, the mechanism fails to account for:

(i) paucity of xenoliths in the diorite and granite (particularly near its contact with the gabbro). It is possible that mixing has been perfect and so few xenoliths are seen.

(ii) if calcic and sodic cores are used in support of this mixing hypothesis (e.g. Larsen 1948), heterogeneity of the higher temperature ferromagnesian minerals, hornblende and biotite, would be expected. However, the hornblendes and biotites in the

diorites are fairly uniform in composition and differ chemically from those in the granites.

(iii) the relative increase in Zr, Ba and Th from basic to acid rocks; Chappell (1966) has fairly convincingly demonstrated for this sort of mixing in the Moonbi granites, that these trace elements decrease in amount in going from basic to acid rocks.

(iv) Zircon abundances are very low in gabbros and basalts (Poldervaart 1956). Thus, if mixing of basic gabbro and granite magma (the latter with abundant zircon) had taken place, one would expect there to be little or no zircon in hornblende and biotite and an abundance in quartz and feldspar. In the Yeoval diorites, zircon is equally distributed throughout all mineral phases. The Zr and Hf of zircons in all mineral phases of the diorite are also very similar.

7.1.3 Primary Dioritic Magma

The premise of a primary dioritic magma is not new; Nockolds (1941) suggested it 26 years ago to account for the Garabal Hill-Glen Fyne rocks. The possibility of a diorite magma is intimately connected with that of the existence of a primary andesite magma derived from the deep crust or the mantle. Evidence supporting a mantle origin of andesite and diorite include the following:

(i) low initial Sr^{87}/Sr^{86} "mantle-type" ratios

(ii) the large volume of andesitic material of fairly uniform chemistry in areas of variable crustal thickness. For

example, Pakiser and Robinson (1966), Woolard (1966) and Eaton (1963) have suggested from seismic and gravity data, that the crust of the western coast of United States (including the Southern California and Sierra Nevada Batholiths) has markedly low values of crustal thickness (approx. 20-25 kms), and in general, subnormal velocity values for the mantle. The effect of crustal thickness is not relevant for the Yeoval and Snowy Mountains diorites because of their much greater age in comparison with the majority of andesites i.e. we cannot say what the crustal thickness was some 400 m.y. ago in these areas.

7.2 ORIGIN OF YEOVAL DIORITES

7.2.1 Nature and Source of Parental Magma

From the information given in previous sections, it is suggested that a parent magma of composition similar to that of the Yeoval "pyroxene-mica diorite" would explain all the observations. A similar conclusion has been reached by a number of workers on both coarse-and fine-grained calc-alkaline associations, e.g. Scottish Caledonian (Nockolds 1941), Southern California Batholith (Larsen 1948), Medicine Lake Highlands (Andersen 1941) Lassen Peak region (Clarke 1915), Crater Lake (Williams 1942). It must be kept in mind that the Yeoval pyroxene-mica diorite is different from the pyroxene-mica diorite of Nockolds (1941).

It is considered that the diorite magma was generated in the lower crust or upper mantle according to either one or the other of two theories suggested by Green and Ringwood (1966) and Green (1967). These theories based on both experimental and natural systems involve derivation of the calc-alkaline association by a two-stage process. "In the first stage, fractional melting of the pyrolite mantle produces undersaturated basaltic magma which rises to higher levels and following fractionation of this magma at depths of less than 20 km, large piles of basalt with an overall quartz-normative composition will result." (Green and Ringwood 1966, p. 315).

The calc-alkaline rocks may be derived in the second stage by either of the following theories:

1. Dry Partial melting of Quartz eclogite at 100-150 kms

If the basalt pile remains dry, and the P-T conditions suitable, it may transform to quartz eclogite and sink back into the mantle. Partial melting of the quartz eclogite under dry conditions at depths of 100-150 kms can produce basaltic andesite and andesite (diorite or quartz diorite).

2. Wet Partial Melting of basaltic material at depths of 30-40 kms, with $P_{H2O} < P_{load}$ -

Introduction of water into the basalt pile results in the formation of amphibolite in the lower parts. "Subsequent heating of the amphibolite, due to renewed or continued volcanic

activity from the mantle, may result in partial melting taking place" (Green 1967).

In both these models the initial bulk composition of the basalt pile and the temperature and depth at which partial melting occurs, will be important factors governing the composition of the derived calc-alkaline magmas. In addition, the rate of progress of the magma to the surface (which strongly influences reaction of the wall-rock and magma (Green and Ringwood 1967)) and degree of crystallisation during this upward movement (O'Hara 1965) will also affect the final composition of the rock.

In addition to providing a mechanism for deriving acidic compositions from a basic parent, the above models also account for a number of other features characteristic of calc-alkaline rocks.

(i) lack of iron enrichment, because the iron-rich phases (garnet or amphibole) remain in the residuum.

(ii) low initial Sr^{87}/Sr^{86} ratios.

(iii) variation composition between and within different members of the calc-alkaline association - this is a function of the bulk composition of the basalt pile, the depth and degree of partial melting (either wet or dry), and the subsequent rise of the magma to the surface.

(iv) volume relationships are overcome since the residuum is in the mantle.

The following properties of the Yeoval diorites suggest a mantle origin:

(i) low initial Sr^{87}/Sr^{86} ratios

(ii) presence of sodic cores in the plagioclase from the pyroxene-mica diorite and "chilled" margin phase of the diorite. Green's (1967) experimental work on calc-alkaline and anorthositic rocks under both wet and dry conditions showed that the An content of plagioclase decreased with increasing pressure. If correlation between his experimental data and the results obtained for the Yeoval plagioclases are made, then the sodic cores (approximately 8% CaO; An 40) would indicate that, under dry conditions (model 1) crystallisation began at pressures of at least 18 kb. This assumes an initial basaltic andesite composition corresponding closely with the composition of the pyroxene-mica diorite. For a quartz diorite composition, the experimental data indicate (dry conditions) that a plagioclase of An 40 would crystallise at pressures near 13.5 kb. For a basaltic andesite composition under wet conditions (model 2), crystallisation occurs of a plagioclase with an An content of 41 at 18 kb compared with An 51.6 at 9 kb. Thus, from these data the plagioclases in the diorite would have begun to crystallise at depths of at least 30-40 kms and pressures greater than 13.5 kb. The crystallisation of the plagioclase may have begun soon after partial melting of the basic material was initiated. Green (1967) has suggested that partial melting of basaltic compositions (at high pressures and

under dry conditions) at lower temperature than those required to produce andesite (40-50% melting), produces liquids enriched in alkalis, relative to silica. The residuum remaining after derivation of such compositions consists mainly of garnet and pyroxene. The liquids produced by such a mechanism may well be high potassium diorites (or andesites) for he states that they may have affinities with some oversaturated syenites found associated with calc-alkaline rocks (Joplin 1965).

Dickinson and Hatherton (1967) suggested that andesitic magmas are generated by events associated with earthquakes of intermediate depth (80-270 km) and rise to the surface without "even undergoing sufficient contamination to mar the pattern of chemical variations established at the sites of partial melting in the mantle". They further suggest an increase of potassium in Circum-Pacific andesites with depth of the Benioff Zone, whereby the "partition of potash between incipient melt and residual crystalline phases should be such that the potash content of the melt rises as confining pressure rises". However, the authors do not suggest that the model predicts the absolute potassium content of the andesitic lavas at the Benioff zone.

7.2.2 Relation of the Gabbro to the Diorite

Before proceeding further with the crystallisation history of the diorite magma, it is important to establish the relationship of the gabbro to the diorite. Unusual features of the gabbro include:

(i) The very high CaO (average 14.8%) and low SiO_2 contents (45.5%), compared with Nockolds (1954) average gabbro (11.07% CaO and 48.36% SiO_2) and "central" basalt (10.07% CaO and 51.33% SiO_2). Also noteworthy are the very low alkali contents in the gabbro (0.9% Na_2O, 0.10% K_2O) compared with Nockolds average gabbro (2.26% Na_2O, 0.56% K_2O).

(ii) The high initial Sr^{87}/Sr^{86} ratio of 0.705 compared with the diorite (0,701.).

(iii) Variable mineralogy-olivine is present in amounts up to 8% and normally co-exists only with clinopyroxene. In other samples containing no olivine, clinopyroxene and orthopyroxene occur in about equal amounts. Also, the rocks containing no olivine have the lowest CaO contents and their plagioclases have the lowest An content (An 80).

(iv) No zoning is present in the plagioclase and they have very high anorthite contents (An 80-87) which are comparable with those of the "accumulative rocks" in the Southern California Batholith (Miller 1937).

(v) The absence of hornblende in the gabbro contrasts with other gabbros occurring with diorites. e.g. Certain phases of the San Marcos gabbro (Miller 1937).

(vi) The presence of a small lens of calcium-silicate hornfels at the margins of the gabbro, and calcite-rich patches patches sporadically distributed throughout the gabbro.

From these observations, it is suggested that the gabbro formed by a mechanism of crystal settling from the diorite magma contaminated by calcium-rich sediment, possibly limestone. Extensive limestone belts occur within 15 miles to the east and south-east of the Yeoval diorites.

Bowen (1928, p. 206) states that addition of limestone or dolomite to basaltic magma causes an endothermic reaction involving the precipitation of magnesian olivine, calcium-rich clinopyroxene and anorthite-rich plagioclases. In the Yeoval rocks, the following reactions may be applicable.

Pyroxene-mica diorite: $Mg_2Si_2O_6 + CaCO_3 \longrightarrow Ca_2Mg_2Si_2O_6 + MgO + CO_2$ (Clinopyroxene)

$2\,MgO + SiO_2 \longrightarrow Mg_2SiO_4$ (olivine)

That is, the addition of limestone locally desilicates the pyroxene-mica diorite magma to the extent that olivine is able to crystallise. At the same time the formation of a CO_2-rich fluid phase would dehydrate the magma since water is partitioned in favour of the fluid phase rather than the melt. This could explain the absence of hornblende. The theory is similar to the classical limestone assimilation hypothesis of Daly (1933) and Shand (1943).

The incorporated material was probably limestone rather than a dolomite because of the normal MgO content of the gabbros and the mineralogy of the calcium-silicate skarn rock.

Support for the limestone-incorporation hypothesis was gained from preliminary results of experimental work. In this, a dry mixture of natural pyroxene-mica diorite composition and 8% CaO was run at 2 kb and varying temperatures (1100-1240°C) in a piston-cylinder apparatus. For comparison, runs were carried out under similar conditions using only the pyroxene-mica diorite composition. The apparatus, techniques and sample preparation have been described in detail by Green and Ringwood (1967). From these runs using both compositions, plagioclase was found to be the liquidus phase at approximately 1200°, followed closely by pyroxene. At lower temperatures (1100-1150°C) the abundance of pyroxene increased relative to plagioclase.

Further evidence that the gabbro crystallised from the diorite magma is suggested by:

(i) the gradation between the gabbro and pyroxene-mica diorite, illustrated by field, petrographic and chemical evidence, given in earlier sections (e.g. see section 3.2).

(ii) The similar compositions of clinopyroxenes from the gabbro and diorite.

(iii) the presence of calcic cores in plagioclase in the "chilled" margin of the diorite which are unzoned and have almost

the same anorthite content as those in the gabbro.

The crystallisation of the gabbro from the parent diorite magma could partly explain the higher K_2O and SiO_2 content of the average quartz-mica diorite; however, this cannot completely explain the high potassium contents when one considers that the areal proportions of the gabbro to diorite are approximately 1:90.

The pyroxenite may also be a crystal accumulate. The textural and chemical evidence (Table 17) indicates that clinopyroxene crystallised early along with plagioclase and minor amounts of olivine and hypersthene leaving a residuum of liquid in the pore spaces which later precipitated a subsilicic hornblende mosaic. A transition to the diorite, similar to that of the gabbro and diorite, is readily discernible.

7.2.3 Depth of Crystallisation of the Diorite Magma

The evidence supporting a shallow depth of crystallisation of the magma is as follows:

(i) The SiO_2 and FeO contents are high, whereas the Al_2O_3, TiO_2 and Na_2O, contents of the hornblende in the diorite are low relative to those crystallised from a high-alumina quartz tholeiite composition at 10 kb, under wet conditions (Green 1967). The bulk composition for the experimental work is not exactly the same as that postulated for the parental diorite magma, but the important oxides, such as SiO_2, FeO and Al_2O_3, are very similar and the same relationships should persist.

(ii) The calcic plagioclase in the diorites - corroded cores and zones in a number of samples of diorites have compositions

of 11-12% CaO (about An_{60}) corresponding closely to plagioclases crystallised from a quartz diorite composition at one atmosphere. (Green 1967).

(iii) The low Al_2O_3 content of the pyroxene in the gabbro and diorite require shallow depths of crystallisation (Green 1963, Green 1967).

(iv) The crystallisation of olivine from a quartz normative liquid (such as the pyroxene-mica diorite) requires low pressure conditions (less than 5 kb) according to Green and Ringwood (1967), Green (1967).

7.2.4 Crystallisation of Plagioclase and its Relation to the Diorite Magma

The mineralogical data given in previous sections, together with the experimental work of Green (1967), indicate that the Yeoval diorite began crystallising at depths greater than 40 kms where sodic plagioclase was the liquidus phase. From the present experimental data at 2kb a more calcic plagioclase (An_{56}) is the liquidus phase. As the Yeoval diorite magma rose toward the surface, a calcic plagioclase (calcic cores) crystallised. The next phase to crystallise was pyroxene (deduced from experimental data, the "chilled" margin of the diorite, and remnant pyroxene grains in the hornblende). With an increase in the amount of water in the magma, possibly associated with the crystallisation of the anhydrous phases, (plagioclase and pyroxene,) hornblende

and biotite began to form. Such speculation is not in conflict with the formation of the gabbro, which is considered to be a local phenomenon. If the field of hornblende had only just been entered at the time of incorporation of limestone, then it is possible for both local dehydration and desilication (leading to the formation of the gabbro) and crystallisation of the diorite magma to occur at the same time. This would account for the transition between the gabbro and the diorite (e.g. rimming of pyroxene by hornblende, crystallisation of a small amount of biotite, zoning in plagioclase, etc).

The crystallisation of up to 25% modal hydrous phases suggests that the diorite magma was possibly saturated with water. An increase in water pressure may have led to corrosion of the outer margins of the plagioclase (e.g. Plate 10) and the development of patchy zoning. After this, sodic rims crystallised (these may or may not be normally zoned). That this was a major event in the crystallisation history of the plagioclase is suggested by the fairly constant composition (An 40) of the sodic rims over a widespread area, Vance (1962, p. 746) has suggested that "The abrupt change to normally zoned (sodic) rims in the zoning sequence is thought to reflect late-stage saturation of the residual melt in volatiles. After saturation, agitation by the escaping volatiles maintains a uniform melt composition equalising the rates of diffusion and crystallisation. This prevents further supersaturation permitting uninterrupted crystallisation of the rims". He bases this postulate on the

plagioclase equilibrium studies in water-saturated systems at high pressure (Yoder et al. 1957). However, he proposes that a decrease in (confining) pressure, associated with rapid upward movement of a water-saturated magma brings about saturation in volatiles.

This is entirely inconsistent with the facts presented above which indicate that the diorite magma crystallised at very shallow depths. Thus Vance's idea (1962, p. 753) of upward movement of magma to account for corrosion and "patchy" zoning of plagioclase in the Yeoval diorites is not substantiated by other evidence. His interpretation (1962, p. 753) of Carr's (1954) thermodynamic data for water-deficient plagioclase systems which he says indicate that a "more sodic plagioclase will crystallise from a given melt at lower pressure than at higher pressure" is in direct conflict with the experimental data of Green (1967) for both dry and wet systems.

The corrosion and "patchy" zoning in the plagioclases from the Yeoval diorite apparently only requires the lowering of the water pressure, possibly by explosive eruption of a volatile phase from the water-saturated magma, rather than rapid upward movement of the magma.

Two main hypotheses have been proposed to explain oscillatory zoning in plagioclase. One theory is that oscillatory zoning results from repeated changes of parameters governing the

crystallisation of plagioclase from the liquid. These parameters include temperature, total pressure, equilibrium water pressure, and liquid composition. The changes are brought about by factors external to the magma, or by the relative movement of crystals and liquid in a large magma chamber. The other is the diffusion-supersaturation theory first proposed by Harloff (1927) and restated by Hills (1936), Vance (1962) and Bottinga et al. (1966). In the first stage of this process the crystal growth rate is faster than diffusion of certain anions and leads to a reduction in the Ca content of the liquid near the crystal face; subsequent crystallisation results in progressively anorthite-poor plagioclase. A tapering off stage ensues, followed by a period during which diffusion is dominant and consequently, supersaturation and deposition takes place of a zone of similar composition to that of the initial calcium-rich zone.

However, as Bottinga et al. (1966) point out, there is no obvious reason why growth should either slow down or cease in order to build up to its original composition. These authors suggest that the plagioclase crystal (without its concentration gradient) might be displaced so that it is once more brought into contact with liquid of the bulk composition. The difference between the theory of Bottinga et al. (1966) and that of Harloff (1927) is that they suggest the flux of Al to the crystal interface regulates the compositional pattern of the zoning

rather than the relative diffusion rates of Ca and Na.

The use of the diffusion theory to explain the oscillatory zoning in the Yeoval plagioclases presents at least one possible problem. This is the occurrence of both normal oscillatory, reverse and "patchy" zoning in crystals only 2-3 mms. apart, or rarely, in the one crystal (Plate 8, Fig. 22). Another is the fairly constant composition (An_{40}) of the outermost portions of the crystals, particularly those which have been corroded. The changes may be associated with an increase in water pressure in the magma, followed by explosive eruption (e,g, see Ewart 1965). If such repeated eruptions took place to form the oscillatory zoning in the Yeoval plagioclases, then one would expect to observe unusual features in other mineral phases. The fact that the biotites and hornblendes from different samples are of similar composition and are not zoned would tend to discount such a theory. It is also difficult to see how such a theory can explain the very fine oscillatory zoning of plagioclase.

It would appear that the oscillatory zoning in the plagioclase from the Yeoval diorites can best be explained by the diffusion-supersaturation theory.

7.3 RELATION OF ORTHOCLASE DIORITES TO OTHER VARIETIES OF DIORITE

The evidence available - field, petrographic, chemical and isotopic - indicates that the orthoclase diorites and other diorites are cogenetic. A summary of these properties include:

(i) the absence of any field contact between the orthoclase diorites and pyroxene and quartz-mica diorites.

(ii) the petrography of the diorites; for example, there is an increase in the amount of potassium feldspar at the expense of plagioclase and femic minerals.

(iii) the silica-variation diagrams given in previous sections (for major and trace elements) strongly suggest that the orthoclase diorites are the end product of the differentiation of the parent dioritic magma.

(iv) the sharp break in the silica-variation diagrams in the 65-75% SiO_2 range and other data, indicates that the orthoclase diorites bear no relation to the granites.

(v) the similar strontium isotope data and fact that the orthoclase diorites plot exactly on the main diorite isochron suggests a close genetic relationship between these rock types.

(vi) Similarity in the composition of the hornblendes and biotites, except for a decrease in the Mg/Fe ratios in the orthoclase diorites.

Fig.44 Compositions of granites from the Yeoval district containing more than 80% normative SiO_2, Ab and Or plotted in terms of these constituents. The projected quartz-alkali feldspar field boundaries and the minima on these boundaries in the system $NaAlSi_3O_8$-$KAlSi_3O_8$-SiO_2-H_2O (Tuttle & Bowen, 1958) are also shown.

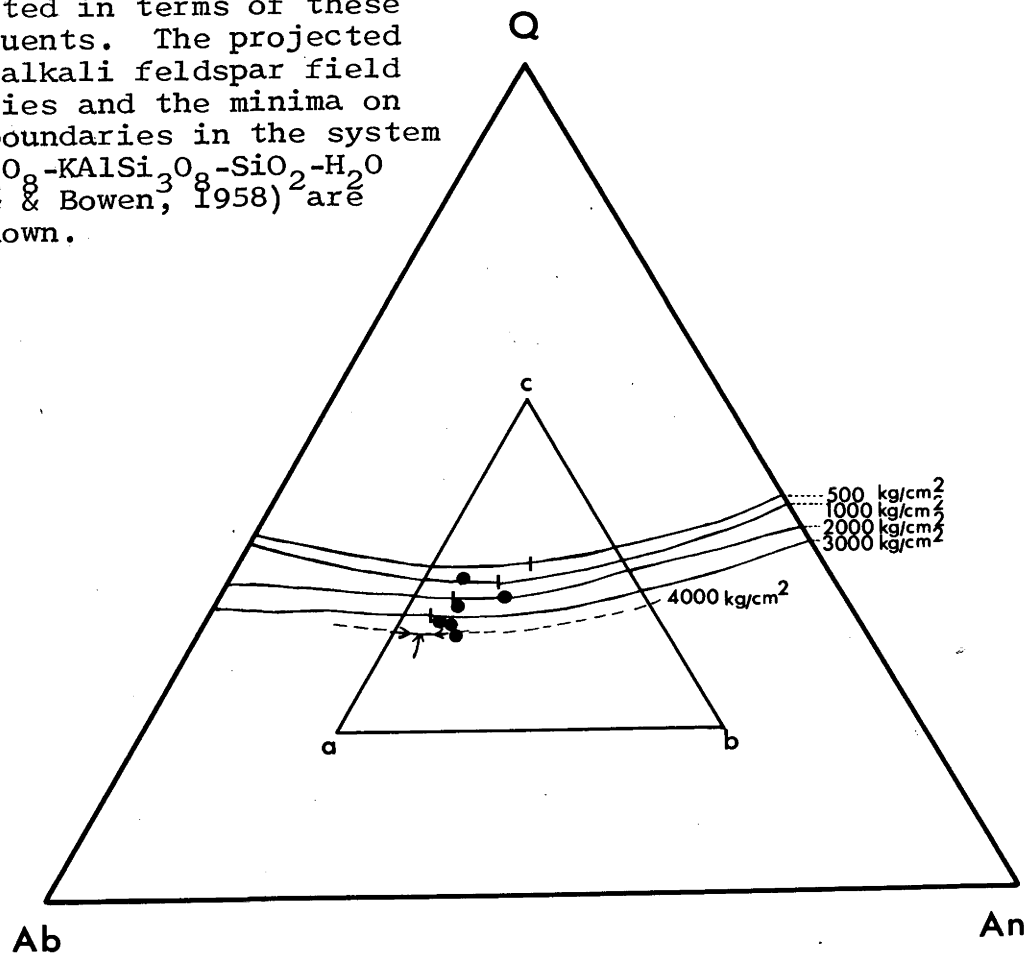

The formation of these rocks may be intimately connected with the accumulation of the gabbro and pyroxenite, and it is again pertinent to mention the closeness in the field of these two rock types. Orthoclase diorites outcrop fairly close to the basic types and are not found in any other area to the south.

7.4 THE PROBLEM OF THE YEOVAL GRANITES

The relative proportions of normative quartz, albite and orthoclase for the Yeoval granites are plotted in Fig. 44. The positions of the quartz-feldspar field boundaries and the "ternary" minima at 500, 1000, 2000, 3000 and 4000 Kg/cm^2 (Tuttle and Bowen, 1958, p. 75, Fig. 38) in the system $NaAlSi_3O_8$ - $KAlSi_3O_8$ - SiO_2 - H_2O are also indicated in the projection. The triangle 'abc' in Fig. 44 is the field of granites (or rhyolites) according to the classification of Tuttle and Bowen (1958, p. 12, Fig. 63). Although the Yeoval granites give a scatter of points, they apparently formed under equilibrium water vapour pressures greater than 2000 Kg/cm^2. This contrasts with Tuttle and Bowen's maxima (p. 79, Fig 42) on the contour diagram for the analysed plutonic rocks in Washington's Tables, which they suggest have crystallised under essentially dry conditions. That the Yeoval granites crystallised under conditions of fairly high water pressures is also suggested by their position on the contour diagram of the distribution of normative albite orthoclase and anothite in all the analysed rocks in Washington's Tables that carry 80% or more normative

Ab + Or + Q (Tuttle and Bowen 1958, p. 136, Fig. 67).

Tuttle and Bowen (1958, p. 129) further classify granites that have a composition in or near Bowen's (1937) "petrogeny's residua system", on the basis of the distribution of the sodium feldspar component between the phases,plagioclase and potassium feldspar. They divide granites into two broad groups:

I. hypersolvus granites characterised by the absence of plagioclase except as a component of perthite.

II. subsolvus granites characterised by both potassium feldspar and plagioclase. This group is still further subdivided into three groups according to the sodium content of the potassium feldspar: the one of interest for the Yeoval rocks is that in which the albite content is greater than 30 per cent by weight.

In the Yeoval rocks, both types are present. There are hypersolvus granites containing only one feldspar (potassium feldspar or perthite) and these are identical in appearance to the hypersolvus granite illustrated in Tuttle and Bowen (1958, Plate 6, Fig. 1). In other Yeoval granites potassium feldspar (perthite) is accompanied by separate crystals of plagioclase. The potassium feldspar contains greater than 30% of the albite component (See Table 29). Support for the postulate that there are two types of granite according to Tuttle and Bowen's classification comes from the observation

that all of the granites regardless of type have approximately the same Na_2O/K_2O ratio of about 1.1, so it is impossible for both plagioclase-bearing and plagioclase-free types to be hypersolvus granites in which one contains some early liquidus-phase plagioclases. An apparent anomaly however is that the potassium feldspars separated from each type are more or less identical in composition. Since the feldspars are very perthitic it is possible that these analyses are an unreliable estimate of the original feldspar compositions: more of the albitic feldspar of the perthite has obviously been separated from potassium feldspar of the hypersolvus granites.

If a correlation with Tuttle and Bowen's (1958, p. 129) data is permissible then the Yeoval granites "can be considered high-temperature rocks (and therefore undoubtedly owe their origin to magmatic processes)".

Kleeman (1965) has suggested that there are two groups of granites falling in the low temperature trough of the $Or-Ab-An-SiO_2$ system. Firstly, those that formed in orogenic areas by melting or partial melting of sedimentary rocks; and secondly, those formed by the differentiation of basic magmas which have assimilated siliceous sedimentary material.

The production of the Yeoval granites by partial melting of geosynclinal-type sedimentary material cannot account for the low initial Sr^{87}/Sr^{86} ratio of 0.703. This would also

preclude the second hypothesis of contamination of a basaltic magma if it is assumed that the basaltic material had an initial Sr^{87}/Sr^{86} of 0.703 to 0.705 corresponding to that of modern basalt magmas in oceanic regions (Gast 1960; Faure and Hurley 1963).

The Yeoval granites are similar in major element abundances to the "Snowy Mountains leucogranites" which are commonly found associated with the batholiths of eastern Australia, particularly those in southern N.S.W. and north eastern Victoria (Kolbe and Taylor 1966; Taylor, Ewart and Capp 1968). These authors point out, however, that certain trace elements are abnormal in their "leucogranites" compared with rhyolites of similar major element chemistry. They considered these abnormalities (e.g. low K/Rb, Ba/Rb, high Th and U) to be due to fractional crystallisation of granodiorite magma. To account for the difference in the trace element chemistry they suggest a partial melting mechanism for the formation of the magmas with "normal" trace element abundances. The presence of fluorite, epidote and tourmaline, often in vughs, in the Yeoval granite indicates that this magma has not entirely lost a late volatile phase which was considered by Taylor et al. (1968) as a possible cause of minor element differences between rhyolites and Snowy Mountains leucogranites.

The normal trace element chemistry and low initial Sr^{87}/Sr^{86} ratio of the Yeoval granites precludes any theory of

origin by refusion of crustal-type material or by fractional crystallisation. These data may be explained by the partial melting of low Rb material such as a rock of basaltic or andesitic composition.

The two mechanisms for the production of dioritic magma cited in the previous section may also give rise to granites; i.e. either dry partial melting of quartz eclogite at 100-150 kms depth (Green and Ringwood, 1966) or, wet partial melting of basic material at depths of 30-40 kms (with $P_{H2O} < P_{LOAD}$) (Green 1967). The experimental data of Green (1967) indicates that the first mechanism of dry partial melting of quartz eclogite (leaving a residuum of garnet and pyroxene) cannot produce liquids of SiO_2 content greater than 70%. Although only limited data are available, it is quite feasible that the second mechanism is operative, whereby the fractional melting under wet conditions at depths of 30-40 kms of basaltic (or andesitic) material results in a residue of subsilicic amphibole and pyroxene, giving rise to rhyolitic (or granitic) liquids. The basic xenoliths found in some granites could represent fragments of this residual material brought up by the granite magma.

In summary, it may be stated that there is no evidence for a genetic relationship between the diorites and granites and a mechanism of wet partial melting of basaltic or andesitic material near the base of the crust or upper mantle can best explain the origin of the granites.

TABLE 48

Comparison of Yeoval Diorite with other similar rock types

	Average Yeoval Diorite	Average High Pot. Andesite	Average Andesite	Benmorite	Tristanite	Average Shoshonite	Average Crust
SiO_2	59.1	59.8	59.5	57.1	56.9	53.58	60.3
TiO_2	0.6	0.79	0.7	1.82	1.83	1.13	1.0
Al_2O_3	16.6	16.7	17.2	16.9	19.3	17.21	15.6
ΣFeO	7.5	5.81	6.10	9.01	5.55	11.85	7.2
MgO	3.9	2.70	3.42	1.11	2.08	3.67	3.9
CaO	7.8	5.98	7.03	3.31	4.60	7.44	5.8
Na_2O	3.9	3.85	3.68	6.43	5.26	3.64	3.2
K_2O	2.9	3.00	1.60	3.96	4.16	3.55	2.5
Rb	76	70	31				85
Ba	622	510	270				425
K+	2.42	2.45	1.33				2.03
Sr	472	380	385				375
K/Rb	317	350	430				240
Ba/Rb	8.2	7.3	8.7				5.0
Rb/Sr	0.16	0.18	0.08				0.23
Y^{3+}	23	22	21				33
Th^{4+}	8.4	6.8	2.2				9.6
U^{4+}	2.0	1.9	0.69				2.7
Zr^{4+}	108	170	110				145
Nb^{5+}	4	4	4.3				20
		Taylor, pers. comm. Ewart and Stipp 1967	Taylor 1967	Tilley and Muir 1964	Tilley and Muir 1964	Joplin 1965	Taylor 1967

7.5 COMPARISON OF THE YEOVAL DIORITES WITH OTHER RELATED ROCKS

The high potassium diorites are not related to any of the fine-grained high potassium rocks such as benmorites or tristanites which are both alkaline associates (Tilley and Muir 1964) and so must be grouped with the calc-alkaline rocks. They are somewhat related in chemical composition to the shoshonites (Joplin 1965), although these apparently have even higher K, P, Sr and Ba contents. High potassium diorites have been reported from the Snowy Mountains, N.S.W. (Joplin 1958) and high potassium andesites from the San Francisco Peaks (Robinson 1913), New Zealand (Ewart and Stipp 1967), Bougainville (Taylor and Blake, in preparation). Typical chemical analyses of andesites, benmorites, tristanites, and shoshonites are compared with the average Yeoval diorite in Table 48. A weighted average for the Yeoval diorites has been calculated on the basis of the surface area of each variety.

The most notable feature of the data in this table and Table 37 is the similarity of the Yeoval diorite and high potassium andesites. A similarity exists in the major element chemistry of the Yeoval diorite and average andesite but the difference in potassium effects the trace element chemistry particularly for elements such as Rb, U, Th, Ba, etc. Thus from the limited data available so far, there is apparently a

transition from very low to high potassium diorites and andesites, e.g. in the Saipan Islands are andesites with potash contents of 0.7% in contrast to those in Bougainville with 3.6% K_2O (Taylor, pers. comm.); and in the Snowy Mountains, N.S.W., are diorites of both low (J. Worden, pers. comm.) and high potassium contents (Joplin 1958). The Yeoval diorites fit into the high potassium category.

The average Yeoval diorite is very similar to the crustal average (Taylor 1967) for Si, Fe, Mg and K. With regard to trace elements, Rb and Th are a little lower, while the K/Rb, Th/K and U/K follow closely the average crustal composition. Al, Ca, Ba and Sr are present in greater concentrations in the diorites.

APPENDICES

APPENDIX I - ANALYTICAL PROCEDURES

1. SAMPLE PREPARATION

Rock samples were reduced to hand-specimen size using a rock splitter with hardened steel jaws. This material was crushed in a large, and then smaller, jaw crusher. The sample was quartered; one part being crushed in an agate cone grinder and finally ground in a mechanical agate mortar to pass 150-mesh silk bolting cloth, another part was reduced in a pulveriser for gamma-ray measurements, and another part crushed to various sizes in the pulveriser for mineral separation.

A check for Fe and Mn contamination from the hardened Mn-steel jaw crushers produced negative results. Eight samples were hand-crushed in a porcelain mortar and prepared in the usual way for XRF analysis. Duplicate runs for each sample showed no significant difference from those crushed in the jaw crushers.

2. X-RAY FLUORESCENCE SPECTROGRAPHY

The procedures for determinations of major and trace elements are discussed in detail by Norrish and Chappell (1966).

3. ELECTRON PROBE

The procedure for analysing rocks by the electron probe is given in Appendix III.

For mineral analyses, both grain mounts (in brass holders and also mounted in epoxy-resin) and polished thin sections were used; the latter particularly for checking zoning in minerals (e.g. plagioclase). The samples were coated with a

thin layer (100-200 A°) of carbon and analysed on an ARL probe (model EMX).

The accelerating voltage used throughout the work (except for Zr and Hf) was 10KV with a specimen current of 0.05 to 0.06 μA. Beam size was of the order of <1-10 μ. Because of the use of natural standards very close to the compositionsof the minerals being analysed, the only corrections applied to the data were beam stability (instrument drift), as monitored by varying specimen current measured on the standards during an analytical run ,and background (measured on each side of the peak).

Zircons - Wavelength interference was not a problem for the general run of the elements. However, for the determination of Zr and Hf in zircon there is the concern of interference of Hf Kα by 2nd order Zr Kα. Although a problem in XRF analysis, investigations using pure Zr and Hf metal standards showed no interference of Hf by Zr on the probe. For the Zr and Hf analyses, natural zircons and pure Zr and Hf metals were used as standards.

Olivine and pyroxene - for these analyses, natural minerals and glasses prepared by T.H. Green and D.H. Green were used as standards.

Amphiboles - Natural hornblendes, analysed by E. Kiss, from the Yeoval diorite and other rocks were used as standards for probe analysis. At least 10-15 crystals from each grain mount (and/or

polished thin section) were analysed in order to achieve a statistical basis for the data. This is necessary (also for the biotites) because of the heterogeneities from grain to grain (see Table 16) which are not so marked with the pyroxenes and olivines.

Biotites - The biotites were analysed for Si, Ti, Al, total Fe, Mn, Mg, and Ca with the electron probe using natural standards (except for Ca), kindly donated by Dr B.W. Chappell. Iron determinations were carried out by E. Kiss and alkalis by the author by flame photometry. The alkalis were checked in some samples using the electron probe. Phosphorous contents differ markedly from 0.009% to 0.137% reflecting the varying number of apatite inclusions in the biotite. No corrections need be applied to the calcium and phosphorous results as suggested by Chappell (1966) because of the technique and standards used for the analyses.

Plagioclase Feldspars - Natural albite and bytownite, and alkali glasses prepared by T.H. Green were used as standards for the plagioclase analysis.

Zoned and unzoned crystals in polished thin sections were traversed using a beam of 1-5 micron diameter and analysed for Ca, Na and K. No volatilisation of Ca or K was apparent but minor loss of Na was observed. This accounts for the variation of Na content in zones with the same Ca contents.

APPENDIX II

COMPARISON OF RUBIDIUM AND STRONTIUM RESULTS OBTAINED BY X-RAY FLUORESCENCE SPECTROGRAPHY AND ISOTOPE DILUTION.

A comparison of values of Rb and Sr are listed in Table 49

For total rock samples, a comparison of Rb results shows good agreement between XRF and I.D. Strontium values, particularly at greater concentrations (i.e. > 400 ppm), are fairly similar but there is no obvious trend (i.e. either high or low XRF values compared with I.D.

The difference between XRF and I.D. results for minerals for most samples is due to a sampling error, in that samples used for I.D. are the coarsest possible, whereas for XRF determinations, crushed powders (-150 mesh) are used. However, where crushed mineral samples have been checked by I.D., fairly consistent, although slightly lower, results are obtained. Such samples are denoted by an asterisk in Table 49.

TABLE 49

Comparison of Rubidium and Strontium Results Obtained by X-Ray Fluorescence Spectrography and Isotope Dilution

Rock or Mineral	Rb		Sr	
	XRF	ID	XRF	ID
G117 TR	83	83	514	510
G113 TR	6	7	244	246
G134A TR	38	38	486	490
G134B TR	22	22	558	566
G140 TR	65	65	572	586
Y205 TR	123	119	404	403
Y206 TR	116	103	413	396
Y64 TR	129	125	32	31
R77 TR	102	97	32	33
Y53 TR	165	159	34	34
Y147B TR	105	109	83	85
Y8 TR	32	31	390	394
G120 TR	95	95	316	320
Y235 TR	89	92	478	512
Y41 TR	109	106	507	499
G120 K-F*	237	245	470	497
Y235 K-F	260	269	443	503
Y41 K-F*	317	325	525	509
Y41 Plag.*	45	45	801	867
Y8 Biot.	316	324	10	15
G120 Biot.	517	554	8	7
Y235 Biot.	344	358	40	64
Y41 Biot.*	436	444	20	23

*crushed mineral sample analysed by XRF & I.D.

APPENDIX III - ROCK ANALYSES USING THE ELECTRON PROBE

INTRODUCTION

Recent years have seen a wide diversity of applications for the electron microprobe in the field of earth sciences, the most important of these being in the fine-scale investigation of mineral phases. However, very few publications are available dealing with the bulk analysis of heterogeneous systems. In an abstract, discussed by KEIL (1967), ARRHENIUS et al. (1964) described the analysis of rocks using a 'pressed powder' and 'fused droplet' technique. In the first method, rock powder of less than 10 μ grain size is pressed into a pellet, the flat surface of which may be coated with carbon and then analysed. In the second method, the powder is fused with an equal amount of borate, reground, and then refused. From this melt, spherules of sample may be obtained on a platinum wire loop welded to a tungsten wire. In the present work an attempt was made, using the electron microprobe, to analyse total rocks which had been melted to form a glass disc and to compare these results with those obtained by chemical and x-ray spectrographic means.

ANALYTICAL TECHNIQUE

SAMPLE PREPARATION - The glass discs are prepared by a 'borate bead' method virtually identical to that described by NORRISH AND CHAPPELL (1967) for the preparation of samples for XRF analysis, so that the same buttons prepared for probe analysis may also be used for XRF analysis. A sample of the crushed rock powder (-150 mesh) weighing 0.14 g is mixed with 0.75 g of

borate mix (for preparation see NORRISH AND CHAPPELL (1967)) and 0.02 g of ammonium nitrate and fused at approximately 1000°C for several minutes in a gold-lined platinum crucible. The ammonium nitrate was used in preference to sodium nitrate to maintain oxidising conditions during melting and as sodium analyses were required. The melt, after thorough mixing, is poured onto a graphite disc (15/16 inch diameter) over which has been placed a brass ring and pressed into a disc using a graphite plunger. (The graphite disc and plunger are kept on a hot plate at about 230°C.) The plunger is withdrawn and the brass ring removed. The glass disc is placed between two asbestos mats on another hot plate at about 200°C and after several minutes the mats are removed from the hot plate to allow the disc to cool slowly. After cooling any projecting edges are removed by rubbing with a file and the disc placed in a 2 inch by 2 inch envelope.

The glass discs are then coated with a conducting medium (usually carbon) and are stored in a desiccator since they tend to be hygroscopic. If the glass surface does lose its lustre through moisture absorbance, or if it is not perfectly smooth and flat, a gentle polishing with 1/4 μ diameter paste will produce a suitable surface for analysis.

It is worth noting that care needs to be taken with weighing of small samples and in the cleaning of the platinum crucible after each sample preparation.

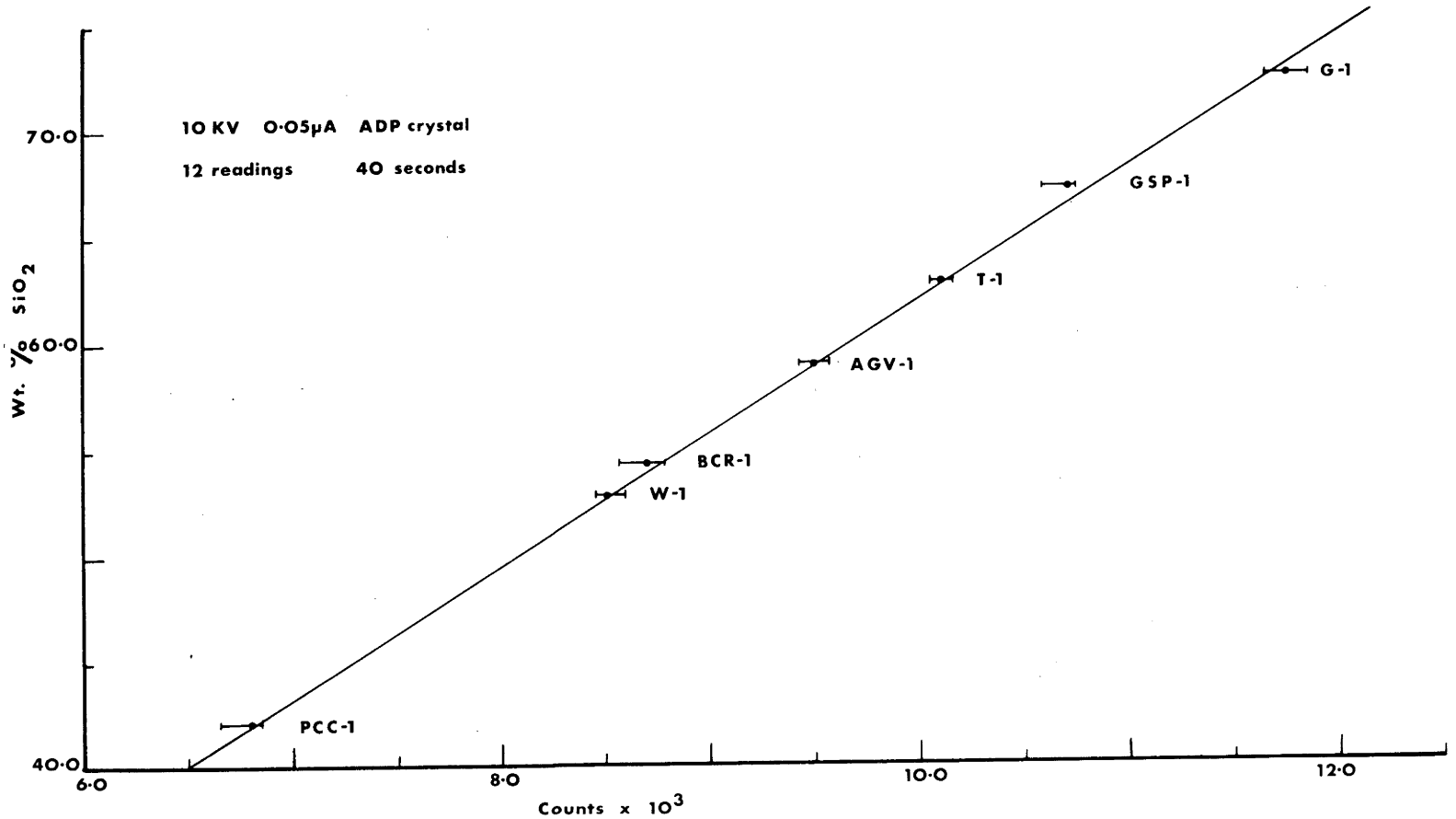

Fig.45 SiO_2 calibration plot for standard rocks.

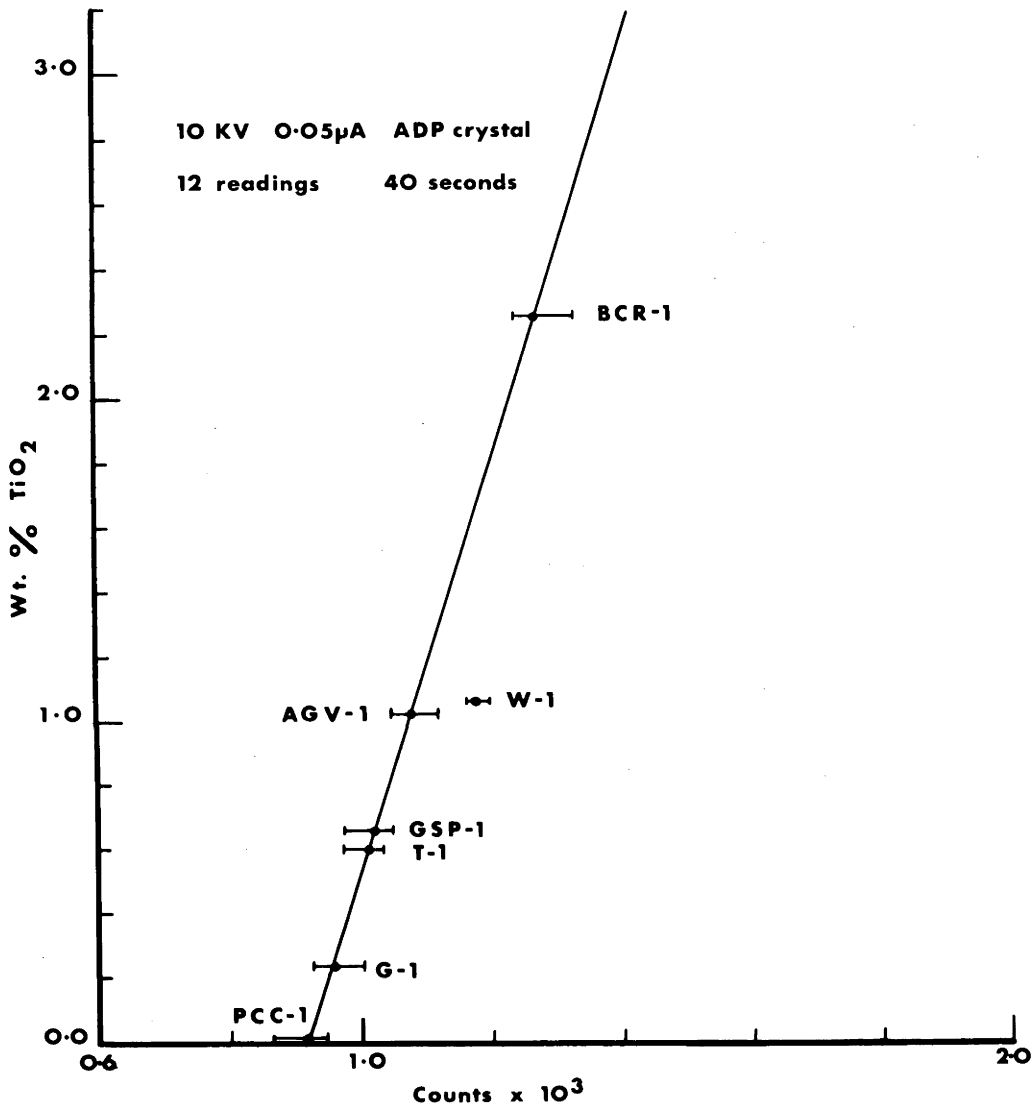

Fig.46 TiO_2 calibration plot for standard rocks.

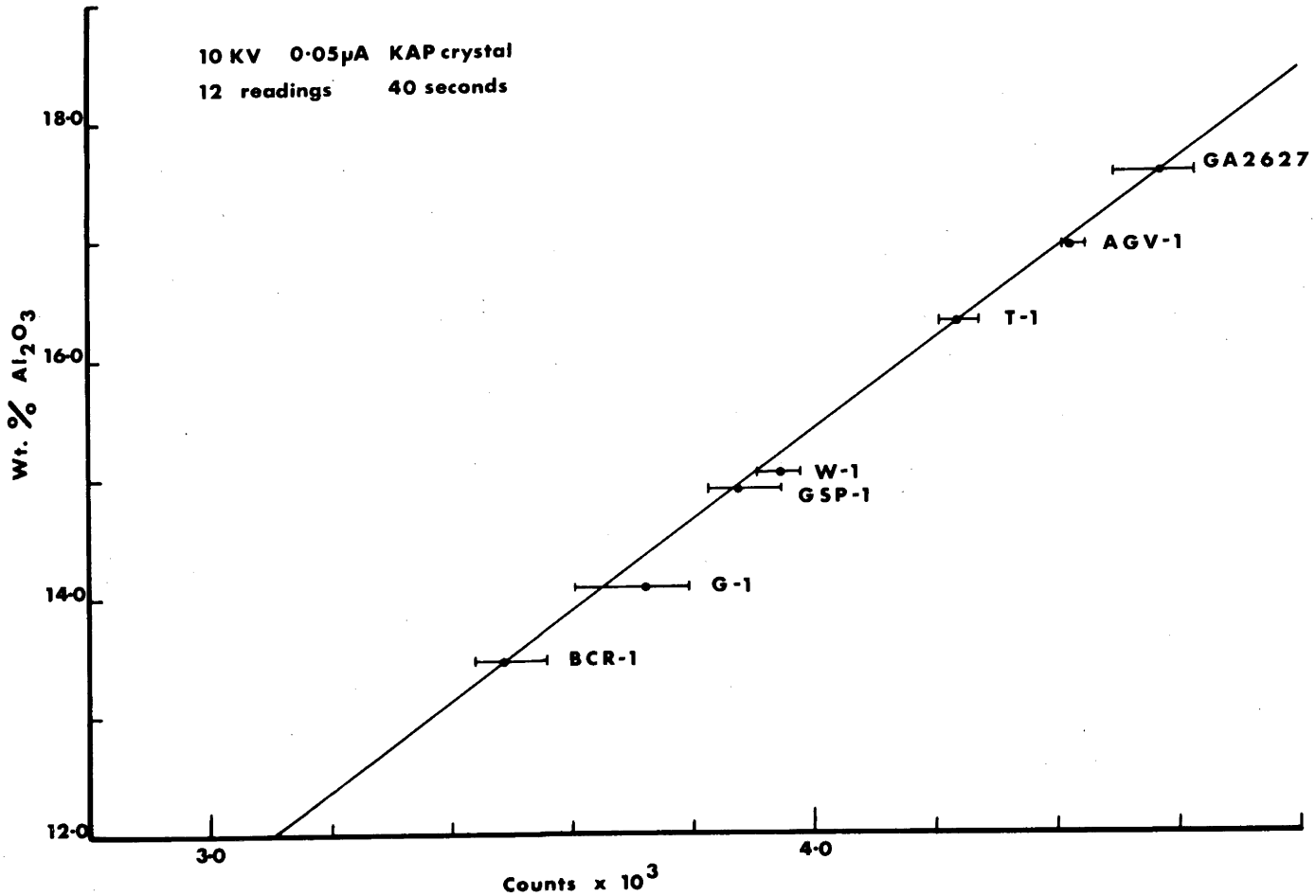

Fig.47 Al_2O_3 calibration plot for standard rocks.

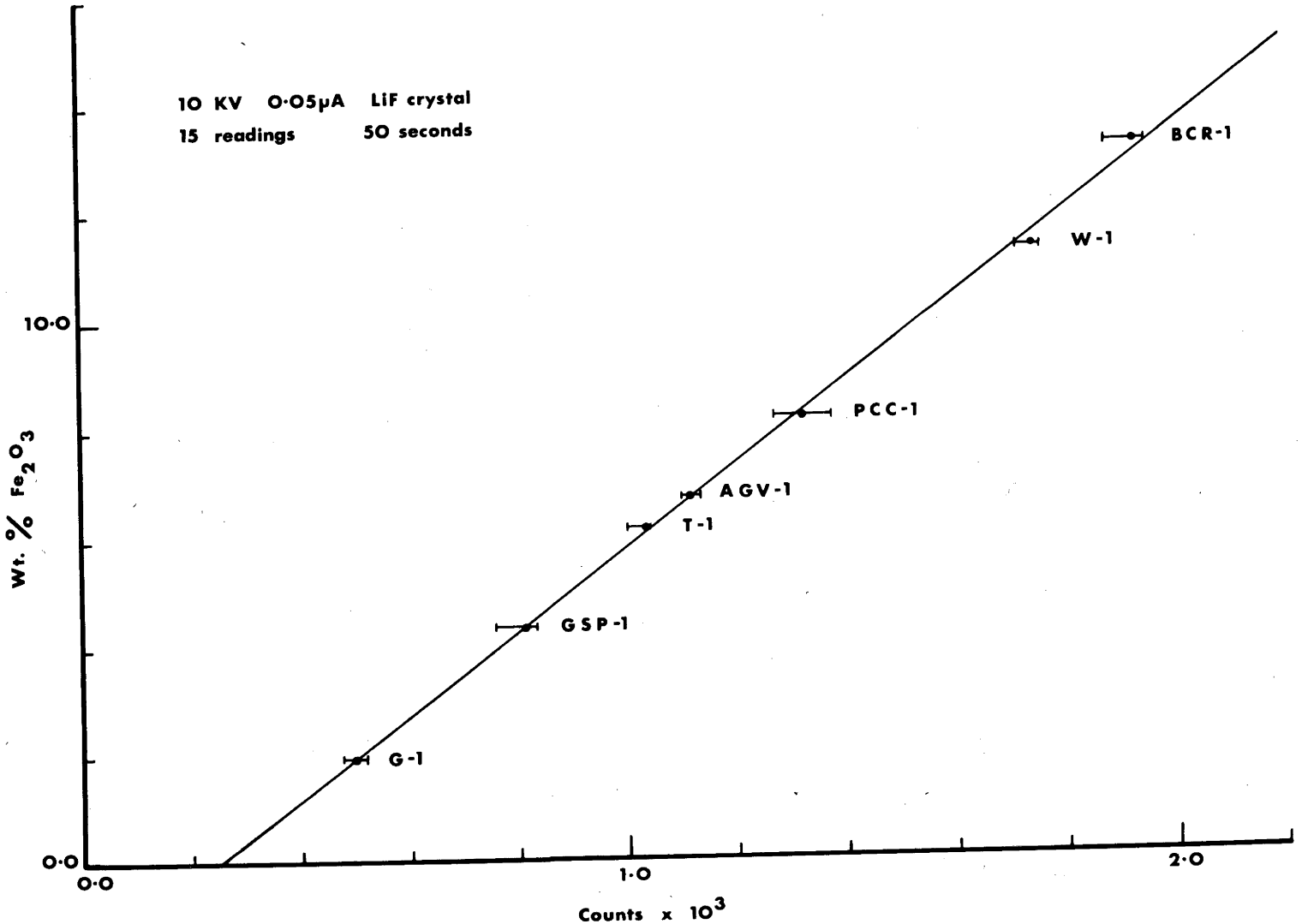

Fig.48 Fe_2O_3 calibration plot for standard rocks.

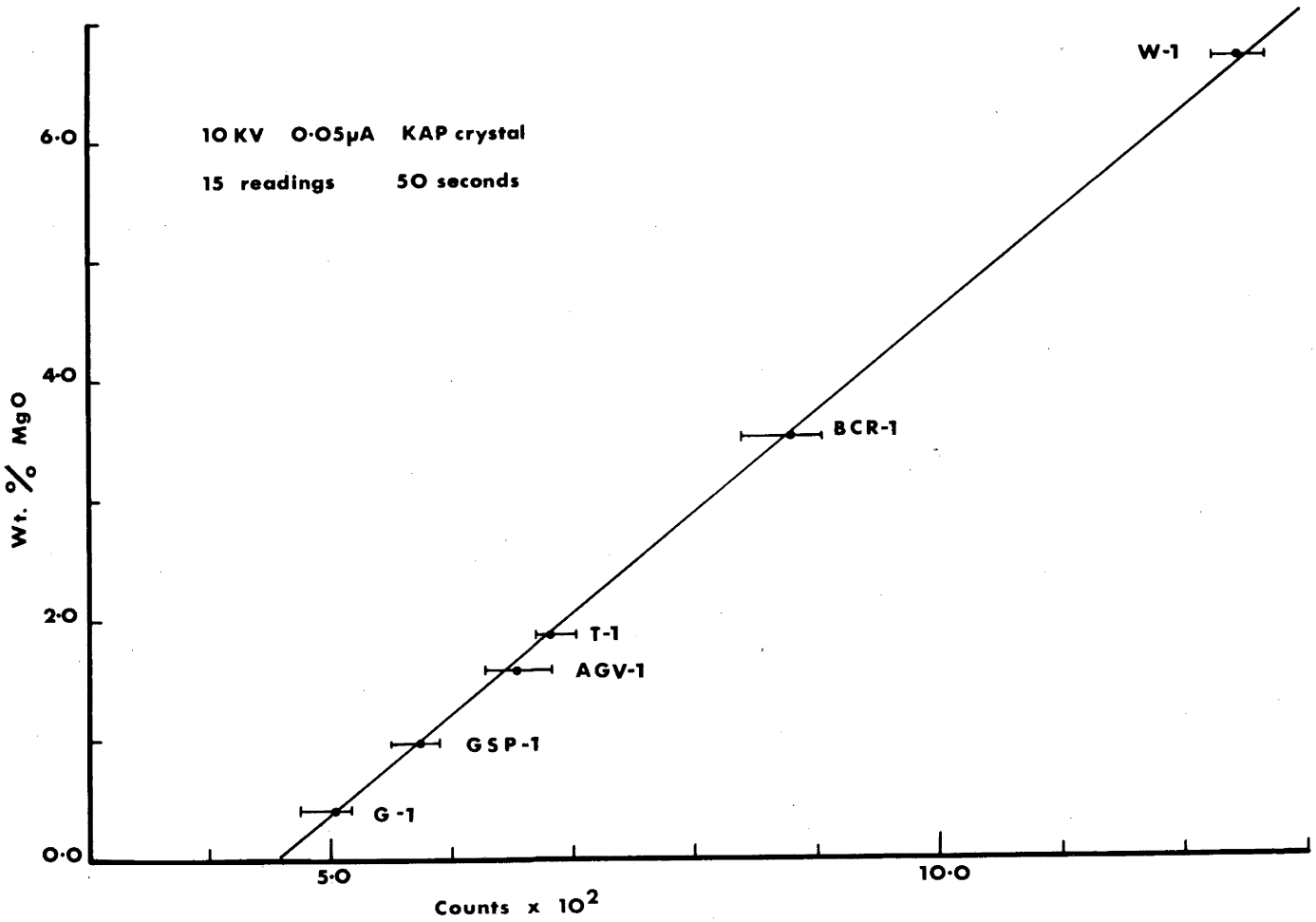

Fig.49 MgO calibration plot for standard rocks.

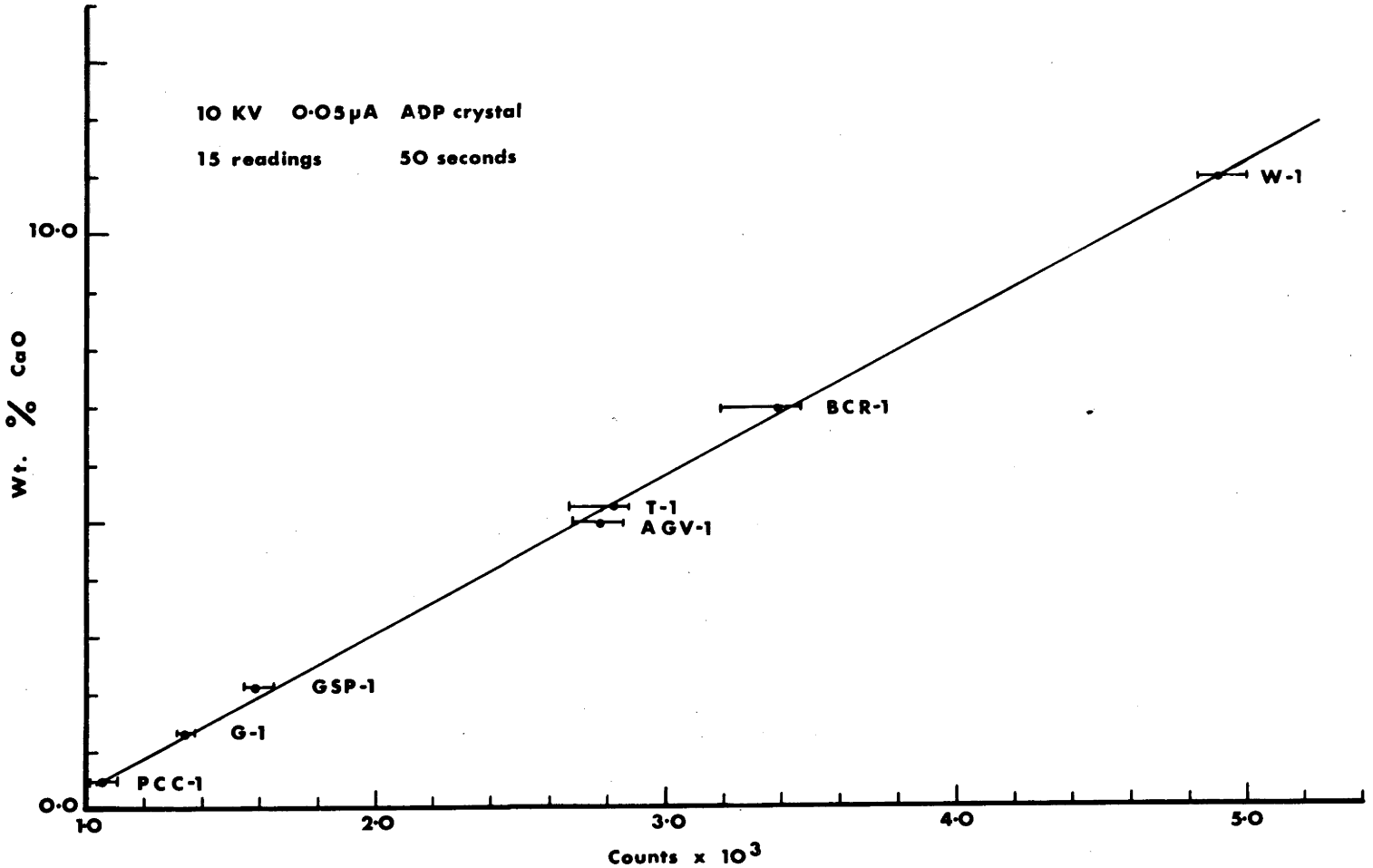

Fig.50 CaO calibration plot for standard rocks.

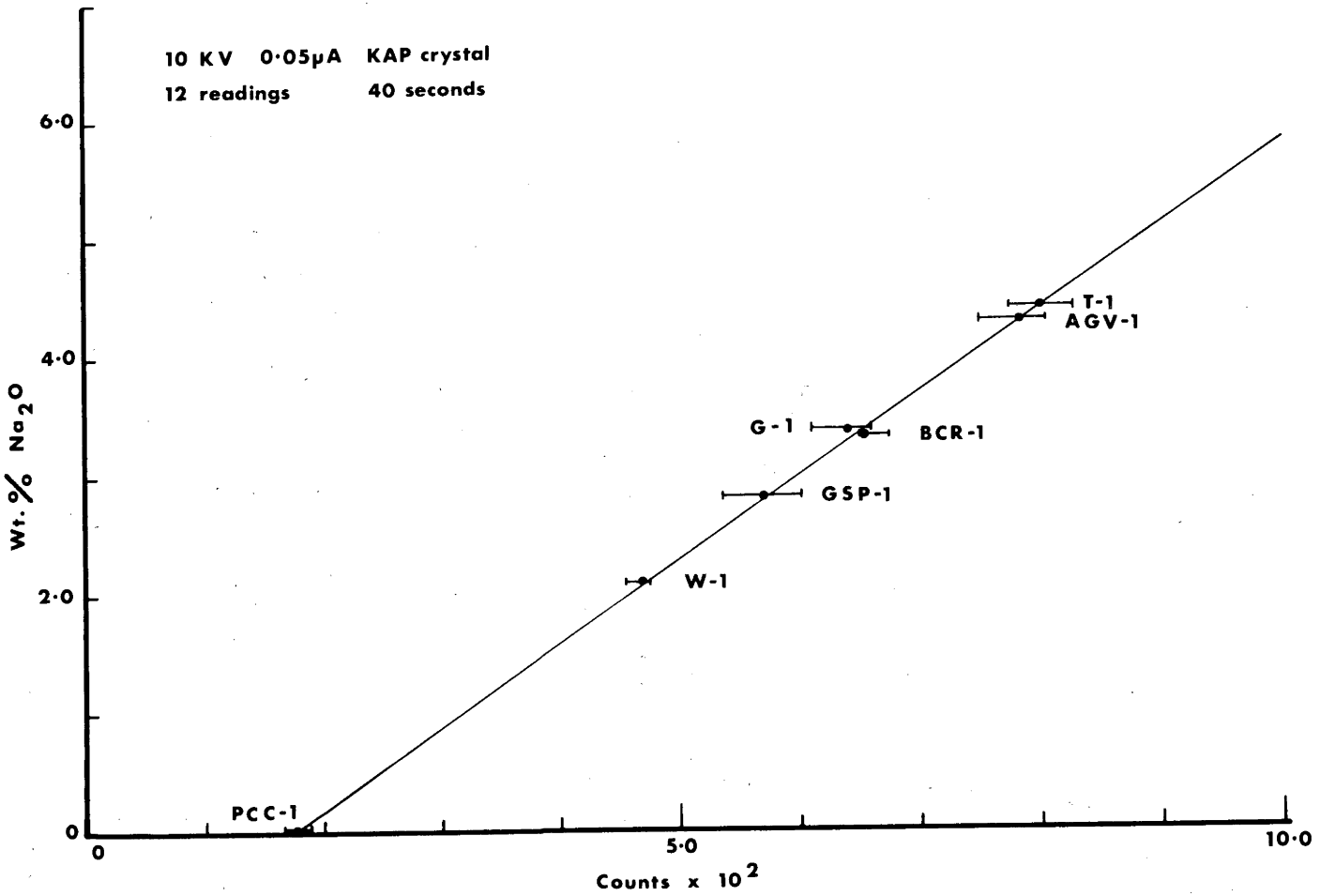

Fig.51 Na_2O calibration plot for standard rocks.

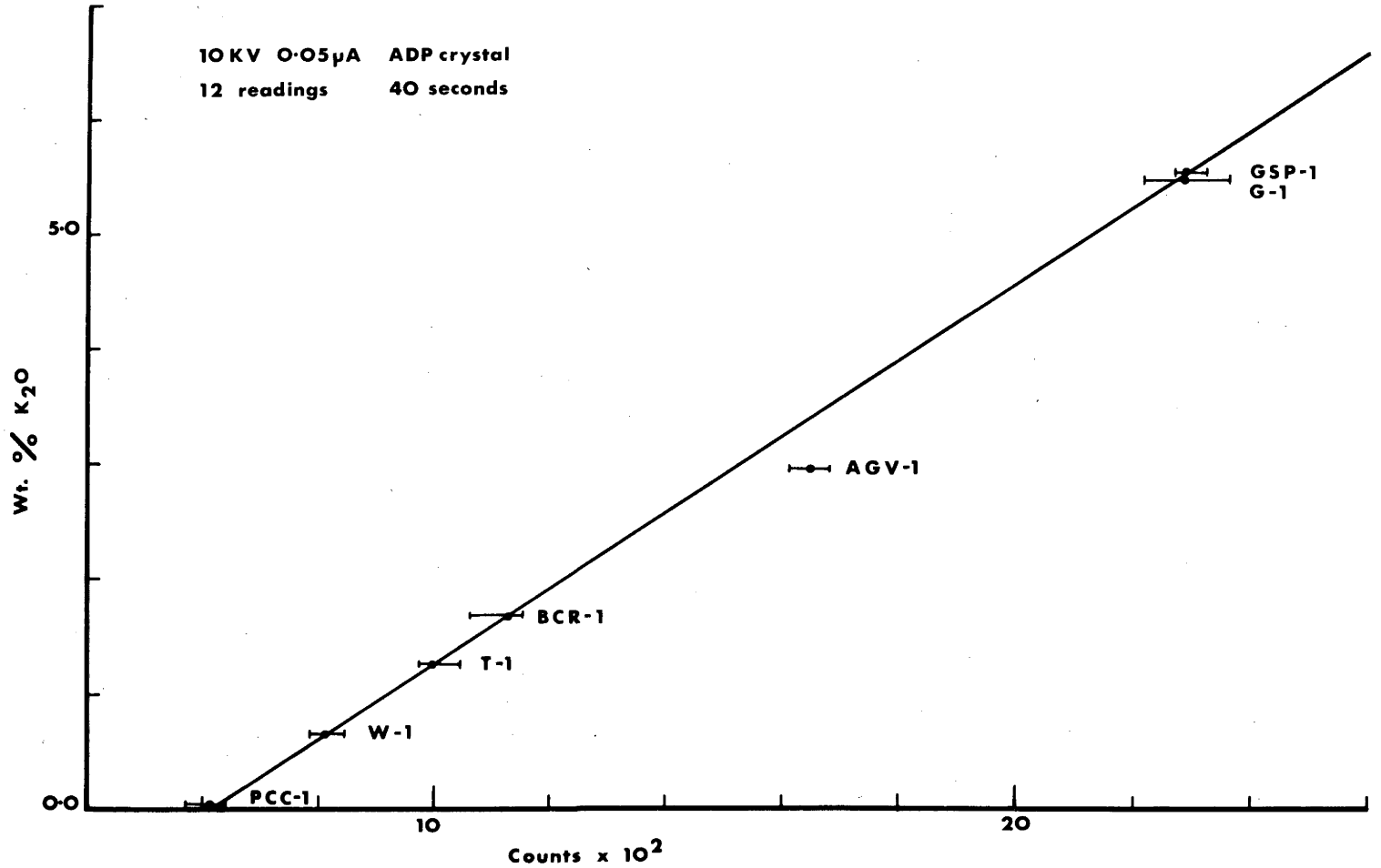

Fig.52 K_2O calibration plot for standard rocks.

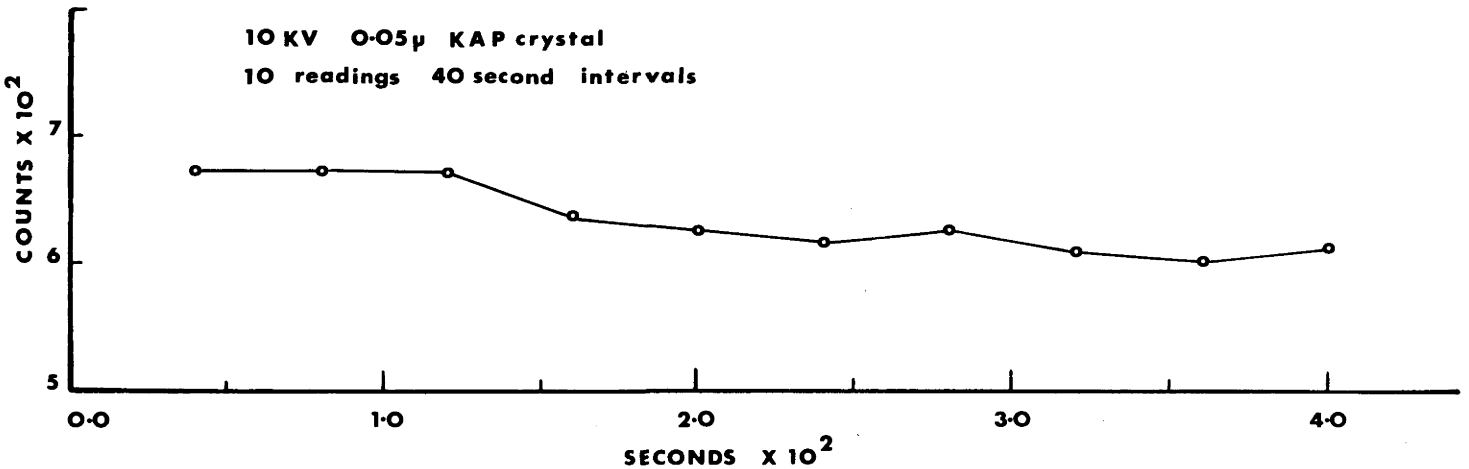

Fig.53 Rate of volatilisation of sodium from the glasses.

ANALYTICAL CONDITIONS - The analyses were carried out on an ARL electron microprobe according to the conditions indicated in the upper left hand corner of the calibration curves (Fig. 45, etc) Elements determined were: Si, Al, Fe, Ca, Mg, Na, K and Ti. Due to low abundance levels and the 1:7 dilution of the samples by the borate mix it was not possible to analyse for Mn and P.

To reduce specimen damage and the effect of any possible sample inhomogeneity, a beam diameter of approximately 50 microns was used and the specimen was continuously moved under the beam at a rate of 96 μ per minute. In addition, the beam was continuously deflected at a rate of 100 c/s over a length of 240 μ thus delineating a rectangle. Using these conditions no sample damage was apparent. To check the homogeneity of the glass discs, complete traverses weremade across the bead in a number of positions. No variations in the concentration of any elements were observed outside normal counting statistics so that fragments of glass may be used if the discs shatter on cooling.

In a study of the volatilisation of socium and potassium in the glass, the electron beam was directed onto the surface where 10 readings were taken at 40 second intervals. No change was observed in the potassium x-ray output but there appeared to be volatilisation of sodium as indicated by the decrease in counts illustrated in Fig. 53. However, volatilisation is not instantaneous (i.e. it does not appear to affect the disc until approximately 2 minutes have lapsed) and since the sample is

TABLE 5Ø

Standard Deviations and Coefficients of Variation for the Standard Rocks

	Standard Deviation (Counts)			Coefficient of Variation (%)			Standard Deviation (Counts)		Coefficient of Variation %		Standard Deviation (Counts)			Coefficient of Variation (%)		
	Fe_2O_3	SiO_2	Al_2O_3	Fe_2O_3	SiO_2	Al_2O_3	CaO	MgO	CaO	Mgo	TiO_2	K_2O	Na_2O	TiO_2	K_2O	Na_2O
G-1	16	80	71	3.1	0.7	1.9	30	14	2.3	2.9	40	98	22	3.0	4.2	3.5
GSP-1	25	48	47	3.3	0.4	1.2	34	8	2.1	1.4	15	19	26	1.5	0.8	5.3
T-1	33	26	30	3.6	0.3	0.7	40	16	1.4	2.3	29	37	28	3.0	3.7	3.8
AGV-1	21	39	12	2.0	0.4	0.3	39	20	1.4	3.0	11	32	25	1.0	1.9	3.2
BCR-1 A	43	85	54	2.7	1.0	1.6	45	43	1.3	4.9	21	44	13	1.8	4.0	2.0
B	42	85	57	2.7	1.0	1.7										
W-1	27	37	37	1.8	0.4	0.9	86	28	1.8	2.2	12	28	10	1.0	3.5	2.1
PCC-1	7	73	21	0.6	1.1	3.8	19	100	1.8	1.8	39	26	11	3.4	3.9	6.0

continuously scanned relative to the beam this effect may be disregarded.

CALIBRATION CURVES - Calibration curves based on the U.S.G.S. standard rocks G-1, W-1, GSP-1 (38/20), AGV-1 (28/12), BCR-1 (44/20) and PCC-1 (71/4) and the standard tonalite T-1 were drawn up using the abundance values of FLEISCHER (1965), THOMAS AND KEMPE (1963), FLANNAGAN (1967), NORRISH AND HUTTON (pers. comm.) and KISS (pers. comm.). A high alumina eclogite (GA2627) analysed by E. KISS (pers. comm.) extended the range of values for Al_2O_3. As initial microprobe analyses for Al_2O_3 were significantly different from the previously reported value for GSP-1 (FLANNAGAN (1967)), further determinations were made by KISS (pers. comm.) using a new method involving DCTA titration which gave an Al_2O_3 content of 14.85%. This lower value is in good agreement with XRF analyses of 14.86% by NORRISH (pers. comm.). Each standard (and sample) was run in duplicate, at least, and the results averaged. Agreement between the duplicates was well within the limits of standard deviation indicated in Table 50. The only correction which needs to be applied to the observed x-ray counts is for beam stability (instrument drift) as monitored by varying specimen current measured on the standards during an analytical run. As the count rates are relatively low, no detector 'dead-time' corrections are required. Absorption and fluorescent corrections are negligible because of the dilution effect and also the presence of lanthanum oxide in the borate mix. As a result

TABLE 51

Linear Regression Analyses for Oxides of the Standard Rocks

		Correlation Coefficient
CaO	: $N = (370.0)P + 866 \pm 50$	0.9998
MgO	: $N = (120.4)P + 475 \pm 30$	0.999
Fe_2O_3	: $N = (128.2)P + 363 \pm 70$	0.998
SiO_2	: $N = (158.0)P + 192 \pm 130$	0.9993
Al_2O_3	: $N = (238.6)P + 357 \pm 50$	0.9998
TiO_2	: $N = (162.4)P + 942 \pm 100$	0.955
K_2O	: $N = (307.6)P + 630 \pm 100$	0.997
Na_2O	: $N = (145.2)P + 171 \pm 25$	0.9985

N = counts

P = % concentration

simple linear calibration plots are produced (see Fig. 45). A linear regression analysis calculated (by least squares) for each oxide gave a correlation coefficient better than 0.99 (Table 51).

The count rates are relatively low and an attempt was made to increase the x-ray output by:

(a) increasing the sample weight - although the count rate was almost doubled when the sample weight was doubled, difficulties arose in the sample digestion, and erratic results were obtained, possibly resulting from button inhomogeneity;

(b) increasing the specimen current and accelerating voltage - both were varied together and in different combinations resulting in considerable specimen damage and poor calibration curves.

The standard deviations and coefficients of variation were calculated for the standard rocks and are presented in Table 50. The standard deviation and coefficient of variation are given for two discs of BCR-1 for Fe_2O_3, SiO_2 and Al_2O_3 and it can be seen that there is good correlation. Similar conditions hold for other duplicates and these statistics also apply to the unknown rocks presented in Table 52.

RESULTS

Samples ranging in composition from basic gabbro through quartz mica diorite to granite were analysed using the electron microprobe, x-ray fluorescence spectrograph and chemical methods. The results are presented in Table 52 along with some K_2O results

TABLE 52

A Comparison of Electron Probe, Chemical and X-ray Spectrographic Results

	GABBRO (W3)			GABBRO (Y187)			QUARTZ MICA DIORITE (G107)			QUARTZ MICA DIORITE (Y161)			QUARTZ MICA DIORITE (Y227)		
	Probe	Chemical	XRF	Probe	Chemical	XRF	Probe	Chemical	XRF	Probe	Chemical	XRF	Probe	Chemical	XRF
SiO_2	45.3	45.83	44.91	47.0	-	45.74	57.7	56.40	56.30	58.6		57.73	58.5		58.82
Al_2O_3	17.2	17.62	17.69	13.6	-	13.55	16.8	16.72	16.73	16.2	16.27	16.41	16.9	16.88	16.94
Fe_2O_3	9.0	9.12	9.02	16.6	17.52	17.43	8.1	7.78	7.87	7.9	7.91	7.92	7.5	7.48	7.58
MgO	11.0	10.86	10.50	5.5	-	5.58	3.2	3.19	3.10	3.2		2.81	3.3		2.98
CaO	14.1	15.36	15.77	10.3	-	10.29	6.6	6.77	6.73	6.5		6.53	6.7		6.66
Na_2O	0.9	0.76	0.76[2]	2.8	3.33	3.33[2]	3.1	3.01	3.01[2]	3.2	2.90	2.90[2]	3.0	2.93	2.93[2]
K_2O	0.1	0.08	0.03(0.04)[1]	0.5	0.50	0.51(0.50)[1]	2.5	2.42	2.34(2.38)[1]	3.1	3.34	2.87	2.5		2.36(2.47)[1]
H_2O+CO_2[2]	1.0	1.00	1.00	1.2	1.17	1.17	1.8	1.80	1.80	2.2	2.24	2.24	1.7	1.72	1.72
TiO_2	0.2	0.22	0.21	3.3	-	3.36	0.7	0.68	0.63	0.5		0.47	0.5		0.54
P_2O_5[2]	0.01	0.007	0.01	0.1	0.084	0.08	0.2	0.24	0.24	0.1	0.13	0.13	0.1	0.11	0.11
MnO[3]	0.14	0.14	0.14	0.3	-	0.29	0.1	0.13	0.18	0.2		0.20	0.2		0.15
TOTAL	99.0	101.00	100.04	101.2		101.33	100.8	99.14	98.93	101.7		100.21	100.9		100.79

1. determined by γ-ray spectroscopy
2. determined chemically
3. determined by XRF

TABLE 52 (continued)

	QUARTZ MICA DIORITE (Y75)			QUARTZ MICA DIORITE (Y41)			QUARTZ MICA DIORITE (Y150)			GRANODIORITE (Y151)			GRANITE (Y43)		
	Probe	Chemical	XRF	Probe	Chemical	XRF	Probe	Chemical	XRF	Probe	Chemical	XRF	Probe	Chemical	XRF
SiO_2	57.3		56.72	59.2		59.71	58.4		59.05	64.8		64.08	75.2	74.23	74.25
Al_2O_3	16.9	16.95	16.38	16.3	16.37	16.28	16.7	16.67	16.49	15.8	15.71	15.92	13.7	13.71	13.64
Fe_2O_3	7.9	7.93	7.93	7.1	6.81	6.80	7.1	7.17	7.12	4.5	4.44	4.55	2.0	1.82	1.88
MgO	3.2		3.12	2.3		2.00	2.6		2.33	1.9		1.90	0.4	0.45	0.45
CaO	7.1		7.06	5.3		5.34	6.7		6.73	4.9		4.76	1.3	1.28	1.18
Na_2O	2.9	2.85	2.85[2]	3.4	3.24	3.24[2]	3.3	2.91	2.91[2]	3.9	3.51	3.51[2]	4.4	3.91	3.91[2]
K_2O	2.4		2.22(2.28)[1]	3.3	3.16	3.13(3.13)[1]	2.5		2.27(2.24)[1]	2.2		1.89(1.99)[1]	3.7	3.63	3.50
H_2O+CO_2[2]	1.9	1.94	1.94	1.8	1.75	1.75	1.4	1.42	1.42	1.2	1.22	1.22	0.5	0.50	0.50
TiO_2	0.7		0.59	0.5		0.62	0.5		0.49	0.4		0.39	0.3	0.28	0.25
P_2O_5[2]	0.1	0.11	0.11	0.1	0.14	0.14	0.1	0.10	0.10	0.1	0.08	0.08	0.1	0.06	0.06
MnO[3]	0.2		0.22	0.2		0.19	0.2		0.22	0.2		0.17	0.1	0.05	0.09
TOTAL	100.6		99.14	99.5		99.20	99.5		99.13	99.90		98.47	101.7	99.92	99.71

1. determined by γ-ray spectroscopy
2. determined chemically
3. determined by XRF

determined by gamma-ray spectroscopy.

Absorption and ignition loss corrections have been applied to the XRF data (NORRISH AND CHAPPELL, 1967), while the microprobe results have been corrected for ignition loss (viz. loss of water, carbon dioxide and other volatiles) during preparation of the glass disc. In order to calculate the total percentages of oxides obtained by the electron microprobe technique, the XRF values for MnO and chemically determined P_2O_5, water and carbon dioxide were used.

DISCUSSION

A good correlation exists between the microprobe, chemical and x-ray spectrographic determinations for Al_2O_3, CaO, MgO and K_2O. For SiO_2, there is fairly good correlation, although there is a tendency for this element to be a little high. The same may be said for TiO_2, but in this case the higher values may be related to the very steep calibration curve. Correlation between the microprobe and other methods for total iron is good except for high values. The sodium values are usually slightly higher than those obtained by flame photometry and it was thought that some buttons may have been contaminated during fusion by the use of inefficiently cleaned platinum crucibles. Six samples were then prepared by fusion in a graphite crucible, but sodium abundances were identical with those obtained using a platinum crucible.

TABLE 53

A Comparison of Analyses Showing the Reproducibility of Runs at Different Times

	Diorite (G107)		Diorite (Y75)		
	Run 1	Run 3	Run 1	Run 2	Run 3
Fe_2O_3	8.0	8.2	7.9	7.8	8.0
SiO_2	57.7	57.8	57.0	57.5	57.4
Al_2O_3	16.8	16.9	16.9	17.0	16.9
MgO	3.1	3.2	3.2	3.2	3.3
CaO	6.6	6.5	6.9	7.3	6.8

The reproducibility of the method is illustrated in Table 53 where results are given for two samples. Analyses were carried out on the discs at intervals of a week. It is of interest to point out that the results in column one for each sample for Fe_2O_3, SiO_2 and Al_2O_3 were obtained on the ARL electron microprobe at the University of New South Wales, Sydney, while the remainder are from the A.N.U. microprobe.

APPENDIX IV - A.N.U. AND YEOVAL SAMPLE NUMBERS

SAMPLE Nos.	A.N.U.	YEOVAL
Gabbros	3502	W1
	3503	W3
	3504	W4
	3505	W6
	3506	W7
	3507	W8
	3508	W9
	3509	W10
	3510	W11
	3511	W12
	3512	W19
	3513	W22
	3514	W25
	3515	W31
	3516	W35
	3517	W39
	3518	W41
	3519	W42
	3520	W46
	3521	W47
	3522	W48
	3523	W49
	3524	W50
	3525	W53
	3526	W54
	3527	W65
	3528	W66
	3529	W70

SAMPLE Nos.	A.N.U.	YEOVAL
Gabbros	3530	W71
	3531	W56
	3532	W58
Pyroxenites	3533	W60
	3534	W61
	3535	G153
Pyroxene-	3536	Y8
mica diorites	3537	G71
	3538	G72
	3539	G154
	3540	G131
Quartz-mica	3541	Y208
diorites	3542	Y224
	3543	Y225
	3544	Y227
	3545	Y237
	3546	Y234
	3547	Y69
	3548	Y235
	3549	Y12
	3550	Y71
	3551	Y67
	3552	Y245A
	3553	Y161
	3554	Y148
	3555	Y167
	3556	Y41
	3557	Y151
	3558	Y150
	3559	Y149
	3560	Y16

SAMPLE Nos.	A.N.U.	YEOVAL
Quartz-mica diorites	3561	Y40
	3562	G106
	3563	G107
	3564	G110
	3565	Y147
	3566	Y5
	3567	Y197
	3568	Y14
	3569	Y75
	3570	Y158
	3571	G120
	3572	G84
	3573	G86
	3574	G90
	3575	G118
	3576	G98
	3577	G99
	3578	G101
	3579	G102
	3580	G105
	3581	G88
	3582	G41
	3583	G91
	3584	Y195
	3585	G92
	3586	G96
	3587	G73
	3588	G55
	3589	G35
	3590	G80
	3591	Y55

SAMPLE Nos.	A.N.U.	YEOVAL
Xenoliths	3592	Y55A
	3593	Y75A
	3594	Y151X
	3595	Y227X
	3596	G90X
	3597	G99X
	3598	Y202A
Aplite	3599	Y41A
: Orthoclase diorites	3600	G57
	3601	G145
	3602	Y205
	3603	Y206
	3604	Y202
	3605	G152
	3606	Y212
	3607	G151
Fine quartz-mica diorites	3608	Y187
	3609	Y189
Tuffs	3610	G116
	3611	G122
	3612	G121
	3613	G123
	3614	G129
	3615	G130
	3616	G130A
Andesitic rocks	3617	G132
	3618	G133
	3619	G128
	3620	G134A
	3621	G134B
	3622	G140

SAMPLE Nos.	A.N.U.	YEOVAL
Andesitic	3623	G139
rocks	3624	G117
	3625	G142
	3626	G143
	3627	G146
	3628	G148
	3629	G149
	3630	G150
Granites	3631	R56
	3632	R67
	3633	R69
	3634	R74
	3635	R75
	3636	R66
	3637	R77
	3638	Y43
	3639	Y53
	3640	Y64
	3641	Y147B
	3642	Y168
	3643	Y173
	3644	R45
	3645	R57
	3646	R41
	3647	R24
	3648	R53
	3649	R76
	3650	Y53A

SAMPLE Nos.	A.N.U.	YEOVAL
Dyke rocks	3651	G127
	3652	G156
	3653	Y229
	3654	G67
	3655	G76
Skarn rocks	3656	W73
	3657	W74
	3658	W75
	3659	W77
	3660	G155
Hornblende gabbro	3661	Y36

Abramovich, I.I. (1959) Uranium and thorium in the intrusive rocks of Central and Western Tuva. Geochemistry, 1959, 442-450.

Akaad, M.K. (1956) The Ardara granitic diapir of County Donegal, Ireland. Q. Jour. Geol. Soc. London., 112, 263-287.

Akhmanova, M.V. and Leonova, L.L. (1961) Investigation of metamictisation of zircons with the aid of infrared absorption spectra. Geochemistry, 1961, 416-431.

Akimoto, S. (1954) Thermo-magnetic study of ferromagnetic minerals contained in igneous rocks. J. Geomag. Geoelect., 6, 1-14.

Akimoto, S. (1955) Magnetic properties of ferromagnetic minerals contained in igneous rocks. Japan. J. Geophys., 1, 1-31.

Aldrich, L.T., Wetherill, G.W., Tilton, G.R. and Davis, G.L. (1956) Half life of ^{87}Rb. Phys. Rev., 103, 1045-1047.

Anderson, C.A. (1941) Volcanoes of the Medicine Lake Highland, California. Univ. Calif. Dept. Geol. Sci., 25, 347-422.

Anderson, J.G.C. (1935) The Arrochar intrusive complex. Geol. Mag., 72, 263-283.

Anderson, J.G.C. (1937) Intrusions of the Glen Falloch Area. Geol. Mag., 74, 450-468.

Arrhenius, G., Fitzgerald, R., Fredriksson, K., Holm, B., Sinkankas, J., Bonatti, E., Bostrom, K., Lynn, D., Mathias, B., Ceballe, T. and Korkisch, J. (1964) Valance band structure and other La Jolla problems in microprobe analysis. Abstr. No.214, Electrochem. Soc. Meet., Washington, 100-103.

Arriens, P.A., Brooks, C., Bofinger, V.M. and Compston, W. (1966) The discordance of mineral ages in granitic rocks resulting from the redistribution of Rb and Sr. J. Geophys. Res., 71(20), 4981-4994.

Bartholome, P. (1961) Co-existing pyroxenes in igneous and metamorphic rocks. Geol. Mag., 98, 346-348.

Bottinga, Y., Kudo, A. and Weill, D. (1966) Some observations on oscillatory zoning and crystallisation of magmatic plagioclase. Am. Min. 51, 792-806.

Bowen, N.L. (1928) The Evolution of Igneous Rocks. Princeton University Press.

Bowen, N.L. (1937) Present high temperature research on silicates and its significance in igneous geology. Am. J. Sci., 33, 1-21.

Brammal, A. and Harwood, H.F. (1932) The Dartmoor granites: their genetic relationships. Q. Jour. Geol. Soc. Lond., 88, 171-234.

Brooks, C. (1966) The effect of mineral age discordancies on total-rock Rb-Sr isochrons of the Heemskirk Granite, Western Tasmania. J. Geophys. Res., 71, 5447-5458.

Brown, I.A. (1928) The geology of the south coast of New South Wales. Part I. The Palaeozoic geology of the Moruya District. Proc. Linn. Soc. N.S.W., 53, 151-192.

Carmichael, I.S.E. (1967) The iron-titanium oxides of salic volcanic rocks and their associated ferromagnesian silicates. Contrib. Min. Pet., 14, 36-64.

Carr, J.M. (1954) Zoned plagioclases in layered gabbros of the Skaergaard intrusion east Greenland. Min. Mag., 30, 367-375.

Chappell, B.W. (1966) Moonbi Granites. Unpub. Ph.D. Thesis, A.N.U.

Chayes, F. (1956) Modal composition of the major members of the Southern California Batholith. Carnegie Institute of Washington Yearbook, 55, 214-216.

Chayes, F. (1964-65) On the level of silica saturation in andesite. Carnegie Inst. Washington, 65, 155-159.

Clark, R.H. (1960) Andesite lavas of the North Island, New Zealand. Inter. Geol. Congress, 21st Session, 13, 123-131.

Clark, F.W. (1915) Analyses of rocks and minerals. U.S. Geol. Surv. Bull., 591, 25-217.

Coats, R.B. (1962) Magma type and crustal structure in the Aleutian arc. Amer. Geophys. Union Monograph, 6, 92-109.

Colditz, M.J. (1948) The petrology of the Silurian Volcanic sequence at Wellington, N.S.W. J. Proc. Roy. Soc. N.S.W., 81, 180-197.

Compston, W. and Jeffery, P.M. (1959) Anomalous 'common strontium' in granite. Nature, 184, 1792-1793.

Compston, W., Lovering, J.F., and Vernon, M.J. (1965) The rubidium-strontium age of the Bishopville aubrite and its component enstatite and feldspar. Geochim. Cosmochim. Acta, 29, 1085-1099.

Cooper, J.A. (1963) The flame photometric determination of potassium in geological materials used for Potassium-Argon dating. Geochim. Cosmochim. Acta, 27, 525-546.

Cruft, E.F. (1966) Minor elements in igneous and metamorphic apatite. Geochim. Cosmochim. Acta, 30, 375-398.

Cruft, E.F., Ingamells, C.O. and Muysson, J. (1965) Chemical analysis and the stoichiometry of apatite. Geochim. Cosmochim. Acta, 29, 581-597.

Daly, R.A. (1933) Igneous rocks and the depths of the earth. McGraw-Hill, New York.

Deans, T. (1938) Igneous rocks from the Aberçorn and Kasama districts, N. Rhodesia. Geol. Mag., 75, 547-558.

Deer, W.A. (1935) The Cairnsmore of Carsphairn igneous complex. Q. Jour. Geol. Soc. Lond., 91, 47-76.

Deer, W.A. (1937) The composition and paragenesis of the biotites of the Carsphairn igneous complex. Min. Mag., 24, 495-502.

Deer, W.A. (1950) The diorites and associated rocks of the Glen Tilt complex, Perthshire. Geol. Mag., 87, 181-195.

Deer, W.A., Howie, R.A. and Zussman, J. (1962a) Rock-Forming Minerals. Vol.1 Ortho and Ring Silicates. Longmans, London.

Deer, W.A., Howie, R.A. and Zussman, J. (1962b) Rock-Forming Minerals. Vol.3 Sheet Silicates. Longmans, London.

Deer, W.A., Howie, R.A. and Zussman, J. (1962c) Rock-Forming Minerals. Vol.5 Non-Silicates. Longmans, London.

Deer, W.A., Howie, R.A. and Zussman, J. (1963a) Rock-Forming Minerals. Vol.2 Chain Silicates. Longmans, London.

Deer, W.A., Howie, R.A. and Zussman, J. (1963b) Rock-Forming Minerals. Vol.4 Framework Silicates. Longmans, London.

Dickinson, W.R. and Hatherton, T. (1967) Andesitic volcanism and seismicity around the Pacific. Science, 157, 801-803.

Eaton, J.P. (1963) Crustal structure from San Francisco, California, to Eureka, Nevada, from seismic refraction measurements. J. Geophys. Res., 68, 5789-5806.

Emerson, D.W. (1962) The Geology of an area to the south west of Dubbo. Unpub. Graduation Thesis. Univ. N.S.W.

Engel, A.E.J. (1963) Geological evolution of North America. Science, 140, 143-152.

Evernden, J.F. and Richards, J.R. (1962) Potassium-argon ages in Eastern Australia. J. Geol. Soc. Aust., 9, 1-50.

Ewart, A. (1963) Petrology and petrogenesis of the Quarternary pumice ash in the Taupo Area, New Zealand. J. Petrol., 4, 392-431.

Ewart, A. (1965) Mineralogy and petrogenesis of the Whakamaru Ignimbrite in the Maraetai area of the Taupo volcanic zone, New Zealand. N.Z. J. Geol. Geophys., 8, 611-677.

Ewart, A. and Stipp, J.J. (1968) Origin of the volcanic rocks of the Central North Island, New Zealand, as indicated by a study of $^{87}Sr/^{86}Sr$ ratios, and Sr, Rb, K, U and Th abundances. Geochim. Cosmochim. Acta, in press.

Faure, G. and Hurley, P.M. (1963) The isotopic composition of strontium in oceanic and continental basalts: application to the origin of igneous rocks. J. Petrol. 4, 31-50.

Flannagan, F.J. (1967) U.S. Geological Survey silicate rock standards. Geochim. Cosmochim. Acta, 31, 289-308.

Fleischer, M. (1955) Hafnium content and hafnium-zirconium ratio in minerals and rocks. U.S. Geol. Surv. Bull. 1021-A.

Fleischer, M. (1965) Summary of data on rock samples G-1 and W-1, 1962-1965. Geochim. Cosmochim. Acta, 29, 1263-1283.

Foster, M.D. (1960) Interpretation of the composition of trioctahedral micas. U.S. Geol. Surv. Prof. Papers, 354B: 11-49.

Frenda, G.A. (1961) The Geology of the Sappa Bulga District. Unpub. Graduation Thesis. Univ. N.S.W.

Gast, P.W. (1960) Limitations on the Composition of the Upper Mantle. J. Geophys. Res., 65, 1287-1297.

Goldsmith, J.R. and Laves, F. (1954) The microcline-sanidine stability relations. Geochim. Cosmochim. Acta, 5, 1-19.

Green, D.H. (1963) Alumina content of enstatite in a Venezuelan high-temperature peridotite. Bull. Geol. Soc. Amer., 74, 1397-1402.

Green, D.H. and Ringwood, A.E. (1967) An experimental investigation of the gabbro to eclogite transformation and its petrological applications. Geochim. Cosmochim. Acta, 31, 767-833.

Green, T.H. (1967) High Pressure Experimental Petrology. Ph.D. Thesis, A.N.U.

Green, T.H. and Ringwood, A.E. (1966) Origin of the Calc-alkaline igneous rock suite. Earth & Planetary Science Letters, 1, 307-316.

Hales, A.L. (1960) Research at the Bernard Price Institute of Geophysical Research, University of Witwatersrand, Johannesburg. Proc. Roy. Soc. Lond., Series A, 258, 1-26.

Hamilton, W. (1964) Origin of high-alumina basalt andesite and dacite magmas. Science, 146, 635-637.

Harloff, C. (1927) Zonal structures in plagioclases. Leidsche Geol. Mededeel., 2, 99-114.

Hasan, S.M. (1959) The Bigga House basic igneous complex, N.S.W. Geol. Mag., 96, 442-452.

Heier, K.S. and Rogers, J.J.W. (1963) Radiometric determination of thorium, uranium and potassium in basalts and in two magmatic differentiation series. Geochim. Cosmochim. Acta, 27, 137-154.

Hills, E.S. (1936) Reverse and oscillatory zoning in plagioclase feldspars. Geol. Mag., 73, 49-56.

Hurley, P.M., Bateman, P.C., Fairbairn, H.W. and Pinson, W.H. (1965) Investigation of initial $^{87}Sr/^{86}Sr$ ratios in the Sierra Nevada plutonic province. Bull. Geol. Soc. Amer., 76, 165-174.

Hutchison, C.S. (1964) A gabbro-granodiorite association in Singapore Island. Q. Jour. Geol. Soc. Lond., 120, 283-297.

Joplin, G.A. (1937) The Ben Bullen plutonic complex, New South Wales. J. Roy. Soc. N.S.W., 70, 69-94.

Joplin, G.A. (1958) Basic and ultrabasic rocks near Happy Jacks and Tumut Pond in the Snowy Mts. of N.S.W. J. Roy. Soc. N.S.W., 91, 120-141.

Joplin, G.A. (1959) On the origin and occurrence of basic bodies associated with discordant bathyliths. Geol. Mag., 96, 361-373.

Joplin, G.A. (1965) A Petrography of Australian Igneous Rocks Angus & Robertson, Sydney.

Keil, K. (1967) The electron microprobe x-ray analyser and its application in mineralogy. Fortschr. Mineral, 44, 4-66.

Kiss, E. (1967) Chemical determination of some major constituents in rocks and minerals. Anal. Chim. Acta, 39, 223-234.

Kleeman, A.W. (1965) The origin of granitic magmas. J. Geol. Soc. Aust., 12, 35-52.

Kleeman, J.D. and Lovering, J.F. (1967) Uranium distribution in rocks by fission-track registration in Lexan Plastic. Science, 156, 512-513.

Kolbe, P. and Taylor, S.R. (1966) Geochemical investigation of the granitic rocks of the Snowy Mountains area, New South Wales. J. Geol. Soc. Aust., 13, 1-25.

Koritnig, S. (1965) Geochemistry of phosphorus - I. The replacement of Si^{4+} by P^{5+} in rock-forming silicate minerals. Geochim. Cosmochim. Acta, 29, 361-372.

Kosterin, A.V., Zuev, V.N. and Shevaleevskii, I.D. (1958) Zr/Hf ratios in zircons in some igneous rocks of Northern Kirgisia. Geochemistry, 1958, 116-119.

Kosterin, A.V., Shevaleevskii, I.D. and Rybalova, E.K. (1960) The Zr/Hf ratio in the zircons of some igneous rocks of the northern slope of the Kuramin Mountain Range. Geochemistry, 1960, 541-545.

Kosterin, A.V., Shevaleevskii, I.D., Rybałova, E.K. and Tolok, K.P. (1963) Zr/Hf ratio in zircons of some igneous rocks of Northern-Kazakhstan. Geochemistry, 1963, 1007-1009.

Kretz, R. (1959) Chemical study of garnet, biotite and hornblende from gneisses of Southwestern Quebec, with emphasis on distribution of elements in co-existing minerals. J. Geol., 67, 371-402.

Kretz, R. (1960) The distribution of certain elements among co-existing calcic pyroxenes, calcic amphiboles and biotites in skarns. Geochim. Cosmochim. Acta, 20, 161-191.

Kretz, R. (1961) Some applications of thermodynamics to co-existing minerals of variable composition. Examples: orthopyroxene-clinopyroxene and orthopyroxene-garnet. J. Geol., 69, 361-387.

Kretz, R. (1963) Distribution of magnesium and iron between orthopyroxene and calcic pyroxene in natural mineral assemblages. J. Geol., 71, 773-785.

Kulp, J.L. (1961) Geologic time-scale. Science, 133, 1105-1114.

Kuno, H. (1960) High-alumina basalt. J. Petrol., 1, 121-145.

Larsen, E.S. (1948) Batholith and associated rocks of Corona, Elsinore, and San Luis Rey Quadrangles, Southern California. Geol. Soc. Am. Mem. 29.

Larsen, E.S. and Draisin, W.M. (1948) Composition of Minerals in the rocks of the Southern California Batholith. Rep. Int. Geol. Congr. XVIII Session (GB) II, 67-69.

Larsen, E.S., Irving, J., Gonyer, F.A. and Larsen, E.S. 3rd., (1936) Petrologic results of a study of the minerals from the Tertiary volcanic rocks of the San Juan Region, Colorado. Am. Min., 21, 679-701.

Larsen, E.S., Irving, J., Gonyer, F.A. and Larsen, E.S. 3rd., (1937) Petrologic results of a study of the minerals from the Tertiary volcanic rocks of the San Juan region, Colorado. Am. Min., 22, 889-905.

Larsen, E.S., Irving, J., Gonyer, F.A. and Larsen, E.S. 3rd., (1938) Petrologic results of a study of the minerals from the Tertiary volcanic rocks of the San Juan region, Colorado. Am. Min., 23, 417-429.

Larsen, L.H. and Poldervaart, A. (1957) Measurement and distribution of zircons in some granitic rocks of magmatic origin. Min. Mag., 31, 544-564.

Leonova, L.L. and Balashov, Yu. A. (1963) Distribution of uranium, thorium and the rare earths in the granitoids of the Susamyr Batholith (Central Tien-Shan). Geochemistry, 1963, 1047-1055.

Lyakhovick, V.V. and Shevaleevskii, I.D. (1962) Zr:Hf ratio in the accessory zircon of granitoids. Geochemistry, 1962, 508-524.

Maggs, D.F. (1963) The stratigraphy of the Yeoval-Cumnock-Manildra region. Unpub. M.Sc. Thesis. Univ. N.S.W.

Matsui, Y. and Banno, S. (1965) Intracrystalline exchange equilibria in silicate solid solutions. Proc. Japan Acad., 41, 461-466.

Matsui, Y., Banno, S. and Hernes, I. (1966) Distribution of some elements among the minerals of Norwegian eclogites. Norsk. geol. Tidsskr., Bind 46, 364-368.

McIntyre, G.A., Brooks, C., Compston, W. and Turek, A. (1966) The statistical assessment of Rb-Sr isochrons. J. Geophys. Res., 71, 5459-5468.

Meliksetyan, B.M. (1960) Zirconium to hafnium ratio in zircons from rocks of Megrin Pluton. Chem. Abs., 1961, 6299b.

Miller, F.S. (1937) Petrology of the San Marcos Gabbro, Southern California. Bull. Geol. Soc. Am., 48, 1397-1426.

Mueller, R.F. (1960) Compositional characteristics and equilibrium relations in mineral assemblages of a metamorphosed iron formation. Am. J. Sci., 258, 449-497.

Mueller, R.F. (1963) Interaction of chemistry and mechanics in magmatism. J. Geol., 71, 759-772.

Murthy, M.V.N. (1957-1961) On the crystallisation of accessory zircon in granitic rocks of magmatic origin. Canad. Min., 6, 260-263.

Nicolaysen, L.O. (1961) Graphic interpretation of discordant age measurements on metamorphic rocks. Ann. N.Y. Acad. Sci., 91, Pt. II, 198-206.

Nockolds, S.R. (1932) The contaminated granite of Bibette Head, Alderney. Geol. Mag., 69, 433-452.

Nockolds, S.R. (1934) The contaminated tonalites of Loch Awe, Argyll. Q. Jour. Geol. Soc. Lond., 90, 302-321.

Nockolds, S.R. (1934) The production of normal rock types by contamination and their bearing on petrogenesis. Geol. Mag., 71, 31-39.

Nockolds, S.R. (1941) The Garabal Hill-Glen Fyne igneous complex. Q. Jour. Geol. Soc. Lond., 96, 451-508.

Nockolds, S.R. (1947) The relation between chemical composition and paragenesis in the biotite micas of igneous rocks. Am. J. Sci., 245, 401-420.

Nockolds, S.R. (1954) Average chemical composition of some igneous rocks. Bull. Geol. Soc. Am., 65, 1007-1032.

Nockolds, S.R. and Allen, R. (1953) The geochemistry of some igneous rock series. Geochim. Cosmochim. Acta, 4, 105-142.

Nockolds, S.R. and Mitchell, R.L. (1948) The geochemistry of some Caledonian plutonic rocks: a study in the relationship between the major and trace elements of igneous rocks and their minerals. Trans. Roy. Soc. Edinb., 61, 533-575.

Norrish, K. and Chappell, B.W. (1966) X-ray Fluorescence Spectrography. In Physical Methods in Determinative Mineralogy, Academic Press, London.

O'Hara, M.J. (1965) Primary magmas and the origin of basalts. Scottish Journ. Geol., 1, 19-40.

Osborn, F.F. (1959) Role of oxygen pressure in the crystallisation and differentiation of basaltic magma. Am. J. Sci., 257, 609-647.

Osborn, F.F. (1962) Reaction series for subalkaline igneous rocks based on different oxygen pressure conditions. Am. Min., 47, 211-226.

Pabst, A. (1928) Observations on inclusions in the granitic rocks of the Sierra Nevada. Univ. Calif. Pub. Geol. Sci., 17, 325-388.

Packham, G.H. (1960) Sedimentary history of part of the Tasman Geosyncline in South-Eastern Australia. Rep. Int. Geol. Congr. Norden, Part 12, Regional Palaeogeography.

Pakiser, L.C. and Robinson, R. (1966) Composition of the continental crust as estimated from seismic observations. Geophysical Monograph No.10, 620-626. The Earth Beneath the Continents. Ed. Steinhart, J.S. and Jefferson Smith, T.

Poldervaart, A. (1949) Three methods of graphical representation of chemical analyses of igneous rocks. Trans. Roy. Soc. S. Africa, 32, 177-188.

Poldervaart, A. (1955) Zircon in rocks. I. Sedimentary Rocks. Am. J. Sci., 253, 433-461.

Poldervaart, A. (1956) Zircon in rocks. II. Igneous Rocks. Am. J. Sci., 254, 521-554.

Powers, H.A. (1932) The lavas of the Modoc Lava-bed Quadrangle, California. Am. Min., 17, 253-294.

Ramberg, H. and DeVore, G. (1951) The distribution of Fe^{++} and Mg^{++} in coexisting olivines and pyroxenes. J. Geol., 59, 193-210.

Read, H.H. and Haq, B.T. (1965) Notes, mainly geochemical, on the granite-diorite complex of the Insch igneous mass, with an addendum on the Aberdeenshire quartz-dolerites. Proc. Geol. Soc., 76, 13-20.

Riley, J.P. (1958) The rapid analysis of silicate rocks and minerals. Anal. Chim. Acta, 19, 413-428.

Ringis, J. (1962) The geology of the Toongi-Sappa Bulga district. Unpub. Graduation Thesis. Univ. N.S.W.

Rittman, A. and El-Hinnawi, E.E. (1961) The application of the zonal method for the distinction between low and high temperature plagioclase feldspars. Schweis. Mineral. Petrog. Mitt., 41, 41-48.

Robinson, H.H. (1913) The San Franciscan volcanic field, Arizona. U.S. Geol. Surv. Prof. Paper, 76.

Rogers, J.J.W. and Ragland, P.C. (1961) Variation of thorium and uranium in selected granitic rocks. Geochem. Cosmochim. Acta, 25, 99-109.

Sahama, Th. G. and Torgeson, D.R. (1949) Some examples of the application of thermochemistry to petrology. J. Geol., 57, 255-262.

Saxone, S.K. (1966) Distribution of elements between co-existing biotite and hornblende in metamorphic Caledonides, lying to the west and north west of Trondheim, Norway. Neves Jehrbuch fur. Mineralogie, Hefte 3, 67-79.

Schmidt, R.G. (1957) Geology of Saipan, Mariana Islands. Chapter B: Petrology of the volcanic rocks. U.S. Geol. Surv. Prof. Paper, 280, B.

Shand, S.J. (1943) Eruptive Rocks Wiley, New York.

Shevaleevskii, I.D., Pavlenko, A.S. and Vainshtein, E.E. (1960) Dependence of the behaviour of zirconium and hafnium on the petrochemical characteristics of igneous and alkali metasomatic rocks. Geochemistry, 1960, 262-272.

Shields, W.R. and Garner, E.L. (1963) Survey of Rb^{85}/Rb^{87} in Minerals. J. Geophys. Res., 68, 2331-2334.

Smirnov, V.A. (1962) Uranium and thorium in igneous rocks of Western Transbaikaliya. Geochemistry, 1962, 1115-1122.

Smith, J.V. (1966) X-ray-emission microanalysis of rock-forming minerals. II. Olivines. J. Geol., 74, 1-16.

Snelling, N.J. (1960) The geology and petrology of the Murrumbidgee batholith, Australia. Q. Jour. Geol. Soc. Lond., 115, 187-217.

Snyder, J.L. (1959) Distribution of certain elements in the Duluth Complex. Geochim. Cosmochim. Acta, 16, 243-277.

Steggles, K.R. (1962) The geology of the Toongi-Dilladerry district. Unpub. Graduation Thesis. Univ. N.S.W.

Steiger, R.H. and Wasserburg, G.J. (1966) Systematics in the Pb^{208}-Th^{232}, Pb^{207}-U^{235}, and Pb^{206}-U^{238}. Nuclear Geophysics, in press.

Summerhayes, C.P. (1966) A geochronological and strontium isotope study on the Garabal Hill-Glen Fyne Igneous complex, Scotland. Geol. Mag., 103, 153-165.

Tauson, L.V. and Stavrov, O.D. (1957) The geochemistry of rubidium in granitoids. Geochemistry, 1957, 819-824.

Taylor, S.R. (1966) The application of trace element data to problems in petrology. Phys. Chem. Earth, 6, 133-213.

Taylor, S.R. (1967) Geochemistry of andesites. In press.

Taylor, S.R. and Blake, D.H. Geochemistry of andesites from Bougainville, Solomon Islands and Fiji. (In preparation).

Taylor, S.R. and White, A.J.R. (1966) Trace element abundances in andesites. Bull. Volcan., Tome 29, 177-194.

Taylor, S.R., Ewart, A., and Capp, A.C. (1968) Leucogranites and rhyolites. Lithos (in press).

Thomas, H.H. and Smith, C.W. (1932) Xenoliths of igneous origin in the Tregastel-Ploumanac'h granite, Cotes du Nord, France. Q. Jour. Geol. Soc. Lond., 88, 274-295.

Thomas, W.K.L. and Kempe, D.R.C. (1963) Standard geochemical sample T-1 Msusule Tonalite. Supplement No.1, 1-6. Geol. Surv. Division, Tanganyika.

Tilley, C.E. (1950) Some aspects of magmatic evolution. Q. Jour. Geol. Soc. Lond., 106, 37-61.

Tilley, C.E. and Muir, I.D. (1964) Intermediate members of the oceanic basalt-trachyte association. Geol. Foren. Stockholm., Forh. 85, 434-443.

Turek, A. (1966) Rubidium-strontium isotopic studies in the Kalgoorlie-Norseman area, Western Australia. Ph.D. Thesis, A.N.U. (Unpub.)

Turner, F.J. and Verhoogen, J. (1960) Igneous and Metamorphic Petrology. 2nd Edition, McGraw-Hill, New York.

Tuttle, O.F. and Bowen, N.L. (1958) Origin of granite in the light of experimental studies in the system $NaAlSi_3O_8$-$KAlSi_3O_8$-SiO_2-H_2O. Geol. Soc. Am. Mem. 74.

Vance, J.A. (1962) Zoning in igneous plagioclase: normal and oscillatory zoning. Am. J. Sci., 260, 746-760.

Vance, J.A. (1965) Zoning in igneous plagioclase: patchy zoning. J. Geol., 73, 636-651.

Volkov, V.P. and Savinova, E.N. (1961) Variation in K/Rb ratio during the evolution of calc-alkalic and alkalic magmas. Geochemistry, 1961, 1227-1236.

Wager, L.R. (1960) The major element variation of the layered series of the Skaergaard intrusion and a re-estimation of the average composition of the hidden layered series and of the successive magmas. J. Petrol., 1, 364-398.

Wager, L.R., Brown, G.M. and Wadsworth, W.J. (1960) Types of igneous cumulates. J. Petrol., 1, 73-85.

Waters, A.C. (1955) Crust of the Earth. Ed. A. Poldervaart, Geol. Soc. Am., Spec. Pap. 62, 703-722.

Wells, A.K. and Bishop, A.C. (1955) An appinitic facies associated with certain granites in Jersey, Channel Islands. Q. Jour. Geol. Soc. Lond., 111, 143-163.

Wells, A.K. and Wooldridge, S.W. (1931) The rock groups of Jersey, with special reference to intrusive phenomena. Proc. Geol. Soc., 42, 178-215.

Whitfield, J.M., Rogers, J.J.W. and Adams, J.A.S. (1959) The relationship between the petrology and the thorium and uranium contents of some granitic rocks. Geochim. Cosmochim. Acta, 17, 248-271.

Whitney, P.R. and Hurley, P.M. (1964) The problem of inherited radiogenic strontium in sedimentary age determinations. Geochim. Cosmochim. Acta, 28, 425-437.

Wilcox, R.E. (1954) Petrology of Paricutin volcano, Mexico. Bull. U.S. Geol. Surv., 965-C, 281-353.

Wilkinson, J.F.G. (1966) Some aspects of calc-alkali rock genesis. J. Roy. Soc. N.S.W., 99, 69-77.

Williams, H. (1932) Geology of the Lassen Peak National Park, California. Univ. Calif. Dept. Geol. Sci. 21, 195-385.

Williams, H. (1935) Newberry volcano of central Oregon. Bull. Geol. Soc. Am., 46, 253-304.

Williams, H. (1942) The geology of Crater Lake National Park, Oregon. Carnegie Institution Washington, Pub. 540.

Wilson, J.T. (1954) In the Earth as a Planet. Ed. Kuiper, G.P. Univ. Chicago Press, 138-214.

Wones, D.R. (1964) Biotite-k feldspar-magnetite as indicators of H_2O pressures during metamorphic and igneous processes. Geol. Soc. Am. Spec. Papers, 82, 228-229.

Woolard, G.P. (1966) Regional isostatic relations in the United States. Geophysical Monograph No.10, 557-594. The Earth Beneath the Continents. Ed. Steinhart, J.S. and Jefferson Smith, T.

Yoder, H.S., Stewart, D.B. and Smith, J.R. (1957) Feldspars. Carnegie Inst. Wash. Year Book, 56, 206-214.